Metabolic inflammation in hepatic and vascular disorders

Strategies to attenuate disease development

Colophon

Metabolic inflammation in hepatic and vascular disorders

Strategies to attenuate disease development

Proefschrift

ter verkrijging van de graad van doctor aan de
Rijksuniversiteit Groningen
op gezag van de
rector magnificus prof. dr. E. Sterken
en volgens besluit van het College voor Promoties.

De openbare verdediging zal plaatsvinden op

woensdag 30 maart 2016 om 12.45 uur

door

Martine Claire Morrison

geboren op 30 juni 1986
te Eindhoven

Promotor
Prof. dr. P. Heeringa

Copromotor
Dr. R. Kleemann

Beoordelingscommissie
Prof. dr. K. N. Faber
Prof. dr. M. H. Hofker
Prof. dr. ir. J. Keijer

"But I don't want to go among mad people," Alice remarked.

"Oh, you can't help that," said the Cat: "we're all mad here. I'm mad. You're mad."

"How do you know I'm mad?" said Alice.

"You must be," said the Cat, "or you wouldn't have come here."

― Lewis Carroll, *Alice in Wonderland*

Table of contents

Chapter 1

General introduction

The global burden of obesity

Although once considered a problem only in high-income countries, obesity is now also on the rise in low- and middle-income countries with prevalences increasing worldwide. In 2014, only a third of the world's population was considered to be of 'normal' weight (body mass index < 25 kg/m^2) and over 600 million adults were obese (body mass index ≥ 30 kg/m^2) [1]. These numbers reflect more than a doubling in the prevalence of obesity since 1980, and this rise is only projected to continue [1]. As obesity is associated with reduced life expectancy [2] and increased all-cause mortality [3] this obesity epidemic may represent one of the greatest threats to global human health.

The World Health Organization defines obesity as "abnormal or excessive fat accumulation that may impair health", and it is commonly classified as a body mass index ≥ 30 kg/m^2. Obesity is associated with several metabolic abnormalities such as abnormal blood cholesterol and triglyceride levels (dyslipidaemia) and elevated blood glucose and insulin levels (hyperglycaemia and hyperinsulinaemia) [4]. These features are thought to contribute to the development of obesity-associated metabolic diseases such as type 2 diabetes (T2D), non-alcoholic fatty liver disease (NAFLD) and cardiovascular disease (CVD), for which obesity is a major risk factor [4]. In addition to these metabolic derangements observed in obese individuals, inflammation has recently emerged as a driving force and potential unifying mechanism behind the pathogenesis of obesity-associated diseases.

Metabolic inflammation

Inflammation is a normal and essential defence mechanism that protects the host from infection and injury. It is the process by which an initial source of cellular injury – an invading pathogen or physical tissue damage – is eliminated in an orchestrated manner. An effective inflammatory response is self-limiting and initiates tissue repair processes, thereby promoting homeostasis at infected or damaged sites. Such regulated inflammatory responses are essential to maintain health.

Over the past few decades, it has become increasingly clear that inflammation can also be triggered by nutrients and metabolic surplus, an inflammatory state that has been coined 'metaflammation' (metabolically triggered inflammation) [5]. In contrast with classical inflammation, as described above, metabolic inflammation is not self-limiting and leads to a state of chronic low-grade inflammation that is considered to be a pathological feature of

obesity-associated diseases such as T2D, NAFLD and CVD [6]. This metabolic inflammatory response involves many components of the classical inflammatory response and is, at later stages, characterised by systemic increases in circulating inflammatory mediators such as cytokines (e.g. Tumour Necrosis Factor-alpha: TNF-α), bioactive lipids (e.g. palmitic acid, ceramides) and acute phase proteins (e.g. C-Reactive Protein: CRP and Serum Amyloid A: SAA) [6]. Obesity – inherently a state of metabolic excess – is characterised by metabolic inflammation: many studies have shown that tissues become inflamed and systemic inflammatory markers are increased in rodent models of obesity as well as in obese humans (e.g. [7-9]).

Mechanisms of metabolic inflammation

Although much remains unknown about the origin or mechanisms of metabolically triggered inflammation, the currently favoured paradigm is that metabolic inflammation is triggered when metabolic excess (surplus energy or macronutrients) is too big for designated metabolic cells (such as adipocytes or hepatocytes) to process. As a result, an inflammatory response is initiated in these specialised metabolic cells, either in direct response to high nutrient levels or in response to the cellular stress or damage that may be the result of metabolic overload, thus mediating the interface between metabolic input and inflammatory output [10]. Although metabolic organs such as the adipose tissue and the liver are likely to be the most susceptible to metabolic overload and inflammation, metabolic inflammation can also develop in other organs (e.g. kidney, brain and vasculature).

Sensing metabolic overload

It is now generally accepted that metabolic overload in metabolic cells results in activation of inflammatory pathways within these cells. Although the initial trigger of the metabolic inflammatory response remains unclear – and may differ according to diet and/or individual susceptibility – several molecules have been proposed to provide the link between metabolism and the immune system: acting as sensors of metabolic overload and activating inflammatory signalling pathways. These molecules belong to the classical pathogen-sensing pathways of the innate immune system, and are thought to be able to recognise excessive nutrient intake as a harmful, stress-related biological event [11].

The innate immune system – the first line of defence against infectious agents – relies on so-called pattern recognition receptors (PRRs) to monitor the extracellular space and intracellular

compartments for the presence of microbes, cell damage or other cellular stressors. These PRRs are able to detect pathogen-associated molecular patterns (PAMPs) as well as endogenous damage and stress signals through damage-associated molecular patterns (DAMPS) [12]. There are several classes of PRRs, of which the Toll-like receptors (TLRs) and the Nod-like receptors (NLRs) have emerged as potentially important regulators of metabolic inflammation [11].

TLRs are a family of membrane-bound pathogen sensing-receptors with at least twelve members in mammalian species, each of which appears to have a distinct function in innate immune recognition [12]. TLR2 and TLR4 are particularly interesting in the context of metabolic inflammation, as they are also broadly expressed by non-immune cells such as adipocytes, hepatocytes and myocytes [13-16] and can be activated by metabolic signals such as saturated fatty acids like palmitate [17-19], ceramides [20], and oxidised low-density lipoproteins (LDL) [21, 22]. Engagement of these TLRs results in the activation of intracellular pro-inflammatory signalling pathways, leading to activation of the transcriptional regulators NFκB and AP-1 [23]. Studies in rodent models of obesity have shown that genetic deletion of TLR2 or a loss-of-function mutation in TLR4 protects against high-fat-diet-induced inflammation [24, 25], thus providing evidence that these receptors may indeed be involved in sensing of metabolic inflammation.

NLRs are cytoplasmic PRRs that assemble into large multimeric protein complexes called inflammasomes. These inflammasomes consist of a sensor molecule (the NLR), the adaptor protein apoptosis-associated speck-like protein containing a CARD (ASC) and the effector protein caspase-1 [26]. The best characterised inflammasome is the NLR family pyrin domain-containing 3 (NLRP3) inflammasome, which can be activated by a variety of PAMPs and DAMPs. Like TLRs, NLRs are also expressed by metabolic cells [27, 28] and they can be activated by metabolic signals such as saturated fatty acids [29, 30] and crystallised cholesterol [31, 32]. In reaction to sensing of a PAMP or DAMP, the inflammasome protein complex is formed and pro-caspase-1 is autoproteolytically cleaved into caspase-1. Active caspase-1 then proteolytically activates the biologically inactive precursors of the cytokines IL-1β and IL-18 into their mature, pro-inflammatory counterparts [33]. These cytokines are released into the extracellular space, where they can bind to their respective receptors and activate pro-inflammatory signalling pathways in an autocrine or paracrine manner, contributing to local organ inflammation. Several studies have shown that genetic deletion of NLRP3-associated genes (i.e. ASC, NLRP3 or Caspase-1) in rodent models of obesity reduces diet-induced inflammation and metabolic disease development [30, 31, 34], suggesting that the

NLRP3 inflammasome contributes to metabolic inflammation.

Inflammatory response to metabolic overload

The activation of a PRR, either by a 'classical' DAMP or PAMP or by nutrient excess, leads to the activation of intracellular signalling pathways that converge on the activation of pro-inflammatory transcription factors to initiate a program of gene expression that enables the mounting of an inflammatory response. In the context of metabolic inflammation, the transcription factor NFκB has frequently been implicated as a key player [35-38]. NFκB is considered the master regulator of inflammatory responses and although it was initially characterised in immune cells, it is now known to be expressed and capable of activation in most cell types [36]. Under resting conditions, NFκB is sequestered in the cytosol by inhibitor of κB (IκB), which prevents its nuclear localisation and transcriptional function. In response to stimulation of PRRs – e.g. by metabolic overload – intracellular signalling pathways converge on the activation of inhibitor of κB kinase (IKK), which phosphorylates IκB and thereby promotes its degradation. This releases NFκB, allowing for its translocation to the nucleus where it promotes transcription of its target genes [39]. Since the NFκB target genes include a wide array of pro-inflammatory cytokines, chemokines and adhesion molecules, activation of NFκB by nutritional overload contributes to immune cell recruitment and amplifies and sustains an inflammatory reaction that ultimately results in organ dysfunction and thereby metabolic disease development [37].

This recruitment of immune cells into tissues is a common component of metabolic diseases. In a classical inflammatory response, the first immune cells that are recruited to an inflammatory site are the neutrophils (polymorphonuclear leukocytes), which mediate the earliest phase of the innate immune response [40]. They respond to chemoattractants that are produced by resident tissue macrophages in response to inflammatory or cellular-damage signals released from parenchymal cells [41]. As the body's first line of defence during acute inflammatory responses, neutrophils are highly efficient, short-lived effector cells that carry a multitude of weapons that are either primarily directed against a wide range of pathogens, or serve as signal molecules for the recruitment and activation of secondary immune cells [42]. The brute force and indiscriminate nature of the potent arsenal of antimicrobial weaponry (e.g. proteases and reactive oxygen species) carried by neutrophils makes them a potential cause of extensive tissue damage, which is thought to contribute to their detrimental role in metabolic disease development [43, 44]. Monocyte-derived macrophages typically follow soon after the neutrophils, but survive much longer at sites of inflammation [40]. The primary function of

these phagocytes is to identify, ingest and destroy pathogens, and they play an important role in the clearance of apoptotic cells and cellular debris. Unlike neutrophils, macrophages are not terminally differentiated and they show a remarkable phenotypic plasticity in response to their environment. During obesity, the macrophage population differs from that of lean subjects not only in number and tissue localisation, but also in inflammatory phenotype [45]. Although neutrophils and macrophages have an essential role in the protection of the host against invading pathogens, their improper recruitment and activation during metabolic inflammation can contribute to amplification and propagation of the initial inflammatory signal, thereby driving organ dysfunction and disease progression.

Defective resolution in metabolic inflammation
While the ideal inflammatory response is self-limiting, metabolic inflammation is chronic in nature. The self-limiting capacity of an inflammatory response relies on the timely initiation of inflammation resolution, which allows for the repair of injured tissues and enables a return to homeostasis. Although inflammation resolution was long thought to be a passive process, it is now recognised to be an active programmed response that is orchestrated by a family of lipid mediators that are derived from essential fatty acids: the specialised pro-resolving mediators (SPMs) [46]. These SPMs, namely resolvins, protectins, and maresins, act as agonists to actively dismantle the inflammatory response, limit further leukocyte recruitment, promote efferocytosis (the uptake and clearance of apoptotic cells, cellular debris and microorganisms by macrophages) and initiate tissue repair mechanisms [47, 48]. Dysfunctional resolution is thought to underlie the aetiology of chronic inflammatory diseases [49], and it has been proposed that defective resolution of inflammation may be pivotal to the sustained inflammatory state that drives metabolic disease development [50]. When resolution of inflammation is defective there is no appropriate termination and clearance of phagocytes, and the resulting sustained presence of activated leukocytes within tissues is associated with collateral tissue damage, amplification of the inflammatory response and persistence of tissue inflammation, ultimately leading to organ dysfunction [50].

Organ dysfunction during metabolic disease development

Adipose tissue dysfunction
The adipose tissue is the primary site of energy storage in the body. When energy intake exceeds energy expenditure (i.e. dietary excess) energy is stored in the adipose tissue in the form of triglycerides, leading to expansion of adipose tissue depots. This adipose tissue

expansion is the result of both adipocyte hyperplasia (increase in cell number) and adipocyte hypertrophy (increase in cell size). In addition to the fact that excess lipids or intermediates of lipid metabolism could directly trigger an inflammatory response by engaging with PRRs as discussed above, it is thought that cellular stress, local hypoxia, intracellular damage (e.g. to membranes or organelles) and eventually necrosis may occur when an adipocyte has reached the limit of its expansion, thus providing additional triggers for inflammation [51, 52]. These inflammatory signals lead to expression of chemotactic signals by adipocytes, resulting in infiltration of immune cells into the adipose tissue [52-54] where they characteristically arrange around necrotic adipocytes in so-called crown-like structures [55]. Secretion of pro-inflammatory cytokines such as IL-1β and TNF-α [9, 56] by these infiltrating immune cells further propagates the inflammatory response. These pro-inflammatory cytokines also stimulate lipolysis [57] and contribute to insulin resistance (discussed below), thus promoting dysfunction of adipose tissue. In addition to these effects within the adipose tissue, it is thought that spillover of inflammatory and metabolic signals from dysfunctional adipose tissue into the circulation may drive the progression of organ dysfunction and metabolic disease in other organs such as the liver and the vasculature [58]. Adipose tissue dysfunction and inflammation is thus widely considered to play a crucial role in obesity-associated metabolic inflammation and disease development [5, 6, 58-60].

Insulin resistance and type 2 diabetes

It is now generally accepted that (metabolic) inflammation can interfere with insulin signalling pathways in various tissues, leading to reduced insulin sensitivity and ultimately to development of insulin resistance and type 2 diabetes (T2D) [61]. Pro-inflammatory cytokines such as TNF-α and IL-1β are thought to interfere with insulin signalling downstream of the insulin receptor, thus making insulin target cells less sensitive to its effects [56, 62, 63]. This means that glucose is not properly cleared from the circulation, leading to increased levels of blood glucose (hyperglycaemia). Of note, recent observations indicate that this interplay between inflammatory cascades and insulin signalling is more complex than generally assumed [64] and show that aggravation of hepatic inflammation does not necessarily worsen insulin resistance [65]. Hyperglycaemia resulting from reduced glucose clearance is further exacerbated by inappropriately increased glucose release from the liver, resulting from the inability of insulin to suppress hepatic gluconeogenesis [66]. In the early stages of insulin resistance, the pancreatic beta cells increase insulin secretion in a compensatory attempt to lower circulating glucose levels. However, this compensation is lost in individuals with overt

type 2 diabetes due to beta cell dysfunction and depletion [67], causing glucose levels to rise uncontrollably.

There is a well-established relationship between increased adiposity – particularly in abdominal visceral fat depots – and reduced whole-body insulin sensitivity in obese subjects [68, 69]. Since the adipose tissue only removes a small fraction of plasma glucose, the expanded adipose tissue depots must also affect insulin sensitivity in other tissues such as skeletal muscle and liver, together resulting in reduced whole-body insulin sensitivity [66]. Rather than developing in parallel in different tissues, different organs may become insulin resistant at different stages of metabolic overload.

Non-alcoholic fatty liver disease
The liver is the primary organ for energy homeostasis as it plays a major role lipid and carbohydrate metabolism. In the fed state, dietary lipids (triglycerides and cholesterol) are absorbed and packed into triglyceride-rich chylomicrons in the intestine, which are transported to the blood through the lymphatic system. At peripheral sites, chylomicron-derived triglycerides are hydrolysed to allow uptake of free fatty acids for energy supply (skeletal muscle and heart) or storage (adipose tissue). The resulting chylomicron remnants (now triglyceride-depleted and cholesterol-enriched) are taken up by the liver where they are metabolised or stored. In the fasted state, the liver ensures the supply of triglycerides to peripheral organs through secretion of very low density lipoproteins (VLDL). The assembly of these triglyceride-rich particles is highly dependent of the availability of triglycerides within the hepatocyte, which may originate from: previously accumulated triglycerides within the hepatocyte; free fatty acids released from adipose tissue, re-esterified in the liver; or triglycerides synthesised in the liver from de novo synthesised free fatty acids. Similarly to chylomicrons, triglycerides from VLDL are hydrolysed at peripheral sites and the resulting VLDL remnants (cholesterol-enriched low-density lipoproteins: LDL) are cleared by the liver. Carbohydrates enter the circulation as glucose, after digestion of complex carbohydrates following a meal. Excess glucose is either converted into glycogen (the primary hepatic storage form of carbohydrates), or used as substrate for de novo lipogenesis. In the fasted state, the liver ensures adequate plasma glucose levels by releasing glucose from stored glycogen (glycogenolysis) or de novo synthesised glucose (gluconeogenesis) [70]. This central role of the liver in the regulation of metabolic homeostasis may make it particularly vulnerable to the effects of metabolic overload.

 The hepatic manifestation of metabolic overload and inflammation is non-alcoholic fatty liver

disease (NAFLD). This chronic liver disease encompasses a spectrum of liver pathologies that ranges from the clinically benign accumulation of lipids (simple steatosis) to the more progressive non-alcoholic steatohepatitis (NASH) which is characterised by hepatic inflammation and fibrosis in addition to hepatic steatosis [71]. The intrahepatocellular accumulation of lipids (mainly triglycerides, but also free fatty acids and cholesterol) in NAFLD is thought to be the result of increased dietary influx, peripheral insulin resistance (which increases free fatty acid flux from the adipose tissue) and increased hepatic de novo lipogenesis [72]. While triglycerides are considered a relatively "safe" storage form of lipids in the liver, it is the build-up of other lipid species such as free fatty acids, diglycerides, ceramides, and free cholesterol that is thought to provide a direct trigger of hepatic inflammation [73]. In addition, circulating factors released from dysfunctional adipose tissue have also been proposed to exert pro-inflammatory effects in the liver [74] and may thereby contribute to the progression of NAFLD. Continued hepatic inflammation then drives the development of hepatic fibrosis, through activation of hepatic stellate cells by pro-inflammatory mediators such as TNF-α and TGF-β, which stimulates their production of collagen [75].

Atherosclerosis

As the underlying cause of myocardial infarction, stroke and sudden cardiac death, atherosclerosis is the major underlying pathology of cardiovascular disease (CVD) [76]. Although atherosclerosis was initially considered a passive accumulation of cholesterol debris on the arterial wall, atherosclerosis is now recognised to be a chronic non-resolving inflammatory disease [77]. It is triggered by an interplay between endothelial dysfunction and subendothelial (intimal) low-density lipoprotein (LDL) retention, and occurs in medium-sized arteries at regions of disturbed blood flow (i.e. at bends or branch points) [78]. Various modifications (such as oxidation) of these retained lipoproteins are thought to mimic PAMPs or DAMPs, thereby triggering an inflammatory response. This leads to activation of endothelial cells and their expression of adhesion molecules. Together with the release of chemokines this attracts leukocytes (primarily monocyte-derived macrophages, but also neutrophils and other immune cells) that subsequently infiltrate the vascular wall and contribute to amplification and perpetuation of the inflammatory response [78].

Targets for intervention in metabolic inflammation

Obviously, lifestyle interventions that focus on reduction of metabolic overload (e.g. restriction of food intake) may at least partly prevent metabolic inflammation and development of metabolic diseases. However, such lifestyle changes are difficult to achieve in the long run,

which urges the development of therapeutics to combat these disorders. The major challenge in the field of metabolic disease is to prevent, dampen, or resolve the metabolic inflammatory response that is the driving force of metabolic disease development (both initiation and progression). This may be achievable by interventions targeted to: A) prevent metabolic overload by changing the macronutrient composition of the diet to prevent nutrient excess, B) inhibit sensing of metabolic overload (i.e. at the level of translation of metabolic to inflammatory signal), C) reduce amplification of the early metabolic inflammatory response, D) stimulate resolution of inflammation to prevent development of chronic inflammatory responses. Herein, we investigated several routes of intervention in metabolic inflammation using both pharmaceutical and nutraceutical approaches, to assess their value in the attenuation of metabolic disease development focusing on NAFLD and atherosclerosis as main disease endpoints.

Aim and outline of this thesis

Although it is considered to be of great importance in the development of obesity-related diseases such as NAFLD and atherosclerosis, much remains unknown about the origin and mechanisms of metabolic overload and inflammation. The aim of this thesis was to further our understanding of metabolic inflammation and investigate the effects of interventions targeted to different aspects of metabolic inflammation on the development of disease endpoints. First, we aimed to unravel the contribution of different organs (liver and adipose tissue) to the development of metabolic inflammation and disease (**chapter 2**). In this chapter we explored the sequence of inflammatory events in adipose tissue and liver during metabolic overload in a longitudinal study in high-fat diet (HFD)-fed C57BL/6J mice, and investigated the contribution of adipose tissue- and liver inflammation to systemic metabolic inflammation and insulin resistance. We then sought evidence for a causal role of inflamed adipose tissue in the development of NAFLD in **chapter 3**. Using HFD-fed C57BL/6J mice, we studied the development of metabolic inflammation in several (visceral) adipose tissue depots and investigated whether surgical removal of inflamed white adipose tissue may reduce hepatic inflammation and thereby attenuate progression of NAFLD to NASH. Next, we studied interventions targeted to a specific factor in metabolic inflammation and investigated whether these may affect metabolic disease development. In **chapter 4** this was the NLRP3 inflammasome, i.e. the sensing of metabolic overload, in which we intervened using a caspase-1 inhibitor. For this we treated HFD-fed LDLr-/-.Leiden mice with a caspase-1 inhibitor in a

therapeutic study protocol, and investigated its effects on adipose tissue inflammation, insulin resistance and hepatic steatosis, inflammation and fibrosis. We then evaluated distinct nutritional strategies to prevent metabolic inflammation and disease, either by changing the macronutrient composition of the diet to reduce metabolic overload, or by adding potentially anti-inflammatory nutrients to the diet. In **chapter 5** we investigated whether replacement of dietary saturated fat with pumpkin seed oil (rich in unsaturated fat) would reduce NAFLD and atherosclerosis development and questioned whether potentially bioactive phytochemicals present only in unrefined pumpkin seed oil may have additional beneficial effects on top of those of the refined oil. For this we fed ApoE*3Leiden mice a cholesterol-containing Western-type diet, in which we replaced part of the saturated fat in this diet (cocoa butter) with either refined or virgin pumpkin seed oil and studied the effects of these interventions on NAFLD and atherosclerosis development. To gain more insight into the potential health effects of phytochemicals, we conducted two studies which either focused on metabolic inflammation in liver during NASH development or metabolic inflammation in vasculature during atherosclerosis development. In **chapter 6** we evaluated the effects of a mixture of phytochemicals (bilberry extract) on the development of NASH and hepatic fibrosis in Western-type diet fed ApoE*3Leiden mice, specifically focusing on the role of cholesterol as an inducer of hepatic inflammation. In **chapter 7** we studied the potential of the phytochemical (-)-epicatechin to prevent metabolic inflammation and atherosclerosis development. We studied the potential anti-inflammatory and anti-atherosclerotic effects of this phytochemical in Western-type diet fed ApoE*3Leiden mice and performed additional mechanistic studies of its anti-inflammatory potential in diet-induced inflammation in human-CRP transgenic mice and NFκB-luciferase reporter mice. Finally, in **chapter 8**, we evaluated a conceptually different strategy to attenuate metabolic inflammation, namely targeting resolution of inflammation using an SPM (Resolvin E1) with particular emphasis on vascular inflammation and atherosclerosis development, using a therapeutic study protocol in Western-type diet fed ApoE*3Leiden mice. The results obtained in these studies and their implications are discussed in **chapter 9**.

References

1. World Health Organization. Fact sheet Obesity and overweight [updated January 2015]. Available from: www.who.int/mediacentre/factsheets/fs311/en/.

2. St-Onge MP, Heymsfield SB. Overweight and obesity status are linked to lower life expectancy. Nutr Rev. 2003;61(9):313-6. doi:10.1301/nr.2003.sept.313-316.

3. de Gonzalez AB, Hartge P, Cerhan JR, Flint AJ,

Hannan L, MacInnis RJ, et al. Body-mass index and mortality among 1.46 million white adults. N Engl J Med. 2010;363(23):2211-9. doi:10.1056 /NEJMoa1000367.

4. Haslam DW, James WPT. Obesity. Lancet. 2005;366(9492):1197-209. doi:10.1016/S0140-6736(05)67483-1.

5. Hotamisligil GS. Inflammation and metabolic disorders. Nature. 2006;444(7121):860-7. doi:10.1038/nature05485.

6. Lumeng CN, Saltiel AR. Inflammatory links between obesity and metabolic disease. J Clin Invest. 2011;121(6):2111-7. doi: 10.1172/JCI57132.

7. Dandona P, Weinstock R, Thusu K, Abdel-Rahman E, Aljada A, Wadden T. Tumor necrosis factor-α in sera of obese patients: fall with weight loss. J Clin Endocrinol Metab. 1998;83(8):2907-10. doi:10.1210 /jcem.83.8.5026.

8. Zhao Y, He X, Shi X, Huang C, Liu J, Zhou S, et al. Association between serum amyloid A and obesity: A meta-analysis and systematic review. Inflamm Res. 2010;59(5):323-34. doi:10.1007/s00011-010-0163-y.

9. Hotamisligil GS, Shargill S, Spiegelman BM. Adipose expression of tumor necrosis factor-α: Direct role in obesity-linked insulin resistance. Science. 1993;259(5091):87-91. doi:10.2307/2880244.

10. Gregor MF, Hotamisligil GS. Inflammatory mechanisms in obesity. Annu Rev Immunol. 2011;29:415-45. doi:10.1146/annurev-immunol-031210-101322.

11. Jin C, Flavell RA. Innate sensors of pathogen and stress: Linking inflammation to obesity. J Allergy Clin Immunol. 2013;132(2):287-94. doi:10.1016 /j.jaci.2013.06.022.

12. Medzhitov R. Toll-like receptors and innate immunity. Nature Reviews Immunology. 2001;1(2) :135. doi:10.1038/35100529.

13. Lin Y, Lee H, Berg AH, Lisanti MP, Shapiro L, Scherer PE. The lipopolysaccharide-activated toll-like receptor (TLR)-4 induces synthesis of the closely related receptor TLR-2 in adipocytes. J Biol Chem. 2000;275(32):24255-63. doi:10.1074/jbc. M002137200.

14. Bès-Houtmann S, Roche R, Hoareau L, Gonthier M-P, Festy F, Caillens H, et al. Presence of functional TLR2 and TLR4 on human adipocytes. Histochem Cell Biol. 2007;127(2):131-7. doi:10.1007/s00418-006-0230-1.

15. Li L, Chen L, Hu L, Liu Y, Sun H-Y, Tang J, et al. Nuclear factor high-mobility group box1 mediating the activation of toll-like receptor 4 signaling in hepatocytes in the early stage of nonalcoholic fatty liver disease in mice. Hepatology. 2011;54(5):1620-30. doi:10.1002/hep.24552.

16. Matsumura T, Degawa T, Takii T, Hayashi H, Okamoto T, Inoue J-i, et al. TRAF6-NF-κB pathway is essential for interleukin-1-induced TLR2 expression and its functional response to TLR2 ligand in murine hepatocytes. Immunology. 2003;109(1):127-36. doi:10.1046/j.1365-2567.2003 .01627.x.

17. Huang S, Rutkowsky JM, Snodgrass RG, Ono-Moore KD, Schneider DA, Newman JW, et al. Saturated fatty acids activate TLR-mediated proinflammatory signaling pathways. J Lipid Res. 2012;53(9):2002-13. doi: 10.1194/jlr.D029546.

18. Snodgrass RG, Huang S, Choi I-W, Rutledge JC, Hwang DH. Inflammasome-mediated secretion of IL-1β in human monocytes through TLR2 activation; Modulation by dietary fatty acids. J Immunol. 2013;191(8):4337-47. doi:10.4049 /jimmunol.1300298.

19. Shi H, Kokoeva MV, Inouye K, Tzameli I, Yin H, Flier JS. TLR4 links innate immunity and fatty acid–induced insulin resistance. J Clin Invest. 2006;116 (11):3015-25. doi:10.1172/JCI28898.

20. Fischer H, Ellström P, Ekström K, Gustafsson L, Gustafsson M, Svanborg C. Ceramide as a TLR4 agonist; a putative signalling intermediate between sphingolipid receptors for microbial ligands and TLR4. Cell Microbiol. 2007;9(5):1239-51. doi: 10.1111/j.1462-5822.2006.00867.x.

21. Chávez-Sánchez L, Garza-Reyes MG, Espinosa-Luna JE, Chávez-Rueda K, Legorreta-Haquet MV, Blanco-Favela F. The role of TLR2, TLR4 and CD36 in macrophage activation and foam cell formation in response to oxLDL in humans. Hum Immunol. 2014;75(4):322-9. doi:10.1016/j.humimm.2014.01 .012.

22. Yang K, Zhang XJ, Cao LJ, Liu XH, Liu ZH, Wang XQ, et al. Toll-like receptor 4 mediates inflammatory cytokine secretion in smooth muscle cells induced by oxidized low-density lipoprotein. PLoS One. 2014;9(4):e95935. doi:10.1371/journal .pone.0095935.

23. Könner AC, Brüning JC. Toll-like receptors: Linking inflammation to metabolism. Trends Endocrinol Metab. 2011;22(1):16-23. doi:10.1016/j.tem.2010 .08.007.

24. Tsukumo DML, Carvalho-Filho MA, Carvalheira JBC, Prada PO, Hirabara SM, Schenka AA, et al.

Loss-of-function mutation in toll-like receptor 4 prevents diet-induced obesity and insulin resistance. Diabetes. 2007;56(8):1986-98. doi:10.2337/db06-1595.

25. Kuo LH, Tsai PJ, Jiang MJ, Chuang YL, Yu L, Lai KTA, et al. Toll-like receptor 2 deficiency improves insulin sensitivity and hepatic insulin signalling in the mouse. Diabetologia. 2011;54(1):168-79. doi:10.1007/s00125-010-1931-5.

26. Latz E, Xiao TS, Stutz A. Activation and regulation of the inflammasomes. Nature Reviews Immunology. 2013;13(6):397-411. doi:10.1038/nri3452.

27. Csak T, Ganz M, Pespisa J, Kodys K, Dolganiuc A, Szabo G. Fatty acid and endotoxin activate inflammasomes in mouse hepatocytes that release danger signals to stimulate immune cells. Hepatology. 2011;54(1):133-44. doi:10.1002/hep.24341.

28. Stienstra R, Joosten LA, Koenen T, van Tits B, van Diepen JA, van den Berg SA, et al. The inflammasome-mediated caspase-1 activation controls adipocyte differentiation and insulin sensitivity. Cell Metab. 2010;12(6):593-605. doi:10.1016/j.cmet.2010.11.011.

29. Wen H, Gris D, Lei Y, Jha S, Zhang L, Huang MT, et al. Fatty acid-induced NLRP3-ASC inflammasome activation interferes with insulin signaling. Nat Immunol. 2011;12(5):408-15. doi:10.1038/ni.2022.

30. Vandanmagsar B, Youm YH, Ravussin A, Galgani JE, Stadler K, Mynatt RL, et al. The NLRP3 inflammasome instigates obesity-induced inflammation and insulin resistance. Nat Med. 2011;17(2):179-88. doi:10.1038/nm.2279.

31. Duewell P, Kono H, Rayner KJ, Sirois CM, Vladimer G, Bauernfeind FG, et al. NLRP3 inflammasomes are required for atherogenesis and activated by cholesterol crystals. Nature. 2010;464(7293):1357-61. doi:10.1038/nature08938.

32. Rajamäki K, Lappalainen J, Öörni K, Välimäki E, Matikainen S, Kovanen PT, et al. Cholesterol crystals activate the NLRP3 inflammasome in human macrophages: A novel link between cholesterol metabolism and inflammation. PLoS One. 2010;5(7):e11765. doi:10.1371/journal.pone.0011765.

33. Guo H, Callaway JB, Ting JPY. Inflammasomes: Mechanism of action, role in disease, and therapeutics. Nat Med. 2015;21(7):677-87. doi:10.1038/nm.3893.

34. Stienstra R, Tack CJ, Kanneganti TD, Joosten LA, Netea MG. The inflammasome puts obesity in the danger zone. Cell Metab. 2012;15(1):10-8. doi:10.1016/j.cmet.2011.10.011.

35. Hotamisligil GS, Erbay E. Nutrient sensing and inflammation in metabolic diseases. Nature Reviews Immunology. 2008;8(12):923-34. doi:10.1038/nri2449.

36. Baker RG, Hayden MS, Ghosh S. NF-κB, inflammation, and metabolic disease. Cell Metab. 2011;13(1):11-22. doi:10.1016/j.cmet.2010.12.008.

37. Tornatore L, Thotakura AK, Bennett J, Moretti M, Franzoso G. The nuclear factor kappa B signaling pathway: Integrating metabolism with inflammation. Trends Cell Biol. 2012;22(11):557-66. doi:10.1016/j.tcb.2012.08.001.

38. Solinas G, Karin M. JNK1 and IKKβ: Molecular links between obesity and metabolic dysfunction. FASEB J. 2010;24(8):2596-611. doi:10.1096/fj.09-151340.

39. Hayden MS, Ghosh S. Shared principles in NF-κB signaling. Cell. 2008;132(3):344-62. doi:10.1016/j.cell.2008.01.020.

40. Abbas AK, Lichtman AH, Pillai S. Cellular and molecular immunology. 7th ed. ed. Philadelphia: Saunders Elsevier; 2011.

41. Soehnlein O, Lindbom L. Phagocyte partnership during the onset and resolution of inflammation. Nature Reviews Immunology. 2010;10(6):427-39. doi:10.1038/nri2779.

42. Amulic B, Cazalet C, Hayes GL, Metzler KD, Zychlinsky A. Neutrophil function: from mechanisms to disease. Annu Rev Immunol. 2012;30(1):459-89. doi:10.1146/annurev-immunol-020711-074942.

43. Döring Y, Drechsler M, Soehnlein O, Weber C. Neutrophils in atherosclerosis: from mice to man. Arterioscler Thromb Vasc Biol. 2015;35(2):288-95. doi:10.1161/atvbaha.114.303564.

44. Xu R, Huang H, Zhang Z, Wang FS. The role of neutrophils in the development of liver diseases. Cellular and Molecular Immunology. 2014;11(3):224-31. doi:10.1038/cmi.2014.2.

45. McNelis JC, Olefsky JM. Macrophages, immunity, and metabolic disease. Immunity. 2014;41(1):36-48. doi:10.1016/j.immuni.2014.05.010.

46. Serhan CN. Pro-resolving lipid mediators are leads for resolution physiology. Nature. 2014;510(7503):92-101. doi:10.1038/nature13479.

47. Serhan CN, Chiang N, Van Dyke TE. Resolving inflammation: dual anti-inflammatory and pro-resolution lipid mediators. Nature Reviews

Immunology. 2008;8(5):349-61. doi:10.1038/nri2294.

48. Headland SE, Norling LV. The resolution of inflammation: Principles and challenges. Semin Immunol. 2015;27(3):149-60. doi:10.1016/j.smim.2015.03.014.

49. Gilroy D, De Maeyer R. New insights into the resolution of inflammation. Semin Immunol. 2015;27(3):161-8. doi:10.1016/j.smim.2015.05.003.

50. Spite M, Clària J, Serhan Charles N. Resolvins, specialized proresolving lipid mediators, and their potential roles in metabolic diseases. Cell Metab. 2014;19(1):21-36. doi:10.1016/j.cmet.2013.10.006.

51. Virtue S, Vidal-Puig A. Adipose tissue expandability, lipotoxicity and the metabolic syndrome — An allostatic perspective. Biochim Biophys Acta. 2010;1801(3):338-49. doi:10.1016/j.bbalip.2009.12.006.

52. Lafontan M. Adipose tissue and adipocyte dysregulation. Diabetes Metab. 2014;40(1):16-28. doi:10.1016/j.diabet.2013.08.002.

53. Weisberg SP, McCann D, Desai M, Rosenbaum M, Leibel RL, Ferrante AW, Jr. Obesity is associated with macrophage accumulation in adipose tissue. J Clin Invest. 2003;112(12):1796-808. doi:10.1172/JCI19246.

54. McNelis Joanne C, Olefsky Jerrold M. Macrophages, Immunity, and Metabolic Disease. Immunity. 41(1):36-48. doi:10.1016/j.immuni.2014.05.010.

55. Cinti S, Mitchell G, Barbatelli G, Murano I, Ceresi E, Faloia E, et al. Adipocyte death defines macrophage localization and function in adipose tissue of obese mice and humans. J Lipid Res. 2005;46(11):2347-55. doi:10.1194/jlr.M500294-JLR200.

56. Jager J, Grémeaux T, Cormont M, Le Marchand-Brustel Y, Tanti J-F. Interleukin-1β-induced insulin resistance in adipocytes through down-regulation of insulin receptor substrate-1 expression. Endocrinology. 2007;148(1):241-51. doi:10.1210/en.2006-0692.

57. Grant RW, Stephens JM. Fat in flames: influence of cytokines and pattern recognition receptors on adipocyte lipolysis. American Journal of Physiology - Endocrinology and Metabolism. 2015;309(3):E205-E13. doi: 10.1152/ajpendo.00053.2015.

58. Klöting N, Blüher M. Adipocyte dysfunction, inflammation and metabolic syndrome. Reviews in Endocrine and Metabolic Disorders. 2014;15(4):277-87. doi:10.1007/s11154-014-9301-0.

59. Osborn O, Olefsky JM. The cellular and signaling networks linking the immune system and

metabolism in disease. Nat Med. 2012;18(3):363-74. doi:10.1038/nm.2627.

60. Grant RW, Dixit VD. Adipose tissue as an immunological organ. Obesity. 2015;23(3):512-8. doi:10.1002/oby.21003.

61. Dandona P, Aljada A, Bandyopadhyay A. Inflammation: the link between insulin resistance, obesity and diabetes. Trends Immunol. 2004;25(1):4-7. doi:10.1016/j.it.2003.10.013.

62. Uysal KT, Wiesbrock SM, Marino MW, Hotamisligil GS. Protection from obesity-induced insulin resistance in mice lacking TNF-alpha function. Nature. 1997;389(6651):610-4. doi: 10.1038/39335.

63. Wellen KE, Hotamisligil GS. Inflammation, stress, and diabetes. J Clin Invest. 2005;115(5):1111-9. doi:10.1172/JCI25102.

64. Gruben N, Shiri-Sverdlov R, Koonen DPY, Hofker MH. Nonalcoholic fatty liver disease: A main driver of insulin resistance or a dangerous liaison? Biochimica et Biophysica Acta (BBA) - Molecular Basis of Disease. 2014;1842(11):2329-43. doi: 10.1016/j.bbadis.2014.08.004.

65. Aparicio-Vergara M, Hommelberg PPH, Schreurs M, Gruben N, Stienstra R, Shiri-Sverdlov R, et al. Tumor necrosis factor receptor 1 gain-of-function mutation aggravates nonalcoholic fatty liver disease but does not cause insulin resistance in a murine model. Hepatology. 2013;57(2):566-76. doi: 10.1002/hep.26046.

66. Gardner DG, Shoback DM, Greenspan FS. Greenspan's basic & clinical endocrinology. 9th ed. ed. New York: McGraw-Hill Medical; 2011.

67. Meier JJ, Bonadonna RC. Role of reduced β-Cell mass versus impaired β-Cell function in the pathogenesis of type 2 diabetes. Diabetes Care. 2013;36(Supplement 2):S113-S9. doi:10.2337/dcS13-2008.

68. Evans DJ, Hoffman RG, Kalkhoff RK, Kissebah AH. Relationship of body fat topography to insulin sensitivity and metabolic profiles in premenopausal women. Metabolism. 1984;33(1):68-75. doi:10.1016/0026-0495(84)90164-1.

69. Abate N, Garg A, Peshock RM, Stray-Gundersen J, Grundy SM. Relationships of generalized and regional adiposity to insulin sensitivity in men. J Clin Invest. 1995;96(1):88-98. doi:10.1172/JCI118083.

70. Campbell I. Liver: metabolic functions. Anaesthesia and Intensive Care Medicine. 2006;7(2):51-4. doi:10.1383/anes.2006.7.2.51.

71. Rinella ME. Nonalcoholic fatty liver disease: A

systematic review. J Am Med Assoc. 2015;313(22):2263-73. doi:10.1001/jama.2015.5370.

72. Tilg H, Moschen AR. Evolution of inflammation in nonalcoholic fatty liver disease: The multiple parallel hits hypothesis. Hepatology. 2010;52(5):1836-46. doi:10.1002/hep.24001.

73. Alkhouri N, Dixon LJ, Feldstein AE. Lipotoxicity in nonalcoholic fatty liver disease: not all lipids are created equal. Expert Rev Gastroenterol Hepatol. 2009;3(4):445-51. doi:10.1586/egh.09.32.

74. Tordjman J, Guerre-Millo M, Clément K. Adipose tissue inflammation and liver pathology in human obesity. Diabetes Metab. 2008;34(6, Part 2):658-63. doi:10.1016/S1262-3636(08)74601-9.

75. Fujii H, Kawada N. Inflammation and fibrogenesis in steatohepatitis. J Gastroenterol. 2012;47(3):215-25. doi:10.1007/s00535-012-0527-x.

76. Lusis AJ. Atherosclerosis. Nature. 2000;407(6801):233-41. doi:10.1038/35025203.

77. Tabas I. Macrophage death and defective inflammation resolution in atherosclerosis. Nature Reviews Immunology. 2010;10(1):36-46. doi:10.1038/nri2675.

78. Tabas I, García-Cardeña G, Owens GK. Recent insights into the cellular biology of atherosclerosis. J Cell Biol. 2015;209(1):13-22. doi:10.1083/jcb.201412052.

High-fat diet induced obesity primes inflammation in adipose tissue prior to liver in C57BL/6j mice

Roel A van der Heijden[1,*], Fareeba Sheedfar[2,5,*], Martine C Morrison[3], Pascal PH Hommelberg[2], Danny Kor[1], Niels J Kloosterhuis[2], Nanda Gruben[2], Sameh A Youssef[4], Alain de Bruin[2,4], Marten H Hofker[1], Robert Kleemann[3], Debby PY Koonen[2,*], and Peter Heeringa[1,*]

[1]University of Groningen, University Medical Center Groningen, Department of Pathology and Medical Biology, Section Medical Biology, Groningen, The Netherlands;
[2]University of Groningen, University Medical Center Groningen, Department of Pediatrics, Section Molecular Genetics, Groningen, The Netherlands;
[3]Department of Metabolic Health Research, Netherlands Organization for Applied Scientific Research (TNO), Leiden, The Netherlands;
[4]Dutch Molecular Pathology Center, Department of Pathobiology, Faculty of Veterinary Medicine, Utrecht University, Utrecht, The Netherlands;
[5]Radboud University Medical Center, Department of Physiology, Nijmegen, The Netherlands
* These authors contributed equally.

Abstract: Metabolic inflammation in adipose tissue and the liver is frequently observed as a result of diet-induced obesity in human and rodent studies. Although the adipose tissue and the liver are both prone to become chronically inflamed with prolonged obesity, their individual contribution to the development of metabolic inflammation remains speculative. Thus, we aimed to elucidate the sequence of inflammatory events in adipose and hepatic tissues to determine their contribution to the development of metabolic inflammation and insulin resistance (IR) in diet-induced obesity. To confirm our hypothesis that adipose tissue (AT) inflammation is initiated prior to hepatic inflammation, C57BL/6J male mice were fed a low-fat diet (LFD; 10% kcal fat) or high-fat diet (HFD; 45% kcal fat) for either 24, 40 or 52 weeks. Lipid accumulation and inflammation was measured in AT and liver. Glucose tolerance was assessed and plasma levels of glucose, insulin, leptin and adiponectin were measured at various time points throughout the study. With HFD, C57BL/6j mice developed a progressive obese phenotype, accompanied by IR at 24 and 40 weeks of HFD, but IR was attenuated after 52 weeks of HFD. AT inflammation was present after 24 weeks of HFD, as indicated by the increased presence of crown-like structures and up-regulation of pro-inflammatory genes *Tnf, Il1β, Mcp1* and *F4/80*. As hepatic inflammation was not detected until 40 weeks of HFD, we show that AT inflammation is established prior to the development of hepatic inflammation. Thus, AT inflammation is likely to have a greater contribution to the development of IR compared to hepatic inflammation.

INTRODUCTION

Obesity and associated metabolic disorders like insulin resistance (IR), type 2 diabetes (T2D) and non-alcoholic fatty liver disease (NAFLD) are marked by a state of inflammation initiated by nutrient overload [1]. Metabolic inflammation in obesity, in contrast to the classical immune response to injury or infection, is modest and without apparent resolution over time [1]. Although it is well established that metabolic

inflammation disrupts cellular metabolism and impairs insulin signalling in metabolically active tissues, the underlying mechanisms are as yet ill-defined [2].

Adipose tissue (AT) is an important site of inflammatory events in obesity. It contains various cell types that all contribute to the inflammatory response during obesity. In addition to regulating fat mass and nutrient homeostasis, adipocytes mediate the inflammatory response through the secretion of adipokines, cytokines, and chemokines that enhance the recruitment of immune cells, especially macrophages, to the AT [3]. These AT macrophages (ATMs) are a major source of pro-inflammatory cytokines and chemokines and once activated can propagate the inflammatory state and interfere with insulin sensitivity in insulin target cells [4]. Although, prolonged nutrient overload results in metabolic inflammation associated with adipocyte expansion and dysfunction, metabolic inflammation in obesity is not restricted to the AT; the liver is also a strong contributor to the development of this type of inflammation [5–7]. Indeed, the production of pro-inflammatory cytokines secreted by resident macrophages in the liver is linked to disruption of hepatic insulin signalling [8]. Consistent with this, enhanced expression of inflammatory genes in the liver following high-fat diet (HFD) feeding is associated with reduced insulin sensitivity in mice [9,10]. Thus, metabolic inflammation in both organs is associated with the development of IR. However, what tissue provides the main contribution to the development of IR remains unknown.

Few studies have addressed the temporal relationship between AT and liver inflammation in the etiology of IR. Nevertheless, it is generally accepted that AT is an important initiator of the inflammatory response to obesity [4,11], engaging in crosstalk with the liver to affect liver metabolism and IR [12,13]. On the contrary, others have shown that this crosstalk in the development of HFD-induced metabolic derangements is bidirectional [14,15]. Furthermore, hepato-specific targeting of endoplasmatic reticulum stress was associated with decreased obesity and AT inflammation in *ob/ob* mice [14], underscoring the existence of crosstalk between the liver and the AT in obesity. The sequence of inflammatory processes in adipose and hepatic tissues in respect to the development of IR thus represents a topic of debate.

This study aims to elucidate the initiation and sequence of inflammatory events in the adipose and hepatic tissues in obesity, and to determine the contribution of these individual inflammatory processes to the overall development of metabolic inflammation and IR. We

hypothesize that liver inflammation comes secondary to adipose tissue inflammation and is of lesser importance to the development of metabolic inflammation and IR in diet-induced obesity.

RESULTS

Body weight gain stabilizes after prolonged HFD-feeding in mice

Body weight and AT mass were measured in mice fed a LFD and HFD for 24, 40 and 52 weeks, at the age of 36, 52 and 64 weeks respectively (Fig. 1A) to assess the development of obesity over time. As expected, we observed a rapid increase in body weight in mice fed a HFD, which was significant from 12 weeks following a diet onwards (Fig. 1B). Body weight gradually increased between mice fed a HFD for 24 weeks and 40 weeks (Fig. 1B; $p<0.001$) and remained at the same level in mice fed a HFD for 52 weeks compared to HFD for 40 weeks (Fig. 1B). In addition, weights of the mesenteric, gonadal/epidydimal and perirenal fat depots were significantly increased in mice fed a HFD for 24, 40 and 52 weeks as compared to their age-matched LFD controls (Fig. 1C-E). We observed no difference in all three fat depots between mice fed a HFD for 24, 40 or 52 weeks (Fig. 1C-E), suggesting a steady degree of adiposity following its initial establishment. Liver weight was significantly higher in mice fed a HFD for 24, 40 and 52 weeks as compared to LFD controls (Fig. 1F).

Improved insulin sensitivity upon prolongation of HFD-feeding in mice

Since obesity is associated with IR, we next monitored insulin sensitivity in mice fed a HFD for 24, 40, and 52 weeks. In mice fed a HFD at all points in time the fasted glucose levels were not affected (Fig. 2A), but fasted insulin levels in mice fed a HFD for 24 and 40 weeks were significantly elevated (Fig. 2B), suggesting a reduction in insulin sensitivity in these mice. Furthermore, we performed an oral glucose tolerance test (OGTT) and measured glucose and insulin levels simultaneously during the OGTT. At 24 weeks of HFD feeding, glucose tolerance was negatively affected, as evidenced by elevated glucose levels during the OGTT (Fig. 2D; $p<0.01$ at $t=90$ and $p<0.05$ at $t=120$, Suppl. 1A; $p<0.05$) when compared to age-matched LFD controls. Furthermore, insulin levels were significantly increased in 24-week HFD fed mice compared to age-matched LFD controls (Fig. 2D, Suppl. 1B), confirming the existence of IR at this point in time. Whole-body glucose tolerance was also significantly impaired in mice fed a HFD for 40 weeks, as mice displayed elevated insulin levels during the OGTT (Fig. 2E,
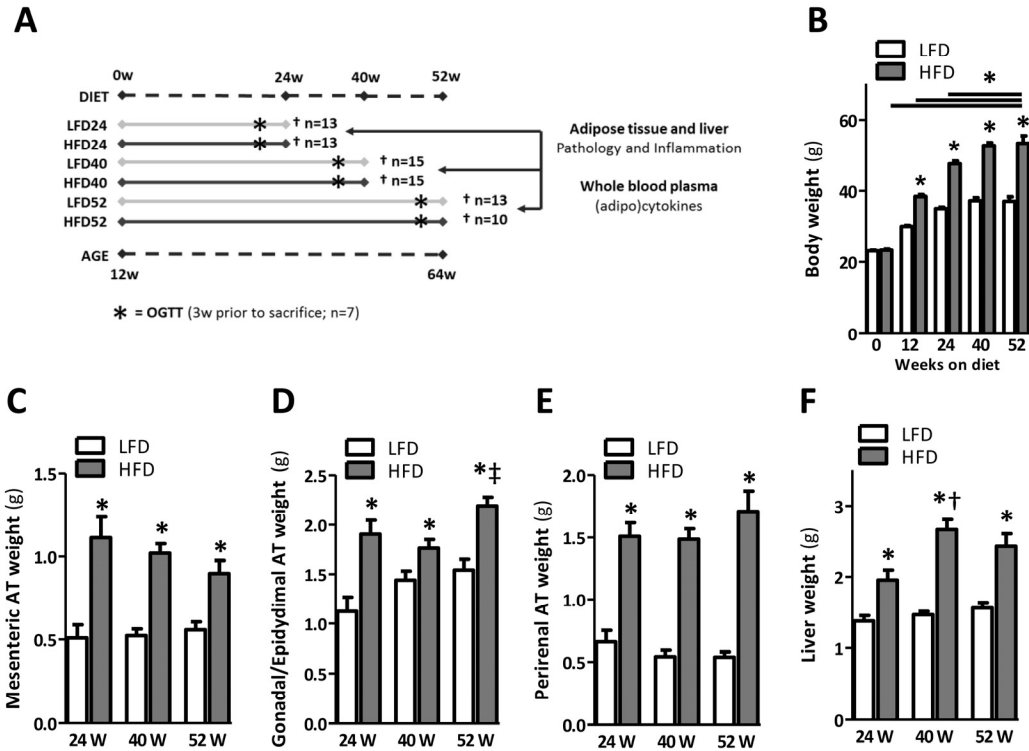
Figure 1. Prolonged HFD-feeding leads to obesity and organ adiposity. (**A**) Experimental design. (**B**) Body weights of mice fed a LFD and HFD shown at the start and at 12, 24, 40 and 52 weeks after a HFD. (**C**) Mesenteric, (**D**) gonadal/epididimal and (**E**) perirenal fat depots weights. (**F**) Liver weight measured upon sacrifice at 24, 40 and 52 weeks. Values shown are means ± SEM (n = 10-15 mice/group). Significance level set at p<0.05. *=significant from LFD at same time point, †=significant from same diet 24w, ‡=significant from same diet 40w.

Suppl. 1B), whereas blood glucose levels remained stable (Fig. 2E, Suppl. 1A). In contrast, we observed no signs of apparent glucose intolerance in mice fed a HFD for 52 weeks, as glucose levels did not differ (Fig. 2F, Suppl. 1A) and plasma insulin was significantly increased only after 15 min following gavage (Fig. 2F, Suppl. 1B). In support of the glucose tolerance data, homeostasis model assessment of IR (HOMA-IR) showed values to be significantly higher in the 24- and 40-week HFD-fed mice as compared to their age-matched LFD controls (Fig. 2C); this suggests a state of IR in mice fed a HFD for 24 and 40 weeks. HOMA-IR was not increased in mice fed a HFD for 52 weeks, confirming the absence of IR in these mice (Fig. 2C).

Inflammation in AT is apparent at 24 weeks of HFD feeding

Hematoxylin and Eosin (H&E) staining of gonadal (epididimal) fat tissues (Fig. 3A) suggested an increased

adipocyte size in mice fed the HFD. The number of cells per mm^2 was significantly reduced by 24, 40, and 52 weeks of HFD-feeding, confirming an increased adipocyte size when compared to LFD age-matched controls (Fig. 3B). Furthermore, crown-like structures (CLS), representing an accumulation of macrophages around dead adipocytes, were apparent in AT samples of mice fed a HFD for 24, 40 and 52 weeks (Fig. 3A, insets). Scoring of CLS confirmed a significant difference to exist between LFD and HFD mice for every time point (Fig. 3C). To confirm the presence of AT inflammation, we next assessed the expression of various inflammatory genes. Indeed, the gene expression levels of the pro-inflammatory cytokine *Tnf* (Fig. 3D) and the genes encoding for proteins involved in macrophage infiltration, *Mcp1* and *F4/80* (Fig. 3E-G), were significantly elevated in the adipose tissue of 24-, 40- and 52-weeks HFD mice compared to LFD mice. *Il1β* was only significantly elevated in HFD mice at the 40-weeks time point (Fig. 3E). Besides these pro-

inflammatory genes, the anti-inflammatory gene *Il-10* was significantly elevated in the AT of HFD mice at 24 and 40 weeks (Fig. 3H). Furthermore, we observed a decrease in *Tnf* and *F4/80* expression in 52-weeks HFD fed mice compared to mice fed a HFD for 40 weeks (Fig. 3D, *Tnf*; p<0.05 and Fig. 3G, *F4/80*; p<0.05), whereas *Il-10* expression increased over time in LFD mice (Fig. 3H, 52-weeks LFD *vs* 24-weeks LFD: p<0.001; 52-weeks LFD *vs* 40-weeks LFD: p<0.05).

Hepatic inflammation gradually develops over time in mice fed a HFD

H&E staining of liver slides (Fig. 4A) indicated the presence of HFD-induced hepatic steatosis from 24 weeks onwards, which was confirmed by a significant elevation in the amount of neutral lipids in the liver (TG; Fig. 4B). Histopathological examination of liver sections showed an increase in steatosis grade at 52 weeks as compared to 24 weeks of HFD-feeding (Fig. 4C; p<0.05), suggesting a progression in the accumulation of hepatic lipids over time. Although prolonged HFD-feeding significantly increased the percentage of microvesicular steatosis over macro-vesicular steatosis, it did not differ over time (Fig. 4D).

Furthermore, we observed a significant increase in the NAFLD activity score (NAS) (Fig. 4E), the number of inflammatory foci (Fig. 4F) and hepatocellular ballooning (Fig. 4G) for all HFD groups as compared to LFD groups. In line with a progression in steatosis grade, we also observed an increase in both the NAS score (Fig. 4E; p<0.05) and the number of inflammatory foci (Fig. 4F; p<0.001) in mice fed a HFD for 40 weeks as compared to the 24-weeks HFD group. To further investigate inflammation we measured the expression of pro- and anti-inflammatory cytokines (*Tnf, Il1ß, Il-10*) and macrophage markers (*Mcp1, F4/80*) in the liver. *Tnf, Il1ß, Il-10, Mcp1, and F4/80* expression was significantly upregulated at 40 weeks of HFD-feeding but not 24 weeks of HFD-feeding compared to mice fed the LFD. Furthermore, no difference was observed in expression level of *Tnf, Mcp1* and *Il-10* at 52 weeks of HFD-feeding, whereas *Il1ß* and *F4/80* were still significantly elevated at this time point (Fig. 4H-L). In addition, *Mcp1* expression was significantly reduced in HFD52 mice compared to HFD40 mice (Fig 4I). We also observed an age-related decline in *F4/80* expression as represented by a significant reduction in *F4/80* in LFD52 mice compared to LFD24 mice (Fig. 4K).
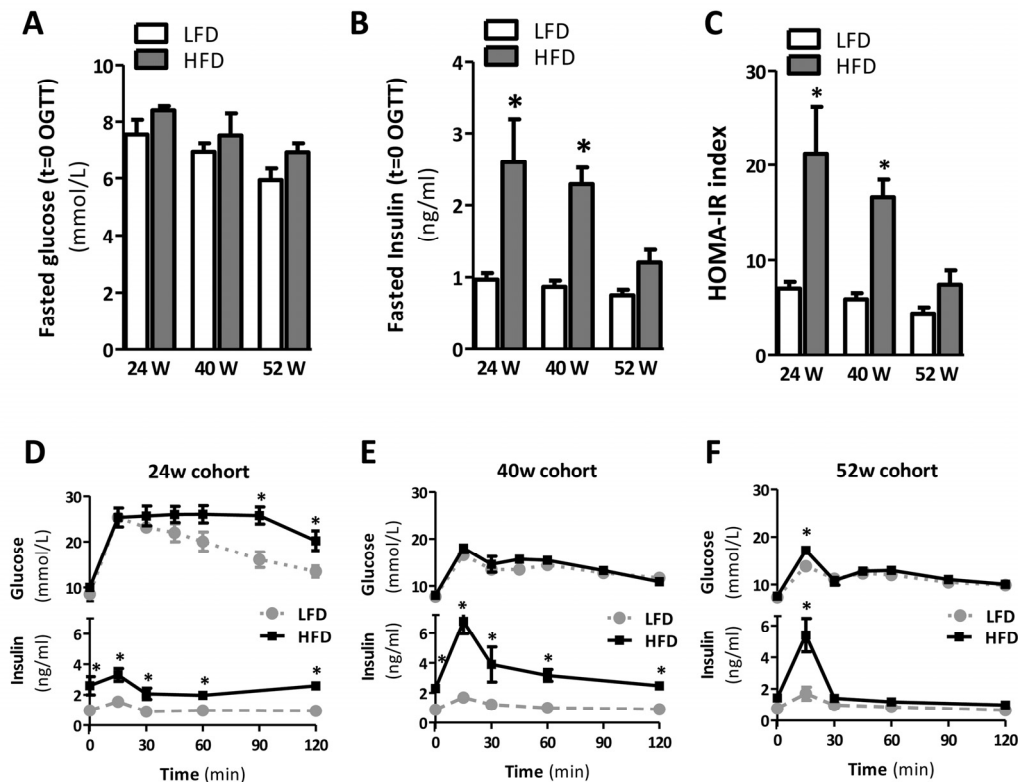
Figure 2. Prolonged HFD is associated with IR after 24 and 40 weeks but not after 52 weeks of HFD. (**A**) Fasted plasma glucose and (**B**) insulin concentrations measured in blood collected prior to oral glucose tolerance test (OGTT). (**C**) Homeostatic model assessment of IR (HOMA-IR) used as a surrogate marker of IR. (**D-F**) Blood glucose (top) and plasma insulin (bottom) levels during OGTT after 24, 40 and 52 weeks of LFD and HFD-feeding. Values shown are means ± SEM (n=7 mice/group). Significance level set at p<0.05. *=significant from LFD at same time point, †=significant from same diet 24w, ‡=significant from same diet 40w.
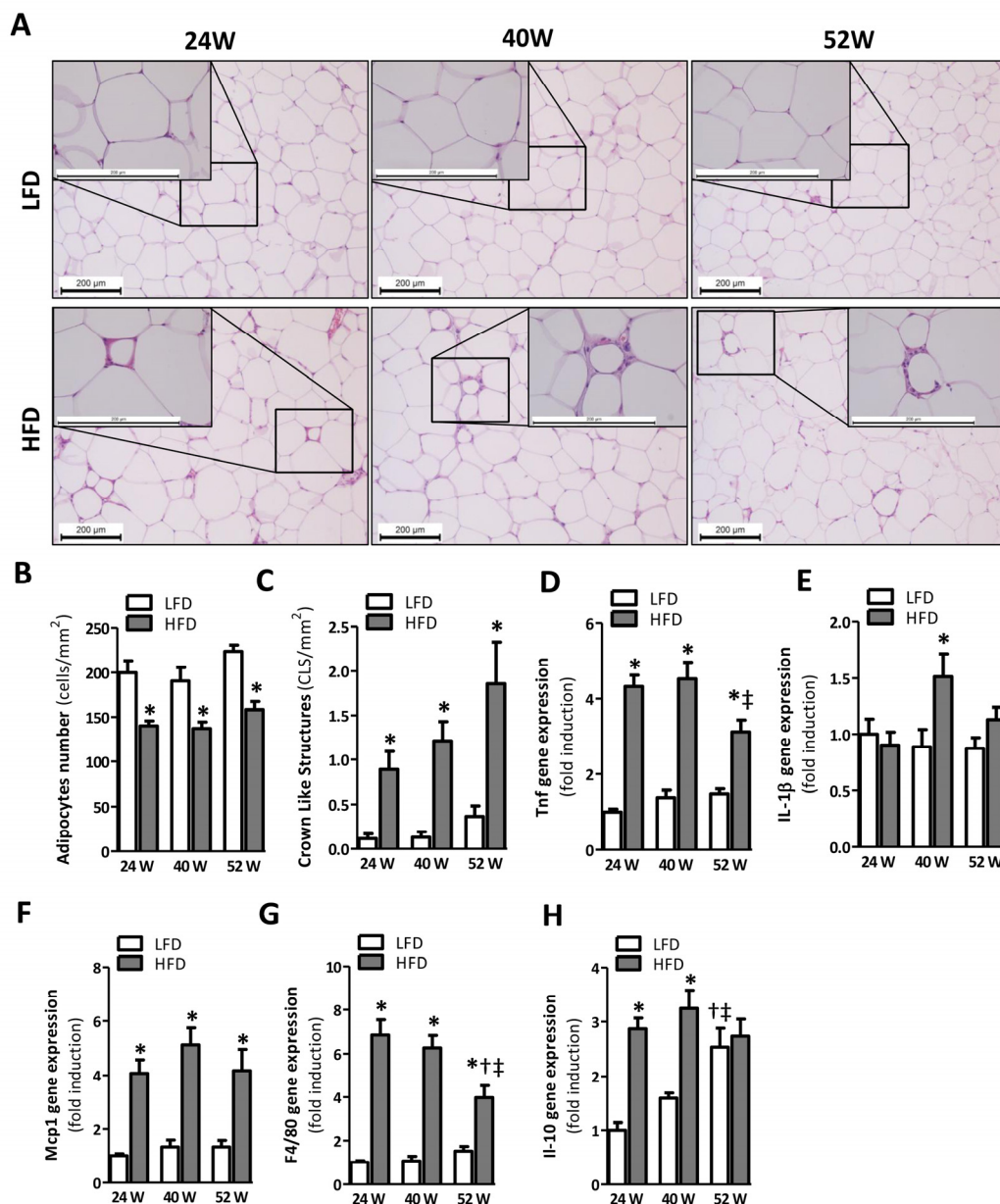
Figure 3. Prolonged HFD-feeding leads to AT inflammation in mice after 24 weeks. **(A)** Representative pictures from H&E-stained AT sections of LFD and HFD mice after 24 (left), 40 (middle) and 52 (right) weeks of diet with crown-like structures (insets). Histologically quantified number of **(B)** adipocytes and **(C)** crown-like structures per mm^2 (n=10-15). **(D-H)** mRNA expression levels of tumor necrosis factor (*Tnf*), interleukin-1β (*Il1β*), monocyte chemotactic protein-1 (*Mcp1*), macrophage marker (*F4/80*) and interleukin-10 (*Il-10*) in the AT. All mRNA expression data were normalized to the LFD24 group and expressed as mean ± SEM (n=7-8). Significance level set at p<0.05. *=significant from LFD at same time point, †=significant from same diet 24w, ‡=significant from same diet 40w.

Plasma adipokine and cytokine levels during prolonged HFD-feeding in mice

Both leptin and adiponectin are associated with obesity, IR and T2D. To investigate the extent to which prolonged HFD-feeding mediates the secretion of leptin and adiponectin, we measured the plasma levels of these adipokines throughout the dietary period. As expected, leptin was significantly increased in mice fed a HFD compared to LFD, reaching a maximum around 24 weeks
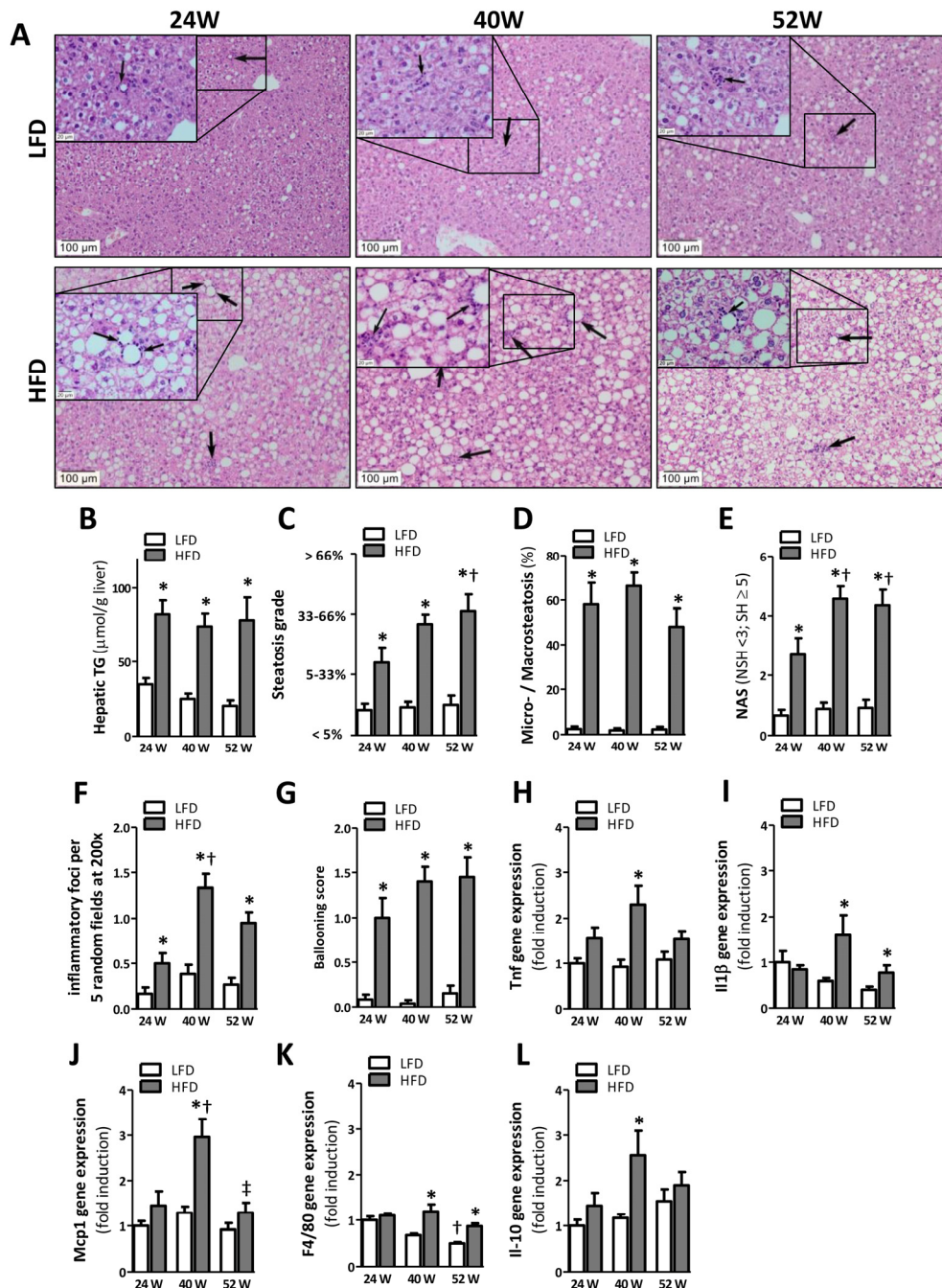
Figure 4. HFD-feeding leads to hepatic steatosis after 24 weeks but inflammation becomes apparent after 40 weeks. (**A**) Representative pictures from H&E-stained liver sections of LFD and HFD mice after 24 (left), 40 (middle) and 52 (right) weeks of diet with inflammatory foci (arrows; insets). (**B**) Quantification of hepatic triglycerides. (**C**) Determination of steatosis grade (0=0-5%; 1=5-33%; 2=33-66%; 3=66-100% coverage), and (**D**) percentage of microvesicular over macrovesicular steatosis. (**E**) Determination of NAFLD Activity Score (NAS; sum of steatosis + lobular inflammation + ballooning), score >5 represents steatohepatitis (SH) and pathological scores <3 non-steatohepatitis (NSH). (**F**) Quantification of inflammatory foci per 5 random fields under 200x magnification and (**G**) determination of ballooning score. (**H-L**) mRNA expression levels of tumor necrosis factor (*Tnf*), monocyte chemotactic protein-1 (*Mcp1*), macrophage marker (*F4/80*), interleukin-1β (*Il1β*), and interleukin-10 (*Il-10*) in the AT. All mRNA expression data were normalized to the LFD24 group and expressed as mean ±SEM (n=7-8). Significance level set at p<0.05. *=significant from LFD at same time point, †=significant from same diet 24w, ‡=significant from same diet 40w.

(Fig. 5A). Plasma leptin concentrations exhibited very strong correlation with body weight (Fig. 5B). Serial adiponectin levels did not change in time or as a result of HFD-feeding (Fig. 5C). After 24 weeks of HFD, the circulating pro-inflammatory mediators, TNF, IL-6, and mKC, as well as the anti-inflammatory mediator IL-10 were up-regulated (Fig. 5D), confirming immunological activation in HFD-fed mice.

DISCUSSION

To date, the detrimental role of metabolic inflammation in the etiology of IR has become irrefutable [10]. Despite the fact that inflammation in AT and liver are both associated with IR, their individual contribution to the development of metabolic inflammation remains elusive. Here, we have explored the temporal relationship between AT and liver inflammation in the development of metabolic inflammation. We show that chronic metabolic inflammation is apparent in the visceral AT depot at 24 weeks of HFD-feeding (Fig. 3), whilst overt hepatic inflammation does not occur until 40 weeks of HFD-feeding (Fig. 4). This implies that AT inflammation precedes hepatic inflammation in mice fed an obesogenic diet. Furthermore, as IR was established before the development of clear hepatic inflammation and did not further progress, our data also suggest that obesity-associated IR is more likely to be associated with AT

inflammation rather than hepatic inflammation.

In agreement with previous reports demonstrating that HFD-feeding favours the development of obesity [10,16], our data show that body weight gain increased rapidly within the initial 12-24 weeks of HFD-feeding (Fig. 1B). Prolonged HFD-feeding in mice led to a further, yet marginal, increase in body weight up to a maximum at about 40 weeks of HFD-feeding. Weight gain then levelled off and weight remained high until the end of the study. Although we used male mice in our study, previous studies observed a similar growth pattern in female mice fed a HFD-diet (60% kcal fat) for up to 12 months [16]. In the female mice the increase in body weight was greater during the first 12 weeks and slower during subsequent weeks of HFD-feeding. Corresponding to the rate of body weight gain in mice fed a HFD, plasma leptin levels were significantly increased compared with mice fed a LFD (Fig. 5). Indeed, as adipocytes expand due to enhanced triglyce-ride storage, leptin secretion increases proportionately [17]. However, leptin levels significantly declined with prolonged HFD-feeding (±30 weeks of HFD-feeding) although body weight remained high (Fig. 5A, B). Leptin levels also declined in mice fed the LFD, suggesting an age-related decline in circulating leptin. This has previously been observed in rodents [18] and also in the human population leptin levels have been found to decline with age [19].

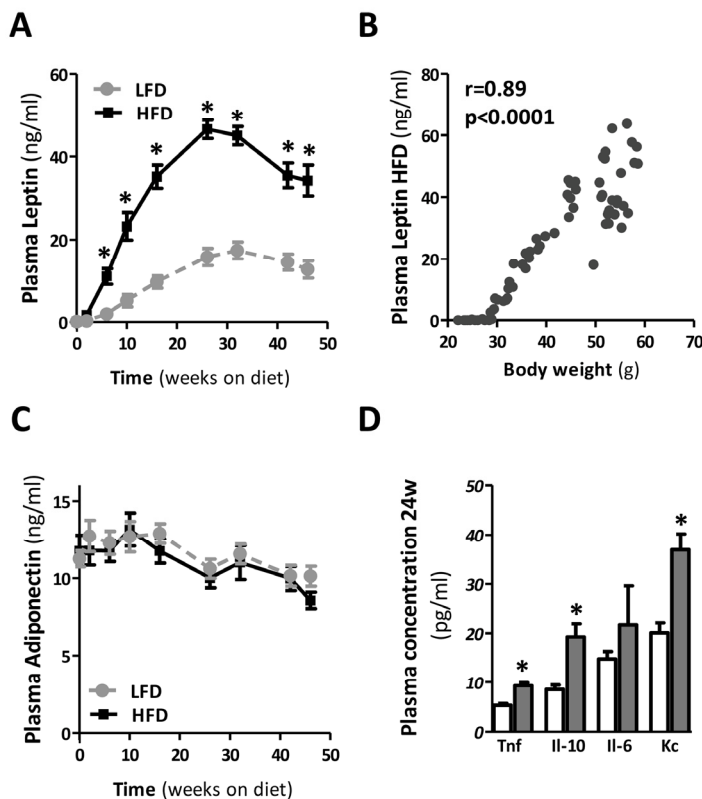**Figure 5. Plasma adipokine and cytokine levels during prolonged HFD in mice.** (**A**) Serial plasma leptin and (**B**) its correlation with body weight, and (**C**) serial plasma adiponectin throughout the dietary intervention. (**D**) Plasma cytokine levels in mice fed a LFD and HFD for 24 weeks. (n=10-15 mice/group). Significance level set at p<0.05. *=significant from LFD at same time point.

Although AT is an important initiator of the inflammatory response to obesity [4], few studies have addressed the temporal relationship between AT and the liver in the development of metabolic inflammation. Here we show that 24 weeks of diet-induced obesity indeed led to an increase in AT inflammation. In contrast to *Tnf, Mcp1* and *F4/80, Il1β* was not elevated at the 24-week time point (Fig. 3D). However, we cannot fully exclude that Il1β was not expressed at this time point, since cytokine expression was not measured in the stromal vascular fraction but in AT lysates only, which may have led to an underrepresentation of the results. Of note, gene expression of the anti-inflammatory cytokine *Il-10* was persistently elevated in HFD mice as well. This is in agreement with previous studies in mice [20] and humans [21] and likely represents a protective response of the body to counteract pro-inflammatory events.

Other longitudinal studies investigating the development of adipose and liver inflammation found that both organs exhibit a very similar response to HFD feeding at the level of transcriptional master regulators [22]. However, the response at the level of genes controlled by these regulators was tissue-specific and, importantly, the authors observed a delayed response in the liver when compared to the AT, which is consistent with our findings. What causes this delayed inflammatory response remains to be elucidated. However, it has been shown that systemically administered cytokines can exert pro-inflammatory effects on the liver. Especially TNF and leptin are known to play a role in the pathogenesis of NAFLD [23,24]. Here, we show that AT inflammation is associated with the enhanced secretion of TNF and leptin to the circulation after 24w of HFD (Fig. 5). Since the visceral AT depot directly drains into the portal circulation, this may support the notion of crosstalk between dysfunctional AT and the liver. Thus, our results indicate that metabolic inflammation in obesity is initiated in the AT and in time progresses to the liver. Therefore, our data suggest that the liver does not play a role in the initial development of metabolic inflammation in mice but may serve as a contributor to metabolic inflammation following its establishment.

Aging is associated with increased visceral adiposity [25,26], AT inflammation and a systemic increase in pro-inflammatory cytokines [27], thus closely resembling the pathophysiology in obesity. Given that this inflamm-aging is linked with various age-associated disorders [28], targeting inflammatory pathways could prevent or alleviate the pathological consequences observed in the course of aging, obesity or both in parallel. Over the last decade mTOR inhibitors,

especially rapamycin, have shown promising effects on extending life- and health span in animal models of aging [29,30] and obesity [31], effects that, at least for obesity, may be attributed to rapamycin's anti-inflammatory properties in the AT [32]. Whether this may be applied to the human setting to increase health span in the growing aging population remains unknown.

Our data also show that IR was induced in mice fed a HFD for 24 weeks compared with LFD mice. Since at this point AT inflammation was present, in the absence of clear hepatic inflammation, this may suggest AT inflammation is more likely to contribute to obesity-associated IR. This observation accords with our previous reports regarding the dissociation of hepatic inflammation and IR and suggests a greater contribution of adipose inflammation to development of IR than hepatic inflammation [33,34]. Our study design, however, does not allow for assessing whether AT inflammation triggers systemic IR or vice versa since at our earliest time point (24 weeks HFD-feeding) both IR and AT inflammation were observed. It has, however, been shown previously that AT inflammation is necessary for long-term but not short-term HFD-induced IR, which is more likely related to acute tissue lipid overload [10].

Nevertheless, our data also show that prolonged HFD feeding is associated with improved insulin sensitivity over time, as we did not observe signs of glucose intolerance in mice fed a HFD for 52 weeks (Fig. 2, Suppl. 1). This increase in insulin sensitivity was already observed in mice fed a HFD for 40 weeks compared to 24 weeks. Although the observed alleviation of IR clearly warrants further study it is known that insulin responses and insulin levels decline with age in the human population [35]. This could reflect beta cell failure in aging, or might be due to alterations in gastric emptying, delayed nutrient absorption, or enhanced insulin sensitivity in older age [36]. Furthermore, an age-related decline in renal function may also affect glucose metabolism and impair insulin secretion [36,37]. Whether any of these factors can explain the amelioration of insulin sensitivity in our study remains to be investigated. In addition, the high serum leptin levels as observed in mice fed the HFD may have resulted in inhibition of insulin release from the pancreas [38]. Furthermore, the apparent improvement in insulin sensitivity in our study may also be related to the attenuated inflammatory phenotype of the AT observed with aging. Indeed, AT of mice fed a 52-week diet of HFD had a reduced expression of the inflammatory genes *Tnf* and *F4/80* in comparison with mice fed a HFD for 40 weeks. Although this could reflect the reciprocal relationship between inflammation

and IR, it should be noted that the reduced expression of inflammatory genes was not paralleled by a reduced number of crown-like structures in the AT (Fig 3C). A similar trend was observed for the liver, in which *Mcp1* expression was significantly reduced in mice fed a HFD for 52 weeks compared with mice at 40 weeks. This may seem paradoxical at first sight, however, this finding may be explained at the macrophage's functional level where it has been reported that with aging macrophages obtain a reduced capacity to become activated into a pro-inflammatory state by chemokines and cytokines [39], thus allowing a similar amount of macrophages to be associated with a reduced cytokine expression with age. Nevertheless, the influx of macrophages to the AT is less impressive with aging and it has been suggested that (pre-) adipocytes, rather than macrophages, are the major source of inflammation in aging [40]. Although we cannot discriminate between the different cell types involved in AT and liver inflammation, aging by itself did not result in upregulation of pro-inflammatory genes and cytokines in LFD52 mice. This is in discrepancy with the study by Wu *et al.* and may be explained by the longer duration (22-24 months) and different strain of mice (C57BL/6JNIA) used in their study. Nevertheless, *Il-10* was significantly increased in time suggesting some degree of age-induced immunological activation in our study.

Taken together, we provide evidence that obesity-induced metabolic inflammation in the AT precedes inflammation in the liver, suggesting that the liver does not play a role in the initial development of metabolic inflammation. Furthermore, we show that hepatic inflammation is of lesser importance to the development of insulin resistance compared to AT inflammation. Therefore, targeting AT inflammation may help to control metabolic inflammation in obesity and aging in mice by both delaying its initiation and subsequent progression to other organs such as the liver. Further research is warranted for successful extrapolation of the research results to human clinical conditions.

MATERIALS AND METHODS

Animals and diet intervention. All procedures were performed with approval of the University of Groningen Ethics Committee for Animal Experiments (experiment registered as 6141B), which adheres to the principles and guidelines established by the European Convention for the Protection of Laboratory Animals. Experiments were carried out on male C57BL/6j mice (Charles River, JAX laboratories, France), individually housed in a temperature-controlled room under a 12 h light-dark cycle with *ad libitum* access to water and food, unless

stated otherwise. After arrival at our laboratories the 6-week old C57BL/6j male mice received a low-fat diet (LFD) containing 10% fat from lard (D12450HY, Research Diets Inc., NJ, USA) for 6 weeks until the start of the experiment, at which time the animals were 12 weeks old. After this run-in period, randomly divided groups of animals were either kept on the LFD or switched to a high-fat diet (HFD) containing 45% fat from lard (D12451, Research Diets Inc.). Experiments were performed on mice after 24, 40 and 52 weeks of HFD-feeding unless stated otherwise. To ensure that observations took place in a state of chronic obesity, animals exhibiting a weight loss >15% at sacrifice, compared with their peak body weight were excluded from the analyses. Six mice were excluded from the study due to the development of dermatitis, that is n=2 in the HFD24 group, n=3 in the HFD52 group, and n=1 in the LFD52 cohort. Final group sizes were n=13 for LFD24, n=13 for HFD24, n=15 for LFD40, n=15 for HFD40, n=13 for LFD52 and n=10 for HFD52.

Oral glucose tolerance test. Three weeks prior to sacrifice subsets of mice (n=7 per group) were fasted for 6 hours and received a glucose bolus (2 g/kg; 40% glucose solution (w/v) by oral gavage. Average gavage volume was 180±13 and 250±24 μl for LFD- and HFD-mice, respectively. Glucose levels were measured with the OneTouch Ultra glucometer (Lifescan Benelux, Beerse, Belgium) before and 15, 30, 45, 60, 90, and 120 minutes after the gavage by puncturing the saphenous vein of the left hind limb. Blood samples collected prior to glucose administration and at 15, 30, 60 and 120 minutes were used to simultaneously assess plasma insulin levels. HOMA-index for systemic IR was calculated as described elsewhere [41].

Analysis of plasma parameters. Plasma insulin was determined by ELISA (Alpco ultrasensitive, Alpco, Tilburg, The Netherlands). Plasma leptin and adiponectin were determined by ELISA (R&D systems, Abingdon, UK). Plasma levels of interleukin IL-1β, IL-2, IL-5, IL-6, IL-10, IL-12 and mKC (CXCL-1), p70, TNF and IFN-γ were measured using Meso Scale Discovery (Gaithersburg, USA) 10-plex multispot Mouse cytokine assay for plasma, according to the manufacturer's instructions. Intra- and inter-assay coefficients of variation were, respectively, IL-10 (15.8 and 31.2%), IL-6 (11,5 and 3.3%), mKC (8.3 and 13.7%) and TNF (6.4 and 16.3%). Concentrations of IFN-γ, IL-12, p70, IL-1β, IL-2, IL-5 were below the detection limit of the assay.

Liver and AT Histology. Three different visceral adipose depots (i.e. surrounding the intestine; mesenteric, the kidney; perirenal, and the gonads;

gonadal/epidydimal) were isolated and weighed at sacrifice. Subsections were partially embedded in paraffin and snap frozen and stored at -80°C for further analyses. The frozen gonadal fat depot was crushed in liquid nitrogen for RNA isolation. Livers were collected, trimmed, and trimmed sections were fixed in 10% paraformaldehyde. Paraffin-embedded liver and AT sections (4 μm) were stained with Hematoxylin/Eosin (H&E) for morphological examination. Scoring of hepatic steatosis and steatohepatitis (NAFLD activity score NAS) was performed in an unbiased manner by two board-certified veterinary pathologists (SAY, AdB) using a method described previously [42].

To estimate adipocyte size, the number of adipocytes per mm^2 was determined on scanned sections by manually counting all the adipocytes in an area of 4-5 mm^2, using Aperio ImageScope (Leica Biosystems Imaging Inc., CA, USA). Slides were scanned with the NanoZoomer 2.0-HT slide scanner from Hamamatsu (Herrsching am Ammersee, Germany).

Liver lipids. Total liver lipids were extracted from the liver according to the Bligh and Dyer method [43], as previously explained [44], and measured biochemically. Hepatic triglycerides (TG) were quantified using commercially available kits (Hitachi, Roche, Woerden, The Netherlands).

Quantitative Real-Time PCR (qRT-PCR). Total RNA was isolated from the liver and AT using RNeasy Mini plus and RNeasy Lipid Tissue Mini kits (Qiagen, Wetburg, Leusden, The Netherlands), respectively, according to the manufacturer's instructions. RNA integrity was determined by agarose gel electrophoresis. RNA quantity (OD-260) and quality (260/OD-280) were determined using an ND-1,000 spectrophotometer (NanoDrop Technologies, Rockland, DE). Total RNA (1 μg) was converted into cDNA using a Quantitect Reverse Transcription kit (Roche, Mannheim, Germany) according to the manufacturer's instructions. Real time PCR (RT-PCR) was performed using a 7900HT system (Applied Biosystems, Warrington, UK) as previously explained [45] by using Power SYBR Green Master Mix (Roche, Mannheim, Germany). Values were corrected using the housekeeping gene Cyclophillin A (*Ppia*). Primer sequences are available in Supplementary Table 1.

Statistical analysis. Data are expressed as means ± standard error of the mean (SEM). Data were statistically analysed using GraphPad Prism (version 5.00 for Windows, GraphPad Software, San Diego, CA, USA). Non-parametric Mann-Whitney U tests were performed for comparing LFD and HFD groups within a time point, and Kruskall Wallis ANOVA with Dunn's post hoc test was used to determine differences between time points within the designated diet. Statistical analyses with p-value smaller than 0.05 were considered significant.

Conflict of interest statement

The authors declare that they have no competing financial interests or other conflicts of interest.

REFERENCES

1. Hotamisligil GS. Inflammation and metabolic disorders. Nature. 2006;444:860–867.

2. Hummasti S, Hotamisligil GS. Endoplasmic reticulum stress and inflammation in obesity and diabetes. Circ. Res. 2010;107:579–591.

3. Cinti S, Mitchell G, Barbatelli G, Murano I, Ceresi E, Faloia E, Wang S, Fortier M, Greenberg AS, Obin MS. Adipocyte death defines macrophage localization and function in adipose tissue of obese mice and humans. J. Lipid Res. 2005;46:2347–2355.

4. Olefsky JM, Glass CK. Macrophages, inflammation, and insulin resistance. Annu. Rev. Physiol. 2010;72:219–246.

5. Shoelson SE, Lee J, Goldfine AB. Inflammation and insulin resistance. J. Clin. Invest. 2006;116:1793–1801.

6. Glass CK, Olefsky JM. Inflammation and lipid signaling in the etiology of insulin resistance. Cell Metab. 2012;15:635–645.

7. Sheedfar F, Di Biase S, Koonen D, Vinciguerra M. Liver diseases and aging: friends or foes? Aging Cell. 2013;12:950–954.

8. Tilg H, Moschen AR. Insulin resistance, inflammation, and non-alcoholic fatty liver disease. Trends Endocrinol. Metab. 2008;19:371–379.

9. Cai D, Yuan M, Frantz DF, Melendez PA, Hansen L, Lee J, Shoelson SE. Local and systemic insulin resistance resulting from hepatic activation of IKK-beta and NF-kappaB. Nat. Med. 2005;11:183–190.

10. Lee YS, Li P, Huh JY, Hwang IJ, Lu M, Kim JI, et al. Inflammation is necessary for long-term but not short-term high-fat diet-induced insulin resistance. Diabetes. 2011;60:2474–2483.

11. Wellen KE, Hotamisligil GS. Inflammation, stress, and diabetes. J. Clin. Invest. 2005;115:1111–1119.

12. De Taeye BM, Novitskaya T, McGuinness OP, Gleaves L, Medda M, Covington JW, Vaughan DE. Macrophage TNF-alpha contributes to insulin resistance and hepatic steatosis in diet-induced obesity. Am. J. Physiol. Endocrinol. Metab. 2007;293:E713–725.

13. Suganami T, Mieda T, Itoh M, Shimoda Y, Kamei Y, Ogawa Y. Attenuation of obesity-induced adipose tissue inflammation in C3H/HeJ mice carrying a Toll-like receptor 4 mutation. Biochem. Biophys. Res. Commun. 2007;354:45–49.

14. Kammoun HL, Chabanon H, Hainault I, Luquet S, Magnan C, Koike T, Ferré P, Foufelle F. GRP78 expression inhibits insulin and ER stress-induced SREBP-1c activation and reduces hepatic steatosis in mice. J. Clin. Invest. 2009;119:1201–1215.

15. Lanthier N, Molendi-Coste O, Cani PD, van Rooijen N, Horsmans Y, Leclercq IA. Kupffer cell depletion prevents but has no therapeutic effect on metabolic and inflammatory changes induced by a high-fat diet. FASEB J. 2011;25:4301–4311.

16. Winzell MS, Ahren B. The High-Fat Diet-Fed Mouse: A Model for Studying Mechanisms and Treatment of Impaired Glucose Tolerance and Type 2 Diabetes. Diabetes. 2004;53:S215–S219.

17. Unger RH, Scherer PE. Gluttony, sloth and the metabolic syndrome: a roadmap to lipotoxicity. Trends Endocrinol. Metab. 2010;21:345–352.

18. Hamrick MW, Ding K-H, Pennington C, Chao YJ, Wu Y-D, Howard B, et al. Age-related loss of muscle mass and bone strength in mice is associated with a decline in physical activity and serum leptin. Bone. 2006;39:845–853.

19. Moller N, O'Brien P, Nair KS. Disruption of the relationship between fat content and leptin levels with aging in humans. J. Clin. Endocrinol. Metab. 1998;83:931–934.

20. Oliveira MC, Menezes-Garcia Z, Henriques MCC, Soriani FM, Pinho V, Faria AMC, Santiago AF, Cara DC, Souza DG, Teixeira MM, Ferreira AVM. Acute and sustained inflammation and metabolic dysfunction induced by high refined carbohydrate-containing diet in mice. Obesity (Silver Spring). 2013; 21:E396-406.

21. Esposito K, Pontillo A, Di Palo C, Giugliano G, Masella M, Marfella R, Giugliano D. Effect of weight loss and lifestyle changes on vascular inflammatory markers in obese women: a randomized trial. JAMA. 2003;289:1799–1804.

22. Liang W, Tonini G, Mulder P, Kelder T, van Erk M, van den Hoek AM, Mariman R, Wielinga PY, Baccini M, Kooistra T, Biggeri A, Kleemann R. Coordinated and interactive expression of genes of lipid metabolism and inflammation in adipose tissue and liver during metabolic overload. PLoS One. 2013;8:e75290.

23. Brunt EM. Nonalcoholic steatohepatitis. Semin. Liver Dis. 2004;24:3–20.

24. Neuschwander-Tetri BA, Caldwell SH. Nonalcoholic steatohepatitis: summary of an AASLD Single Topic Conference. Hepatology. 2003;37:1202–1219.

25. Matsuzawa Y, Shimomura I, Nakamura T, Keno Y, Kotani K, Tokunaga K. Pathophysiology and pathogenesis of visceral fat obesity. Obes. Res. 1995;3 Suppl 2:187S–194S.

26. Kuk JL, Saunders TJ, Davidson LE, Ross R. Age-related changes in total and regional fat distribution. Ageing Res. Rev. 2009;8:339–348.

27. Koster A, Stenholm S, Alley DE, Kim LJ, Simonsick EM, Kanaya AM, et al. Body fat distribution and inflammation among obese older adults with and without metabolic syndrome. Obesity (Silver Spring). 2010;18:2354–2361.

28. Tchkonia T, Morbeck DE, Von Zglinicki T, Van Deursen J, Lustgarten J, Scrable H, Khosla S, Jensen MD, Kirkland JL. Fat tissue, aging, and cellular senescence. Aging Cell. 2010;9:667–684.

29. Miller RA, Harrison DE, Astle CM, Baur JA, Boyd AR, de Cabo R, et al. Rapamycin, but not resveratrol or simvastatin, extends life span of genetically heterogeneous mice. J. Gerontol. A. Biol. Sci. Med. Sci. 2011;66:191–201.

30. Wilkinson JE, Burmeister L, Brooks S V, Chan C-C, Friedline S, Harrison DE, Hejtmancik JF, Nadon N, Strong R, Wood LK, Woodward MA, Miller RA. Rapamycin slows aging in mice. Aging Cell. 2012;11:675–682.

31. Leontieva O V, Paszkiewicz GM, Blagosklonny M V. Weekly administration of rapamycin improves survival and biomarkers in obese male mice on high-fat diet. Aging Cell. 2014;13:616–622.

32. Jiang H, Westerterp M, Wang C, Zhu Y, Ai D. Macrophage mTORC1 disruption reduces inflammation and insulin resistance in obese mice. Diabetologia. 2014;57:2393–2404.

33. Funke A, Schreurs M, Aparicio-Vergara M, Sheedfar F, Gruben N, Kloosterhuis NJ, Shiri-Sverdlov R, Groen AK, van de Sluis B, Hofker MH, Koonen DPY. Cholesterol-induced hepatic inflammation does not contribute to the development of insulin resistance in male LDL receptor knockout mice. Atherosclerosis. 2014;232:390–396.

34. Aparicio-Vergara M, Hommelberg PPH, Schreurs M, Gruben N, Stienstra R, Shiri-Sverdlov R, Kloosterhuis NJ, de Bruin A, van de Sluis B, Koonen DPY, Hofker MH. Tumor necrosis factor receptor 1 gain-of-function mutation aggravates nonalcoholic fatty liver disease but does not cause insulin resistance in a murine model. Hepatology. 2013;57:566–756.

35. Chang AM, Halter JB. Aging and insulin secretion. Am. J. Physiol. Endocrinol. Metab. 2003;284:E7–12.

36. Bryhni B, Arnesen E, Jenssen TG. Associations of age with serum insulin, proinsulin and the proinsulin-to-insulin ratio: a cross-sectional study. BMC Endocr. Disord. 2010;10:21.

37. Henriksen JH, Tronier B, Bülow JB. Kinetics of circulating endogenous insulin, C-peptide, and proinsulin in fasting nondiabetic man. Metabolism. 1987;36:463–468.

38. Nasrallah MP, Ziyadeh FN. Overview of the physiology and pathophysiology of leptin with special emphasis on its role in the kidney. Semin. Nephrol. 2013;33:54–65.

39. Sebastián C, Lloberas J, Celada A. Molecular and cellular aspects of macrophage aging in Handbook on Immunosenescence. Dordrecht: Springer Netherlands; 2009.

40. Wu D, Ren Z, Pae M, Guo W, Cui X, Merrill AH, Meydani SN. Aging up-regulates expression of inflammatory mediators in mouse adipose tissue. J. Immunol. 2007;179:4829–4839.

41. Turner RC, Holman RR, Matthews D, Hockaday TD, Peto J. Insulin deficiency and insulin resistance interaction in diabetes: estimation of their relative contribution by feedback analysis

from basal plasma insulin and glucose concentrations. Metabolism. 1979;28:1086–1096.

42. Kleiner DE, Brunt EM, Van Natta M, Behling C, Contos MJ, Cummings OW, et al. Design and validation of a histological scoring system for nonalcoholic fatty liver disease. Hepatology. 2005;41:1313–1321.

43. Bligh EG, Dyer WJ. A rapid method of total lipid extraction and purification. Can. J. Biochem. Physiol. 1959;37:911–917.

44. Sheedfar F, Vermeer M, Pazienza V, Villarroya J, Rappa F, Cappello F, Mazzoccoli G, Villarroya F, van der Molen H, Hofker MH, Koonen DP, Vinciguerra M. Genetic ablation of macrohistone H2A1 leads to increased leanness, glucose tolerance and energy expenditure in mice fed a high fat diet. Int. J. Obes. (Lond). 2015; 39:331-338.

45. Sheedfar F, Sung MM, Aparicio-Vergara M, Kloosterhuis NJ, Miquilena-Colina ME, Vargas-Castrillón J, et al. Increased hepatic CD36 expression with age is associated with enhanced susceptibility to nonalcoholic fatty liver disease. Aging (Albany. NY). 2014;6:281–295.

SUPPLEMENTARY MATERIAL

A

B
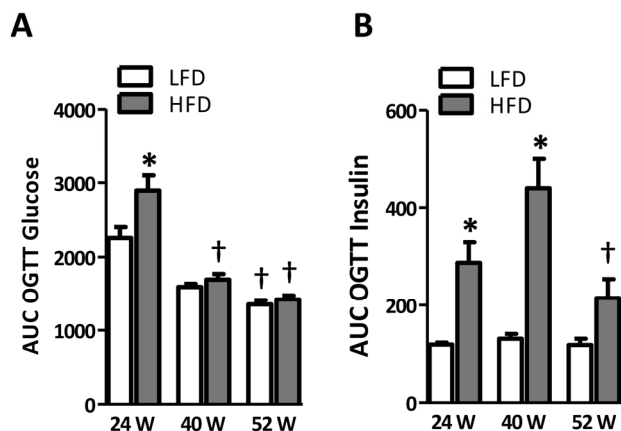
Supplementary Figure 1. Glucose and insulin during OGTT. (**A**) Glucose and (**B**) insulin homeostasis during oral glucose tolerance test (OGTT) quantified by area under curve (AUC) based on data in Fig. 2B-E. Significance level set at p<0.05. *=significant from LFD at same time point, †=significant from same diet 24w, ‡=significant from same diet 40w.

Supplementary Table 1. Primer sequences applied for gene expression analyses in AT and liver. Primer sequences for *Tnf, Mcp1, Il-1β, F4/80, Ppia* and *Il-10*

Gene	Forward primer 5'-3'	Reverse primer 5'-3'
F4/80	TGTGTCGTGCTGTTCAGAACC	AGGAATCCCGCAATGATGG
Mcp1	GCTGGAGAGCTACAAGAGGATCA	ACAGACCTCTCTCTTGAGCTTGGT
Il1β	TGCAGCTGGAGAGTGTGG	TGCTTGTGAGGTGCTGATG
Il10	GCTCTTACTGACTGGCATGAG	CGCAGCTCTAGGAGCATGTG
Tnf	GTAGCCCACGTCGTAGCAAAC	AGTTGGTTGTCTTTGAGATCCATG
Ppia	TTCCTCCTTTCACAGAATTATTCCA	CCGCCAGTGCCATTATGG

Surgical removal of inflamed epididymal white adipose tissue attenuates the development of non-alcoholic steatohepatitis in obesity

Abstract

Background: Non-alcoholic fatty liver disease (NAFLD) is strongly associated with abdominal obesity. Growing evidence suggests that inflammation in specific depots of white adipose tissue (WAT) plays a key role in NAFLD progression, but experimental evidence for a causal role of WAT is lacking. **Methods:** A time-course study in C57BL/6J mice was performed to establish which WAT depot is most susceptible to develop inflammation during high-fat diet (HFD)-induced obesity. Crown-like structures (CLS) were quantified in epididymal (eWAT), mesenteric (mWAT) and inguinal/subcutaneous (iWAT) WAT. The contribution of inflamed WAT to NAFLD progression was investigated by surgical removal of a selected WAT depot and compared to sham surgery. Plasma markers were analysed by ELISA (cytokines/adipokines) and lipidomics (lipids). **Results:** In eWAT, CLS were formed already after 12 weeks of HFD which coincided with maximal adipocyte size and fat depot mass, and preceded establishment of non-alcoholic steatohepatitis (NASH). By contrast, the number of CLS was low in mWAT and iWAT. Removal of inflamed eWAT after 12 weeks (eWATx group) followed by another 12 weeks of HFD feeding, resulted in significantly reduced NASH in eWATx. Inflammatory cell aggregates (-40%; $p<0.05$) and inflammatory gene expression (e.g. TNFα, -37%; $p<0.05$) were attenuated in livers of eWATx mice, while steatosis was not affected. Concomitantly, plasma concentrations of circulating pro-inflammatory mediators, viz. leptin and specific saturated and monounsaturated fatty acids, were also reduced in the eWATx group. **Conclusions**: Intervention in NAFLD progression by removal of inflamed eWAT attenuates the development of NASH and reduces plasma levels of specific inflammatory mediators (cytokines and lipids). These data support the hypothesis that eWAT is causally involved in the pathogenesis of NASH.

Published as:

Introduction

Non-alcoholic fatty liver disease (NAFLD) is a significant health problem and the most common form of chronic liver disease worldwide [1, 2]. The prevalence of NAFLD parallels the steady increases in the rates of obesity, and consumption of saturated fat is positively associated with the risk of NAFLD [3]. Clinicopathologically, NAFLD comprises a wide spectrum of liver damage ranging from bland steatosis (NAFL) to non-alcoholic steatohepatitis (NASH), fibrosis and ultimately cirrhosis [4]. Bland steatosis is benign whereas NASH is characterised by hepatocyte injury, TNFα-mediated inflammation [4], and a high risk of liver-related morbidity and mortality [2].

The pathogenesis of NAFLD is not fully understood, and the factors that contribute to disease progression from bland steatosis to NASH remain enigmatic. Epidemiological and human observational studies do provide indications that progressive NAFLD is strongly associated with white adipose tissue (WAT) inflammation, insulin resistance, and elevated circulating levels of inflammatory mediators including certain adipokines and lipids [5-10]. Furthermore, longitudinal rodent studies demonstrated that high fat diet (HFD)-induced expression of inflammatory genes in WAT precedes the development of NASH in disease models with obesity, suggesting a potential role of inflamed WAT in NAFLD progression [11]. Also, the severity of the NAFLD pathology appears to be closely linked to WAT dysfunction, i.e. hypertrophy of adipocytes combined with macrophage infiltration, formation of crown-like structures (CLS) and enhanced expression of inflammatory genes [12]. Hence, it has been postulated that obesity-induced inflammation in WAT is critical for the development of NAFLD [13, 14] but experimental evidence for an involvement of WAT is still lacking.

WAT is a complex endocrine organ that is composed of different depots among which the intra-abdominal (e.g. epididymal and mesenteric) and subcutaneous (e.g. inguinal) WAT depots [15, 16]. These depots are thought to play different roles in energy storage and inflammation [14-16] and may thus have different contributions to the pathogenesis of NAFLD. The temporal development of inflammation (i.e. CLS formation) in WAT depots has not been systematically investigated and it is not known whether a particular depot is more prone than others to become inflamed during HFD-induced obesity and associated NAFLD.

The present time-course study analyses HFD-evoked changes in epididymal (eWAT), mesenteric (mWAT) and inguinal WAT (iWAT) with specific emphasis on adipocyte hypertrophy and WAT inflammation (CLS formation). To that end, a cohort of male C57BL/6J

mice was treated with HFD for a period of 24 weeks. Groups of mice were sacrificed at regular intervals, and compared with chow controls. Longitudinal histological analyses revealed that a particular depot (eWAT) is highly susceptible to develop inflammation with pronounced CLS formation already after 12 weeks. In a separate experiment, the inflamed eWAT depot of obese HFD-fed mice was surgically removed (after 12 weeks on a HFD) to examine a potential role of eWAT in the subsequent development of NASH. Our results provide evidence that inflamed eWAT plays an important role in the pathogenesis of NASH. Analysis of adipokines and circulating lipids by lipidomics supports the view that circulating inflammatory factors derived from eWAT mediate NASH development.

Materials and methods

Animals and housing

Animal experiments were approved by an independent Animal Care and Use Committee and were in compliance with European Community specifications for the use of laboratory animals.

Time-course cohort study: Male 9-week old wild-type C57BL/6J mice (n=84) were obtained from Charles River Laboratories (L'Arbresle Cedex, France). After an acclimatisation period of 3 weeks on chow diet (R/M-H, Ssniff Spezialdieten GmbH, Soest, Germany; containing: 33 kcal% protein, 58 kcal% carbohydrate and 9 kcal% fat), mice were matched into 7 groups of n=12 mice each based on body weight. One group was sacrificed after matching to define the starting condition of the experiment (t=0). Three groups were treated with high-fat diet (HFD; D12451, Research Diets Inc., New Brunswick, USA; with 20 kcal% protein, 35 kcal% carbohydrate and 45 kcal% fat from lard) and three control groups remained on chow. Mice had ad libitum access to food and water and groups were sacrificed after 6, 12 and 24 weeks on diet respectively. Plasma samples were collected after 5h fasting at 4-week intervals. Animals were sacrificed by CO_2 asphyxiation, a serum sample was collected by heart puncture; and liver, epididymal (eWAT), mesenteric (mWAT) and inguinal (iWAT) WAT were isolated. A part of the tissues was fixed in formalin and paraffin-embedded for histological analysis, another part was snap-frozen in liquid nitrogen and stored at -80°C for real-time polymerase chain reaction (RT-PCR).

Surgical removal of the epididymal adipose tissue depot (eWAT): In a separate HFD-feeding experiment the contribution of eWAT to NASH development was analysed. Male 9-week old wild-type C57BL/6J mice (Charles River Laboratories, L'Arbresle Cedex, France) were

acclimatised for three weeks and matched in two groups (n=15/group) based on body weight and fasting plasma insulin concentrations after 12 weeks of HFD feeding. All mice were injected subcutaneously with carprofen analgesic (5 mg/kg) 30 minutes prior to surgery and anaesthetised with isoflurane during surgery. In the eWATx group, both eWAT fat pads were surgically removed through a mid-ventral abdominal incision as described [17]. Testes were visualised and the attached epididymal fat pads were carefully removed and weighed, without damaging the testicular blood supply. In the sham group, a mid-ventral incision was made and the epididymal fat pads were visualised, i.e. fat pads were pulled out, but were left intact and placed back inside the peritoneal cavity. One animal from the eWATx group died during surgery and was therefore excluded from the study. Daily food intake and body weight regain were evaluated to determine recovery from surgery. After surgery, mice continued HFD feeding for another 12 weeks and were then sacrificed for histological evaluation of livers.

Histological, biochemical, lipidomic and gene expression analyses
A detailed description of biochemical, lipidomic and gene expression analyses is provided in Supplement 1. For histological analysis of livers, 5-μm-thick cross sections were stained with Haematoxylin-Eosin (HE). NAFLD was scored blindly using a general scoring system for rodent models which is based on the human NAS grading criteria [18]. Briefly, microvesicular steatosis and macrovesicular steatosis were scored separately and expressed as a percentage of the cross-sectional area. Hepatic inflammation was analysed by counting the number of inflammatory foci per field at a 100x magnification (view size 3.1 mm^2) in five different fields per specimen. For WAT, paraffin-embedded cross sections (5 μm thick) were stained with Haematoxylin-Phloxine-Saffron (HPS) for quantification of adipocyte size and CLS using an Olympus BX51 microscope and CellˆD software (Olympus, Zoeterwoude, the Netherlands). The number of CLS was counted in 5 fields (100x magnification) per mouse and depot and data were expressed as number of CLS per 1000 adipocytes.

Statistical analysis
All data are presented as mean±SEM. Significance of differences in continuous variables between HFD-fed and chow-fed animals was tested using Student's t-tests. Changes over time between the different HFD groups (t=0, 6, 12 and 24 weeks) were statistically analysed by One-way ANOVA and Tukey post-hoc tests (for normally distributed variables). Non-normally distributed variables were tested by non-parametric Kruskal-Wallis test followed by Mann-Whitney U tests. Statistical significance of differences between SHAM and eWATx was tested using unpaired one-sided t-tests. Paired two-sided t-tests were used to calculate the significance

of induction of inflammatory mediators in plasma (fatty acids and adipokines) between week 12 and week 24 (i.e. before and after surgery) within each group. Results were considered statistically significant at p<0.05. Analyses were performed using Graphpad Prism software (version 6, Graphpad Software Inc. La Jolla, USA).

Results

Time-resolved analysis of HFD-induced obesity, hyperinsulinemia and hyperglycemia in a cohort of mice

Mice had an average body weight of 26.2±1.0 g at the start of the experiment (t=0). Body weight was already significantly higher in mice on a HFD compared with control mice after 4 weeks of diet feeding and HFD-fed mice reached a final body weight of 51.6±0.8g versus 33.3±0.7g in chow-fed control mice at 24 weeks of diet feeding (Fig. 1A). HFD feeding significantly increased fasting plasma insulin (8.2±0.2 ng/mL) compared with chow (1.6±0.2 ng/mL) (Fig. 1B). The HFD effect on insulin was accompanied by a significant increase in fasting plasma glucose (15.1±0.5 mM), compared with chow (10.9±0.4 mM) (Fig. 1C).
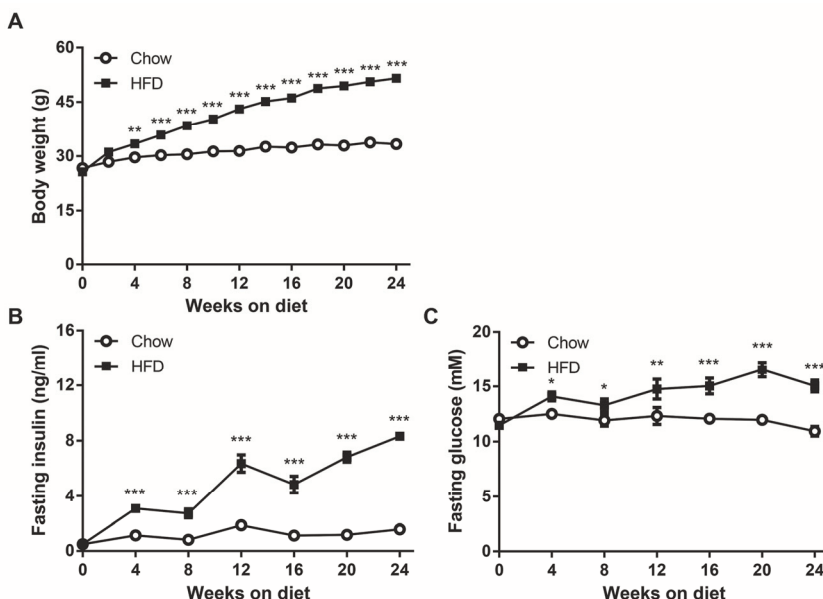

Figure 1. Time-course analysis of the effect of HFD on body weight and metabolic parameters. (A) HFD feeding increased body weight compared with chow control diet. HFD feeding gradually increased fasting plasma concentrations of (B) insulin and (C) glucose compared with chow. Data are mean±SEM (n=12/group per time point), *p<0.05,**p<0.01,***p<0.001 versus chow control.

Plasma triglyceride concentrations were comparable between HFD- and chow-treated groups and decreased slightly over time (not shown). Altogether, these data show that HFD-treated mice developed obesity, hyperinsulinaemia and hyperglycaemia, all of which are associated with NAFLD.

HFD feeding induces liver steatosis by week 12 which progresses to NASH

Livers collected after t=0, 6, 12 and 24 weeks of diet feeding were analysed for presence of steatosis and inflammatory cell aggregates to evaluate development of NASH (representative images shown in Fig. 2A). HFD feeding resulted in modest steatosis by week 12 which intensified significantly towards the end of the study, while chow-fed mice showed no steatosis and had normal liver histology at all time points (not shown). Quantification of distinct forms of steatosis, i.e. micro- and macrovesicular steatosis, demonstrated a gradual increase in HFD-induced microvesicular steatosis over time (Fig. 2B). In contrast, macrovesicular steatosis (a hallmark of overt human NASH [4]) had hardly developed by week 12, but was significantly increased in week 24 (Fig. 2C). HFD-induced liver steatosis could be attributed to significant increases in liver triglycerides as measured biochemically in corresponding liver homogenates (Fig. 2D). Lobular inflammation was specifically induced by HFD (Fig. 2E), not by chow, and showed a time pattern similar to that of macrovesicular steatosis.
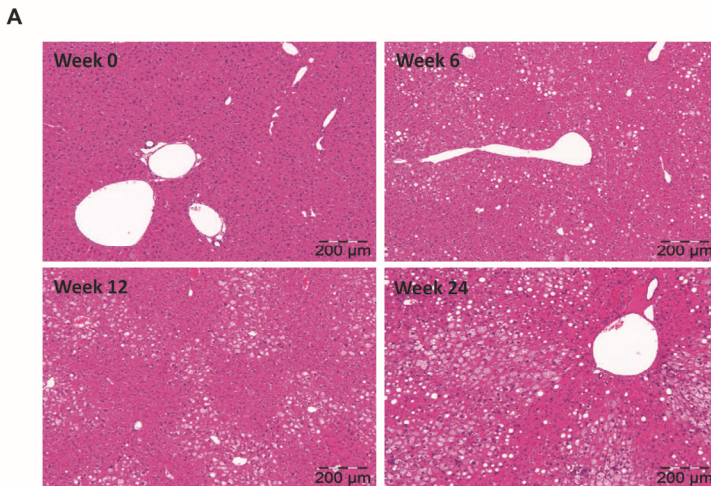

Figure 2. Time-resolved development of NAFLD induced by HFD feeding. (A) Representative photomicrographs of HE-stained liver cross sections of mice treated with HFD for 0, 6, 12 or 24 weeks (magnification 100x). *Figure continued on next page.*
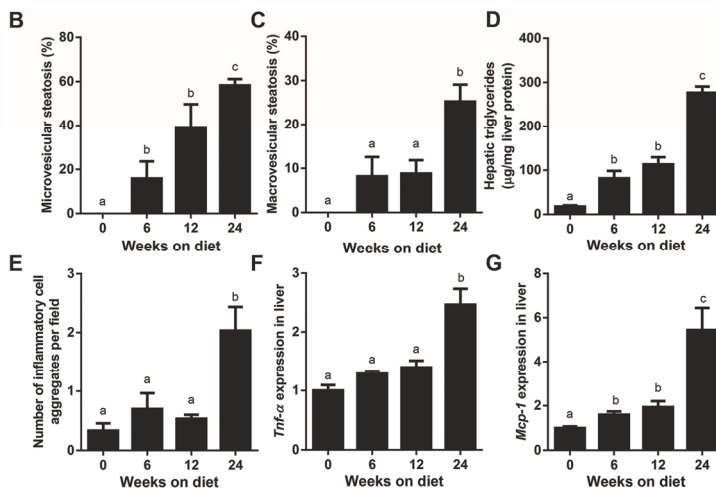
Figure 2 (*continued*). Histological analysis of (B) microvesicular and (C) macrovesicular steatosis as a percentage of the cross-sectional area (n=6-12/group per time point). (D) Biochemical quantification of hepatic triglyceride content (n=11-12/group). (E) Development of lobular inflammation in liver over time defined as the number of inflammatory cell aggregates (n=6-12/group per time point) per field at 100x magnification. (F) Gene expression of TNF-α and (G) MCP-1 in liver over time. Data (n=8/group) are expressed as fold-change in gene expression relative to t=0. Data are mean±SEM. [a,b,c] Mean values with unlike letters differ significantly from each other (p<0.05).

More specifically, the number of inflammatory cell aggregates (an indicator of lobular inflammation [18]) remained low until week 12 and increased significantly by week 24. HFD-induced lobular inflammation was accompanied by significantly increased TNF-α and MCP-1/Ccl2 gene expression in livers at t=24 weeks (Fig. 2F-G).Taken together, these data demonstrate that 12 weeks of HFD feeding resulted in bland steatosis which progressed to NASH by week 24 as demonstrated by the establishment of pronounced macrovesicular steatosis and lobular inflammation.

Epididymal WAT depot is prone to develop HFD-induced inflammation

We next examined whether the epididymal (eWAT), mesenteric (mWAT) and inguinal (iWAT) depots differ in their susceptibility to develop inflammation during HFD feeding, and defined the time point at which CLS formation started in the various depots. HFD feeding led to an increase in the mass of eWAT, mWAT and iWAT depots over time (Fig. 3A), while the mass of the depots remained unchanged on chow (not shown). eWAT mass was increased strongly by week 6 and reached a maximum already in week 12 (2.4±0.1g). In contrast, the mass of mWAT and iWAT increased continuously over time until the end of the experiment (Fig. 3A). In all WAT depots, adipocytes increased in size during HFD feeding, indicating that

adipocyte expansion is a generic response of all WAT depots. However, the adipocytes in eWAT rapidly reached a maximal size by week 6 (Fig. 3B). Adipocytes in the other depots were still smaller at this time point and their size increased more slowly and gradually until the end of the study. Notably, first CLS were observed specifically in eWAT by week 6, and their numbers were increased greatly by week 12 when the maximal capacity of eWAT seemed to be reached (viz. maximal mass and maximal adipocyte size) (Fig. 3C). CLS formation in eWAT was more rapid and pronounced than in mWAT and iWAT (Fig. 3C-D) indicating that eWAT is most prone to develop HFD-induced inflammation. In mWAT, CLS numbers increased later than in eWAT (by week 24), at the time that maximal average adipocyte size was reached, essentially as observed in eWAT. These observations show that the expandability of a depot (and its adipocytes) is limited and that this depot-specific restriction seems critical for the development of inflammation. In all, our time-resolved histological analyses show that HFD-induced WAT inflammation starts in a specific depot (eWAT) and increases strongly when eWAT has expanded maximally (at t=12 weeks). Importantly, eWAT inflammation coincides with bland steatosis and hence precedes the development of NASH.
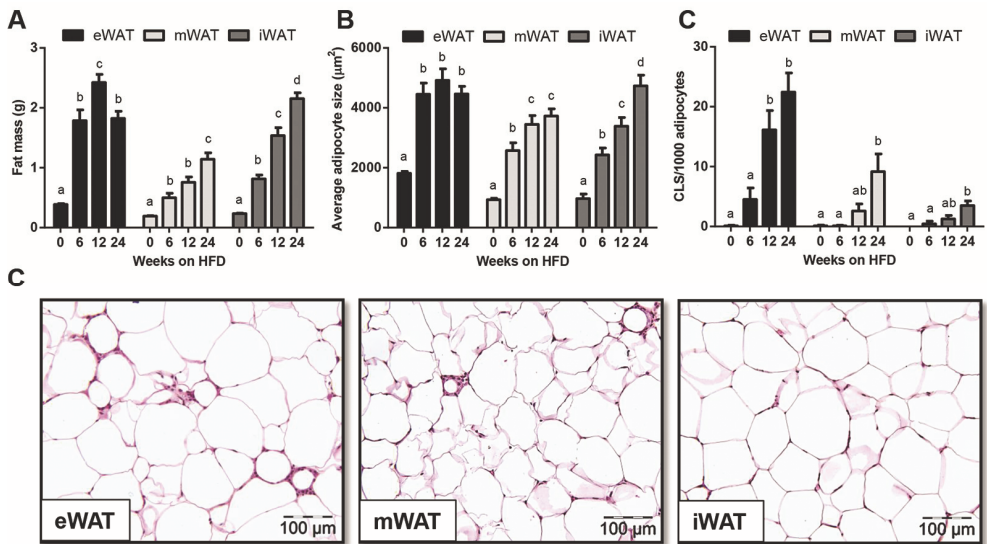
Figure 3. Effect of HFD feeding on the quantity and inflammatory state of the epididymal (eWAT), mesenteric (mWAT) and inguinal (iWAT) white adipose tissue (WAT) depots. (A) Mass of eWAT, mWAT and iWAT depot during HFD-feeding time-course experiment (n=12/group per time point). (B) Development of adipocyte cell size of the different WAT depots quantified by morphometric analysis of HPS-stained sections. (C) Quantitative analysis of the number of crown-like structures (CLS) in the different WAT depots over time (n=8-12/group per time point). (D) Representative images of HPS-stained cross-sections of eWAT, mWAT and iWAT after 24 weeks of HFD (magnification 200x). Data are mean±SEM. [a,b,c,d] Mean values with unlike letters differ significantly from each other ($p<0.05$).

Surgical removal of inflamed eWAT attenuates NASH development

To examine whether eWAT is causally involved in the progression of liver steatosis to NASH, we performed a separate HFD-feeding experiment in which eWAT was surgically removed in one group (eWATx) and compared with a SHAM surgery control group (SHAM). The surgery was performed after 12 weeks of HFD feeding, i.e. at the time point at which livers in the above time-course experiment were steatotic and eWAT was inflamed.

Body weight at the time of surgery was comparable between SHAM and eWATx groups (SHAM: 42.3±1.2 g, and eWATx: 42.3±0.9 g; Fig. 4A). On average, 1.9±0.1 g of eWAT was removed and this reduction in fat mass was reflected in the body weight of eWATx mice on the day after surgery (SHAM: 41.6±1.7 g; and eWATx: 39.5±1.2 g, not shown). CLS were abundantly present in this tissue, confirming pronounced inflammation at the time of surgery (Fig. 4B).
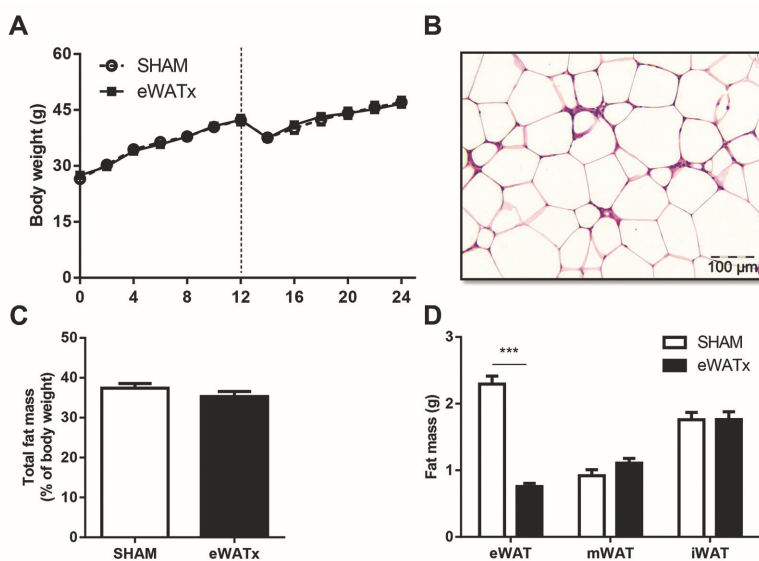
Figure 4. Effect of surgical removal of eWAT on body weight and other WAT depots. Mice were fed HFD and, on average, 1.9 gram of eWAT was carefully removed after 12 weeks of HFD. (A) Body weight development of the eWATx and SHAM group. The dashed line indicates the time point of surgery. (B) Representative image of a HPS-stained eWAT cross-section showing presence of inflammatory cells and CLS at time of removal (magnification 200x). (C) Analysis of total fat mass measured by EchoMRI in week 24 of HFD. (D) Mass of eWAT, mWAT and iWAT isolated at the end of the study (24 weeks of HFD) in eWATx and SHAM group. The eWAT mass of eWATx mice was significantly lower than in SHAM. Data also show that mWAT and iWAT did not compensate for the removed eWAT. Data are mean±SEM (n=14-15/group),***$p<0.001$ versus SHAM.

Food intake was comparable between the eWATx and SHAM group throughout the study. The total body weight at the end of the experiment was 47.1±1.3 g in SHAM and 46.7±0.9 g in eWATx, and whole-body fat mass determined by EchoMRI was slightly lower in eWATx mice (not significant, Fig. 4C), while lean mass was comparable between the groups (SHAM: 29.1±0.6 g vs. eWATx: 29.7 ±0.4 g, ns). Fasting plasma glucose concentrations increased during the experiment, essentially as observed in the time-course study, and hyperglycaemia was comparable between groups (SHAM: 14.6±0.7 mM vs. eWATx: 15.2±0.6 mM; ns). Isolation of individual fat depots after sacrifice in week 24 showed that eWAT mass was significantly reduced in eWATx mice (Fig. 4D). The mass of mWAT, iWAT (Fig. 4D), retroperitoneal WAT and brown AT (not shown) was comparable between groups indicating that these depots did not compensate for the removed eWAT. Also, the weight of heart and kidneys was comparable between the groups (not shown).

Histological analysis of livers revealed that eWATx mice exhibited a similar degree of micro- and macrovesicular steatosis to SHAM mice (Fig. 5A-C). Biochemical analysis of liver triglycerides showed no significant difference between the groups (SHAM: 160.8±18.9 µg/mg liver protein vs. eWATx: 170.5±16.2 µg/mg liver protein; ns). Minor liver lipids (cholesteryl esters and free cholesterol) were also comparable between the groups (data not shown). Remarkably, eWATx livers displayed a significantly reduced number of inflammatory cell aggregates indicating attenuated NASH development upon eWAT removal (Fig. 5D). Reduced liver inflammation was substantiated by a significantly reduced gene expression of TNF-α (Fig. 5E) and MCP-1 (trend p=0.08; Fig. 5F) in eWATx livers.
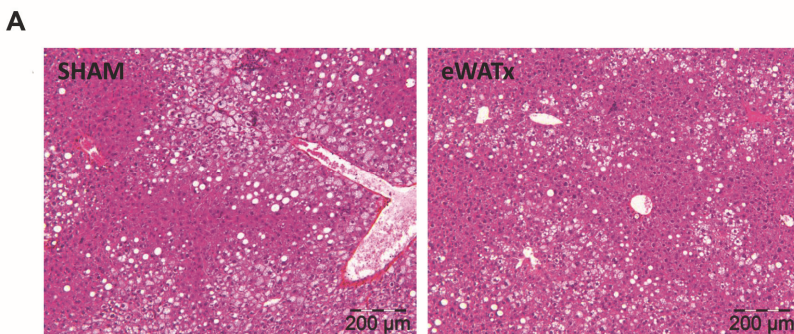
Figure 5. Effect of surgical removal of eWAT on NAFLD development. (A) Representative images of HE-stained liver sections (magnification 100x). *Figure continued on next page.*
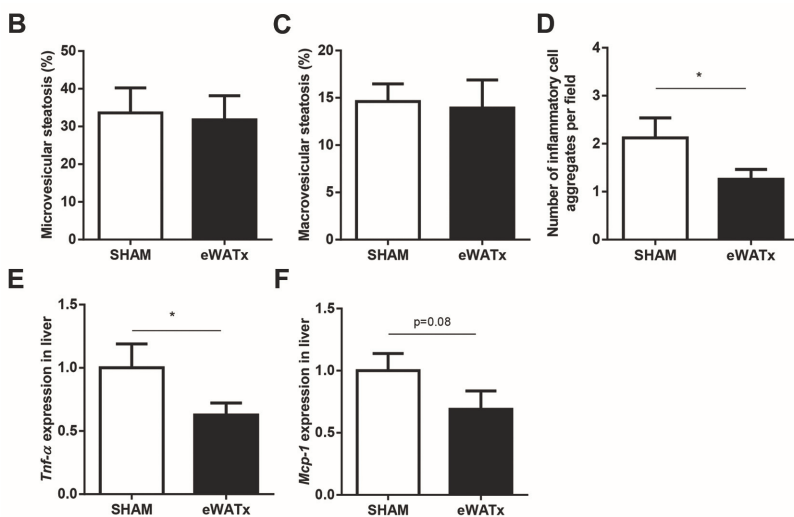
Figure 5 (*continued*). Quantification of (B) microvesicular steatosis and (C) macrovesicular steatosis as percentage of the cross-sectional liver area (n=14-15/group). (D) Number of inflammatory cell aggregates in livers of eWATx and SHAM mice. Liver gene expression of (E) TNF-α and (F) MCP-1 in eWATx and SHAM. Real-time PCR data are expressed as fold-change in gene expression relative to SHAM (n=8/group). Data are mean±SEM,*$p<0.05$.

Surgical removal of eWAT affects circulating levels of pro-inflammatory mediators

The effects of eWAT removal on adipokines and lipids associated with NAFLD development were assessed. In eWATx, the IL-6 serum concentrations were slightly lower (5.5±2.6 pg/ml) than in SHAM (7.0±2.5 pg/ml, not shown) but the difference was not statistically significant. The eWATx and SHAM groups also had comparable plasma concentrations of MCP-1 (86.6±11.7 pg/ml vs. 80.8±13.3 pg/ml; ns) and adiponectin (13.6±1.1 μg/ml vs. 14.3±1.2 μg/ml; ns). In contrast, plasma leptin concentrations increased significantly in SHAM mice and this increase was not observed in eWATx mice (Fig. 6A). Plasma leptin levels correlated positively (r^2=0.7; p=0.01) with hepatic Mcp-1 expression, suggesting a link to hepatic inflammation.

We next profiled circulating (pro-inflammatory) lipids using lipidomics to define the most abundant lipid species in plasma (Fig. 6B), and subsequently analysed whether eWATx removal affected the levels of these lipids (Table 1). Saturated fatty acids (SFA) were the most abundant lipid species after 12 weeks of HFD feeding (prior to surgery), followed by monounsaturated fatty acids (MUFA), and n-6 and n-3 polyunsaturated fatty acids (PUFA) (Fig. 6B). Within the SFA, C16:0 (palmitic acid), C18:0 (stearic acid) and C14:0 (myristic acid) were most abundant. Within the class of MUFA C18:1n9 (oleic acid) and C16:1n7 (palmitoleic acid) were circulating at high levels, and within the PUFA, C20:4n3 (eicosatetraenoic acid) and C18:2n6 (linoleic acid) were most abundant.
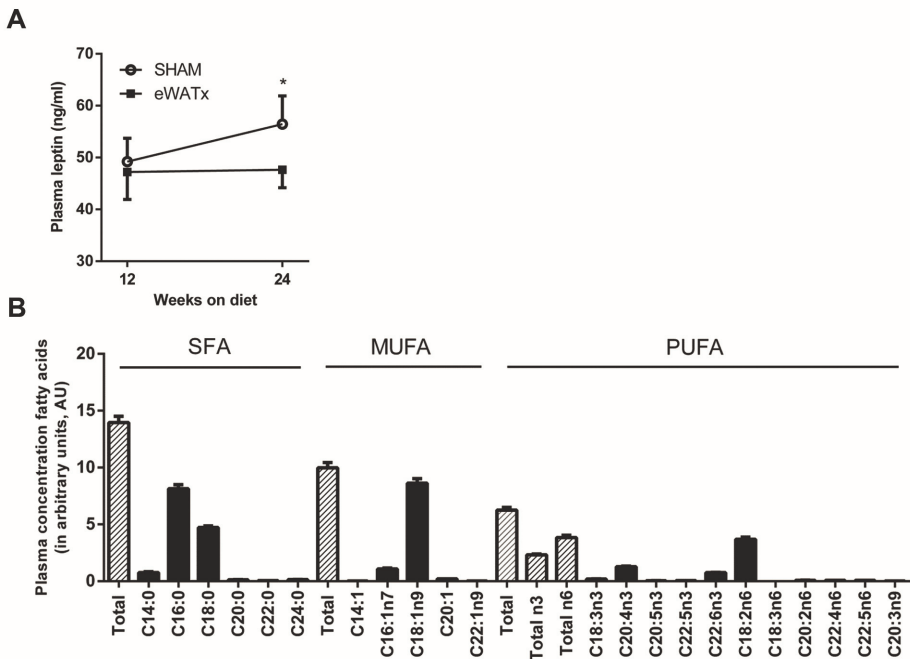
Figure 6. Effect of surgical removal of eWAT on circulating inflammatory mediators and lipids. (A) Plasma concentrations of leptin prior to surgery at 12 weeks of HFD, and at the end of the experiment (24 weeks) in eWATx and SHAM group. Data are mean±SEM,*p<0.05 according to paired Student's t-test. (B) Profiling of plasma lipids after 12 weeks of HFD by lipidomic analysis. Fasting plasma was collected before surgery. The levels of saturated free fatty acids (SFA), monounsaturated fatty acids (MUFA) and polyunsaturated fatty acids (PUFA) are shown and the most abundant lipid species of each category are indicated. Data are mean±SEM and expressed as arbitrary units (AU) relative to internal standard.

Table 1 shows that the levels of total SFA, and palmitic acid in particular (+1.4; p<0.05), increase in SHAM while such an increase was not observed in eWATx. Myristic acid and several of the less abundant SFA (C20:0, C22:0, C24:0) decreased significantly after eWAT removal. Furthermore, total MUFA increased strongly over time in SHAM (+3.7; p<0.05), mainly due to significant rises in palmitoleic, oleic and eicosenoic acids. In contrast, there was no significant change over time in any of the MUFA in the eWATx group. Total PUFA levels increased in both SHAM (+2.0) and eWATx (+1.5). The observed changes in SFA and MUFA support the notion that removal of eWAT prevents the development of a pro-inflammatory state.

Table 1. Change in plasma fatty acid levels in SHAM and eWATx

Fatty acid	SHAM (Δ change)	eWATx (Δ change)
Saturated fatty acids	1.3 ± 0.8	-0.3 ± 1.0
Myristic acid (C14:0)	0.02 ± 0.1	-0.3 ± 0.2
Palmitic acid (C16:0)	1.4 ± 0.5*	-0.1 ± 0.6
Stearic acid (C18:0)	-0.03 ± 0.3	0.4 ± 0.2
Arachidic acid (C20:0)	-0.01 ± 0.0	-0.05 ± 0.0*
Behenic acid (C22:0)	-0.01 ± 0.0	-0.04 ± 0.0*
Lignoceric acid (C24:0)	-0.02 ± 0.0	-0.1 ± 0.1*
Monounsaturated fatty acids	3.7 ± 0.9*#	0.8 ± 0.8
Myristoleic acid (C14:1)	0.0 ± 0.0	0.0 ± 0.0
Palmitoleic acid (C16:1n7)	0.5 ± 0.2*	0.2 ± 0.1
Oleic acid (C18:1n9)	3.1 ± 0.8*#	0.6 ± 0.7
Eicosenoic acid (C20:1)	0.1 ± 0.0*	0.03 ± 0.0
Erucic acid (C22:1n9)	0.004 ± 0.0	-0.003 ± 0.0
Polyunsaturated fatty acids	2.0 ± 0.6*	1.5 ± 0.4*
Total n-6 fatty acids	1.7 ± 0.5*	1.0 ± 0.3*
Total n-3 fatty acids	0.3 ± 0.1*	0.5 ± 0.1*
Linoleic acid (C18:2n6)	1.7 ± 0.5*	1.0 ± 0.3*
γ-linolenic acid (C18:3n6)	0.0 ± 0.0	0.0 ± 0.0
Eicosadienoic acid (C20:2n6)	0.03 ± 0.0*	0.02 ± 0.0*
Adrenic acid (C22:4n6)	0.02 ± 0.0*	0.03 ± 0.0*
Docosapentaenoic acid (C22:5n6)	0.02 ± 0.0*	0.01 ± 0.0
α-linolenic acid (C18:3n3)	0.1 ± 0.0	0.2 ± 0.0
Eicosatetraenoic acid (C20:4n3)	0.1 ± 0.1	0.3 ± 0.1*
Eicosapentaenoic acid (C20:5n3)	0.01 ± 0.0	0.01 ± 0.0*
Docosapentaenoic acid (C22:5n3)	0.01 ± 0.0*	0.02 ± 0.0*
Docosahexaenoic acid (C22:6n3)	0.1 ± 0.0*	0.1 ± 0.0*
Mead acid (C20:3n9)	0.01 ± 0.0*	0.01 ± 0.0*

Delta (Δ) change in plasma lipids between week 12 and 24, i.e. before and after surgery. Data are in arbitrary units (mean±SEM). *$p \leq 0.05$ indicates significant changes over time within a group. #$p < 0.05$ indicates significant difference between SHAM (n=11) and eWATx (n=12).

Discussion

NAFLD is strongly associated with obesity but the pathogenesis of the disease, and in particular the role of WAT, is poorly understood. It has been proposed that inflammation in WAT may play a critical role in obesity-induced NAFLD development [4, 14, 19, 20], but evidence for causality is lacking. This study shows that HFD-induced inflammation in eWAT develops more rapidly than in mWAT or iWAT, and that this inflammation precedes overt NASH. Notably, pronounced CLS formation was observed in eWAT once the adipocytes of this tissue did not further increase in size and the depot had reached a maximal mass (week 12 of HFD feeding). A subsequent experiment showed that removal of the inflamed eWAT depot at week 12 attenuates liver inflammation and reduces the development of NASH. Removal of eWAT affected the circulating levels of specific pro-inflammatory mediators among which leptin and specific lipids (e.g. palmitic acid), providing a rationale for the observed hepatoprotective effect.

The time-course analysis of HFD-induced NAFLD shows that a particular intra-abdominal depot in mice, eWAT, is prone to develop tissue inflammation characterised by presence of macrophages and CLS. Consistent with this finding, other groups have reported that eWAT of obese HFD-treated mice exhibits a higher number of CLS than mesenteric and subcutaneous (inguinal) WAT depots [21, 22]. Differences in macrophage content appear already to exist in lean C57BL/6 mice: Altinas et al. [21] showed that the subcutaneous depot differs from the intra-abdominal depots with respect to immune cell composition and density. For instance, the density of solitary adipose tissue macrophages (ATM) in subcutaneous WAT is much lower than in intra-abdominal depots such as eWAT [21]. Hence, the relatively high number of solitary ATM in eWAT may predispose this depot to develop CLS more rapidly in response to HFD than other depots analysed in this study. In obese subjects, CLS are also more prevalent in abdominal (omental) WAT than in subcutaneous WAT [5, 23] suggesting that, in humans, intra-abdominal depots are also more prone to become inflamed than subcutaneous depots, and that our observations are not restricted to mice.

We found that the number of CLS in eWAT increased strongly once this depot had reached a maximal mass and concomitantly no further increase in adipocyte size was observed. In line with this, other groups have reported that the weight of eWAT typically does not exceed about 2.5 grams [12, 22, 24, 25]. This limitation in eWAT mass has been observed with different diets and in different strains of mice pointing to a generic threshold of eWAT independent of the experimental conditions employed. Consistent with this, Virtue and Vidal-Puig [26] proposed

that organisms possess a maximum capacity for adipose expansion, and failure in the capacity for adipose tissue expansion, rather than obesity per se may underlie the development of inflammation. Indeed, also in the case of mWAT, CLS numbers increased at week 24, i.e. after the average adipocyte size had reached a maximum. Little is known about the mediators that control WAT expansion during diet-induced obesity. It is possible that localised cytokine production limits further WAT expansion: Salles et al. [27] showed that TNF-α knockout mice have two-fold more eWAT mass than wild-type mice during HFD feeding. In support of this notion, increased TNF-α gene expression in eWAT was observed after attainment of maximal adipocyte size in an experiment conducted under conditions comparable to those applied herein [22]. Together, our time-resolved analysis of the inflammatory component in diet-induced obesity shows that WAT inflammation develops sequentially across depots.

C57BL/6 mice constitute a frequently used model to study diet-induced obesity and associated comorbidities. For the interpretation of these studies, it is important to recognise that development of inflammation upon HFD-feeding is a very complex and dynamic process involving multiple tissues, including WAT and liver [11, 15]. As demonstrated herein, the different WAT depots become inflamed at specific time points during HFD feeding, rather than simultaneously. Because animal studies often analyse a single WAT depot (frequently the eWAT) at one particular time point during HFD feeding, conclusions about the condition of 'adipose tissue in general' or the inflammatory state in other depots should be made with caution. Our results support a more comprehensive analysis of WAT (with precise specification of the intra-abdominal depots analysed), and advocates the study of the cross-talk between organs in NAFLD. For instance, between 12 and 24 weeks of HFD, i.e. the period in which eWAT was inflamed and did not further expand, we observed a pronounced increase in triglyceride concentrations in the liver. This supports the concept that, once the expansion limit of a particular WAT depot has been reached, adipose tissue ceases to store energy efficiently and lipids begin to accumulate as ectopic fat in other tissues [26].

In patients, the accumulation of intra-abdominal WAT is strongly associated with progressive NASH [9]. In this study, hepatic inflammation and fibrosis augmented incrementally with increases in intra-abdominal fat mass. Importantly, intra-abdominal fat of patients was directly associated with liver inflammation and fibrosis independent of insulin resistance and hepatic steatosis [9, 10]. Consistent with this, removal of eWAT in the present study attenuated NASH development without an effect on hyperinsulinemia, hyperglycemia and liver steatosis. A possible explanation for the strong association between abdominal WAT mass and NASH

severity in the liver may lie in the anatomical distance between both tissues. Inflammatory mediators from the intra-abdominal depots can reach the liver relatively easily (venous drainage via the portal vein) [28]. In contrast, associations between systemically drained adipose tissue depots (e.g. the deep layer of subcutaneous WAT in the abdominal area) and NASH are rare [29] suggesting that these depots only play a minor role in the pathogenesis of NASH.

While the above studies mainly focused on the quantity of adipose tissue, increasing evidence also points to a role of its inflammatory state. Livers of obese subjects with inflamed intra-abdominal (omental) WAT contain more fibro-inflammatory lesions than livers of equally obese subjects without WAT inflammation [5, 10]. This observation suggests that inflammation in a specific WAT depot contributes to the inflammatory component in human NASH. The present study supports this view, because surgical removal of inflamed eWAT reduced liver inflammation (about 40% fewer inflammatory aggregates). Of note, intra-abdominal eWAT in mice has no human equivalent and our findings should not be generalised with respect to the role of other WAT depots. Because of the close relationship between visceral obesity and NASH development in patients [9], it is possible that inflamed visceral WAT depots, such as mesenteric WAT, may contribute to NASH in a way similar to eWAT. For instance, mesenteric WAT develops similar features of inflammation to those observed in eWAT, including formation of CLS during WAT expansion and expression of pro-inflammatory mediators (e.g. cytokines, adipokines, fatty acids), in both mice [30, 31] and humans [32, 33]. Furthermore, pro-inflammatory mediators that are released by mesenteric WAT can not only reach the liver via systemic drainage (like eWAT) but also via the portal vein, which constitutes a more direct connection to the liver [28]. However, additional studies are needed to investigate the contribution of inflamed mesenteric WAT to NASH development.

Specific circulating factors have been proposed as inducers of liver inflammation in NASH [19, 20]. Among these mediators are cytokines/adipokines (including IL-6, TNF-α, leptin, and adiponectin) and specific lipids with reported activities on liver cells [4, 13, 14, 19]. Of the adipokines measured in the present study, only plasma leptin differed between the eWATx and the SHAM group. Several studies have shown that leptin exerts pro-inflammatory and pro-fibrogenic effects on liver cells [34, 35]. For instance, leptin stimulates hepatic stellate cells to express the pro-inflammatory cytokine MCP-1 [34], a chemotactic factor and critical mediator of lobular inflammation [36]. In line with this, we observed that plasma leptin concentrations correlated with MCP-1 gene expression in the liver. Besides

cytokines/adipokines, certain lipid mediators (e.g. SFA with TLR4 binding properties) have also been implicated in the pathogenesis of NASH. For example, *in vitro* studies have shown that SFA, and in particular palmitic acid, can trigger inflammation via the NFκB pathway and thereby induce TNF-α production [37]. In SHAM mice, palmitic acid levels increased significantly between 12 and 24 weeks of HFD feeding, i.e. during the progression from NAFL to NASH. This increase was not observed in eWATx mice and in line with this, hepatic TNF-α expression was lower than in SHAM mice. A total plasma lipid analysis in humans showed that obese subjects with NAFL and NASH have significantly elevated MUFA levels relative to lean controls [38]. Among these MUFA were palmitoleic acid and oleic acid, which also increased after surgery in SHAM while they did not change significantly in eWATx. The observed increases in MUFA (both in humans and mice) may be an adaptive response to protect the liver from the lipotoxic effects of SFA (i.e. palmitic acid). As MUFAs themselves can suppress liver inflammation in mice [39], it is thus likely that increased levels of palmitic acid in SHAM mice are critical for the development of liver inflammation.

Collectively, this study demonstrates that obesity-induced inflammation develops progressively across various WAT depots, starting in eWAT. Surgical excision of inflamed eWAT shows that this depot participates in the development of NASH. Hence, interventions that target WAT may have significant therapeutic benefit for the treatment of NASH in the context of obesity.

Acknowledgements

Declaration of interests

The authors declare that they have no conflict of interest.

References

1. de Alwis NM, Day CP. Non-alcoholic fatty liver disease: the mist gradually clears. J Hepatol. 2008;48 Suppl 1:S104-12. doi:10.1016/j.jhep.2008.01.009.

2. Loomba R, Sanyal AJ. The global NAFLD epidemic. Nature Reviews Gastroenterology and Hepatology. 2013;10(11):686-90. doi:10.1038/nrgastro.2013.171.

3. Musso G, Gambino R, De Michieli F, Cassader M, Rizzetto M, Durazzo M, et al. Dietary habits and their relations to insulin resistance and postprandial lipemia in nonalcoholic steatohepatitis. Hepatology. 2003;37(4):909-16. doi:10.1053/jhep.2003.50132.

4. Tiniakos DG, Vos MB, Brunt EM. Nonalcoholic

fatty liver disease: Pathology and pathogenesis. Annu Rev Pathol. 2010;5:145-71. doi:10.1146/annurev-pathol-121808-102132.

5. Cancello R, Tordjman J, Poitou C, Guilhem G, Bouillot JL, Hugol D, et al. Increased infiltration of macrophages in omental adipose tissue is associated with marked hepatic lesions in morbid human obesity. Diabetes. 2006;55(6):1554-61. doi:10.2337/db06-0133.

6. Krawczyk K, Szczesniak P, Kumor A, Jasinska A, Omulecka A, Pietruczuk M, et al. Adipohormones as prognostric markers in patients with nonalcoholic steatohepatitis (NASH). J Physiol Pharmacol. 2009;60 Suppl 3:71-5.

7. Lemoine M, Ratziu V, Kim M, Maachi M, Wendum D, Paye F, et al. Serum adipokine levels predictive of liver injury in non-alcoholic fatty liver disease. Liver International. 2009;29(9):1431-8. doi:10.1111/j.1478-3231.2009.02022.x.

8. Nehra V, Angulo P, Buchman AL, Lindor KD. Nutritional and metabolic considerations in the etiology of nonalcoholic steatohepatitis. Dig Dis Sci. 2001;46(11):2347-52. doi:10.1023/A:1012338828418.

9. van der Poorten D, Milner KL, Hui J, Hodge A, Trenell MI, Kench JG, et al. Visceral fat: A key mediator of steatohepatitis in metabolic liver disease. Hepatology. 2008;48(2):449-57. doi:10.1002/hep.22350.

10. Tordjman J, Poitou C, Hugol D, Bouillot J-L, Basdevant A, Bedossa P, et al. Association between omental adipose tissue macrophages and liver histopathology in morbid obesity: Influence of glycemic status. J Hepatol. 2009;51(2):354-62. doi:10.1016/j.jhep.2009.02.031.

11. Liang W, Tonini G, Mulder P, Kelder T, van Erk M, van den Hoek AM, et al. Coordinated and interactive expression of genes of lipid metabolism and inflammation in adipose tissue and liver during metabolic overload. PLoS One. 2013;8(9):e75290. doi:10.1371/journal.pone.0075290.

12. Duval C, Thissen U, Keshtkar S, Accart B, Stienstra R, Boekschoten MV, et al. Adipose tissue dysfunction signals progression of hepatic steatosis towards nonalcoholic steatohepatitis in C57BL/6 mice. Diabetes. 2010;59(12):3181-91. doi:10.2337/db10-0224.

13. Suganami T, Tanaka M, Ogawa Y. Adipose tissue inflammation and ectopic lipid accumulation. Endocr J. 2012;59(10):849-57. doi:10.1507/endocrj.EJ12-0271.

14. Tordjman J, Guerre-Millo M, Clément K. Adipose tissue inflammation and liver pathology in human obesity. Diabetes Metab. 2008;34(6, Part 2):658-63. doi:10.1016/S1262-3636(08)74601-9.

15. Caesar R, Manieri M, Kelder T, Boekschoten M, Evelo C, Muller M, et al. A combined transcriptomics and lipidomics analysis of subcutaneous, epididymal and mesenteric adipose tissue reveals marked functional differences. PLoS One. 2010;5(7):e11525. doi:10.1371/journal.pone.0011525.

16. Cinti S. The adipose organ: morphological perspectives of adipose tissues. The Proceedings of the Nutrition Society. 2001;60(3):319-28. doi:10.1079/PNS200192.

17. Harris RB, Hausman DB, Bartness TJ. Compensation for partial lipectomy in mice with genetic alterations of leptin and its receptor subtypes. American Journal of Physiology - Regulatory, Integrative and Comparative Physiology. 2002;283(5):R1094-103. doi:10.1152/ajpregu.00339.2002.

18. Liang W, Menke AL, Driessen A, Koek GH, Lindeman JH, Stoop R, et al. Establishment of a general NAFLD scoring system for rodent models and comparison to human liver pathology. PLoS One. 2014;9(12):e115922. doi:10.1371/journal.pone.0115922.

19. Mirza MS. Obesity, visceral fat, and NAFLD: Querying the role of adipokines in the progression of nonalcoholic fatty liver disease. ISRN gastroenterology. 2011;2011:592404. doi:10.5402/2011/592404.

20. Tilg H, Moschen AR. Evolution of inflammation in nonalcoholic fatty liver disease: The multiple parallel hits hypothesis. Hepatology. 2010;52(5):1836-46. doi:10.1002/hep.24001.

21. Altintas MM, Azad A, Nayer B, Contreras G, Zaias J, Faul C, et al. Mast cells, macrophages, and crown-like structures distinguish subcutaneous from visceral fat in mice. J Lipid Res. 2011;52(3):480-8. doi:10.1194/jlr.M011338.

22. Strissel KJ, Stancheva Z, Miyoshi H, Perfield JW, 2nd, DeFuria J, Jick Z, et al. Adipocyte death, adipose tissue remodeling, and obesity complications. Diabetes. 2007;56(12):2910-8. doi:10.2337/db07-0767.

23. Harman-Boehm I, Bluher M, Redel H, Sion-Vardy N, Ovadia S, Avinoach E, et al. Macrophage infiltration into omental versus subcutaneous fat across different populations: effect of regional adiposity and the comorbidities of obesity. J Clin

Endocrinol Metab. 2007;92(6):2240-7. doi:10.1210/jc.2006-1811.

24. Lagathu C, Christodoulides C, Tan CY, Virtue S, Laudes M, Campbell M, et al. Secreted frizzled-related protein 1 regulates adipose tissue expansion and is dysregulated in severe obesity. Int J Obes. 2010;34(12):1695-705. doi:10.1038/ijo.2010.107.

25. Larter CZ, Yeh MM, Van Rooyen DM, Teoh NC, Brooling J, Hou JY, et al. Roles of adipose restriction and metabolic factors in progression of steatosis to steatohepatitis in obese, diabetic mice. J Gastroenterol Hepatol. 2009;24(10):1658-68. doi:10.1111/j.1440-1746.2009.05996.x.

26. Virtue S, Vidal-Puig A. Adipose tissue expandability, lipotoxicity and the metabolic syndrome — An allostatic perspective. Biochim Biophys Acta. 2010;1801(3):338-49. doi:10.1016/j.bbalip.2009.12.006.

27. Salles J, Tardif N, Landrier JF, Mothe-Satney I, Guillet C, Boue-Vaysse C, et al. TNFalpha gene knockout differentially affects lipid deposition in liver and skeletal muscle of high-fat-diet mice. Journal of Nutritional Biochemistry. 2012;23(12):1685-93. doi:10.1016/j.jnutbio.2011.12.001.

28. Item F, Konrad D. Visceral fat and metabolic inflammation: The portal theory revisited. Obes Rev. 2012;13 Suppl 2:30-9. doi:10.1111/j.1467-789X.2012.01035.x.

29. Tordjman J, Divoux A, Prifti E, Poitou C, Pelloux V, Hugol D, et al. Structural and inflammatory heterogeneity in subcutaneous adipose tissue: relation with liver histopathology in morbid obesity. J Hepatol. 2012;56(5):1152-8. doi:10.1016/j.jhep.2011.12.015.

30. Kwon EY, Shin SK, Cho YY, Jung UJ, Kim E, Park T, et al. Time-course microarrays reveal early activation of the immune transcriptome and adipokine dysregulation leads to fibrosis in visceral adipose depots during diet-induced obesity. BMC Genomics. 2012;13:450. doi:10.1186/1471-2164-13-450.

31. Murano I, Barbatelli G, Parisani V, Latini C, Muzzonigro G, Castellucci M, et al. Dead adipocytes, detected as crown-like structures, are prevalent in visceral fat depots of genetically obese mice. J Lipid Res. 2008;49(7):1562-8. doi:10.1194/jlr.M800019-JLR200.

32. Bigornia SJ, Farb MG, Mott MM, Hess DT, Carmine B, Fiscale A, et al. Relation of depot-specific adipose inflammation to insulin resistance in human obesity.

Nutrition and Diabetes. 2012;2:e30. doi:10.1038/nutd.2012.3.

33. Fain JN, Madan AK, Hiler ML, Cheema P, Bahouth SW. Comparison of the release of adipokines by adipose tissue, adipose tissue matrix, and adipocytes from visceral and subcutaneous abdominal adipose tissues of obese humans. Endocrinology. 2004;145(5):2273-82. doi:10.1210/en.2003-1336.

34. Aleffi S, Petrai I, Bertolani C, Parola M, Colombatto S, Novo E, et al. Upregulation of proinflammatory and proangiogenic cytokines by leptin in human hepatic stellate cells. Hepatology. 2005;42(6):1339-48. doi:10.1002/hep.20965.

35. Ikejima K, Honda H, Yoshikawa M, Hirose M, Kitamura T, Takei Y, et al. Leptin augments inflammatory and profibrogenic responses in the murine liver induced by hepatotoxic chemicals. Hepatology. 2001;34(2):288-97. doi:10.1053/jhep.2001.26518.

36. Marra F, Tacke F. Roles for chemokines in liver disease. Gastroenterology. 2014;147(3):577-94.e1. doi:10.1053/j.gastro.2014.06.043.

37. Shi H, Strader AD, Woods SC, Seeley RJ. The effect of fat removal on glucose tolerance is depot specific in male and female mice. American Journal of Physiology - Endocrinology and Metabolism. 2007;293(4):E1012-20. doi:10.1152/ajpendo.00649.2006.

38. Puri P, Wiest MM, Cheung O, Mirshahi F, Sargeant C, Min HK, et al. The plasma lipidomic signature of nonalcoholic steatohepatitis. Hepatology. 2009;50(6):1827-38. doi:10.1002/hep.23229.

39. Guo X, Li H, Xu H, Halim V, Zhang W, Wang H, et al. Palmitoleate induces hepatic steatosis but suppresses liver inflammatory response in mice. PLoS One. 2012;7(6):e39286. doi:10.1371/journal.pone.0039286.

Supplemental data

Supplement 1 Detailed material and methods

<u>Biochemical analyses of circulating factors:</u> Plasma was obtained via tail vein bleeding after a 5-hour fast at multiple time points throughout the study. Plasma glucose was quantified using the hexokinase method (Instruchemie, Delfzijl, The Netherlands) and plasma insulin was determined by ELISA (Ultrasensitive mouse insulin ELISA, Mercodia, Uppsala, Sweden). Leptin and adiponectin plasma levels and Mcp-1 serum levels were determined by ELISA (all R&D Systems Ltd., Abington, UK). Serum concentrations of IL-6 and TNF-alpha were quantified by quantikine ELISA assay (R&D Systems Ltd.). TNF-alpha levels were below the detection limit and therefore excluded from the analysis. Lipidomic analysis was performed in plasma samples collected after 5 hours of fasting and according an well-established method for polar lipids, and without hydrolysis of lipids as reported earlier [1]. Reported lipids were identified and quantified using respective specific standards, except for C14:1 (reported as myristoleic acid) and C20:1 (reported as eicosenoic acid). Lipids are expressed as arbitrary units (AU) relative to internal standard.

<u>Analysis of intrahepatic triglycerides:</u> For determination of liver triglycerides, lipids were extracted from liver homogenates using the Bligh and Dyer method [2]. High performance thin-layer chromatography (HPTLC) was then used to separate the extracted lipids with a silica-gel-60 pre-coated plate. Density areas were measured with a Hewlett Packard Scanjet 4500c and lipid concentrations were calculated by Tina software (version-2.09).

<u>Body composition:</u> Total body fat and lean mass in SHAM and eWATx mice was determined using a NMR Echo MRI whole body composition analyser (EchoMRI LLC, Houston, TX, USA) after week 24 of HFD feeding. Total body fat mass was expressed as percentage of total body weight.

<u>Real-time polymerase chain reaction (RT-PCR) gene expression analysis:</u> Total RNA was extracted with RNA Bee Total RNA Isolation Kit (Bio-Connect, Huissen, the Netherlands). RNA concentration was determined using Nanodrop 1000 (Isogen Life Science, De Meern, the Netherlands) and RNA quality was measured using 2100 Bioanalyzer (Agilent Technologies, Amstelveen, the Netherlands). One microgram of total RNA was used to generate cDNA for RT-PCR (High-capacity RNA-to-cDNA kit; 4387406, Life Technologies, Bleiswijk, the Netherlands). RT-PCR was performed in duplicate on a Fast-7500 using TaqMan gene

expression assays (Life Technologies) and specific probes for TNF-α (*Tnf*, Mm00443258_m1) and MCP-1(*Ccl2*, Mm00441242_m1). Glyceraldehyde 3-phosphate dehydrogenase (*Gapdh*; 4308313) and hypoxanthine-guanine phosphoribosyltransferase (*Hprt*; Mm00446968_m1) were used as housekeeping genes. Changes in gene expression were calculated using the comparative Ct (ΔΔCt) method and expressed as fold-change relative to mean expression of control.

References Supplement 1:

1. Wopereis S, Radonjic M, Rubingh C, Erk M, Smilde A, Duyvenvoorde W, et al. Identification of prognostic and diagnostic biomarkers of glucose intolerance in ApoE3Leiden mice. Physiol Genomics. 2012;44(5):293-304. doi: 10.1152/physiolgenomics.00072.2011.
2. Bligh EG, Dyer WJ. A rapid method of total lipid extraction and purification. Can J Biochem Physiol. 1959;37(8):911-7. doi:10.1139/o59-099.

Replacement of dietary saturated fat by PUFA-rich pumpkin seed oil attenuates non-alcoholic fatty liver disease and atherosclerosis development, with additional health effects of virgin over refined oil

Abstract

Background and aims: As dietary saturated fatty acids are associated with metabolic and cardiovascular disease, a potentially interesting strategy to reduce disease risk is modification of the quality of fat consumed. Vegetable oils represent an attractive target for intervention, as they largely determine the intake of dietary fats. Furthermore, besides potential health effects conferred by the type of fatty acids in a vegetable oil, other minor components (e.g. phytochemicals) may also have health benefits. Here, we investigated the potential long-term health effects of isocaloric substitution of dietary fat (i.e. partial replacement of saturated by unsaturated fats), as well as putative additional effects of phytochemicals present in unrefined (virgin) oil on development of non-alcoholic fatty liver disease (NAFLD) and associated atherosclerosis. For this, we used pumpkin seed oil, because it is high in unsaturated fatty acids and a rich source of phytochemicals. **Methods:** ApoE*3Leiden mice were fed a Western-type diet (CON) containing cocoa butter (15% w/w) and cholesterol (1% w/w) for 20 weeks to induce risk factors and disease endpoints. In separate groups, cocoa butter was replaced by refined (REF) or virgin (VIR) pumpkin seed oil (comparable in fatty acid composition, but different in phytochemical content). **Results:** Both oils improved dyslipidaemia, with reduced (V)LDL-cholesterol and triglyceride levels in comparison with CON, and additional cholesterol-lowering effects of VIR over REF. While REF did not affect plasma inflammatory markers, VIR reduced circulating serum amyloid A and soluble vascular adhesion molecule-1. NAFLD and atherosclerosis development was modestly reduced in REF, and VIR strongly decreased liver steatosis and inflammation as well as atherosclerotic lesion area and severity. **Conclusions:** Overall, we show that an isocaloric switch from a diet rich in saturated fat to a diet rich in unsaturated fat can attenuate NAFLD and atherosclerosis development. Phytochemical-rich virgin pumpkin seed oil exerts additional anti-inflammatory effects resulting in more pronounced health effects.

Introduction

Cardiometabolic diseases such as non-alcoholic fatty liver disease (NAFLD) and cardiovascular disease (CVD) constitute a major health burden in modern societies. Accumulating evidence suggests that NAFLD, besides increasing liver morbidity and mortality, is associated with development of atherosclerosis, the major underlying pathology of CVD [1]. As dyslipidaemia and chronic inflammation are recognised to drive the development of NAFLD as well as atherosclerosis [2-4], dietary regimens that influence one or both of these risk factors may be of great preventive and possibly even therapeutic benefit. Support for this concept comes from epidemiological and experimental studies that show that the type of dietary fat consumed plays an important role in the development of both NAFLD and associated CVD (reviewed in [5, 6]). Therefore, a potentially interesting strategy to reduce cardiometabolic risk is a modification of the quality of fat in diets. This is further supported by results from a recent systematic review indicating that partial replacement of saturated fat by unsaturated fat may reduce CVD risk [7].

The daily intake of dietary fats is largely determined by vegetable oils, which makes them an attractive target for intervention. The more so, since besides potential health effects conferred by the type of fatty acids in a vegetable oil, other minor components of an oil (e.g. phytochemicals) may also significantly contribute to cardiometabolic health. Typically, vegetable oils are consumed in their fully refined form that consists almost exclusively of triglycerides. Virgin oils on the other hand, the completely unrefined first press form of an oil, are rich in a collection of phytochemicals (e.g. vitamins E and K, phytosterols and polyphenols) that may influence the critical risk factors dyslipidaemia as well as inflammation [8, 9].

Herein we investigated the potential long-term health effects of substitution of dietary saturated fat by unsaturated fat from refined oil, as well as putative additional effects of the unrefined counterpart rich in phytochemicals (virgin oil). For this, we used pumpkin seed oil, because it is high in unsaturated fatty acids (about 80%) and known to contain large amounts of phytochemicals [10, 11]. In short-term studies, pumpkin seed oil has been shown to reduce surrogate markers of liver health [12] and improve dyslipidaemia [13-15]. However, potential anti-inflammatory properties have not been examined and its effects on cardiometabolic disease endpoints are unknown.

The ApoE*3Leiden (E3L) mouse is a well-established diet-inducible model for NAFLD [16] and atherosclerosis [17]. The model develops human-like dyslipidaemia, inflammation and disease endpoints in response to a well-defined Western-type diet, containing cocoa butter

(±60% saturated fat) as the major fat source [17, 18]. This diet also contains cholesterol (1% w/w), which is required for induction of dyslipidaemia, inflammation and disease endpoints [16, 18, 19]. Groups of E3L mice were fed the Western-type control diet (CON) or pumpkin seed oil-substituted diets, REF (refined oil) and VIR (virgin oil) for 20 weeks, all of which contained 1% cholesterol. The refined and virgin pumpkin seed oils were comparable in fatty acid profile but differed in phytochemical content. This allowed us to define the health effects of refined pumpkin seed oil, as well as the additional effects of the phytochemicals present in its unrefined counterpart. Plasma lipids and markers of inflammation were monitored over time and NAFLD and atherosclerosis endpoints were scored according to established human grading systems ([20-22]). Results from this study indicate that an isocaloric switch from a diet rich in saturated fat to a diet rich in unsaturated fat has beneficial effects on risk factors, and that phytochemical-rich virgin oil has additional anti-inflammatory properties and more strongly reduces disease endpoints.

Materials and methods

All animal experiments were approved by an independent Ethical Committee on Animal Care and Experimentation (DEC-Zeist, the Netherlands) and were in compliance with European Community specifications regarding the use of laboratory animals. Female ApoE*3Leiden transgenic (E3L) mice were obtained from the breeding facility of TNO Metabolic Health Research, Leiden, the Netherlands, and were characterised for expression of human APOE by ELISA. 12-week old E3L mice were matched into 3 groups based on plasma cholesterol and triglycerides. All animals were group-housed (3-4 mice per cage) in the SPF animal facility of TNO Metabolic Health Research, in a temperature-controlled room on a 12 hour light/dark cycle and had free access to food and water. Diets were based on a standardised atherogenic Western-type diet (WTD) that contains 15% cocoa butter, 1% corn oil, 40.5% sucrose, 20% acid casein, 10% corn starch and 6.2% cellulose (all w/w; diet-T; AB-Diets, Woerden, the Netherlands), supplemented with 1% (w/w) cholesterol (Sigma-Aldrich, Zwijndrecht, the Netherlands). Control mice (CON, n=18) were fed this standard WTD, while the treatment groups received the WTD with 9% (w/w of total diet) of the cocoa butter replaced by either 9% refined pumpkin seed oil (REF, n=15; Bunge Ltd., White Plains, USA) or 9% virgin pumpkin seed oil (VIR, n=15; Bunge Ltd). As the cholesterol in this diet is required to induce inflammation and dyslipidaemia [16, 18, 19], the cholesterol concentration was the same (1%) in all three groups.

Detailed methods of the analysis of the composition of the cocoa butter and pumpkin seed oils are described in Supplement 1: Detailed materials and methods. Briefly, the fatty acid composition was determined by gas chromatography, the total phenolic content was determined spectrophotometrically by the Folin-Ciolcalteau method, and individual phenolic content of the pumpkin seed oils was determined by LC-QTOF-MS.

Food intake was measured per cage (3-4 mice per cage) every 4 weeks, expressed as the average food intake per mouse per day. The energy content of the diets was determined by bomb calorimetry. Blood samples were collected from the tail vein after a 4h fasting period for EDTA plasma isolation at week 0, 3, 6, 12 and 20 of the study. Total plasma cholesterol and triglyceride levels were measured in these fasted plasma samples by commercially available enzymatic assays (cholesterol CHOD-PAP 11491458 and triglycerides GPO-PAP 11488872, Roche, Woerden, The Netherlands). For lipoprotein profile analysis, pooled plasma samples were fractionated using an ÅKTA fast protein liquid chromatography system (Pharmacia, Roosendaal, the Netherlands) and analysed as reported [23]. Plasma levels of soluble vascular adhesion molecule 1 (sVCAM-1; R&D Systems, Abingdon, UK) and serum amyloid A (SAA; Life Technologies, Bleiswijk, the Netherlands) were determined by ELISA. ALAT and ASAT levels were measured in serum (unfasted sample from terminal blood, specified below) using a spectrophotometric activity assay (Reflotron Plus system, Roche). After 20 weeks of dietary treatment, mice were sacrificed by CO_2 asphyxiation and blood was collected via cardiac puncture for serum collection (unfasted). Hearts and livers were collected, and fixed in formalin and embedded in paraffin for atherosclerosis analysis (heart) and NAFLD analysis (liver).

Histological analysis of NAFLD and atherosclerosis development

For NAFLD analysis, 3 μm liver sections (medial lobe) were stained with haematoxylin and eosin and analysed blindly using an adapted scoring method for human NAFLD [20, 24]. Briefly, steatosis was expressed as the percentage of the total liver cross section affected by microvesicular steatosis or macrovesicular steatosis. Hepatic inflammation was analysed by counting the number of inflammatory foci per section at a 100× magnification.

Atherosclerosis was analysed blindly in 4 serial cross sections (5 μm, at 50 μm intervals) of the valve area of the aortic root. Cross sections were stained with haematoxylin-phloxine-saffron (HPS) for morphometric analysis of lesion number and area (using cell^D software, version 2.7; Olympus Soft Imaging Solutions, Hamburg, Germany) and analysis of lesion severity. Lesion severity was scored according to the classification of the American Heart

Association (AHA) [21, 22]. This scoring system was used to distinguish five lesion types: Type I (early fatty streak): up to ten foam cells in the intima, no other changes; Type II (regular fatty streak): ten or more foam cells in the intima, no other changes; Type III (mild plaque): foam cells in the intima with presence of a fibrotic cap; Type IV (moderate plaque): progressive lesion, infiltration into media, elastic fibres intact; Type V (severe plaque): structure of media severely disrupted with fragmented elastic fibres, cholesterol crystals, calcium deposits and necrosis may be present. The lesional macrophage content was assessed by immunohistochemical staining of MAC-3 (CD107b)-positive cells (purified rat anti-mouse CD107b antibody, BD Biosciences, Breda, the Netherlands) in cross-sections adjacent to those used for the atherosclerosis analysis. The MAC-3 positive area for each individual plaque was measured using an automated macro in the image processing software ImageJ (version 1.48, NIH, Bethesda, MD, USA; [25]) and expressed as the percentage of total plaque area that was positively stained for MAC-3. The number of lesions was counted in 4 cross sections and expressed as the average per cross section. Furthermore, the number of lesion-free (undiseased) segments was counted and expressed as a percentage of the total number of segments (N.B. each aortic cross-section is divided into 3 segments that are demarcated by the aortic valves, making a total of 12 segments analysed per mouse).

Hepatic gene expression analyses
Total RNA was extracted from liver tissue using RNA Bee Total RNA Isolation Kit (Bio-Connect, Huissen, the Netherlands). Spectrophotometric analysis of RNA concentration was performed using Nanodrop 1000 (Isogen Life Science, De Meern, the Netherlands) and quality of RNA was assessed using a 2100 Bioanalyzer (Agilent Technologies, Amstelveen, the Netherlands). cDNA was synthesised using a High Capacity RNA-to-cDNA™ Kit (Life Technologies, Bleiswijk, the Netherlands). Hepatic gene expression analyses were performed by RT-PCR on a 7500 Fast Real-Time PCR System (Applied Biosystems by Life Technologies) using TaqMan® Gene Expression Assays (Life Technologies). Transcripts were quantified using TaqMan® Gene Expression Assays (Life Technologies) and the following primer/probe-sets for *Srebf1* (Mm00550338_m1), *Fasn* (Mm00662319_m1), *Dgat1* (Mm00515643_m1), *Ppara* (Mm00440939_m1), *Cpt1a* (Mm01231183_m1), *Acox1* (Mm00443579_m1), *Ccl2* (Mm00441242_m1), *Tnf* (Mm00443258_m1), *Il1b* (Mm00434228_m1) and the endogenous controls *Hprt* (Mm00446968_m1) and *Ppif* (Mm01273726_m1). Changes in gene expression were calculated using the comparative Ct ($\Delta\Delta$Ct) method and expressed as fold-change relative to CON.

Hepatic lipid analysis

Lipids were extracted from liver homogenates using the Bligh and Dyer method [26] and separated by high performance thin layer chromatography (HPTLC) on silica gel plates as described previously [27]. Lipid spots were stained with color reagent (5g $MnCl_2 \cdot 4H_2O$, 32ml 95–97% H_2SO_4 added to 960ml $CH_3OH:H_2O$ 1:1 v/v) and triglycerides, cholesteryl esters and free cholesterol were quantified using TINA version 2.09 software (Raytest, Straubenhardt, Germany).

Statistical analyses

All data are presented as mean±SEM. Statistical analyses were performed using SPSS software (version 22, IBM, Armonk, USA). For normally distributed variables, significance of differences between groups was tested by one-way ANOVA, followed by Fisher's Least Significant Difference (LSD) Post-Hoc Test. In case of heterogeneity between groups, variables were analysed by ANOVA using Brown-Forsythe for differences between groups followed by Dunnett's T3 Post-Hoc Test. Non-normally distributed variables were tested by non-parametric Kruskal-Wallis test followed by Mann-Whitney U tests. To test the hypothesis that both pumpkin seed oils may have beneficial effects relative to control and that the virgin oil may have additional beneficial effects over its refined counterpart, a one-sided p-value≤0.05 was considered statistically significant.

Results

The refined and virgin pumpkin seed oils used in this study were comparable in fatty acid composition (Table 1). Both oils contained 81% unsaturated fatty acids, most of which consisted of linoleic acid (C18:2n-6, 64%) and oleic acid (C18:1n-9, 17%). The virgin oil contained more phytochemicals than its refined counterpart (Table 2). Virgin pumpkin seed oil was rich in benzoic acid, vanillic acid, ferulic acid, rutin and *p*-coumaric acid, many of which were below the detection limit in the refined oil. Overall, the total phenolic content was 7.7-fold higher in the virgin oil than in the refined oil.

To investigate potential health effects of these oils on NAFLD and atherosclerosis, E3L mice were fed a standardised Western type control diet (CON) or the same diet substituted with 9% (w/w) refined pumpkin seed oil (REF) or 9% (w/w) virgin pumpkin seed oil (VIR) for 20 weeks. All diets contained 1% (w/w) cholesterol and were comparable in energy content as quantified by bomb calorimetry (CON: 20.2 kJ/g, REF: 20.0 kJ/g and VIR: 20.4 kJ/g) and food intake was

comparable between groups (Supplemental Fig. 1). The treatments were well tolerated and body weight increased slightly over time (percentage body weight gain relative to t=6: CON: 12.3±1.3%, REF: 8.9±1.8%, VIR: 11.1±1.6%, n.s.) in all groups (Supplemental Fig. 2).

Table 1. Fatty acid composition of cocoa butter and refined and virgin pumpkin seed oil.

		Cocoa butter	Refined pumpkin seed oil	Virgin pumpkin seed oil
Poly-unsaturated fatty acids (% of total)		**2.8**	**64.4**	**64.0**
C18:2	Linoleic acid (n-6)	2.7	64.1	63.9
C18:3	alpha-Linolenic acid (n-3)	0.1	0.3	0.1
Mono-unsaturated fatty acids (% of total)		**33.0**	**17.0**	**17.8**
C18:1	Oleic acid	32.8	16.6	17.1
C16:1	Palmitoleic acid	0.2	0.3	0.2
C20:1	Eicosanoic acid	n.d.	0.1	0.4
Saturated fatty acids (% of total)		**63.7**	**18.0**	**18.1**
C16:0	Palmitic acid	26.7	12.8	12.8
C18:0	Stearic acid	35.7	4.5	4.5
C20:0	Arachidic acid (Eicosanoic acid)	1.0	0.3	0.3
C22:0	Behenic acid (Docosanoic acid)	0.2	0.2	0.2
C14:0	Myristic acid (Tetradecanoic acid)	0.1	0.1	0.1
C24:0	Lignoceric acid (Tetracosanoic acid)	n.d.	0.1	0.1
Trans fatty acids (% of total)		n.d.	0.7	0.2
C18:2T	Trans linoleic acid	n.d.	0.7	0.2

n.d. = not detected

Table 2. Phytochemical content of cocoa butter and refined and virgin pumpkin seed oil

	Cocoa butter	Refined pumpkin seed oil	Virgin pumpkin seed oil
Tocopherols (ppm)	246	386	577
Tocotrienols (ppm)	7	123	121
Vitamin K (µg/100g)	3.5	52.3	68.0
Total phenolic content (mg gallic acid/kg oil)	8.3	3.6	27.7
Benzoic acid (µM)	n.d.	0.1	19.3
p-coumaric acid (nM)	n.d.	n.d.	200
Vanillic acid (nM)	791	n.d.	300
Ferulic acid (nM)	n.d.	n.d.	300
Rutin (nM)	n.d.	n.d.	4
Isomer of 3-hydroxybenzoic acid (nM)	n.d.	50	8000
Isomer of protocatechuic acid (nM)	n.d.	n.d.	700
Isomer of caffeic acid (nM)	n.d.	n.d.	60
Isomer of ferulic acid (nM)	456	30	100
Isomer of naringenin (nM)	162	n.d.	2100
Isomer of 4-hydroxyphenylpropionic (nM)	522	10	700

n.d. = not detected, Tocopherols = sum of α, β, γ and δ (δ was n.d.). Tocotrienols = sum of α, γ and δ.
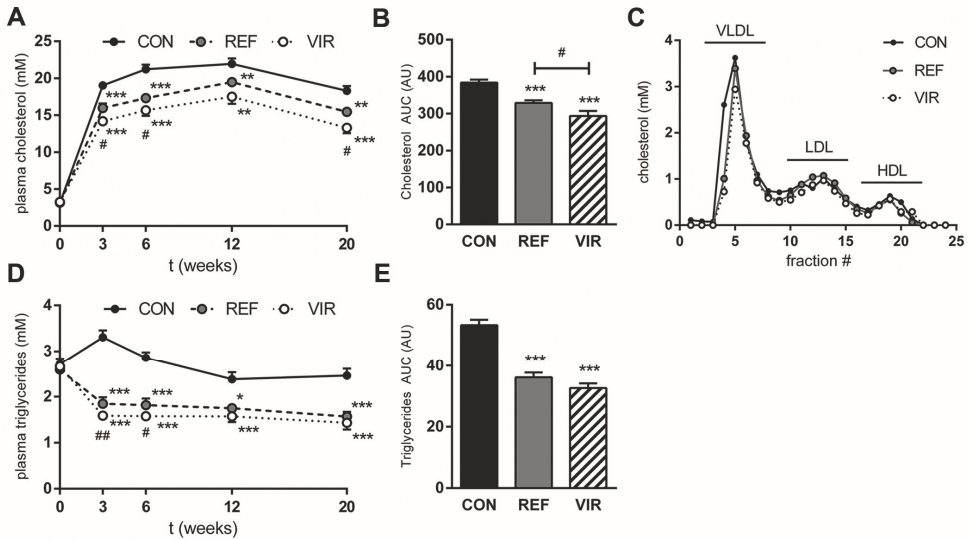
Figure 1. Refined and virgin pumpkin seed oils have beneficial effects on plasma lipids in cholesterol-fed ApoE*3Leiden mice. Mice were fed a Western type diet (CON) containing cocoa butter (15% w/w of diet) for 20 weeks. The cocoa butter was in part replaced by refined pumpkin seed oil (REF) or virgin pumpkin seed oil (VIR) (each 9% w/w of diet). (A) Plasma cholesterol levels over the course of the study, showing lower levels in REF and VIR-fed animals. (B) Area under the curve analysis (AUC, expressed in arbitrary units; AU) of plasma cholesterol levels (t=0 until t=20 weeks) shows additional cholesterol-lowering effect of VIR compared with REF. (C) Lipoprotein profile for cholesterol distribution in VLDL, LDL and HDL-sized particles shows cholesterol-lowering effect mainly confined to VLDL-sized particles. (D) Plasma triglycerides over the course of the study were lowered by both REF and VIR. (E) Area under the curve analysis of plasma triglyceride levels (t=0 until t=20 weeks) shows a reduction by VIR and REF. Data are mean±SEM. * p≤0.05, ** p≤0.01, *** p≤0.001 compared with CON. # p≤0.05, ## p≤0.01 for VIR compared with REF.

Both pumpkin seed oils improve dyslipidaemia, with additional beneficial effects of virgin oil over refined oil

Plasma cholesterol levels rose rapidly in CON animals within the first 3 weeks and remained relatively stable until the end of the study (Fig. 1A) with an average of 19.20±0.39 mM. Both REF and VIR animals had significantly lower fasting plasma cholesterol levels compared with CON at all time points (Fig. 1a). Area under the curve (AUC) analysis of the plasma cholesterol levels throughout the study period showed a significantly lower AUC for cholesterol in VIR (293.6±13.6 AU),than in REF (328.8±7.0 AU, p≤0.05, Fig. 1B), indicating additional cholesterol-lowering properties of VIR. These cholesterol-lowering effects were mainly confined to the VLDL-sized particles (Fig. 1C). In CON animals, fasting plasma triglycerides remained at a stable and elevated level during the study (average 2.67±0.09 mM, (Fig. 1D).

Both pumpkin seed oils decreased fasting plasma triglyceride levels within the first 3 weeks of the study and levels remained stable at this low level thereafter (average REF 1.79±0.08 mM, average VIR 1.63±0.07 mM, Fig. 1D). Overall, VIR treatment did not have additional beneficial effects on plasma triglyceride levels relative to REF as is also shown by results from the AUC analysis for plasma triglyceride levels (Fig. 1E). Together, these results indicate that the observed lipid-lowering effects are predominantly attributable to the replacement of saturated by unsaturated dietary fat.
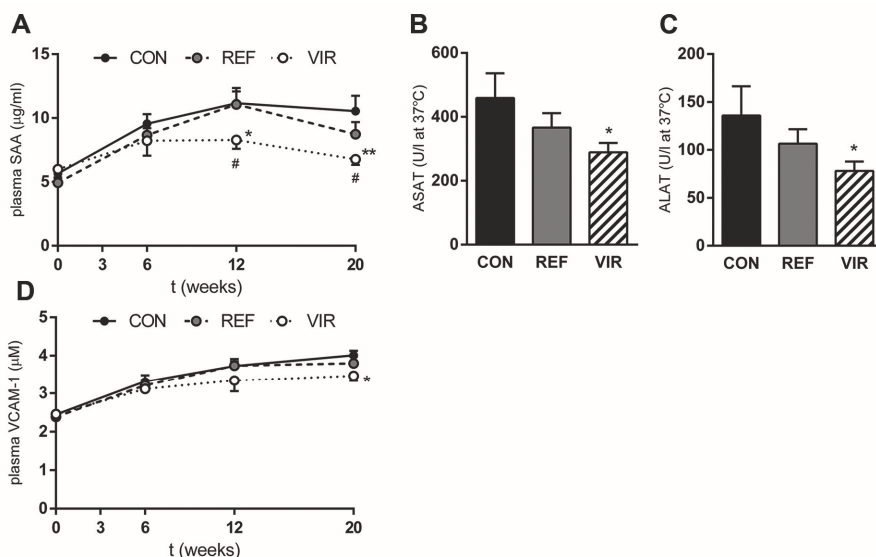

Figure 2. Virgin pumpkin seed oil reduces circulating markers of inflammation in cholesterol-fed ApoE*3Leiden mice. Mice were fed a Western type control diet (CON) or CON diet containing 9% refined pumpkin seed oil (REF) or 9% virgin pumpkin seed oil (VIR) for 20 weeks. (A) Plasma SAA levels were reduced by VIR. Liver damage markers (B) ASAT and (C) ALAT were reduced by VIR but not by REF. (D) Plasma sVCAM-1 levels in VIR animals were lower throughout the duration of the study. Data are mean±SEM. * $p \leq 0.05$, ** $p \leq 0.01$ compared with CON. # $p \leq 0.05$ for VIR compared with REF.

Virgin pumpkin seed oil reduces circulating markers of liver and vascular inflammation
CON diet induced plasma levels of SAA, a marker of liver inflammation, from 5.65±0.34 µg/ml at t=0 to 10.55±1.21 µg/ml at the end of the study (Fig. 2A). SAA levels in REF animals were comparable to CON, while VIR attenuated SAA induction and plasma levels were significantly lower than CON at t=12 and t=20 weeks (6.77±0.44 µg/ml at t=20, -36%, $p \leq 0.01$, Fig. 2A). In line with this effect on SAA, serum levels of the hepatocellular damage markers ASAT and

ALAT were not affected by REF, and VIR significantly reduced both ASAT (p≤0.05) and ALAT levels (p≤0.05) (Fig. 2B-C). Besides inducing liver inflammation, CON diet also gradually induced plasma levels of vascular inflammation marker sVCAM-1 from 2.45±0.09 μg/ml at t=0 to 4.01±0.12 μg/ml at t=20 weeks (Fig. 2D). Levels of sVCAM-1 were not affected by REF, but VIR animals showed lower sVCAM-1 throughout the study period and this effect reached significance at t=20 weeks (3.47±0.14 μg/ml, -14%, p≤0.05, Fig. 2d). These data show that the phytochemicals in virgin pumpkin seed oil are responsible for the observed anti-inflammatory effects on circulating liver and vascular inflammation markers.

Virgin pumpkin seed oil attenuates development of NAFLD

Refined pumpkin seed oil reduced liver weight by 12% (CON: 5.9±0.2% of terminal body weight, REF: 5.2±0.2%, p≤0.05, Fig. 3A) and this effect was even stronger in VIR (-19%), with liver weights reduced to 4.8±0.1% of terminal body weight (p≤0.01, Fig. 3A). Histological examination of the livers from CON animals revealed that NAFLD developed in these mice up to the stage of non-alcoholic steatohepatitis (NASH). CON mice displayed distinctive morphological hallmarks of NASH (pronounced steatosis and lobular infiltration of inflammatory cells) and the observed pathology was less severe in REF and VIR animals (representative photomicrographs shown in Fig. 3B). Quantitative scoring of NAFLD revealed that macrovesicular steatosis tended to be lower in REF (-26%, p=0.08) and was significantly reduced with VIR (-45%, p≤0.01) (Fig. 3C). Microvesicular steatosis was less pronounced in both REF and VIR (-41% and -65%, respectively), but this effect did not reach statistical significance (Supplemental Fig. 3). Biochemical analysis of hepatic lipid levels confirmed the histologically observed antisteatotic effects of the pumpkin seed oils, showing reduced hepatic triglyceride content in both REF and VIR (-17%, p≤0.01 and -23%, p≤0.001 respectively, Fig. 3D). Hepatic cholesterol levels, in both esterified (Fig. 3E) and unesterified (Fig. 3F) form, were affected only in VIR, with slightly but statistically significantly reduced levels of these lipid species in this group. Consistent with the observed effects on plasma inflammation markers, infiltration of inflammatory cells was moderately lowered by REF (-29%, n.s.), while VIR strongly and significantly reduced lobular inflammation (73%, p≤0.001 vs CON, p≤0.001 vs REF; Fig. 3G).
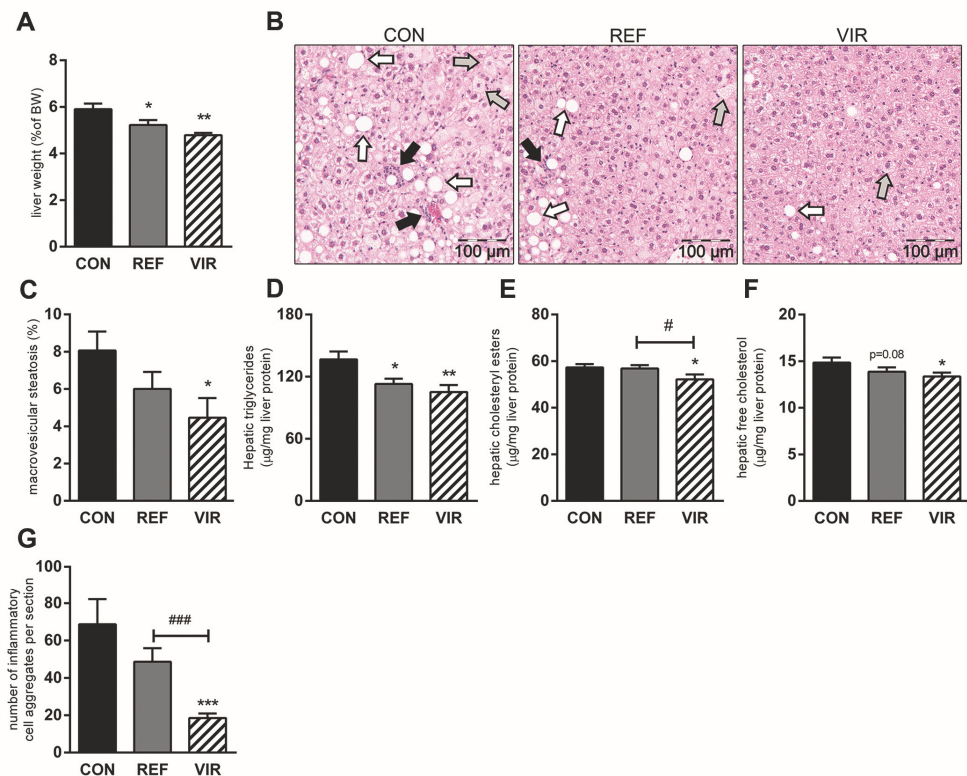
Figure 3. Virgin pumpkin seed oil attenuates development of NAFLD in cholesterol-fed ApoE*3Leiden mice. Mice were fed a Western type control diet (CON) or CON diet containing 9% refined pumpkin seed oil (REF) or 9% virgin pumpkin seed oil (VIR) for 20 weeks. (A) Liver weight (expressed as percentage of terminal body weight) was reduced by REF and VIR. (B) representative photomicrographs of HE-stained liver sections show presence of micro- (grey arrows) and macro-(white arrows)vesicular steatosis and inflammatory cell clusters (black arrows) in CON-fed animals, which was less pronounced in REF and more strongly reduced in VIR. (C) Histological quantitative scoring of macrovesicular steatosis showed significant reduction in VIR. (D) Hepatic triglyceride levels (biochemically determined) were reduced in both REF and VIR while only VIR significantly reduced (E) hepatic cholesteryl ester content and (F) free (unesterified) cholesterol levels. G: Histological quantification of number of inflammatory cell aggregates revealed a significant attenuation of hepatic inflammation by VIR. Data are mean±SEM. * $p \leq 0.05$, ** $p \leq 0.01$, *** $p \leq 0.001$ compared with CON. # $p \leq 0.05$, ### $p \leq 0.001$ for VIR compared with REF.

Atherosclerosis development is reduced with virgin pumpkin seed oil

Atherosclerotic lesion area and number were quantified histologically in the valve area of the aortic root. CON diet induced pronounced atherosclerosis with a total lesion area of 143765±17286 μm² per cross-section (Fig. 4A-B). The total lesion area was reduced with REF (100594±14726 μm², -30%, $p \leq 0.05$, Fig. 4A-B) and an even stronger effect was observed in VIR (82766±15164 μm², -42%, $p \leq 0.01$, Fig. 4A-B). Refined morphological analysis of lesion severity revealed that the atherosclerotic lesion area in CON animals was mostly made up of

large and advanced lesions (severe lesion types IV and V; Fig. 4C). The observed decrease in total lesion area with REF and VIR was attributable to a significant reduction in the total area of these severe lesions specifically. Furthermore, immunohistochemical analysis of lesional macrophage content (MAC-3 positive area) showed that while there was no effect of REF or VIR on the macrophage content of mild type III lesions (not shown), the macrophage area in type V (severe) lesions was significantly reduced by both pumpkin seed oils (Fig. 4D). In CON animals, 14.4±3.4% of the type 5 lesion area was MAC-3 positive and this was reduced to 6.16±1.26% in REF (p≤0.05 compared with CON) and 8.33±3.0% in VIR (p≤0.05 compared with CON). A similar, although non-significant, reduction was observed in type IV lesions (Supplemental Fig. 3). The number of lesions (CON: 3.4±0.24; REF: 2.9±0.36; VIR: 2.6±0.21 lesions per cross section; S4 Fig) and the percentage of lesion-free aortic segments (CON: 5.6±2.3; REF: 12.2±4.3; VIR: 9.5±3.3%; Supplemental Fig. 3) were comparable among the groups. However the average size per lesion was significantly reduced by both oils (REF: -25%, p≤0.05; VIR: -37%, p≤0.01, Fig. 4e), altogether indicating an effect on lesion growth rather than on the initiation of new lesions.
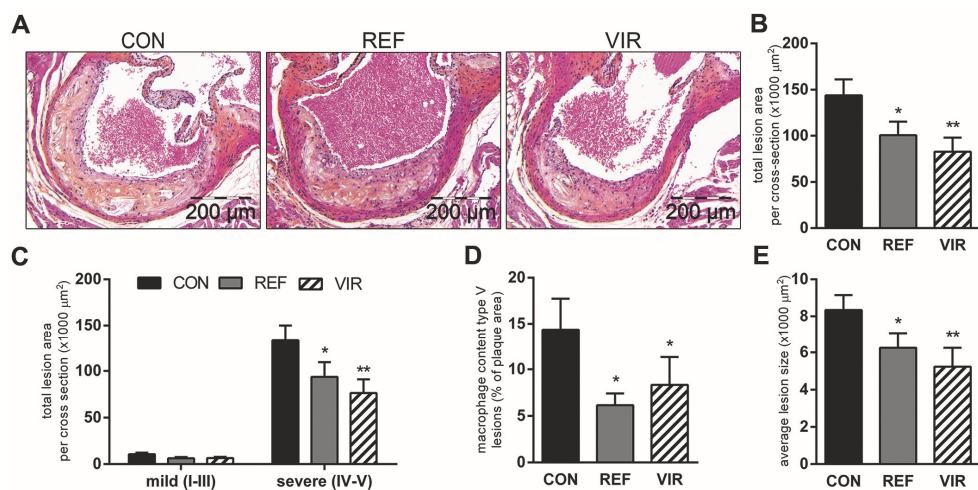
Figure 4. Atherosclerosis development is reduced with virgin pumpkin seed oil. Mice were fed a Western type control diet (CON) or CON diet containing 9% refined pumpkin seed oil (REF) or 9% virgin pumpkin seed oil (VIR) for 20 weeks. (A) representative photomicrographs of HPS-stained cross sections of the aortic root show pronounced development of atherosclerosis in CON animals, which was less pronounced in REF and strongly reduced by VIR. (B) Morphometric analysis of lesion area revealed a significant decrease in atherosclerotic lesion area by REF and VIR. (C) Anti-atherogenic effects of pumpkin seed oils are specific on severe lesion types. (D) Average lesion size was reduced in REF and VIR. (E) Immunohistochemical staining for MAC-3 (CD107b) followed by quantification of positively stained area showed that both REF and VIR reduced the macrophage content of type V lesions. Data are mean±SEM. * p≤0.05, ** p≤0.01 compared with CON.

Figure 5. Refined and virgin pumpkin seed oils modulate lipid metabolism and inflammatory gene expression. Mice were fed a Western type control diet (CON) or CON diet containing 9% refined pumpkin seed oil (REF) or 9% virgin pumpkin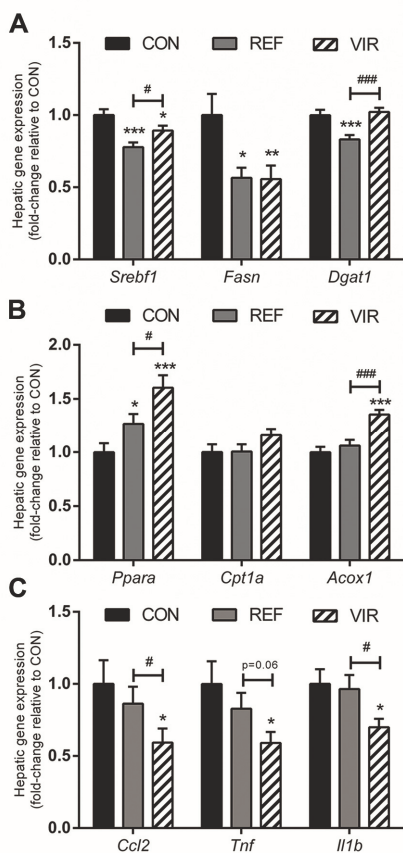 seed oil (VIR) for 20 weeks. (A) Hepatic lipogenic gene expression (*Srebf1, Fasn, Dgat1*) was reduced in both REF and VIR. (B) Hepatic expression of genes involved in fatty acid catabolism (*Ppara, Cpt1a, Acox1*) was upregulated in VIR and to a lesser extent in REF. (C) Only VIR reduced hepatic expression of inflammatory genes (*Ccl2, Tnf, IL1b*). All gene expression data are expressed as fold-change relative to CON. Data are mean±SEM. * p≤0.05, ** p≤0.01, *** p≤0.001 compared with CON, # p≤0.05, ### p≤0.001 for VIR compared with REF.

Both pumpkin seed oils have beneficial effects on hepatic lipid metabolism while only virgin pumpkin seed oil reduces inflammation

To provide insight into the underlying processes modulated by VIR and REF, hepatic mRNA expression of genes involved in lipid metabolism and inflammation was analysed. In line with the observed hypolipidaemic and antisteatotic effects of REF and VIR, expression of genes involved in lipogenesis was reduced by both pumpkin seed oils (Fig. 5A). Expression of SREBP-1c (*Srebf1*), a master transcriptional regulator of de novo fatty acid and triglyceride

synthesis [28] was reduced significantly in both REF (fold-change relative to CON: 0.78±0.03, p≤0.001) and VIR (0.89±0.03, p≤0.01). In line with this, the expression of the SREBP-1c target gene Fatty acid synthase (*Fasn*), the main biosynthetic enzyme in fatty acid synthesis [29], was also reduced in both REF (0.57±0.07, p≤0.05) and VIR (0.56±0.09, p≤0.01). Expression of Diacylglycerol acyltransferase-1 (*Dgat1*), which catalyses the final step in triglyceride synthesis [30], was significantly reduced in REF (0.83±0.03, p≤0.001), but unaffected in VIR. Together, these results provide indication that the de novo synthesis of lipids is reduced in pumpkin seed oil-fed animals.

Furthermore, mRNA expression analysis of genes involved in the catabolism of fatty acids (Fig. 5B) revealed that pumpkin seed oil, particularly in its virgin form, may also stimulate the breakdown of lipids. Expression of Peroxisome proliferator activated receptor α (*Ppara*), the main regulator of β-oxidation [31] was increased in both REF (1.27±0.09, p≤0.05) and VIR (1.61±0.11, p≤0.001), with additional beneficial effects of VIR over REF (p≤0.05). Carnitine palmitoyl transferase I (*Cpt1a*), which catalyses the transport of fatty acids into the mitochondria [32] was not increased in REF (1.01±0.07) or VIR (1.16±0.06). Expression of Acyl-CoA oxidase (*Acox1*) which catalyses the first step of β-oxidation [33], was unaffected by REF (1.06±0.05), while it was significantly increased in VIR (1.36±0.04, p≤0.001). Altogether these results indicate a stimulating effect of VIR on β-oxidation while the effects of REF on this process appear to be less pronounced.

Investigation of hepatic inflammatory gene expression (Fig. 5C) revealed an anti-inflammatory effect of VIR specifically, further strengthening the notion that phytochemicals in virgin pumpkin seed oil rather than the fatty acid composition of the oil per se are responsible for the observed anti-inflammatory effects. Expression of Monocyte chemoattractant protein-1 (*Ccl2*), which plays an important role in the recruitment of myeloid-derived monocytes [34] was not significantly affected by REF (0.86±0.12), while it was strongly reduced in VIR (0.59±0.10, p≤0.05). Similarly, expression of the pro-inflammatory cytokines Tumour necrosis factor alpha (*Tnf*) and Interleukin 1 beta (*Il1b*) was significantly reduced by VIR (0.59±0.08, p≤0.05 for *Tnf*; 0.70±0.06, p≤0.05 for *Il1b*) but not by REF (0.83±0.11 for *Tnf*; 0.96±0.10 for *Il1b*).

Discussion

In the study described herein, we demonstrate the potential long-term health effects of substitution of dietary fat (i.e. replacement of saturated by unsaturated fats), as well as putative

additional effects of phytochemicals present in unrefined (virgin) oil. In a humanised model of disease, we show that both refined and virgin pumpkin seed oils markedly improve plasma lipids (cholesterol, triglycerides) and virgin pumpkin seed oil also reduced circulating markers of systemic and vascular inflammation. In the long run, both pumpkin seed oils attenuated the development of NAFLD and atherosclerosis, with a more pronounced effect of VIR in disease prevention.

Several epidemiological studies have shown that the development of NAFLD and CVD is associated with the type of dietary fat consumed [5-7]. To mimic diet-related long-term disease development in humans, we used the E3L model in which NAFLD and CVD are inducible by diet. These mice have a humanised lipoprotein profile, and cholesterol feeding results in a moderate elevation of plasma cholesterol (to about 18-20 mM) and combined development of NAFLD and atherosclerosis. Under the experimental conditions employed, lipid and inflammatory risk markers of future NAFLD and atherosclerosis are already induced after a few weeks, thus allowing the study of interventions on surrogate markers of disease, under conditions relevant for humans [17, 19, 23, 35].

Replacement of a part of the cocoa butter by pumpkin seed oil markedly diminished the induction of circulating risk factors (cholesterol, triglycerides, SAA, sVCAM-1), which is in line with the short-term effects of other pumpkin seed oil preparations tested in humans and animals [12, 14, 15]. As these studies employed different pumpkin seed oil preparations at different doses and treatment regimens (in capsules or by oral gavage, as an addition to the regular diet), they provide evidence for a general health benefit of pumpkin seed oil, independent of how it is prepared and administered (i.e. replacement of dietary fat, or on top of regular diet).

In the present study we exchanged a part of the main fat in the CON diet, which is cocoa butter (15% w/w of the diet), with pumpkin seed oil (9% w/w of the diet) which modifies the quality of fat consumed, without affecting the caloric density of the diet. More specifically, the main fatty acids present in cocoa butter are stearic acid (C18:0, 35.7%), palmitic acid (C16:0, 26.7%) and oleic acid (C18:1n-9, 32.8%), while linoleic acid (C18:2n-6, 2.7%) is only present in very small amounts. Replacing part of this cocoa butter with pumpkin seed oil, primarily increases the intake of linoleic acid and reduces the intake of oleic acid and the saturated fatty acids (SFA) stearic acid and palmitic acid. Linoleic acid is an essential n-6 poly-unsaturated fatty acid (PUFA) that is reported to have beneficial effects on plasma lipids (reviewed in [36]), in line with the results described herein. A possible rationale for the observed lipid-lowering effects

may be found in activation of the transcription factor PPAR-α, which is known to be activated more strongly by PUFA than SFA [37]. Activation of this master regulator of lipid metabolism reportedly activates beta-oxidation in the liver and lowers plasma triglyceride levels as well as LDL cholesterol [38], consistent with observed reductions in plasma lipids in the present study. Gene expression analyses in the present study revealed an increased expression of PPAR-α in both pumpkin seed oil-fed groups, suggesting that transcriptional activity of this transcriptional regulator may be increased. Virgin pumpkin seed oil had additional effects on the expression and activation (demonstrated by increased expression of the PPAR-α target gene Acox1) of PPAR-α relative to the refined oil, indicating that phytochemicals present only in the virgin oil may have PPAR-α-activating properties. This is in line with findings by others, showing increased PPAR-α and PPAR-α target gene expression by tocopherols [39] and various polyphenol-rich mixtures (e.g. Apple polyphenols [40], Bilberry extract [41] and Walnut extract [42]). In contrast, there was no additional effect of the virgin oil on the reduction of lipogenic gene expression, thus indicating that these effects are attributable to the modification of the fatty acid composition of the diet, rather than effects of bioactive phytochemicals. More specifically, PUFAs are known to suppress SREBP-1c (the dominant transcriptional regulator of lipogenic genes) and rates of lipogenesis in rodents [43], in line with the effects of the PUFA-enriched pumpkin seed oil diets described herein. Remarkably, effects on lipogenic gene expression were more pronounced in the refined oil than in the virgin oil, suggesting that phytochemicals present in the virgin oil may attenuate these anti-lipogenic effects. Triglyceride and cholesterol-lowering effects comparable to those observed herein were also reported in long-term studies in E3L mice treated with long-chain PUFAs [44] or a PUFA-rich food supplement [45], as well as a pharmacological PPAR-α activator [23]. Overall, the reductions of plasma cholesterol achieved with the pumpkin seed oils are remarkably pronounced (-15% for REF, -24% for VIR). This effect is in the range typically achieved with low-doses of hypocholesterolaemic drugs such as HMG-CoA reductase inhibitors (statins) in the E3L mouse as well as in patients [46, 47].

While both pumpkin seed oils had beneficial effects on dyslipidaemia, only VIR reduced markers of inflammation SAA and sVCAM-1, indicating that minor components that are present in VIR but not in REF may have anti-inflammatory properties. These anti-inflammatory effects may be conferred by specific phytochemicals, including polyphenolic compounds, of which virgin pumpkin seed oil is a rich source. The total phenolic content of the VIR preparation used in the present study was 8-fold higher than in REF. Polyphenols are

widely recognised for their anti-inflammatory effects [48-50], and have frequently been reported to be protective against the development of NAFLD and cardiovascular disease, both in epidemiological and experimental studies [51, 52]. Under comparable experimental conditions and in the same mouse model, individual polyphenols were found to attenuate atherosclerotic lesion progression towards severe lesions [19, 35], which is consistent with the observed prevention of development of severe, vulnerable atherosclerotic lesions with pumpkin seed oil. Pumpkin seed oil contains a complex mixture of polyphenols and other bioactive phytochemicals and it is unlikely that observed beneficial effects are confined to a single phytochemical or one single mechanism. It is more likely that multiple bioactives affect multiple mechanisms (alone or in combination) that culminate in the net anti-inflammatory effects observed as has been demonstrated with other complex mixtures of bioactives [13, 45, 53-55].

Replacement of cocoa butter with pumpkin seed oil reduces the intake of palmitic acid by 50% (from 4% of total diet to 2% of total diet). Although palmitic acid is known to have pro-inflammatory effects on liver cells, the intake of this fatty acid was comparable in REF and VIR groups and can thus not explain the marked anti-inflammatory effects of VIR. However, it is likely that the increased intake in dietary PUFAs and the reduced intake of palmitic acid, as achieved with both oils, contributed to the reduction of liver inflammation as a marked (29%) decrease in inflammatory cell content was already observed with REF.

Overall, we show that a simple lifestyle modification, i.e. a switch in the type of fat consumed without reducing total fat or calorie intake, can make a significant contribution to reducing metabolic and cardiovascular disease risk. Partial replacement of the saturated fat-rich cocoa butter with refined pumpkin seed oil was sufficient to improve the risk factor dyslipidaemia, and affect development of NAFLD and atherosclerosis. Additional anti-inflammatory effects, conferred by minor components present only in the virgin oil, lead to profound reductions in disease endpoints. Importantly, the observed effects were achieved in a translational diet-induced disease model, with moderately increased plasma lipids and low-grade metabolic inflammation as is typical for high-risk populations in humans. Under these conditions, pumpkin seed oil represents a powerful means to improve dyslipidaemia, and, particularly when used in its virgin form, reduce chronic inflammation and prevent long-term disease development.

Acknowledgements

Financial support

Declaration of interests

The authors of this manuscript have the following competing interests: This study is funded in part by Bunge Ltd. PMS is an employee of Bunge Ltd.

References

1. Armstrong MJ, Adams LA, Canbay A, Syn WK. Extrahepatic complications of nonalcoholic fatty liver disease. Hepatology. 2014;59(3):1174-97. doi:10.1002/hep.26717.
2. Farrell GC, van Rooyen D, Gan L, Chitturi S. NASH is an inflammatory disorder: Pathogenic, prognostic and therapeutic implications. Gut Liver. 2012;6(2):149-71. doi:10.5009/gnl.2012.6.2.149.
3. Fon Tacer K, Rozman D. Nonalcoholic fatty liver disease: Focus on lipoprotein and lipid deregulation. Journal of Lipids. 2011;2011:783976. doi:10.1155/2011/783976.
4. Weber C, Noels H. Atherosclerosis: current pathogenesis and therapeutic options. Nat Med. 2011;17(11):1410-22. doi:10.1038/nm.2538.
5. Ferramosca A, Zara V. Modulation of hepatic steatosis by dietary fatty acids. World J Gastroenterol. 2014;20(7):1746-55. doi:10.3748/wjg.v20.i7.1746.
6. Michas G, Micha R, Zampelas A. Dietary fats and cardiovascular disease: Putting together the pieces of a complicated puzzle. Atherosclerosis. 2014;234(2):320-8. doi:10.1016/j.atherosclerosis.2014.03.013.
7. Schwab U, Lauritzen L, Tholstrup T, Haldorssoni T, Riserus U, Uusitupa M, et al. Effect of the amount and type of dietary fat on cardiometabolic risk factors and risk of developing type 2 diabetes, cardiovascular diseases, and cancer: a systematic review. Food Nutr Res. 2014;58:eCollection 2014. doi:10.3402/fnr.v58.25145.
8. Gylling H, Plat J, Turley S, Ginsberg HN, Ellegard L, Jessup W, et al. Plant sterols and plant stanols in the management of dyslipidaemia and prevention of cardiovascular disease. Atherosclerosis. 2014;232(2):346-60. doi:10.1016/j.atherosclerosis.2013.11.043.
9. Khurana S, Venkataraman K, Hollingsworth A, Piche M, Tai TC. Polyphenols: Benefits to the

cardiovascular system in health and in aging. Nutrients. 2013;5(10):3779-827. doi:10.3390/nu5103779.

10. Andjelkovic M, Van Camp J, Trawka A, Verhé R. Phenolic compounds and some quality parameters of pumpkin seed oil. European Journal of Lipid Science and Technology. 2010;112(2):208-17. doi:10.1002/ejlt.200900021.

11. Rezig L, Chouaibi M, Msaada K, Hamdi S. Chemical composition and profile characterisation of pumpkin (Cucurbita maxima) seed oil. Industrial Crops and Products. 2012;37(1):82-7. doi:10.1016/j.indcrop.2011.12.004.

12. al-Zuhair H, Abd el-Fattah AA, Abd el Latif HA. Efficacy of simvastatin and pumpkin-seed oil in the management of dietary-induced hyper-cholesterolemia. Pharmacol Res. 1997;35(5):403-8. doi:10.1006/phrs.1997.0148.

13. Allison GL, Lowe GM, Rahman K. Aged garlic extract and its constituents inhibit platelet aggregation through multiple mechanisms. J Nutr. 2006;136(3 Suppl):782S-8S.

14. Gossell-Williams M, Hyde C, Hunter T, Simms-Stewart D, Fletcher H, McGrowder D, et al. Improvement in HDL cholesterol in postmenopausal women supplemented with pumpkin seed oil: pilot study. Climacteric. 2011;14(5):558-64. doi:10.3109/13697137.2011.563882.

15. Gossell-Williams M, Lyttle K, Clarke T, Gardner M, Simon O. Supplementation with pumpkin seed oil improves plasma lipid profile and cardiovascular outcomes of female non-ovariectomized and ovariectomized Sprague-Dawley rats. Phytother Res. 2008;22(7):873-7. doi:10.1002/ptr.2381.

16. Morrison MC, Liang W, Mulder P, Verschuren L, Pieterman E, Toet K, et al. Mirtoselect, an anthocyanin-rich bilberry extract, attenuates non-alcoholic steatohepatitis and associated fibrosis in ApoE *3Leiden mice. J Hepatol. 2015;62:1180-6. doi:10.1016/j.jhep.2014.12.011.

17. Zadelaar S, Kleemann R, Verschuren L, de Vries-Van der Weij J, van der Hoorn J, Princen HM, et al. Mouse models for atherosclerosis and pharmaceutical modifiers. Arterioscler Thromb Vasc Biol. 2007;27(8):1706-21. doi:10.1161/ATVBAHA.107.142570.

18. Kleemann R, Verschuren L, van Erk MJ, Nikolsky Y, Cnubben NH, Verheij ER, et al. Atherosclerosis and liver inflammation induced by increased dietary cholesterol intake: A combined transcriptomics and metabolomics analysis. Genome Biol. 2007;8(9):R200. doi:10.1186/gb-2007-8-9-r200.

19. Morrison M, van der Heijden R, Heeringa P, Kaijzel E, Verschuren L, Blomhoff R, et al. Epicatechin attenuates atherosclerosis and exerts anti-inflammatory effects on diet-induced human-CRP and NFkappaB in vivo. Atherosclerosis. 2014;233(1):149-56. doi:10.1016/j.atherosclerosis.2013.12.027.

20. Liang W, Menke AL, Driessen A, Koek GH, Lindeman JH, Stoop R, et al. Establishment of a general NAFLD scoring system for rodent models and comparison to human liver pathology. PLoS One. 2014;9(12):e115922. doi:10.1371/journal.pone.0115922.

21. Stary HC, Chandler AB, Dinsmore RE, Fuster V, Glagov S, Insull W, Jr., et al. A definition of advanced types of atherosclerotic lesions and a histological classification of atherosclerosis. A report from the Committee on Vascular Lesions of the Council on Arteriosclerosis, American Heart Association. Arterioscler Thromb Vasc Biol. 1995;15(9):1512-31. doi:10.1161/01.ATV.15.9.1512.

22. Stary HC, Chandler AB, Glagov S, Guyton JR, Insull W, Jr., Rosenfeld ME, et al. A definition of initial, fatty streak, and intermediate lesions of atherosclerosis. A report from the Committee on Vascular Lesions of the Council on Arteriosclerosis, American Heart Association. Arterioscler Thromb Vasc Biol. 1994;14(5):840-56. doi:10.1161/01.ATV.14.5.840.

23. Kooistra T, Verschuren L, de Vries-van der Weij J, Koenig W, Toet K, Princen HM, et al. Fenofibrate reduces atherogenesis in ApoE*3Leiden mice: evidence for multiple antiatherogenic effects besides lowering plasma cholesterol. Arterioscler Thromb Vasc Biol. 2006;26(10):2322-30. doi:10.1161/01.ATV.0000238348.05028.14.

24. Kleiner DE, Brunt EM, Van Natta M, Behling C, Contos MJ, Cummings OW, et al. Design and validation of a histological scoring system for nonalcoholic fatty liver disease. Hepatology. 2005;41(6):1313-21. doi:10.1002/hep.20701.

25. Schneider CA, Rasband WS, Eliceiri KW. NIH Image to ImageJ: 25 years of image analysis. Nature methods. 2012;9(7):671-5. doi:10.1038/nmeth.2089.

26. Bligh EG, Dyer WJ. A rapid method of total lipid extraction and purification. Can J Biochem Physiol. 1959;37(8):911-7. doi:10.1139/o59-099.

27. Liang W, Lindeman JH, Menke AL, Koonen DP, Morrison M, Havekes LM, et al. Metabolically

induced liver inflammation leads to NASH and differs from LPS- or IL-1beta-induced chronic inflammation. Lab Invest. 2014;94(5):491-502. doi:10.1038/labinvest.2014.11.

28. Jeon TI, Osborne TF. SREBPs: Metabolic integrators in physiology and metabolism. Trends Endocrinol Metab. 2012;23(2):65-72. doi:10.1016/j.tem .2011.10.004.

29. Chirala SS, Wakil SJ. Structure and function of animal fatty acid synthase. Lipids. 2004;39(11):1045-53. doi:10.1007/s11745-004-1329-9.

30. Cases S, Smith SJ, Zheng YW, Myers HM, Lear SR, Sande E, et al. Identification of a gene encoding an acyl CoA:diacylglycerol acyltransferase, a key enzyme in triacylglycerol synthesis. Proc Natl Acad Sci U S A. 1998;95(22):13018-23. doi:10.1073/pnas.95.22.13018.

31. Mandard S, Muller M, Kersten S. Peroxisome proliferator-activated receptor alpha target genes. Cell Mol Life Sci. 2004;61(4):393-416. doi:10.1007 /s00018-003-3216-3.

32. Bonnefont JP, Djouadi F, Prip-Buus C, Gobin S, Munnich A, Bastin J. Carnitine palmitoyl-transferases 1 and 2: Biochemical, molecular and medical aspects. Mol Aspects Med. 2004;25(5-6):495-520. doi:10.1016/j.mam.2004.06.004.

33. Reddy JK, Hashimoto T. Peroxisomal beta-oxidation and peroxisome proliferator-activated receptor alpha: an adaptive metabolic system. Annu Rev Nutr. 2001;21:193-230. doi:10.1146/annurev .nutr.21.1.193.

34. Xu L, Kitade H, Ni Y, Ota T. Roles of chemokines and chemokine receptors in obesity-associated insulin resistance and nonalcoholic fatty liver disease. Biomolecules. 2015;5(3):1563-79. doi: 10.3390/biom5031563.

35. Kleemann R, Verschuren L, Morrison M, Zadelaar S, van Erk MJ, Wielinga PY, et al. Anti-inflammatory, anti-proliferative and anti-atherosclerotic effects of quercetin in human in vitro and in vivo models. Atherosclerosis. 2011;218(1):44-52. doi:10.1016/j.atherosclerosis.2011.04.023.

36. Monteiro J, Leslie M, Moghadasian MH, Arendt BM, Allard JP, Ma DW. The role of n-6 and n-3 polyunsaturated fatty acids in the manifestation of the metabolic syndrome in cardiovascular disease and non-alcoholic fatty liver disease. Food and Function. 2014;5(3):426-35. doi:10.1039/c3fo60551e.

37. Wahli W, Michalik L. PPARs at the crossroads of lipid signaling and inflammation. Trends Endocrinol Metab. 2012;23(7):351-63. doi:10.1016

/j.tem.2012.05.001.

38. Staels B, Dallongeville J, Auwerx J, Schoonjans K, Leitersdorf E, Fruchart JC. Mechanism of action of fibrates on lipid and lipoprotein metabolism. Circulation. 1998;98(19):2088-93. doi:10.1161/01 .CIR.98.19.2088.

39. Kim DY, Kim J, Ham HJ, Choue R. Effects of d-α-tocopherol supplements on lipid metabolism in a high-fat diet-fed animal model. Nutr Res Pract. 2013;7(6):481-7. doi:10.4162/nrp.2013.7.6.481.

40. Xu Z-R, Li J-Y, Dong X-W, Tan Z-J, Wu W-Z, Xie Q-M, et al. Apple polyphenols decrease atherosclerosis and hepatic steatosis in ApoE−/− mice through the ROS/MAPK/NF-κB pathway. Nutrients. 2015;7(8):5324. doi:10.3390/nu7085324.

41. Takikawa M, Inoue S, Horio F, Tsuda T. Dietary anthocyanin-rich bilberry extract ameliorates hyperglycemia and insulin sensitivity via activation of AMP-activated protein kinase in diabetic mice. J Nutr. 2010;140(3):527-33. doi:10.3945/jn.109 .118216.

42. Shimoda H, Tanaka J, Kikuchi M, Fukuda T, Ito H, Hatano T, et al. Effect of polyphenol-rich extract from walnut on diet-induced hypertriglyceridemia in mice via enhancement of fatty acid oxidation in the liver. J Agric Food Chem. 2009;57(5):1786-92. doi:10.1021/jf803441c.

43. Xu J, Nakamura MT, Cho HP, Clarke SD. Sterol regulatory element binding protein-1 expression is suppressed by dietary polyunsaturated fatty acids. A mechanism for the coordinate suppression of lipogenic genes by polyunsaturated fats. J Biol Chem. 1999;274(33):23577-83. doi:10.1074/jbc .274.33.23577.

44. Wielinga PY, Harthoorn LF, Verschuren L, Schoemaker MH, Jouni ZE, van Tol EA, et al. Arachidonic acid/docosahexaenoic acid-supplemented diet in early life reduces body weight gain, plasma lipids, and adiposity in later life in ApoE*3Leiden mice. Molecular Nutrition and Food Research. 2012;56(7):1081-9. doi:10.1002/mnfr .201100762.

45. Verschuren L, Wielinga PY, van Duyvenvoorde W, Tijani S, Toet K, van Ommen B, et al. A dietary mixture containing fish oil, resveratrol, lycopene, catechins, and vitamins E and C reduces atherosclerosis in transgenic mice. J Nutr. 2011;141(5):863-9. doi:10.3945/jn.110.133751.

46. van de Steeg E, Kleemann R, Jansen HT, van Duyvenvoorde W, Offerman EH, Wortelboer HM, et al. Combined analysis of pharmacokinetic and

efficacy data of preclinical studies with statins markedly improves translation of drug efficacy to human trials. The Journal of Pharmacology and Experimental Therapeutics. 2013;347(3):635-44. doi:10.1124/jpet.113.208595.

47. Verschuren L, Kleemann R, Offerman EH, Szalai AJ, Emeis SJ, Princen HM, et al. Effect of low dose atorvastatin versus diet-induced cholesterol lowering on atherosclerotic lesion progression and inflammation in apolipoprotein E*3-Leiden transgenic mice. Arterioscler Thromb Vasc Biol. 2005;25(1):161-7. doi:10.1161/01.ATV.0000148866 .29829.19.

48. Biesalski HK. Polyphenols and inflammation: Basic interactions. Curr Opin Clin Nutr Metab Care. 2007; 10(6):724-8. doi:10.1097/MCO.0b013e3282f0cef2.

49. Gonzalez R, Ballester I, Lopez-Posadas R, Suarez MD, Zarzuelo A, Martinez-Augustin O, et al. Effects of flavonoids and other polyphenols on inflammation. Crit Rev Food Sci Nutr. 2011;51 (4):331-62. doi:10.1080/10408390903584094.

50. Rahman I, Biswas SK, Kirkham PA. Regulation of inflammation and redox signaling by dietary polyphenols. Biochem Pharmacol. 2006;72(11): 1439-52. doi:10.1016/j.bcp.2006.07.004.

51. Aguirre L, Portillo MP, Hijona E, Bujanda L. Effects of resveratrol and other polyphenols in hepatic steatosis. World J Gastroenterol. 2014;20(23):7366-80. doi:10.3748/wjg.v20.i23.7366.

52. Arts IC, Hollman PC. Polyphenols and disease risk in epidemiologic studies. Am J Clin Nutr. 2005;81(1 Suppl):317S-25S.

53. Farrell N, Norris G, Lee SG, Chun OK, Blesso CN. Anthocyanin-rich black elderberry extract improves markers of HDL function and reduces aortic cholesterol in hyperlipidemic mice. Food and Function. 2015;6:1278-87. doi:10.1039/c4fo01036a.

54. Janega P, Klimentova J, Barta A, Kovacsova M, Vrankova S, Cebova M, et al. Red wine extract decreases pro-inflammatory markers, nuclear factor-kappaB and inducible NOS, in experimental metabolic syndrome. Food and Function. 2014;5(9):2202-7. doi:10.1039/c4fo00097h.

55. Tang CC, Lin WL, Lee YJ, Tang YC, Wang CJ. Polyphenol-rich extract of Nelumbo nucifera leaves inhibits alcohol-induced steatohepatitis via reducing hepatic lipid accumulation and anti-inflammation in C57BL/6J mice. Food and Function. 2014;5(4):678-87. doi:10.1039/c3fo60478k.

Supplemental data

Supplement 1. Detailed Material and Methods

<u>Extraction of phenolic compounds from pumpkin seed oils</u>: A liquid-liquid extraction (LLE) was used to isolate the phenolic fraction of the cocoa butter and pumpkin seed oil samples, both refined and virgin. The extraction was carried out following the method described by Suarez et al. [1] with some modifications. Briefly, 20 mL of methanol:water (80:20, v/v) was added to 5 g of oil and homogenized for 2 min with a Ultraturrax (IKA Labortechnik). After that, two phases were separated by centrifugation at 637×g for 10min and the hydroalcoholic phase was transferred to a balloon. This step was repeated twice and the extracts were combined in the balloon. Then, the hydroalcoholic extracts were rotatory evaporated up to a syrupy consistency at 31 ◦C and were dissolved in 5 mL of acetonitrile. Afterwards, the extract was washed three times with 10 mL of n-hexane and the rejected n-hexane was treated with 5 mL of acetonitrile. The acetonitrile solution was finally rotatory evaporated to dryness and then re-dissolved in 1 mL of acetonitrile and maintained at −18 ◦C before the chromatographic analysis. 5 μL of the eluate was directly injected into the LC-QTOF-MS. Extractions were carried out in triplicate.

<u>LC-QTOF-MS analysis of phenolic extracts from pumpkin seed oils</u>: The analysis of the phenolic compounds and their metabolitesin the oil samples was carried out by means of an LC-QTOF-MS system consisted of a LC-Agilent 1290Series (Agilent Technologies, Palo Alto, U.S.A.) coupled to a 6540 ESI-QTOF (Agilent Technologies) operated in negative electrospray ionization mode (ESI-). Separation was carried out using a Zorbax SB-Aq column (3.5μm, 150mm x 2.1mm i.d.) equipped with a Pre-Column Zorbax SB-C18 (3.5μm, 15mm x 2.1mm i.d.) also from Agilent. Drying gas temperature was 350°C and the flow rate was held at 12 l/min. On the other hand pressure of the gas nebulizer was 45 psi and the capillary voltage was set at 4000 V. The fragmentor was set at 120V, the skimmer at 65V and the OCT 1RF Vpp was set at 750V.

During the analysis, the column was kept at 25°C and the flow rate was 0.4 mL/min. The solvent composition was solvent A: milli-Q water/acetic acid (99.8:0.2 v/v) and solvent B: acetonitrile. Solvent B was initially 5% and was gradually increased reaching 55% at 10 minutes and 95% at 12 min. Then it was maintained isocratically up to 15 min and after that it was reduced to 5% in 1 minute and was held at initial conditions during 8 minutes to re-equilibrate the column. The injection volume was set at 5 μl.

References Supplement: 1

1. Suarez M, Macia A, Romero MP, Motilva MJ. Improved liquid chromatography tandem mass spectrometry method for the determination of phenolic compounds in virgin olive oil. J Chromatogr A. 2008;1214(1-2):90-9. doi:10.1016/j.chroma.2008.10.098.
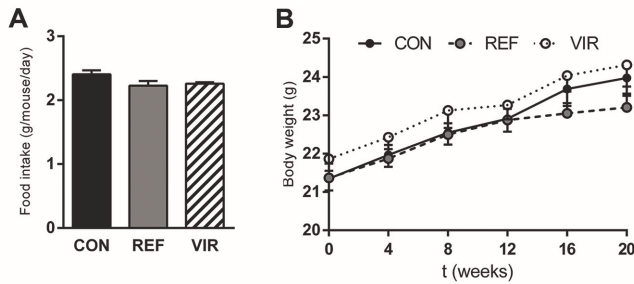
Supplemental Figure 1. Refined and virgin pumpkin seed oils do not affect food intake or body weight in ApoE*3Leiden mice. Mice were fed a Western type diet (CON) containing 9% refined pumpkin seed oil (REF) or 9% virgin pumpkin seed oil (VIR) for 20 weeks. (A) Average food intake was measured per cage in group-housed mice (3-4 mice per cage) and did not differ between groups. (B) Body weight was not affected by either VIR or REF and increased gradually over time. Data are mean±SEM.
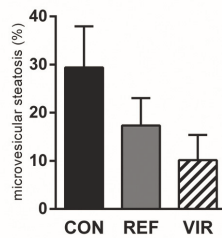
Supplemental Figure 2. Refined and virgin pumpkin seed oils do not affect microvesicular steatosis in ApoE*3Leiden mice. Mice were fed a Western type diet (CON) containing 9% refined pumpkin seed oil (REF) or 9% virgin pumpkin seed oil (VIR) for 20 weeks. Microvesicular hepatosteatosis (% of total liver cross section affected) was not reduced by REF or VIR. Data are mean±SEM.
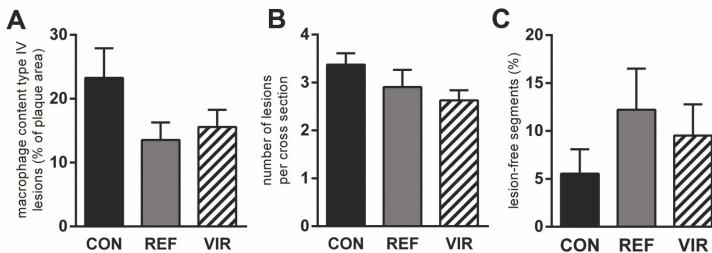
Supplemental Figure 3. Refined and virgin pumpkin seed oils do not affect number of lesions or lesion-free segments ApoE*3Leiden mice. Mice were fed a Western type diet (CON) containing 9% refined pumpkin seed oil (REF) or 9% virgin pumpkin seed oil (VIR) for 20 weeks. (A) Immunohistochemical staining for MAC-3 (CD107b) followed by quantification of positively stained area showed that the macrophage content of type IV lesions was not significantly reduced by REF or VIR. (B) number of lesions per cross section were not reduced by REF or VIR. (C) REF and VIR did not increase the percentage of lesion-free segments. Data are mean±SEM

Mirtoselect, an anthocyanin-rich bilberry extract, attenuates non-alcoholic steatohepatitis and associated fibrosis in ApoE*3Leiden mice

Abstract

Background & Aims: Anthocyanins may have beneficial effects on lipid metabolism and inflammation and are demonstrated to have hepatoprotective properties in models of restraint-stress- and chemically-induced liver damage. However, their potential to protect against non-alcoholic steatohepatitis (NASH) under conditions relevant for human pathogenesis remains unclear. Therefore, we studied the effects of the standardized anthocyanin-rich extract Mirtoselect on diet-induced NASH in a translational model of disease. **Methods:** ApoE*3Leiden mice were fed a Western-type cholesterol-containing diet without (HC) or with 0.1% (w/w) Mirtoselect (HCM) for 20 weeks to study effects on diet-induced NASH. **Results:** Mirtoselect attenuated HC-induced hepatic steatosis, as observed by decreased macro- and microvesicular hepatocellular lipid accumulation and reduced hepatic cholesteryl-ester content. This anti-steatotic effect was accompanied by local anti-inflammatory effects in liver, as demonstrated by reduced inflammatory cell clusters and reduced neutrophil infiltration in HCM. On a molecular level, HC-diet significantly induced hepatic expression of pro-inflammatory genes *Tnf*, *Emr1*, *Ccl2*, *Mpo*, *Cxcl1* and *Cxcl2* while this induction was less pronounced or significantly decreased in HCM. A similar quenching effect was observed for HC-induced pro-fibrotic genes, *Acta2* and *Col1a1* and this anti-fibrotic effect of Mirtoselect was confirmed histologically. Many of the pro-inflammatory and pro-fibrotic parameters positively correlated with intrahepatic free cholesterol levels. Mirtoselect significantly reduced accumulation and crystallisation of intrahepatic free cholesterol, providing a possible mechanism for the observed hepatoprotective effects. **Conclusions:** Mirtoselect attenuates development of NASH, reducing hepatic lipid accumulation, inflammation and fibrosis, possibly mediated by local anti-inflammatory effects associated with reduced accumulation and crystallisation of intrahepatic free cholesterol.

Introduction

Non-alcoholic fatty liver disease (NAFLD) is the most common cause of chronic liver disease in Western countries [1, 2]. It constitutes a spectrum of liver injury, ranging from the clinically benign intrahepatic accumulation of lipids (steatosis), to the more progressive non-alcoholic steatohepatitis (NASH). In addition to hepatic lipid accumulation, NASH is characterised by hepatic inflammation, i.e. infiltration of immune cells [3] and can further progress to fibrosis, cirrhosis and hepatocellular carcinoma. Although the mechanisms by which NASH progresses are not completely understood, it is thought that dysregulation of cholesterol homeostasis and subsequent accumulation of free (unesterified) cholesterol are linked to the pathogenesis of NASH in humans (reviewed in reference [4]). In line with this notion, emerging experimental evidence implicates free cholesterol as a potential trigger of inflammation [5] as well as a possible driving factor in the development of fibrosis [6, 7]. A recent study in experimental and human NASH revealed that intrahepatic accumulation of free cholesterol can lead to the formation of cholesterol crystals in hepatocyte lipid droplets, which may form an important trigger for the progression of simple steatosis to NASH [8].

The anthocyanins, a subclass of the polyphenols, comprise a large group of bioactive compounds that are considered to have many health-promoting effects [9], including cholesterol-lowering [10, 11] and anti-inflammatory effects [12] which may mediate potential hepatoprotective properties [13]. Here we studied the effects of the standardised anthocyanin-rich bilberry (*Vaccinium myrtillus L.*) extract Mirtoselect on the development of NASH. This extract has been demonstrated to reduce circulating makers of inflammation in humans [14, 15] and has beneficial effects in restraint-stress- [16, 17] and chemically-induced [18] models of liver damage. However, its hepatoprotective potential in diet-induced metabolic inflammation and liver disease is unclear. Therefore we studied effects of Mirtoselect on NASH in ApoE*3Leiden (E3L) mice, a translational model of disease [19]. These mice develop diet-induced dyslipidaemia and inflammation on a high-fat/high-cholesterol diet [20], and ultimately develop NASH with fibrosis. Earlier studies have shown that E3L mice are sensitive to nutritional [21] and pharmacological [19] interventions, and show human-like responses to hypolipidaemic compounds [19, 22].

Combined histological, biochemical, and gene expression analyses revealed that Mirtoselect reduces development of NASH, attenuating both steatosis and inflammation as well as the development of hepatic fibrosis. These effects were associated with a reduction in hepatic free

cholesterol accumulation and cholesterol crystal formation.

Materials and methods

Animal experiments

Experiments were approved by an independent Animal Care and Use Committee and were in compliance with European Community specifications regarding the use of laboratory animals. ApoE*3Leiden mice (E3L) were used because they allow study of diets and nutrients on lipids (including cholesterol) and liver inflammation [19, 23, 24].

Female E3L mice were fed a Western-type diet (15% cocoa butter, 1% corn oil, 40.5% sucrose, 20% acid casein, 10% corn starch and 6.2% cellulose; diet-T; AB-Diets, Woerden, the Netherlands), supplemented with 1% (w/w) cholesterol (Sigma-Aldrich, Zwijndrecht, the Netherlands) for 20 weeks. The study included a 4-week run-in during which all mice received this diet, after which they were matched for plasma cholesterol and triglycerides into 3 experimental groups (n=15/group). Control animals (HC) continued to receive the Western-type diet for the remainder of the study, while Mirtoselect-treated animals (HCM) received the HC diet with addition of 0.1% (w/w) Mirtoselect (Indena S.A.S., Paris, France). This standardised bilberry (*Vaccinium myrtillus L.*) extract contains 36% anthocyanins. An ageing reference group (REF) received the same Western-type diet mentioned above, but without cholesterol supplementation. Food intake and body weight were monitored throughout the study. Every 4 weeks, blood samples were collected via tail vein bleeding after a 4h fast, for isolation of EDTA plasma. Animals were sacrificed by CO_2 asphyxiation after 16 weeks of dietary treatment to collect livers. The medial lobe was fixed in formalin and embedded in paraffin for histological analysis of NASH and the left lobe was snap frozen in liquid nitrogen and stored at -80°C for cryosectioning, liver lipid- and mRNA-expression analyses.

Histological, biochemical and hepatic gene expression analyses

A detailed description of (immuno)histological, biochemical, and gene expression analyses is provided in Supplement 1: Detailed materials and methods. Briefly, development of NASH was assessed histologically using an adapted grading method for human NASH [25, 26]. Plasma lipids were determined with commercially available enzymatic assays and liver lipids were analysed by HPTLC, as described previously [27]. Hepatic gene expression analyses were performed by RT-PCR, using TaqMan® Gene Expression Assays (Life Technologies, Bleiswijk, the Netherlands) and changes in gene expression were calculated using the comparative

Ct (ΔΔCt) method, expressed as fold-change relative to REF. Illumina microarray analysis of hepatic gene expression was performed following established normalisation and quality control protocols followed by gene enrichment analysis across pathways and biological processes as described [23]. p65-NFκB activity was determined in liver homogenates by DNA-binding ELISA (TransAM® p65-NFκB Chemi Kit, Active Motif, La Hulpe, Belgium) according to manufacturer's instructions and as described [26].

Statistical analyses

All data are presented as mean ± SD. Statistical analyses were performed using SPSS software (version 22, IBM, Armonk, USA). For normally distributed variables, significance of differences between groups was tested by one-way ANOVA, with Dunnett's Multiple Comparison Post-Hoc Test to compare HC vs REF and HC vs HCM. In case of heterogeneity between groups, variables were analysed by ANOVA using Brown-Forsythe for differences between groups with Dunnett's T3 Post-Hoc Test. Non-normally distributed variables were tested by non-parametric Kruskall-Wallis test followed by Mann-Whitney U. A p-value<0.05 was considered statistically significant.

Results

Mirtoselect attenuates hepatic steatosis and hepatocellular damage

Treatments were well tolerated and there was no effect of Mirtoselect on food intake or body weight (Supplemental Fig. 1A-B). HC-feeding induced hepatosteatosis relative to REF, as observed histologically by a non-zonal accumulation of lipid macrovesicles and microvesicles in hepatocytes (Fig. 1A). Mirtoselect attenuated the development of hepatic steatosis (Fig. 1A), completely preventing the HC-induced increase in macrovesicular steatosis (p<0.001, Fig. 1B) and strongly decreasing microvesicular steatosis (p=0.027, Fig. 1C). Analysis of intrahepatic lipid composition revealed that this increase in hepatic steatosis in HC was mainly attributable to an accumulation of lipids esterified to cholesterol (cholesteryl esters), the concentration of which was significantly lower in HCM (p=0.008, Fig. 1D). Comparably, hepatic triglyceride levels (i.e. lipids esterified to glycerol) tended to build up in HC, but no increase was observed in HCM (Fig. 1E). In association with steatosis, HC-feeding resulted in a pronounced induction of hepatocellular hypertrophy, the development of which was markedly reduced in HCM (p=0.034, Supplemental Fig. 2). In HC-fed animals, some of these hypertrophic cells were deficient in cytokeratin 18 (CK 18) compared with neighbouring cells (Fig. 1F), indicating loss of cytoskeletal function and hepatocellular damage as seen in ballooning cells in
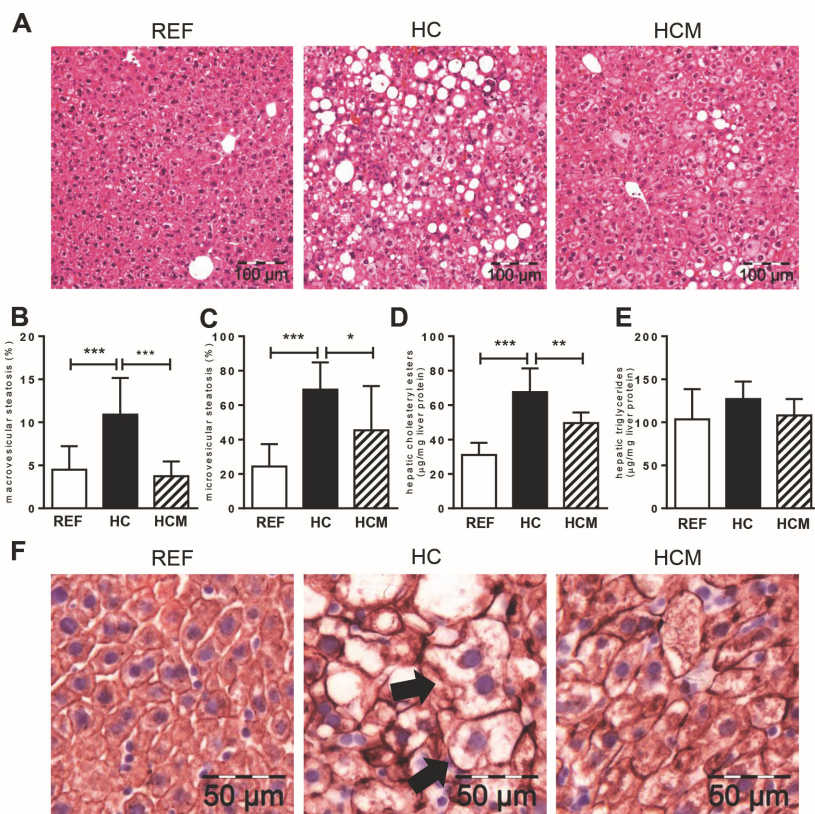
Figure 1. Mirtoselect attenuates hepatic steatosis in cholesterol-fed E3L-mice. (A) Representative photomicrographs of liver sections of reference, high-cholesterol control and Mirtoselect-treated mice. Mirtoselect attenuated HC-diet-induced (B) macrovesicular and (C) microvesicular steatosis. (D) Hepatic steatosis in HC-mice was mainly attributable to accumulation of cholesteryl-esters, the build-up of which was decreased by Mirtoselect. (E) Hepatic triglycerides tended to accumulate in HC, which was not observed in HCM. (F) In HC-fed animals, some hypertrophic cells were CK18-deficient compared with neighbouring cells (arrows); presence of these cells was reduced in HCM. REF: non-cholesterol-fed reference, HC: high-cholesterol control, HCM: high-cholesterol+Mirtoselect. Data are mean±SD. *p<0.05, **p<0.01, ***p<0.001 compared with HC.

human NASH [28, 29]. In Mirtoselect-treated mice, only very few enlarged CK-18 deficient cells were observed (Fig. 1F), indicating a reduction in hepatocellular damage.

Mirtoselect reduces hepatic inflammation

In addition to hepatosteatosis, a defining characteristic of NASH is the presence of hepatic inflammation, which can be observed histologically as the lobular infiltration of inflammatory cells, i.e. inflammatory aggregates containing mononuclear cells (F4/80-positive cells of the monocyte/macrophage lineage) and polymorph nuclear cells (MPO-positive granulocytes,

i.e. neutrophils). In comparison with REF, the number of inflammatory cell aggregates increased strongly in HC, and this HC-induced hepatic inflammatory response was fully blunted with Mirtoselect (p<0.001, Fig. 2A). Investigation of hepatic *Emr1* (F4/80) gene expression revealed that the influx of inflammatory cells was partly attributable to macrophages, which was supported by increased gene expression levels of *Ccl2* (MCP-1), a mediator of monocyte recruitment (Fig 2B-C). Mirtoselect did not affect expression of *Emr1* or *Ccl2* (Fig. 2B-C), indicating that its anti-inflammatory effect may impair the influx of another immune cell type.
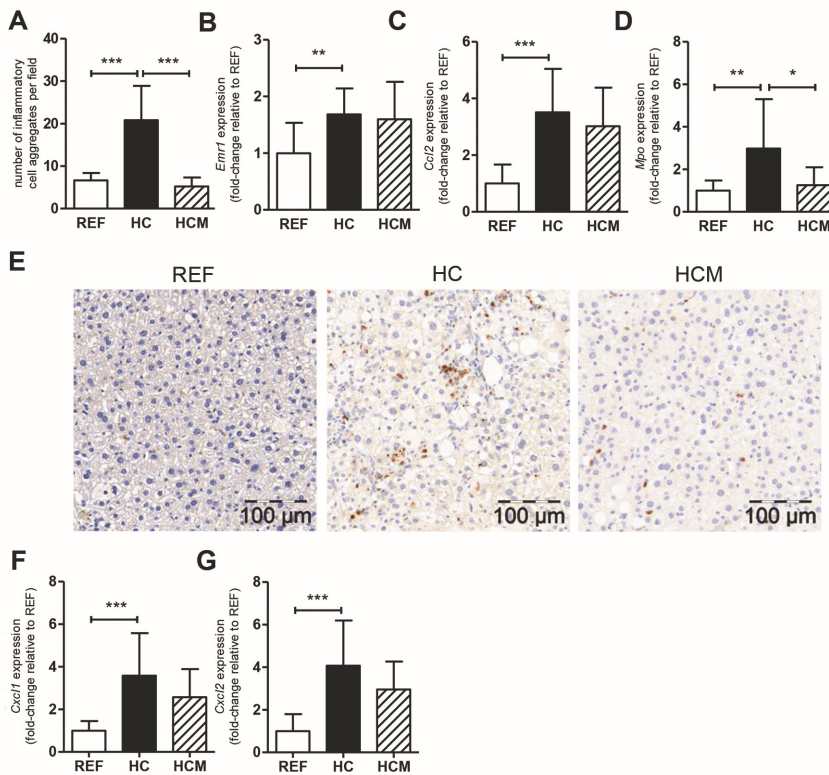
Figure 2. Mirtoselect reduces hepatic inflammation in cholesterol-fed E3L-mice. (A) The number of HC-induced inflammatory cell aggregates was reduced by Mirtoselect. HC-diet induced (B) *Emr1* and (C) *Ccl2* gene expression was not affected by Mirtoselect. Mirtoselect reduced HC-induced (D) *Mpo* gene expression and (E) number of MPO-positive cells as determined immunohistochemically. HC-induced gene expression of neutrophil chemoattractants (F) *Cxcl1* and (G) *Cxcl2* was less pronounced in HCM. REF: non-cholesterol-fed reference, HC: high-cholesterol control, HCM: high-cholesterol+Mirtoselect. Data are mean±SD. *p<0.05, **p<0.01, ***p<0.001 compared with HC.

Hepatic gene expression analysis of the neutrophil marker *Mpo* showed that *Mpo* expression was increased in HC animals and this induction was completely prevented in HCM animals (p=0.034, Fig. 2D). Immunohistochemical staining of MPO-positive cells confirmed the mRNA expression data and showed that HC induced neutrophil infiltration, which was attenuated by HCM (Fig. 2E). In line with these findings, the expression of two neutrophil chemoattractants – *Cxcl1* and *Cxcl2* – was upregulated strongly and significantly by HC feeding while induction of these chemokines was less pronounced in HCM animals (*Cxcl1*: p=0.327, *Cxcl2*: p=0.131, Fig. 2F-G).

Mirtoselect attenuates hepatic fibrosis

Continued hepatic inflammation is thought to drive the progression of NASH, ultimately resulting in the development of hepatic fibrosis. Histochemical staining of hepatic collagen content by Picro-Sirius Red staining demonstrated that the HC diet caused liver fibrosis, characterised by periportal, pericentral and perisinusoidal deposition of collagen. This HC-induced fibrosis was much less pronounced in HCM (Fig. 3A). In line with these histological observations, biochemical analysis of hepatic collagen content revealed a pronounced increase in collagen content in HC compared with REF, which was significantly reduced in HCM (p=0.034, Fig. 3B) and hepatic gene expression analysis of *Col1a1* showed significantly increased expression in HC compared with REF, while Mirtoselect quenched this effect and significantly reduced *Col1a1* expression compared with HC (p=0.011, Fig. 3C). Additionally, HC diet significantly induced expression of the hepatic stellate cell activation marker *Acta2* (α-SMA) (Fig. 3D), as well as the pro-fibrotic cytokines *Tgfb1* (TGF-β) and *Tnf* (TNF-α) (Fig. 3E-F). In line with the attenuating effect of Mirtoselect on hepatic fibrosis development, the induction of these genes was less pronounced, although non-significantly, in HCM (*Acta2*: p=0.173, *Tgfb1*: p=0.174, *Tnf*: p=0.096, Fig. 3D-F). Subsequent microarray pathway analysis revealed that many genes downstream of TGF-β were affected, indicating strongly and significantly activated TGF-β signalling in HC compared with REF (z=7.539, p=2.5E 51). Mirtoselect strongly inhibited activation of this pathway (z=-4.862, p=3.3E-20 compared with HC). Consistent with this, the process 'Hepatic fibrosis/hepatic stellate cell activation', was strongly activated in HC compared with REF and Mirtoselect suppressed this activation (Supplemental Fig. 3). Together, our data demonstrate that HC-feeding induced histopathological and molecular hallmarks of NASH and fibrosis and that Mirtoselect significantly attenuated disease development.
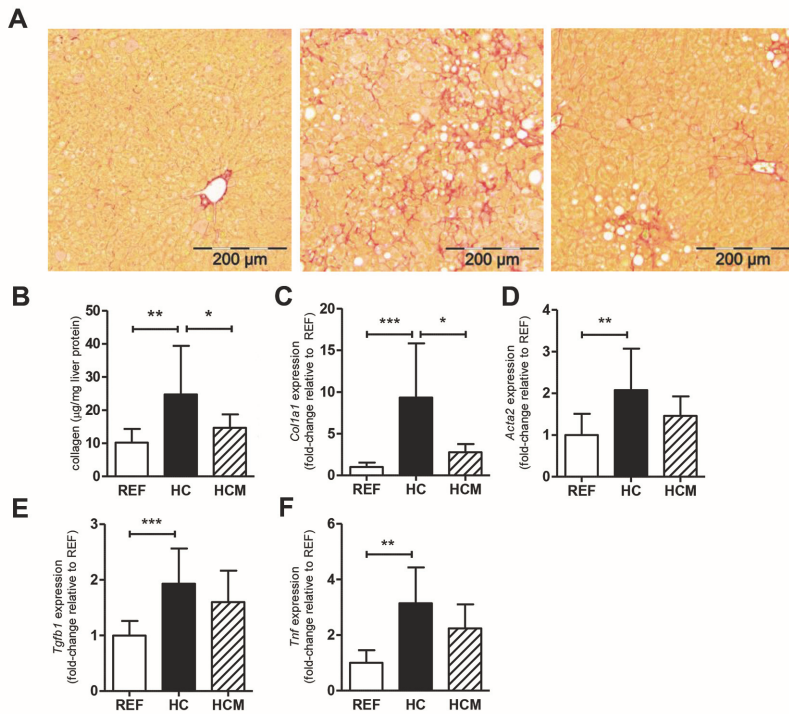
Figure 3. Development of hepatic fibrosis in cholesterol-fed E3L-mice reduced by Mirtoselect. (A) Representative photomicrographs of picro-sirius red-stained liver sections show reduction of HC-induced collagen content in Mirtoselect-treated mice, which was confirmed by (B) biochemical analysis of hepatic collagen content. (C) Induction of *Col1a1* gene expression is prevented by Mirtoselect. Gene expression of hepatic stellate cell activation marker (D) *Acta2* as well as pro-fibrotic cytokines (E) *Tgfb1* and (F) *Tnf* was induced by HC, while this induction was less pronounced in HCM. REF: non-cholesterol-fed reference, HC: high-cholesterol control, HCM: high-cholesterol+Mirtoselect. Data are mean±SD. *p<0.05, **p<0.01, ***p<0.001 compared with HC.

Intrahepatic free cholesterol correlates with development of NASH and is reduced by Mirtoselect

To gain more insight into the metabolic-inflammatory processes that drive the development of NASH and hepatic fibrosis and the effects of Mirtoselect thereupon, we next analysed a possible metabolic trigger of inflammation: cholesterol. HC-feeding induced dyslipidaemia with increased plasma total cholesterol compared with REF, specifically in the VLDL- and LDL-sized particles. Mirtoselect did not affect circulating cholesterol levels or lipoprotein profile (Supplemental Fig. 4) pointing to a hepatoprotective effect within the liver tissue. As intrahepatic free cholesterol is a very potent inducer of liver inflammation [23] and is elevated intrahepatically in human NASH [30, 31], we determined free cholesterol concentrations in freshly prepared liver homogenates and correlated them with histology scores and gene

expression data. Both hepatic inflammation (number of inflammatory clusters observed histologically, p<0.001), and hepatic fibrosis (hepatic *Col1a1* expression, p=0.007) were positively correlated with hepatic free cholesterol levels (Fig. 4A-B). Further strengthening this notion, we also observed positive significant correlations of hepatic free cholesterol levels with the expression level of many of the investigated pro-inflammatory and pro-fibrotic parameters (i.e. *Ccl2*, *Cxcl1*, *Cxcl2*, *Acta2*, *Tgfb1* and *Tnf*, shown in Supplemental Fig. 5). Importantly, Mirtoselect fully blunted the disease-associated increase in hepatic free cholesterol, the concentrations of which were comparable to REF and significantly lower than in HC (p=0.008, Fig. 4C). To further examine the link between cholesterol and inflammation and the effects of Mirtoselect thereupon we analysed activation of inflammatory pathways by microarray as well as biochemically. HC diet significantly induced TNF-α and IL-1β signalling (TNF-α: z= 7.539, p=2.5E-51; IL-1β: z=6.516, p=4.70E-30; vs REF) and activated the downstream pro-inflammatory transcription factor NFκB (z=6.245, p4.82E-14 vs REF). Consistent with this, hepatic free cholesterol levels were positively correlated with biochemically measured transcriptional activation of p65-NFκB (R^2=0.51, p=0.021), providing a link between cholesterol and inflammation. Mirtoselect significantly reduced p65-NFκB activity relative to HC (fold-change relative to REF: 1.15±0.11 in HC vs 0.98±0.05 in HCM, p=0.032).

More detailed analysis of processes that may underlie observed effects of Mirtoselect on hepatic cholesterol accumulation showed that plasma markers of cholesterol uptake (plant sterols to cholesterol ratio and cholestanol to cholesterol ratio) or cholesterol biosynthesis (lathosterol to cholesterol ratio) were not affected in HCM (Supplemental Fig. 6). Also, microarray analysis confirmed absence of an effect of Mirtoselect on cholesterol biosynthesis but revealed a significant activation of FXR in HCM (z=2.190, p=7.64E-03) and showed that genes involved in bile acid synthesis, bile acid conjugation and bile salt secretion (e.g. *Bsep*, *Cyp27a1*) were upregulated in HCM.

Refined microscopic analysis of liver cross-sections under polarised light revealed that HC-feeding caused pronounced formation of large birefringent crystals within a considerable amount of the macrovesicular lipid droplets, while these crystals were hardly observed in Mirtoselect-treated animals (even in the few regions containing macrovesicles, Fig. 4D-E). These birefringent crystals stained positively with filipin (Fig. 4F), which forms a fluorescent complex with free cholesterol specifically, indicating that the observed birefringence is attributable to crystallised free cholesterol. Detailed examination of the liver cross-sections under bright field and polarised light microscopy revealed that many of the hepatocytes

containing these crystals were devoid of normal cellular morphology and organisation. The prevention of this intrahepatic cholesterol crystal formation by Mirtoselect provides a possible rationale for its observed hepatoprotective properties.
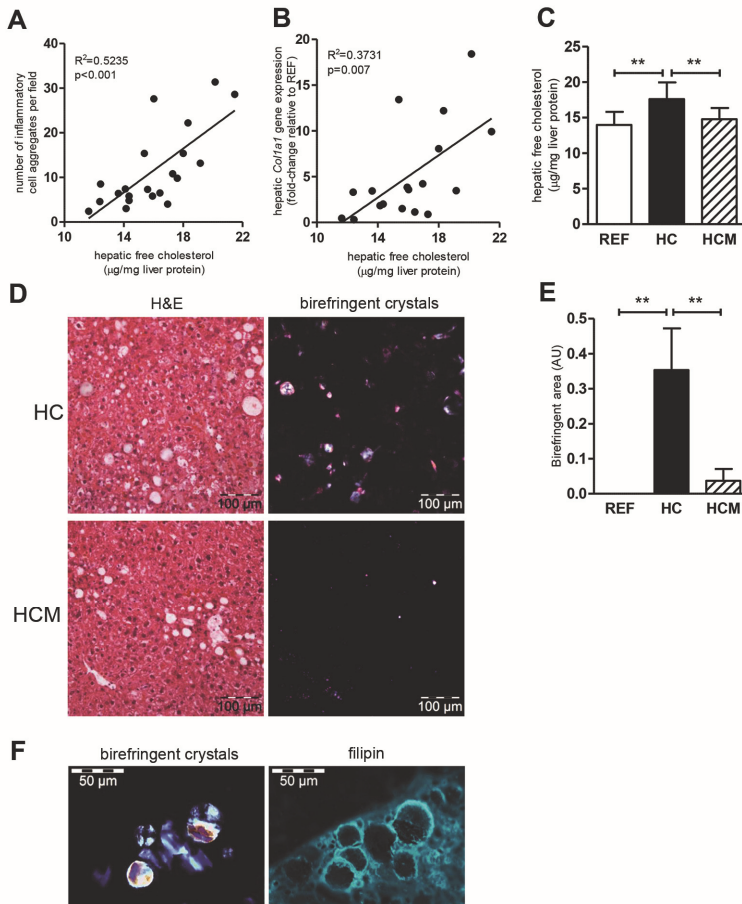
Figure 4. Mirtoselect reduces intrahepatic free cholesterol accumulation and crystallisation in cholesterol-fed E3L-mice. Intrahepatic free cholesterol levels correlated with hepatic inflammation (inflammatory aggregates per field; A) and hepatic fibrosis (*Col1a1* expression; B). (C) HC-induced hepatic free cholesterol accumulation was not observed in HCM. (D) Representative photomicrographs of liver cryosections (same field under bright-field and polarised-light microscopy) reveal presence of birefringent crystals in HC that were hardly observed in HCM. (E) Quantification of birefringent area shows strong HC-induced increase that is not observed in HCM. (F) Birefringent crystals stained prominently with free-cholesterol staining filipin (same field under polarised-light and fluorescent microscopy). REF: non-cholesterol-fed reference, HC: high-cholesterol control, HCM: high-cholesterol+Mirtoselect. Data are mean±SD. **p<0.01 compared with HC.

Discussion

We investigated the potential hepatoprotective properties of a standardised anthocyanin-rich extract (Mirtoselect) in a diet-induced, translational model of NASH with fibrosis. We show that Mirtoselect protects against the development of NASH, reducing hepatic steatosis, hepatic inflammation and hepatic fibrosis, associated with decreased accumulation and crystallisation of intrahepatic free cholesterol. The observed hepatoprotective effects of Mirtoselect were achieved at a dosage that translates to an anthocyanin intake of around 300mg/day in humans, an intake that is achievable by diet [12, 32, 33].

HC diet-feeding induced intrahepatic lipid accumulation characterised by macro- and micro-vesicular steatosis, which was mainly attributable to an increase in lipids esterified to cholesterol. Mirtoselect strongly reduced this intrahepatic accumulation of lipids. Experimental support for these observed anti-steatotic effects is provided by results from earlier studies that report improved hepatic cholesterol homeostasis in rodents treated with similar concentrations of anthocyanin-rich extracts [10, 34] or individual anthocyanins [35]. Although these studies were not performed under conditions leading to NAFLD/NASH, they do provide a possible mechanism for the observed reduction in intrahepatic cholesterol: intervention with anthocyanins was found to increase bile acid synthesis [34, 35] and faecal sterol excretion [10, 35], thereby reducing intrahepatic cholesterol accumulation [10, 35] which is consistent with our observations of FXR activation by Mirtoselect. Although it is the anthocyanin fraction of Mirtoselect that is considered to be the principal bioactive fraction of the extract, it is unknown which of these anthocyanins or other possibly bioactive constituents (alone or in combination), may be responsible for the observed effects.

In addition to reducing hepatic steatosis Mirtoselect also attenuated hepatic inflammation, completely preventing the HC-induced increase in inflammatory cell aggregates. This anti-inflammatory effect was largely attributable to an effect specifically on the influx of MPO-positive neutrophils, the infiltration of which is recognised as a defining characteristic of inflammation in human NASH [36]. The exact role of neutrophils in the pathogenesis of NASH remains to be elucidated [37], but their ability to release a potent cocktail of reactive oxygen species and proteases implicates them as potential cause of extensive tissue damage [38] that may contribute to amplification of the inflammatory response as well as development of fibrosis. We observed a marked reduction of neutrophils in livers of Mirtoselect-treated mice, but only a modest effect on the hepatic expression of neutrophil chemoattractants *Cxcl1* and

Cxcl2, suggesting additional mechanisms outside the liver. Indeed, it has been demonstrated that anthocyanins can attenuate the induction of chemokine receptors such as CXCR2 [39], which is required for neutrophil chemotaxis.

Although inflammation is recognised to play an important role in the development of NASH, the nature of the trigger for this inflammatory component remains unclear. Lipotoxicity caused by the build-up of toxic lipid species is thought to play an important role, but the specific lipid species that mediate hepatic lipotoxicity have not been identified with certainty [40]. While triglycerides are the main accumulating lipid species in human NASH, recent studies have implicated free cholesterol as a potential trigger for disease progression [4]. The experimental conditions chosen for the present study emphasize the role of cholesterol in NASH, and limit the study of hepatic triglyceride accumulation. Results from epidemiological studies that link dietary cholesterol intake to increased risk and severity of NAFLD [41, 42] and cirrhosis [43] provide indications that cholesterol may play a causal role in NASH development. In support of this notion, free cholesterol is increased intrahepatically in human [30, 31] and experimental NASH [44] and modulation of hepatic free cholesterol levels by diet [44] or pharmacological intervention [45] is closely linked to the severity of experimental NASH. Furthermore, there are indications that cholesterol-lowering agents (e.g. statins, ezetimibe) may improve NASH in patients with hypercholesterolaemia [46, 47]. Mechanistic studies have shown that free cholesterol accumulation in Kupffer cells [48] and hepatic stellate cells (HSC) [6, 7] promotes inflammation and exacerbates fibrosis (e.g. increased TNF-α and CCL2 expression by Kupffer cells and increased COL1A1 expression in HSC). Results from the study described herein show that intrahepatic free cholesterol levels are positively correlated with many factors that contribute to or reflect progressive development of NASH (e.g. *Ccl2*, *Cxcl1*, *Cxcl2*, *Col1a1*, *Acta2*, *Tnf*, and *Tgfb1*). The observed activation of inflammatory signalling routes (IL-1β, TNF-α, TGF-β) by HC as well as the positive correlation between free cholesterol and NFκB activity, point to NFκB activation as an effector of cholesterol-induced inflammation, which is in line with previous observations [23, 27]. Mirtoselect decreases the build-up of this cytotoxic lipid species and associated NFκB activation, thereby providing a possible explanation for its beneficial effects on NAFLD development.

A recently emerging mechanism of cellular toxicity associated with free cholesterol accumulation is intracellular cholesterol crystallisation, which can happen when the concentration of free cholesterol reaches a very high level [49]. Cholesterol crystals, particularly when they are very small (nm range), can trigger inflammation through inflammasome

activation [5, 50]. Besides putative pro-inflammatory effects of cholesterol crystals [5, 50], it is plausible that the sheer size of the intrahepatocellular cholesterol crystals observed in the present study (with diameters ranging up to 50 μm) would also cause extensive physical damage to the cells containing them. Indeed, the formed cholesterol crystals may damage cells by physically disrupting the integrity of intracellular structures [49], in line with observations in the present study. Furthermore, cellular damage can result in the release of damage associated molecular patterns (DAMPs), which leads to neutrophil recruitment [37] further enhancing the inflammatory response. Additional support for this mechanism is provided by results from human studies that demonstrate that cholesterol crystals distinguish NASH from simple steatosis [8] and that this accumulation and crystallisation of free cholesterol within steatotic hepatocytes may be an important trigger for disease progression.

Overall, we show that Mirtoselect has beneficial effects in NASH, improving hepatic steatosis, inflammation and fibrosis. Furthermore, we demonstrate the presence of cholesterol crystals and associated tissue damage in NASH and show that dietary intervention with Mirtoselect prevents this accumulation and crystallisation of free cholesterol, providing a possible rationale for its hepatoprotective effects. Given the moderate dose of Mirtoselect used, this study suggests that intervention with naturally occurring, well-tolerated polyphenols may constitute a powerful approach to retard NASH development.

Acknowledgements

Financial support

Declaration of interests

The authors declare that they have no conflict of interest, including any conflict of interest with the manufacturer of the test compound used herein.

References

1. Browning JD, Szczepaniak LS, Dobbins R, Nuremberg P, Horton JD, Cohen JC, et al. Prevalence of hepatic steatosis in an urban population in the United States: Impact of ethnicity. Hepatology. 2004;40(6):1387-95. doi:10.1002/hep.20466.

2. Clark JM. The epidemiology of nonalcoholic fatty liver disease in adults. J Clin Invest. 2006;40 Suppl 1:S5-10. doi:10.1097/01.mcg.0000168638.84840.ff.

3. Fujii H, Kawada N. Inflammation and fibrogenesis in steatohepatitis. J Gastroenterol. 2012;47(3):215-25. doi:10.1007/s00535-012-0527-x.

4. Musso G, Gambino R, Cassader M. Cholesterol metabolism and the pathogenesis of non-alcoholic steatohepatitis. Prog Lipid Res. 2013;52(1):175-91. doi:10.1016/j.plipres.2012.11.002.

5. Duewell P, Kono H, Rayner KJ, Sirois CM, Vladimer G, Bauernfeind FG, et al. NLRP3 inflammasomes are required for atherogenesis and activated by cholesterol crystals. Nature. 2010;464(7293):1357-61. doi:10.1038/nature08938.

6. Teratani T, Tomita K, Suzuki T, Oshikawa T, Yokoyama H, Shimamura K, et al. A high-cholesterol diet exacerbates liver fibrosis in mice via accumulation of free cholesterol in hepatic stellate cells. Gastroenterology. 2012;142(1):152-64.e10. doi:10.1053/j.gastro.2011.09.049.

7. Tomita K, Teratani T, Suzuki T, Shimizu M, Sato H, Narimatsu K, et al. Free cholesterol accumulation in hepatic stellate cells: Mechanism of liver fibrosis aggravation in nonalcoholic steatohepatitis in mice. Hepatology. 2014;59(1):154-69. doi:10.1002/hep.26604.

8. Ioannou GN, Haigh WG, Thorning D, Savard C. Hepatic cholesterol crystals and crown-like structures distinguish NASH from simple steatosis. J Lipid Res. 2013;54(5):1326-34. doi:10.1194/jlr.M034876.

9. He J, Giusti MM. Anthocyanins: Natural colorants with health-promoting properties. Annu Rev Food Sci Technol. 2010;1:163-87. doi:10.1146/annurev.food.080708.100754.

10. Liang Y, Chen J, Zuo Y, Ma KY, Jiang Y, Huang Y, et al. Blueberry anthocyanins at doses of 0.5 and 1 % lowered plasma cholesterol by increasing fecal excretion of acidic and neutral sterols in hamsters fed a cholesterol-enriched diet. Eur J Nutr. 2013;52(3):869-75. doi:10.1007/s00394-012-0393-6.

11. Qin Y, Xia M, Ma J, Hao Y, Liu J, Mou H, et al. Anthocyanin supplementation improves serum LDL- and HDL-cholesterol concentrations associated with the inhibition of cholesteryl ester transfer protein in dyslipidemic subjects. Am J Clin Nutr. 2009;90(3):485-92. doi:10.3945/ajcn.2009.27814.

12. Jennings A, Welch AA, Spector T, Macgregor A, Cassidy A. Intakes of anthocyanins and flavones are associated with biomarkers of insulin resistance and inflammation in women. J Nutr. 2014;144(2):202-8. doi:10.3945/jn.113.184358.

13. Valenti L, Riso P, Mazzocchi A, Porrini M, Fargion S, Agostoni C. Dietary anthocyanins as nutritional therapy for nonalcoholic fatty liver disease. Oxid Med Cell Longev. 2013;2013:145421. doi:10.1155/2013/145421.

14. Karlsen A, Paur I, Bohn SK, Sakhi AK, Borge GI, Serafini M, et al. Bilberry juice modulates plasma concentration of NF-kappaB related inflammatory markers in subjects at increased risk of CVD. Eur J Nutr. 2010;49(6):345-55. doi:10.1007/s00394-010-0092-0.

15. Kolehmainen M, Mykkanen O, Kirjavainen PV, Leppanen T, Moilanen E, Adriaens M, et al. Bilberries reduce low-grade inflammation in individuals with features of metabolic syndrome. Molecular Nutrition and Food Research. 2012;56(10):1501-10. doi:10.1002/mnfr.201200195.

16. Bao L, Abe K, Tsang P, Xu JK, Yao XS, Liu HW, et al. Bilberry extract protect restraint stress-induced liver damage through attenuating mitochondrial dysfunction. Fitoterapia. 2010;81(8):1094-101. doi:10.1016/j.fitote.2010.07.004.

17. Bao L, Yao XS, Yau CC, Tsi D, Chia CS, Nagai H, et al. Protective effects of bilberry (Vaccinium myrtillus L.) extract on restraint stress-induced liver damage in mice. J Agric Food Chem. 2008;56(17):7803-7. doi:10.1021/jf800728m.

18. Domitrovic R, Jakovac H. Effects of standardized bilberry fruit extract (Mirtoselect(R)) on resolution of CCl4-induced liver fibrosis in mice. Food Chem Toxicol. 2011;49(4):848-54. doi:10.1016/j.fct.2010.12.006.

19. Zadelaar S, Kleemann R, Verschuren L, de Vries-Van der Weij J, van der Hoorn J, Princen HM, et al. Mouse models for atherosclerosis and pharmaceutical modifiers. Arterioscler Thromb

Vasc Biol. 2007;27(8):1706-21. doi:10.1161/ATVBAHA.107.142570.

20. Duivenvoorden I, Voshol PJ, Rensen PC, van Duyvenvoorde W, Romijn JA, Emeis JJ, et al. Dietary sphingolipids lower plasma cholesterol and triacylglycerol and prevent liver steatosis in APOE*3Leiden mice. Am J Clin Nutr. 2006;84(2):312-21.

21. Morrison M, van der Heijden R, Heeringa P, Kaijzel E, Verschuren L, Blomhoff R, et al. Epicatechin attenuates atherosclerosis and exerts anti-inflammatory effects on diet-induced human-CRP and NFkappaB in vivo. Atherosclerosis. 2014;233(1):149-56. doi:10.1016/j.atherosclerosis.2013.12.027.

22. van de Steeg E, Kleemann R, Jansen HT, van Duyvenvoorde W, Offerman EH, Wortelboer HM, et al. Combined analysis of pharmacokinetic and efficacy data of preclinical studies with statins markedly improves translation of drug efficacy to human trials. The Journal of Pharmacology and Experimental Therapeutics. 2013;347(3):635-44. doi:10.1124/jpet.113.208595.

23. Kleemann R, Verschuren L, van Erk MJ, Nikolsky Y, Cnubben NH, Verheij ER, et al. Atherosclerosis and liver inflammation induced by increased dietary cholesterol intake: A combined transcriptomics and metabolomics analysis. Genome Biol. 2007;8(9):R200. doi:10.1186/gb-2007-8-9-r200.

24. Verschuren L, Wielinga PY, van Duyvenvoorde W, Tijani S, Toet K, van Ommen B, et al. A dietary mixture containing fish oil, resveratrol, lycopene, catechins, and vitamins E and C reduces atherosclerosis in transgenic mice. J Nutr. 2011;141(5):863-9. doi:10.3945/jn.110.133751.

25. Kleiner DE, Brunt EM, Van Natta M, Behling C, Contos MJ, Cummings OW, et al. Design and validation of a histological scoring system for nonalcoholic fatty liver disease. Hepatology. 2005;41(6):1313-21. doi:10.1002/hep.20701.

26. Liang W, Lindeman JH, Menke AL, Koonen DP, Morrison M, Havekes LM, et al. Metabolically induced liver inflammation leads to NASH and differs from LPS- or IL-1beta-induced chronic inflammation. Lab Invest. 2014;94(5):491-502. doi:10.1038/labinvest.2014.11.

27. Wielinga PY, Yakala GK, Heeringa P, Kleemann R, Kooistra T. Beneficial effects of alternate dietary regimen on liver inflammation, atherosclerosis and renal activation. PLoS One. 2011;6(3):e18432. doi:10.1371/journal.pone.0018432.

28. Caldwell S, Ikura Y, Dias D, Isomoto K, Yabu A, Moskaluk C, et al. Hepatocellular ballooning in NASH. J Hepatol. 2010;53(4):719-23. doi:10.1016/j.jhep.2010.04.031.

29. Zatloukal K, Stumptner C, Fuchsbichler A, Fickert P, Lackner C, Trauner M, et al. The keratin cytoskeleton in liver diseases. J Pathol. 2004;204(4):367-76. doi:10.1002/path.1649.

30. Caballero F, Fernandez A, De Lacy AM, Fernandez-Checa JC, Caballeria J, Garcia-Ruiz C. Enhanced free cholesterol, SREBP-2 and StAR expression in human NASH. J Hepatol. 2009;50(4):789-96. doi:10.1016/j.jhep.2008.12.016.

31. Puri P, Baillie RA, Wiest MM, Mirshahi F, Choudhury J, Cheung O, et al. A lipidomic analysis of nonalcoholic fatty liver disease. Hepatology. 2007;46(4):1081-90. doi:10.1002/hep.21763.

32. Cassidy A, Mukamal KJ, Liu L, Franz M, Eliassen AH, Rimm EB. High anthocyanin intake is associated with a reduced risk of myocardial infarction in young and middle-aged women. Circulation. 2013;127(2):188-96. doi:10.1161/CIRCULATIONAHA.112.122408.

33. Hertog MG, Hollman PC, Katan MB, Kromhout D. Intake of potentially anticarcinogenic flavonoids and their determinants in adults in The Netherlands. Nutr Cancer. 1993;20(1):21-9. doi:10.1080/01635589309514267.

34. Mauray A, Felgines C, Morand C, Mazur A, Scalbert A, Milenkovic D. Bilberry anthocyanin-rich extract alters expression of genes related to atherosclerosis development in aorta of apo E-deficient mice. Nutrition, Metabolism and Cardiovascular Diseases. 2012;22(1):72-80. doi:10.1016/j.numecd.2010.04.011.

35. Wang D, Xia M, Gao S, Li D, Zhang Y, Jin T, et al. Cyanidin-3-O-beta-glucoside upregulates hepatic cholesterol 7alpha-hydroxylase expression and reduces hypercholesterolemia in mice. Molecular Nutrition and Food Research. 2012;56(4):610-21. doi:10.1002/mnfr.201100659.

36. Brunt EM, Janney CG, Di Bisceglie AM, Neuschwander-Tetri BA, Bacon BR. Nonalcoholic steatohepatitis: a proposal for grading and staging the histological lesions. Am J Gastroenterol. 1999;94(9):2467-74. doi:10.1111/j.1572-0241.1999.01377.x.

37. Xu R, Huang H, Zhang Z, Wang FS. The role of neutrophils in the development of liver diseases. Cellular and Molecular Immunology. 2014;11(3):224-31. doi:10.1038/cmi.2014.2.

38. Kubes P, Mehal WZ. Sterile inflammation in the liver. Gastroenterology. 2012;143(5):1158-72. doi:10.1053/j.gastro.2012.09.008.

39. Kang MK, Li J, Kim JL, Gong JH, Kwak SN, Park JH, et al. Purple corn anthocyanins inhibit diabetes-associated glomerular monocyte activation and macrophage infiltration. American Journal of Physiology - Renal Physiology. 2012;303(7):F1060-9. doi:10.1152/ajprenal.00106.2012.

40. Farrell GC, van Rooyen D, Gan L, Chitturi S. NASH is an inflammatory disorder: Pathogenic, prognostic and therapeutic implications. Gut Liver. 2012;6(2):149-71. doi:10.5009/gnl.2012.6.2.149.

41. Musso G, Gambino R, De Michieli F, Cassader M, Rizzetto M, Durazzo M, et al. Dietary habits and their relations to insulin resistance and postprandial lipemia in nonalcoholic steatohepatitis. Hepatology. 2003;37(4):909-16. doi:10.1053/jhep.2003.50132.

42. Yasutake K, Nakamuta M, Shima Y, Ohyama A, Masuda K, Haruta N, et al. Nutritional investigation of non-obese patients with non-alcoholic fatty liver disease: the significance of dietary cholesterol. Scand J Gastroenterol. 2009;44(4):471-7. doi:10.1080/00365520802588133.

43. Ioannou GN, Morrow OB, Connole ML, Lee SP. Association between dietary nutrient composition and the incidence of cirrhosis or liver cancer in the United States population. Hepatology. 2009;50(1):175-84. doi:10.1002/hep.22941.

44. Van Rooyen DM, Larter CZ, Haigh WG, Yeh MM, Ioannou G, Kuver R, et al. Hepatic free cholesterol accumulates in obese, diabetic mice and causes nonalcoholic steatohepatitis. Gastroenterology. 2011;141(4):1393-403, 403.e1-5. doi:10.1053/j.gastro.2011.06.040.

45. Van Rooyen DM, Gan LT, Yeh MM, Haigh WG, Larter CZ, Ioannou G, et al. Pharmacological cholesterol lowering reverses fibrotic NASH in obese, diabetic mice with metabolic syndrome. J Hepatol. 2013;59(1):144-52. doi:10.1016/j.jhep.2013.02.024.

46. Ekstedt M, Franzen LE, Mathiesen UL, Holmqvist M, Bodemar G, Kechagias S. Statins in non-alcoholic fatty liver disease and chronically elevated liver enzymes: a histopathological follow-up study. J Hepatol. 2007;47(1):135-41. doi:10.1016/j.jhep.2007.02.013.

47. Yoneda M, Fujita K, Nozaki Y, Endo H, Takahashi H, Hosono K, et al. Efficacy of ezetimibe for the treatment of non-alcoholic steatohepatitis: An open-label, pilot study. Hepatol Res. 2010;40(6):566-73. doi:10.1111/j.1872-034X.2010.00644.x.

48. Leroux A, Ferrere G, Godie V, Cailleux F, Renoud ML, Gaudin F, et al. Toxic lipids stored by Kupffer cells correlates with their pro-inflammatory phenotype at an early stage of steatohepatitis. J Hepatol. 2012;57(1):141-9. doi:10.1016/j.jhep.2012.02.028.

49. Tabas I. Consequences of cellular cholesterol accumulation: Basic concepts and physiological implications. J Clin Invest. 2002;110(7):905-11. doi:10.1172/JCI16452.

50. Samstad EO, Niyonzima N, Nymo S, Aune MH, Ryan L, Bakke SS, et al. Cholesterol crystals induce complement-dependent inflammasome activation and cytokine release. J Immunol. 2014;192(6):2837-45. doi:10.4049/jimmunol.1302484.

Supplemental data

Supplement 1. Detailed Material and Methods

<u>Histological assessment of NASH</u>: NASH development was assessed in haematoxylin and eosin-stained liver sections (3 μM) by analysis of steatosis and inflammation, the two key features of NASH. Steatosis was determined at a 40× magnification by analysis of macro-vesicular and microvesicular steatosis and hepatocellular hypertrophy (hepatocyte size >1.5x normal diameter [1]), expressed as the percentage of the total liver slice area affected (considering only the area of the slice occupied by hepatocytes). Hepatocellular damage was assessed by immunohistochemical staining of cytokeratin 18 (CK18), which can be used to investigate cytoskeletal injury as observed in ballooning cells in human NASH [2]. For this, 8 μM cryosections were fixed in formalin and stained with an anti-CK18 antibody (ab27553, Abcam, Cambridge, UK). Hepatic inflammation was analysed by counting the number of inflammatory foci per field at a 100× magnification (view size 3.1 mm^2) in five different fields per specimen, and was expressed as the average number of foci per field. Neutrophils were identified immunohistochemically using an anti-myeloperoxidase antibody (ab9535; Abcam, Cambridge, UK) and the number of myeloperoxidase-positive inflammatory clusters was counted in the same manner as described above for the number of inflammatory foci. Hepatic collagen content was stained histochemically using Picro-Sirius Red staining (Chroma, WALDECK-Gmbh, Münster, Germany).

Frozen liver sections (8 μM) were fixed in formalin, stained with haematoxylin and eosin and subsequently examined by bright-field microscopy with or without a polarising filter to investigate the presence of birefringent crystals. To examine co-localisation of these crystals with hepatic unesterified 'free' cholesterol, frozen liver sections (8 μM) were stained with filipin (Filipin III from Streptomyces filipinensis, Sigma-Aldrich, Zwijndrecht, the Netherlands), which forms a fluorescent complex with free cholesterol but not with esterified sterols [3]. Liver sections were fixed in formalin for 15 min, then treated with 10% FBS in PBS for 30 min, followed by incubation with filipin (4 mg/ml in DMSO, diluted to 125 μg/ml in 10% FBS) for 1h. Slides were examined by fluorescence microscopy and bright-field microscopy with a polarising filter.

<u>Liver lipid analysis</u>: Lipids were extracted from liver homogenates using the Bligh and Dyer method [4] and separated by high performance thin layer chromatography (HPTLC) on silica gel plates as described previously [5]. Lipid spots were stained with colour reagent (5 g

MnCl$_2$4H$_2$O, 32 ml 95–97% H$_2$SO$_4$ added to 960 ml CH$_3$OH:H$_2$O 1:1 v/v) and triglycerides, cholesteryl esters and free cholesterol were quantified using TINA version 2.09 software (Raytest, Straubenhardt, Germany).

Biochemical analyses: Hepatic collagen content was measured in formalin-fixed, paraffin-embedded liver sections by quantitative colorimetric determination of hydroxyproline residues, obtained by acid hydrolysis of collagen (Total Collagen Assay, Quickzyme Biosciences, Leiden, the Netherlands) and expressed per mg liver protein.

Total plasma cholesterol and triglyceride levels were measured by commercially available enzymatic assays (cholesterol CHOD-PAP 11491458 and triglycerides GPO-PAP 11488872, Roche, Woerden, the Netherlands). Lipoprotein profiles were determined in pooled plasma, fractionated using an ÄKTA fast protein liquid chromatography system (Pharmacia, Roosendaal, The Netherlands) and analysed as reported [6].

p65-NFκB activity was determined in liver homogenates by DNA-binding ELISA (TransAM® p65-NFκB Chemi Kit, Active Motif, La Hulpe, Belgium) according to manufacturer's instructions and as described previously [1]. This assay determines the amount of active transcription factor (equal amounts of protein were used) by measuring its binding capacity to a consensus binding site in the presence of a competitive or a mutated (non-competitive) oligonucleotide, to correct for non-specific DNA binding. Data are expressed as fold-change relative to REF.

Gas chromatography analysis of neutral sterols in plasma: Plasma samples were pooled (n=5 pools per group) before treatment with alkaline methanol at 37°C for 90 minutes, using 5α-cholestane (Sigma-Aldrich) as an internal standard. Neutral sterols were then extracted with chloroform and subsequently silylated by DMF-Sil-Prep (Grace Davison Discovery Sciences, Deerfield, USA). Neutral sterol derivatives were separated on a 25 m×0.25 mm capillary GC column (CP Sil 5B, Varian Chrompack International, Middelburg, the Netherlands) in a 3800 gas chromatograph (Varian Chrompack International) equipped with a flame ionisation detector. The injector and the flame ionisation detector were kept at 300°C. The column temperature was programmed from 230 to 280°C. Quantitation was based on the area ratio of the individual neutral sterol to that of the internal standard 5α-cholestane.
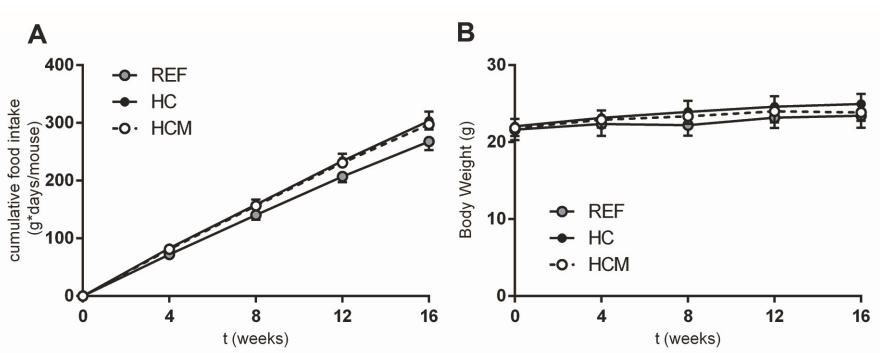
mRNA expression analyses: Total RNA was extracted with RNA Bee Total RNA Isolation Kit (Bio-Connect, Huissen, the Netherlands). RNA concentration was determined spectrophotometrically using Nanodrop 1000 (Isogen Life Science, De Meern, the Netherlands)

and RNA quality was assessed using 2100 Bioanalyzer (Agilent Technologies, Amstelveen, the Netherlands). cDNA was synthesised using a High Capacity RNA-to-cDNA™ Kit (Life Technologies, Bleiswijk, the Netherlands). Transcripts were quantified using TaqMan® Gene Expression Assays (Life Technologies) and the following primer/probe-sets for *Emr1* (Mm00802529_m1), *Ccl2* (Mm00441242_m1), *Mpo* (Mm01298424_m1), *Cxcl1* (Mm04207460_m1), *Cxcl2* (Mm00436450_m1), *Col1a1* (Mm00801666_g1), *Tgfb1* (Mm00441724_m1), *Tnf* (Mm00443258_m1), *Acta2* (Mm01546133_m1), and the endogenous controls *Ppif* (Mm01273726_m1), *Hprt* (Mm00446968_m1) and *Gapdh* (4308313). Changes in gene expression were calculated using the comparative Ct ($\Delta\Delta$Ct) method and expressed as fold-change relative to REF.

<u>Microarray gene expression analysis</u>: Microarray analysis was performed on individual samples from REF, HC and HCM animals (n=10 per group). Biotin-labeled cRNA was synthesized from total RNA using the Illumina TotalPrep RNA Amplification Kit (Ambion, Huntington, UK). The biotinylated cRNA was hybridised onto the MouseRef-8 v2 expression BeadChip (Illumina, San Diego CA, USA). Illumina's Genomestudio v1.1.1 software was used for data extraction, using the default settings as advised by Illumina. All the quality control data of this BeadChip were within the specifications of the microarray service provider (Service XS, Leiden, the Netherlands). The probe-level background-subtracted expression values were used as input for lumi package [7] of the R/Bioconductor (http://www.bioconductor.org; http://www.r-project.org) to perform quality control and quantile normalisation. Unexpressed probes (p>0.01 in all experiments) were removed from further analysis, and 13312 probes remained in the analysis. Differentially expressed probes were identified using the limma package of R/Bioconductor [8] and the threshold for significance was set at p-values <0.01. Selected differentially expressed probes (DEPs) were used as an input for pathway analysis through Ingenuity Pathway Analysis suite (www.ingenuity.com, accessed 2014) and Ingenuity Pathway Analysis (IPA) software. This analysis determines the activation state of pathways and processes based on the observed differential gene expression in relation to the number of genes present in that particular pathway or process. This results in an overlap p-value and activation z-score for each gene in the IPA knowledgebase. The activation z-score indicates activation (positive z-score) or inhibition (negative z-score) of a particular pathway or biological process. An activation z-score >2 or <-2 indicates significant activation or inhibition of a pathway or process.

References Supplement 1:

1. Liang W, Lindeman JH, Menke AL, Koonen DP, Morrison M, Havekes LM, et al. Metabolically induced liver inflammation leads to NASH and differs from LPS- or IL-1beta-induced chronic inflammation. Lab Invest. 2014;94(5):491-502. doi:10.1038/labinvest.2014.11.
2. Caldwell S, Ikura Y, Dias D, Isomoto K, Yabu A, Moskaluk C, et al. Hepatocellular ballooning in NASH. J Hepatol. 2010;53(4):719-23. doi:10.1016/j.jhep.2010.04.031.
3. Maxfield FR, Wustner D. Analysis of cholesterol trafficking with fluorescent probes. Methods Cell Biol. 2012;108:367-93. doi:10.1016/B978-0-12-386487-1.00017-1.
4. Bligh EG, Dyer WJ. A rapid method of total lipid extraction and purification. Can J Biochem Physiol. 1959;37(8):911-7. doi:10.1139/o59-099.
5. Wielinga PY, Yakala GK, Heeringa P, Kleemann R, Kooistra T. Beneficial effects of alternate dietary regimen on liver inflammation, atherosclerosis and renal activation. PLoS One. 2011;6(3):e18432. doi:10.1371/journal.pone.0018432.
6. Kooistra T, Verschuren L, de Vries-van der Weij J, Koenig W, Toet K, Princen HM, et al. Fenofibrate reduces atherogenesis in ApoE*3Leiden mice: evidence for multiple antiatherogenic effects besides lowering plasma cholesterol. Arterioscler Thromb Vasc Biol. 2006;26(10):2322-30. doi:10.1161/01.ATV.0000238348.05028.14.
7. Du P, Kibbe WA, Lin SM. lumi: a pipeline for processing Illumina microarray. Bioinformatics (Oxford, England). 2008;24(13):1547-8. doi:10.1093/bioinformatics/btn224.
8. Wettenhall JM, Smyth GK. limmaGUI: a graphical user interface for linear modeling of microarray data. Bioinformatics (Oxford, England). 2004;20(18):3705-6. doi:10.1093/bioinformatics/bth449.

Supplemental Figure 1. Effect of Mirtoselect on food intake and body weight in ApoE*3Leiden mice. Mirtoselect (0.1% w/w) did not affect (A) food intake or (B) body weight in cholesterol-fed (1% w/w) ApoE*3Leiden mice. REF: non-cholesterol-fed reference, HC: high-cholesterol control, HCM: high-cholesterol + Mirtoselect. Data are mean±SD.
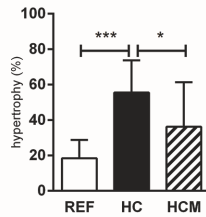
Supplemental Figure 2. Effect of Mirtoselect on hepatocellular hypertrophy in ApoE*3Leiden mice. Mirtoselect (0.1% w/w) reduced HC-diet-induced hepatocellular hypertrophy (size>1.5x normal diameter) in cholesterol-fed (1% w/w) ApoE*3Leiden mice. REF: non-cholesterol-fed reference, HC: high-cholesterol control, HCM: high-cholesterol+Mirtoselect. Data are mean±SD. *p<0.05, ***p<0.001 compared with HC.
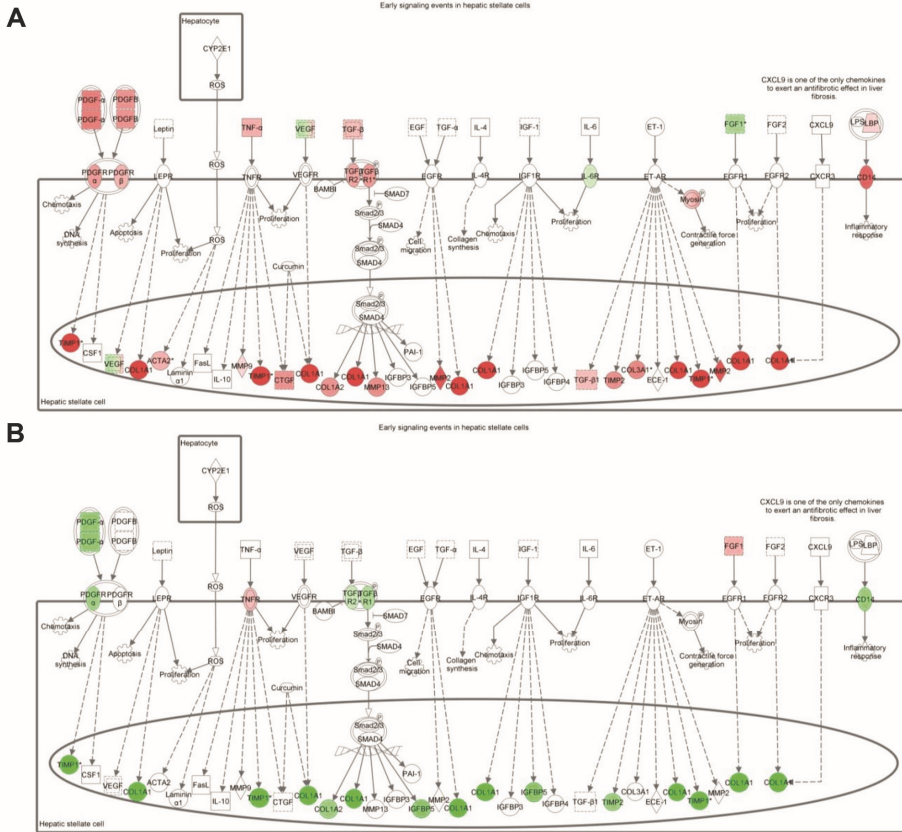
Supplemental Figure 3. Mirtoselect reduces hepatic stellate cell activation in cholesterol-fed ApoE*3Leiden mice
Mirtoselect (0.1% w/w) reduces activation of hepatic stellate cells in cholesterol-fed (1% w/w) ApoE*3Leiden mice. Hepatic microarray analysis followed by Ingenuity pathway analysis shows activation of this process in HC compared with REF (A), as demonstrated by upregulation (red) of most genes involved, and reduced activation in HCM compared with HC (B) as demonstrated by downregulation (green) of most genes involved. REF: non-cholesterol-fed reference, HC: high-cholesterol control, HCM: high-cholesterol+Mirtoselect.
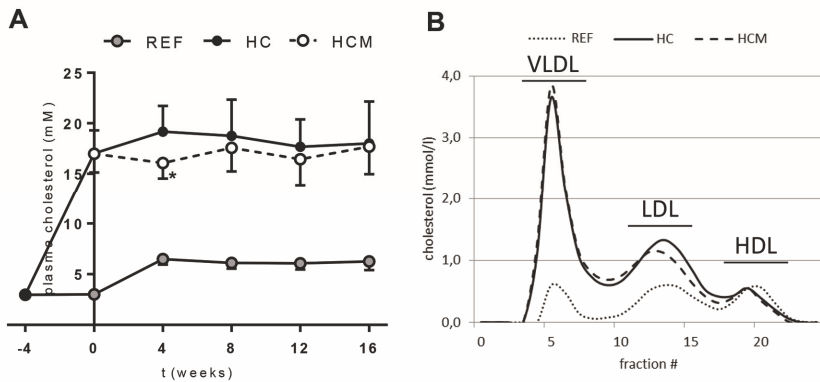
Supplemental Figure 4. Effects of Mirtoselect on plasma cholesterol and lipoprotein profile in ApoE*3Leiden mice. Mirtoselect (0.1% w/w) did not affect plasma cholesterol levels (A) or lipoprotein profile (as determined by FPLC at t=16 weeks; B) in cholesterol-fed (1% w/w) ApoE*3Leiden mice, apart from a transient decrease in plasma cholesterol at t=4 weeks. REF: non-cholesterol-fed reference, HC: high-cholesterol control, HCM: high-cholesterol + Mirtoselect. Data are mean±SD. * p<0.05 compared with HC control.
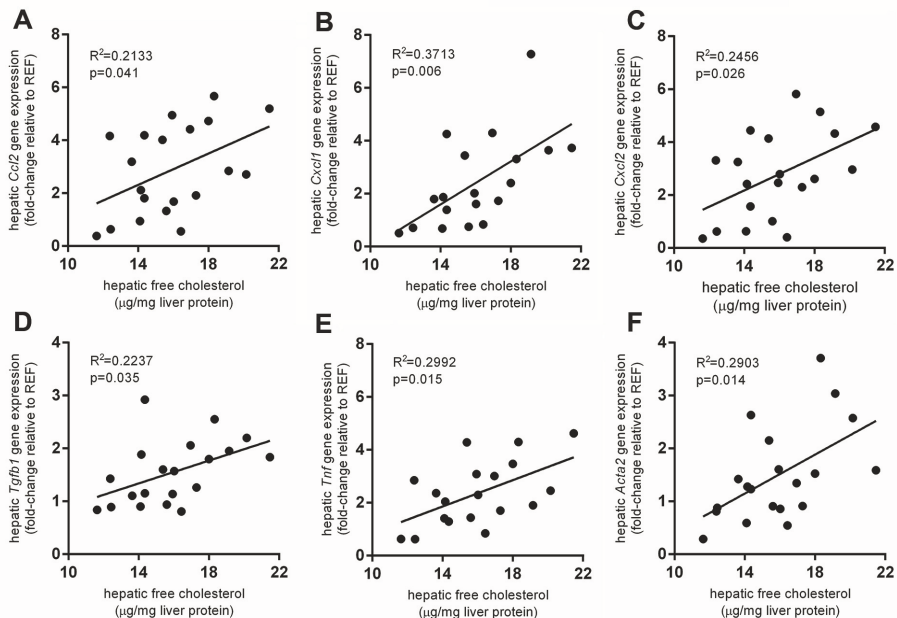
Supplemental Figure 5. Correlation of intrahepatic free cholesterol levels with hepatic expression of pro-inflammatory and pro-fibrotic factors in ApoE*3Leiden mice. Intrahepatic free cholesterol levels, as determined by HPTLC, correlated with hepatic mRNA expression of pro-inflammatory and pro-fibrotic factors *Ccl2* (A), *Cxcl1* (B), *Cxcl2* (C), *Tgfb1* (D), *Tnf* (E) and *Acta2* (F) after 16 weeks of dietary treatment in ApoE*3Leiden mice. Strength and statistical significance of the correlations was tested using Pearson's correlation coefficient analysis.
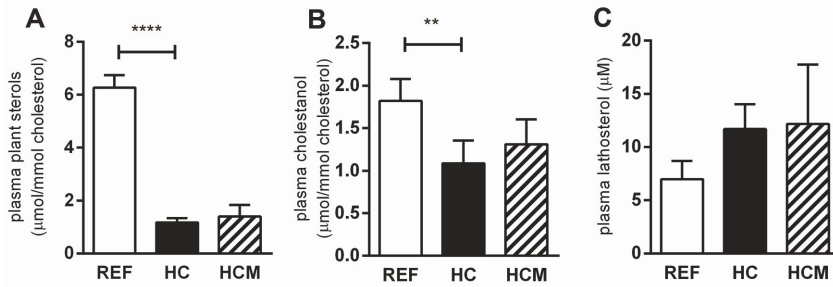
Supplemental Figure 6. Mirtoselect does not affect plasma markers of intestinal cholesterol uptake or cholesterol biosynthesis in ApoE*3Leiden mice. Mirtoselect (0.1% w/w) did not affect plasma markers of intestinal cholesterol absorption or cholesterol biosynthesis in cholesterol-fed (1% w/w) ApoE*3Leiden mice. Mirtoselect does not affect (A) plasma levels of intestinal cholesterol absorption markers: plant sterol (sum of campesterol, stigmasterol and b-sitosterol) to cholesterol ratio or (B) plasma cholestanol to cholesterol ratio, and has no effect on (C) plasma levels of the cholesterol biosynthesis marker: plasma lathosterol to cholesterol ratio. REF: non-cholesterol-fed reference, HC: high-cholesterol control, HCM: high-cholesterol+Mirtoselect. Data are mean±SD. *p<0.05, **p<0.01 compared with HC.

Chapter 7

Epicatechin attenuates atherosclerosis and exerts anti-inflammatory effects on diet-induced human-CRP and NFκB *in vivo*

Abstract

Objective: Previous studies investigating flavanol-rich foods provided indications for potential cardioprotective effects of these foods, but the effects of individual flavanols remain unclear. We investigated whether the flavanol epicatechin can reduce diet-induced atherosclerosis, with particular emphasis on the cardiovascular risk factors dyslipidaemia and inflammation. **Methods:** ApoE*3Leiden mice were fed a cholesterol-containing atherogenic diet with or without epicatechin (0.1% w/w) to study effects on early- and late-stage atherosclerosis (8w and 20w). *In vivo* effects of epicatechin on diet-induced inflammation were studied in human-CRP transgenic mice and NFκB-luciferase reporter mice. **Results:** Epicatechin attenuated atherosclerotic lesion area in ApoE*3Leiden mice by 27%, without affecting plasma lipids. This anti-atherogenic effect of epicatechin was specific to the severe lesion types, with no effect on mild lesions. Epicatechin mitigated diet-induced increases in plasma SAA (in ApoE*3-Leiden mice) and plasma human-CRP (in human-CRP transgenic mice). Microarray analysis of aortic gene expression revealed an attenuating effect of epicatechin on several diet-induced pro-atherogenic inflammatory processes in the aorta (e.g. chemotaxis of cells, matrix remodelling), regulated by NFκB. These findings were confirmed immunohistochemically by reduced lesional neutrophil content in HCE, and by inhibition of diet-induced NFκB activity in epicatechin-treated NFκB-luciferase reporter mice. **Conclusions:** Epicatechin attenuates development of atherosclerosis and impairs lesion progression from mild to severe lesions in absence of an effect on dyslipidaemia. The observed reduction of circulating inflammatory risk factors by epicatechin (e.g. SAA, human-CRP), as well as its local anti-inflammatory activity in the vessel wall, provide a rationale for epicatechin's anti-atherogenic effects.

Introduction

Cardiovascular disease (CVD) is the leading cause of death worldwide. Its major underlying pathology is atherosclerosis, a complex, multi-factorial disease that is driven by dyslipidaemia and chronic inflammation [1]. Accumulation of lipids and inflammatory cells in the arterial wall promotes formation of mild lesions known as fatty streaks. Over time, continuous inflammatory stress drives progression of these early-stage mild lesions into late-stage severe lesions that are characterised by extensive vascular remodelling.

Diet is an important determinant of CVD risk [2, 3]. Epidemiologic studies have provided consistent evidence that the incidence of CVD is associated with diets rich in saturated fat [4], which may be mediated by increased levels of circulating inflammatory factors (e.g. liver-derived SAA, CRP, reviewed in [5, 6]). In contrast, a diet rich in fruit and vegetables is associated with decreased levels of inflammatory markers [7-9] and may attenuate the development of CVD [10]. The polyphenols, a large group of bioactive compounds ubiquitous in plant-derived foods, are considered a potential mediator of these cardioprotective effects [11]. The flavanol subclass of the polyphenols in particular has been studied extensively in relation to its putative cardioprotective properties [12]. The majority of these studies investigated health benefits of flavanol-rich foods such as tea and cocoa, and report reduced risk of myocardial infarction [13], CVD [14, 15], stroke [16] and atherosclerotic disease mortality [17]. Results from numerous human intervention studies on the effects of these flavanol-rich foods provide further support for possible cardioprotective effects of these foods, although their effects on the CVD risk factors – plasma lipids and inflammatory markers – are not always consistent (recently reviewed in [18, 19]).

Of the flavanols, (-)-epicatechin is considered as an important candidate that may be responsible for beneficial effects of these flavanol-rich foods [20], and a strong inverse relationship with CVD mortality has been reported for (-)-epicatechin specifically [21]. These results indicate a beneficial role for epicatechin in atherogenesis, all the more so because epicatechin has been shown to have anti-inflammatory [22] and anti-oxidative [23] properties *in vivo*. In the latter study, Loke et al. reported a small (-14%), non-significant effect of epicatechin on total lesion area in apoE-/- mice, despite clear anti-oxidative effects of epicatechin. As apoE is involved in lipid metabolism as well as inflammatory processes, and apoE-/- mice lack this factor completely, the apoE-/- model is not optimally suited to study diet-induced dyslipidaemia and inflammation in the development of atherosclerosis [24].

Here, we studied the effects of epicatechin on atherosclerosis in ApoE*3Leiden (E3L) mice, an alternative model for atherosclerosis that does allow for investigation of effects on dyslipidaemia and inflammation throughout the atherogenic process. When fed a high-fat/high-cholesterol diet, E3L mice develop mild dyslipidaemia with a human-like lipoprotein profile, low-grade inflammation and atherosclerosis characterised by moderate progression through the stages of disease, allowing for controlled analysis of early- and late-stage processes [24, 25]. Atorvastatin was used as a cholesterol-reducing pharmaceutical reference. For a more thorough characterisation of the effects of epicatechin on diet-induced inflammation we used specific models of liver and whole-body inflammation: human-CRP transgenic mice [26] and NFκB-luciferase reporter mice [27], respectively. Histological analysis of early- and late stage atherosclerosis in E3L mice showed that epicatechin reduces atherosclerosis by attenuating progression to severe lesions. Biochemical analyses together with aortic genome profiling provide indication that these anti-atherogenic effects may at least partly be explained by epicatechin's anti-inflammatory properties.

Materials and methods

Animal experiments

Experiments were approved by an independent Animal Care and Use Committee and were in compliance with European Community specifications regarding the use of laboratory animals.

Atherosclerosis experiments: Female ApoE*3-Leiden transgenic (E3L) mice, characterised by ELISA, were fed an atherogenic Western-type diet for a four-week run-in period. This diet contains 15% cocoa butter, 1% corn oil, 40.5% sucrose, 20% acid casein, 10% corn starch and 6.2% cellulose (diet-T; AB-Diets, Woerden, the Netherlands), and was supplemented with 1% (w/w) cholesterol (Sigma-Aldrich, Zwijndrecht, the Netherlands). After run-in on this high-cholesterol (HC) diet, mice were matched for plasma cholesterol and triglycerides into 4 treatment groups (n=15 each). The control group continued to receive the HC diet, and the epicatechin-treated group (HCE) received the HC diet supplemented with 0.1% (w/w) (-)-epicatechin (Chromadex Inc., Irvine, USA) for 16 weeks. Two reference groups were included: an 0.01% (w/w) atorvastatin-treated pharmaceutical reference group (HCA) (Lipitor, Pfizer, Capelle a/d Ijssel, the Netherlands) and an ageing reference group (REF) that received the Western-type diet without cholesterol supplementation. Plasma epicatechin concentration in HCE mice was determined in pooled plasma (n=15 animals per pool, non-fasted) by HPLC-MS/MS on an Agilent HPLC 1200 Series with a Zorbax SB-Aq column

(3.5 μm, 150 mm × 2.1 mm i.d.) (both Agilent Technologies, Palo Alto, USA)) as previously described [28].

EDTA plasma samples were collected from the tail vein after a 4h fasting period. Body weight and food intake were monitored throughout the study. Animals were sacrificed by CO_2 asphyxiation after 16 weeks of dietary treatment to collect hearts, aortas and kidneys. Hearts were fixed in formalin and embedded in paraffin for atherosclerosis analysis. Descending aortas were snap-frozen in liquid nitrogen and stored at -80°C for microarray analysis.

In an independent early-stage atherosclerosis experiment, female E3L mice were matched for plasma cholesterol and triglycerides into an HC and an HCE group (n=15 each). Mice were fed the diets described above, without a run-in period. After 8 weeks of dietary treatment, animals were sacrificed by CO_2 asphyxiation and hearts were collected for atherosclerosis analysis as described above.

Diet-induced inflammation experiments: Human-CRP transgenic mice carry a 31-kb human DNA fragment containing the human-CRP gene including the entire human-CRP promoter. Male mice were characterised by human-CRP ELISA (R&D Systems, Abingdon, UK) and matched into 2 treatment groups (n=10-14) based on plasma human-CRP. Mice were fed standard mouse chow (ssniff® R/M-H, ssniff Spezialdiäten, Soest, Germany) without or with epicatechin (0.06% w/w) for 2 weeks followed by a high-fat diet (45% kcal% fat D12451, Research Diets, New Brunswick, USA) without (HF) or with (-)-epicatechin (0.1% w/w, HFE) for 3 weeks. To correct for the higher food intake on the chow diet compared with the fat-containing diets, the epicatechin concentration was adjusted to achieve a comparable daily intake. EDTA plasma was collected from the tail vein (non-fasted) before and after HFD-feeding for human-CRP measurements. NFκB-luciferase reporter mice carry a transgene for the firefly luciferase gene, coupled with three binding sites for NF-κB. This transgene is flanked by insulator sequences from the chicken [β]-globin gene to reduce genomic interference [27]. Female mice were characterised by RT-PCR. NF-κB activity was monitored non-invasively by *in vivo* molecular imaging in an IVIS spectrum *in vivo* imaging system (Caliper Life Sciences, Hopkinton, USA). Mice were anaesthetised using 2.5% isoflurane, and ventral fur was removed by shaving. Images were acquired 5 min after intraperitoneal injection of D-Luciferin (150 mg/kg, Caliper Life Sciences), with an exposure time of 30s. Living imaging 4 software (Caliper Life Sciences) was used to quantify the signal. Mice were matched into 2 experimental groups according to baseline NFκB activity. Mice were fed HC diet (n=15) or HCE diet (n=7) for 7 days after which diet-induced NFκB activity was determined.

Histological, biochemical and microarray analyses

A detailed description of histological, biochemical and microarray analyses is provided in Supplement 1. Detailed materials and methods. Briefly, atherosclerosis was scored histologically using an adapted grading method for human atherosclerosis, and the plasma parameters and histological and RT-PCR analyses of renal pathology were quantified as described [29]. Illumina microarray analysis of aortic gene expression was performed following established normalisation and quality control protocols [25] as well as pathway analysis [30].

Statistical analysis

All data are presented as mean±SD. The atherosclerosis experiments investigated the null hypothesis that epicatechin may not exert beneficial anti-atherosclerotic effects relative to the untreated control (HC). Significance of differences between HCE and HC animals was tested using one-sided t-tests. The reference groups (REF and HCA) were not required to test the null hypothesis and were used to control the experimental conditions of the disease model. The experiments in the inflammation models investigated the potential effects of epicatechin in preventing diet-induced inflammation. Paired one-sided t-tests were used to calculate the significance of induction of inflammation within each group. Statistical tests were performed using SPSS software (version 20, IBM, Armonk USA) or Graphpad Prism software (version 5.03, Graphpad Software Inc., La Jolla, USA). A p-value ≤ 0.05 was considered statistically significant.

Results

Epicatechin attenuates atherosclerosis development without effect on plasma lipids

All treatments were well tolerated and food intake and body weight were comparable in HC and HCE (Supplemental Table 1) throughout the 16-week study period. The calculated daily dose of epicatechin in HCE was 110±11 mg/kg body weight, based on food intake measurements. HCE diet-feeding resulted in an average plasma epicatechin concentration of 4.2 μM, i.e. within the micromolar range achievable in humans [31]. The atherogenic HC-diet induced pronounced atherosclerosis in HC relative to REF, with a total atherosclerotic lesion area in the aortic root of 515190±265747 μm^2 compared with 11797±11822 μm^2 in REF (Fig. 1A). Epicatechin treatment significantly attenuated the development of atherosclerosis by 27% (375495±205386 μm^2, Fig. 1A-B). As expected, atherosclerosis development was strongly reduced in atorvastatin-treated reference mice (100148±108685 μm^2). Epicatechin had no effect on the microvasculature (HC-induced kidney injury) as assessed histologically (not shown).
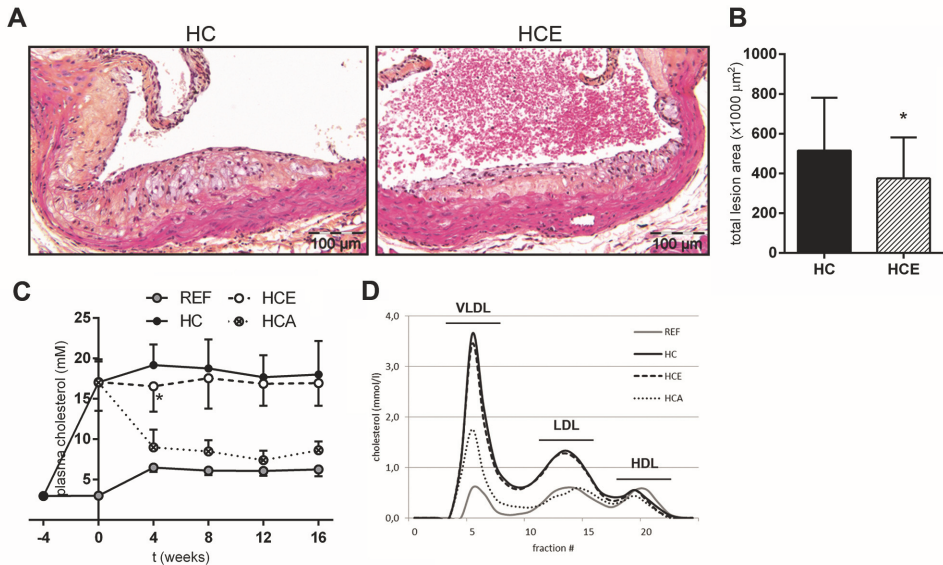
Figure 1. Effects of 16-week epicatechin-treatment (0.1% w/w in atherogenic HC diet) on atherosclerosis and plasma lipids in E3L mice. (A) representative photomicrographs of the aortic root area showing smaller and less severe atherosclerotic lesions in HCE compared with HC. (B) total atherosclerotic lesion area quantified in serial cross-sections of the aortic valve area (n=15/group). (C) plasma cholesterol levels over the time-course of the intervention. (D) lipoprotein profile for cholesterol distribution in VLDL, LDL and HDL-sized particles. REF: reference, HC: high cholesterol, HCE: high cholesterol + epicatechin, HCA: high cholesterol + atorvastatin. Data are mean±SD. *p≤0.05 compared with HC.

Dyslipidaemia is a major risk factor for atherosclerosis development. HC-diet feeding strongly increased plasma cholesterol levels (17.05±2.84 mM) relative to REF (6.24±0.66 mM) within the first 4 weeks and levels remained stable for the rest of the study, with an average of 18.14±3.17 mM (Fig. 1C). The increase in plasma cholesterol observed in HC was confined to the atherogenic VLDL- and LDL-sized particles (Fig. 1D). Addition of epicatechin to the diet had no effect on total plasma cholesterol levels and lipoprotein profile, except a small transient decrease in total cholesterol after 4 weeks of treatment. In line with its well-known lipid-lowering properties, atorvastatin treatment strongly and rapidly decreased plasma cholesterol and levels remained low until the end of the study (average 8.38±1.60 mM, a 54% reduction). Atorvastatin treatment reduced cholesterol in the VLDL and LDL-sized particles specifically. Plasma triglyceride levels were not affected by epicatechin and were slightly reduced by atorvastatin treatment (Supplemental Table 1).

These results indicate that the anti-atherogenic effect of epicatechin is independent of an effect on plasma lipids. We therefore continued by investigating the effects of epicatechin on inflammation, a second important risk factor in atherosclerosis.

Epicatechin does not affect monocyte adhesion to the endothelium

An important inflammatory process in atherosclerosis is the attachment of monocytes to the endothelial cell layer, which is mediated by adhesion molecules. Epicatechin feeding did not reduce plasma levels of the endothelial cell adhesion molecules sE-selectin and sVCAM-1 (Supplemental Table 2) and did not reduce monocyte expression of the adhesion molecules CD11a, CD11b, CD49d and CD162 as analysed by flow cytometry (Supplemental Table 2). In line with these findings, histological quantification of the number of monocytes adherent to the endothelial cell layer revealed that monocyte adhesion to the endothelium was not reduced in epicatechin-treated animals (not shown).

Epicatechin attenuates diet-induced expression of circulating inflammatory markers

Epicatechin-treated animals showed lower SAA levels than HC throughout the study period, and this effect reached significance at week 16 (Fig. 2A). Because SAA, secreted by the liver, can participate in disease progression throughout the development of atherosclerosis, the total SAA exposure (area under the curve) was calculated. SAA exposure was also significantly reduced compared with HC (Fig. 2B). This anti-inflammatory effect was substantiated in an independent experiment in mice expressing human-CRP, another liver-derived acute phase response protein and CVD risk factor. In control animals, HF-feeding significantly induced plasma human-CRP levels , while supplementation with epicatechin completely prevented this diet-induced increase in plasma human-CRP (Fig. 2C).
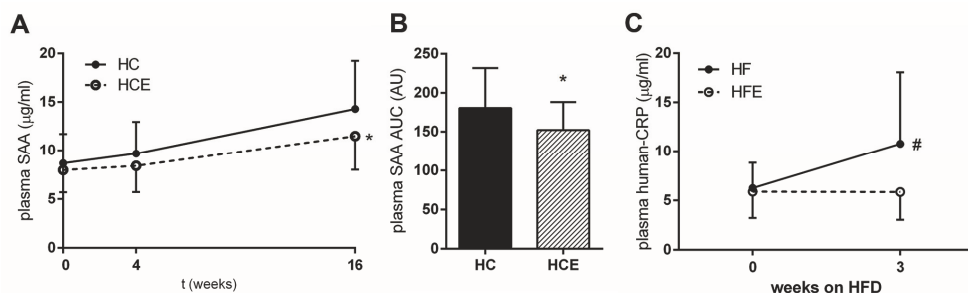
Figure 2. Effects of epicatechin on diet-induced inflammation in E3L mice and human-CRP transgenic mice.
(A) HC diet increases plasma SAA concentration during atherogenesis in E3L mice, epicatechin attenuates this effect (n=15/group). (B) SAA exposure (area under curve) in E3L mice. (C) HF-diet induces plasma human-CRP levels in human-CRP transgenic mice (HF; n=14) which is prevented by epicatechin (HFE; n=10). Data are mean±SD. *p<0.05 compared with HC, #p≤0.05 for increase within group.

Together, these data demonstrate that epicatechin quenched the formation of the liver-derived pro-atherogenic factors SAA and human-CRP.

Effect of epicatechin on lesion severity in early- and late-stage atherosclerosis

To provide insight into which stage of the atherosclerotic disease process may be affected by epicatechin, we performed a refined morphological analysis of lesion severity. This analysis revealed that the anti-atherosclerotic effect of epicatechin was specific to the severe lesions (type IV and V), the area of which was 27% lower in HCE than in HC (Fig. 3A). There was no difference between HC and HCE animals in the total area of mild lesions (type I-III, Fig. 3A), but epicatechin-treated animals did have significantly more lesion-free segments (10% in HCE compared with 2% in HC, Fig. 3B).
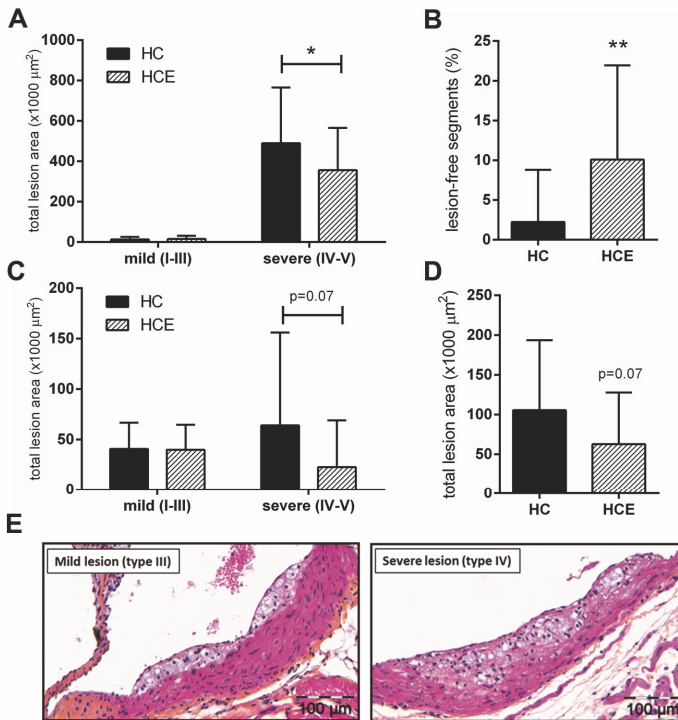
Figure 3. Refined analysis of anti-atherosclerotic effects of epicatechin in late-(16w) and early-(8w) stage atherosclerosis. (A) total lesion area of mild (type I-III) and severe (type IV-V) lesions after 16w treatment. (B) percentage of lesion-free segments after 16w treatment. (C) total lesion area of mild and severe lesions after 8w treatment. (D) total lesion area in the aortic root after 8w treatment. (E) representative photomicrographs of type III and type IV lesions showing progressive infiltration of plaque into the media. Data are mean±SD. *p≤0.05, **p≤0.01 compared with HC.

To investigate whether this effect is attributable to an effect of epicatechin on early atherosclerosis development, E3L mice were fed the HC or HCE diet for 8 weeks, which resulted in a greater relative contribution of mild lesions to the total lesion area (Fig. 3C). There was no effect of epicatechin on the prevalence of mild lesions and, consistent with the long-term experiment, epicatechin tended to reduce the severe lesion types as well as the total lesion area (Fig. 3C-D). The overall reduction in atherosclerotic lesion area was 40% (Fig. 3D). Together, these data confirm the anti-atherosclerotic potential of epicatechin and suggest a specific effect of epicatechin on the progression from mild to severe lesions, a transition that is characterised by progression of the atherosclerotic plaque into the media of the vessel wall (representative photomicrographs shown in Fig. 3E). This lesion progression requires matrix remodelling, which is mediated by processes related to vascular inflammation.

Epicatechin attenuates vascular inflammation and NFκB activity

To explore the mechanisms by which epicatechin may exert this effect on lesion progression we performed a microarray analysis of genome-wide gene expression changes in the descending aorta, followed by gene set enrichment analysis across pathways and biological processes. Compared with REF, HC differentially expressed 173 genes ($p<0.01$) and 271 genes were differentially expressed in HCE compared with HC ($p<0.01$). Geneset enrichment analysis of these 173 genes regulated by HC demonstrated activation of the biological processes "Chemotaxis of cells" ($p=0.03$, $Z=2.076$) and "Accumulation of myeloid cells" ($p=0.008$, $Z=2.198$), which confirmed induction of pro-atherogenic vascular inflammatory processes following HC-diet feeding. Of these 173 genes, a substantial number (77 genes including *Ccrl1*, *Ccl7*, *S100A8*) were inversely regulated by epicatechin. This is illustrated for the process "Chemotaxis of cells" in Fig. 4A, showing inverse regulation for many of the genes involved. Collectively, this indicates that the inflammatory effect of HC was attenuated by epicatechin, suggesting a reduced overall inflammatory milieu in the aorta. This damping effect of epicatechin on vascular inflammation was substantiated by results from immunohistochemical staining of lesional neutrophils, which revealed a decrease in the number of neutrophils in lesions from epicatechin-treated animals (Fig. 4B-C). The attenuation of HC-induced vascular inflammation by epicatechin was accompanied by effects on several genes involved in matrix degradation and remodelling (*Adam4*, *Adam21*, *Adam22*, *Mmp12*, *Mmp13* and *Timp1*; all upregulated by HC, $p<0.05$), the induction of which was globally quenched in HCE providing further mechanistic support for the observed effects on lesion progression.
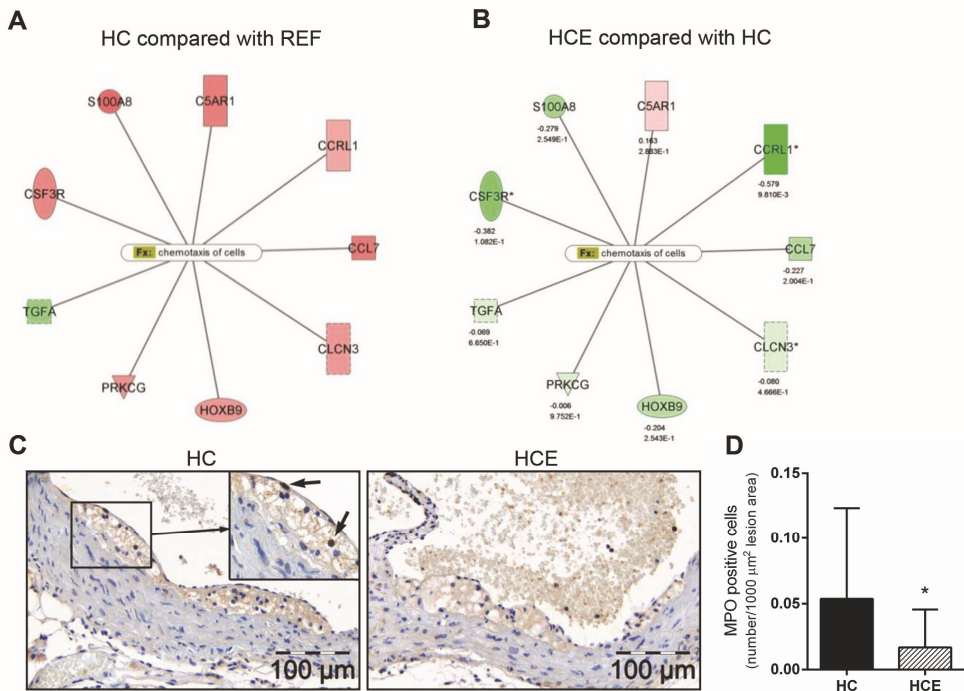
Figure 4. Effects of epicatechin on vascular inflammation. (A-B) inversely regulated genes in the process 'chemotaxis of cells' as determined by aortic microarray analysis and Ingenuity pathway analysis. (A) subset of differentially regulated genes by HC compared with REF (all p<0.01) showing upregulation (red) of most genes involved. (B) downregulation (green) of the same subset of genes by HCE compared with HC (*Ccrl1*: p<0.01) indicating inverse anti-inflammatory effect of epicatechin. (C) representative photomicrographs of atherosclerotic lesions immunohistochemically stained for myeloperoxidase-positive neutrophils. (D) quantification of lesional neutrophils in HC and HCE, showing reduced number of neutrophils in HCE. Data are mean±SD. *p≤0.05 compared with HC.

As many of the quenched chemotaxis- and matrix remodelling-associated genes as well as the liver-derived factors SAA and human-CRP are controlled by the inflammatory master regulator NFκB, we investigated whether epicatechin would quench HC diet-induced NFκB activation *in vivo*. An independent experiment was performed in NFκB-luciferase reporter mice using non-invasive bioluminescence imaging. Relative to baseline, HC diet-induced activation of NFκB was mainly observed in the abdominal and heart region (Fig. 5A). Epicatechin supplementation to the diet indeed prevented this activation of NFκB, and photon counts remained comparable to baseline levels (Fig. 5B). This further substantiates the anti-inflammatory capacity of epicatechin *in vivo*.
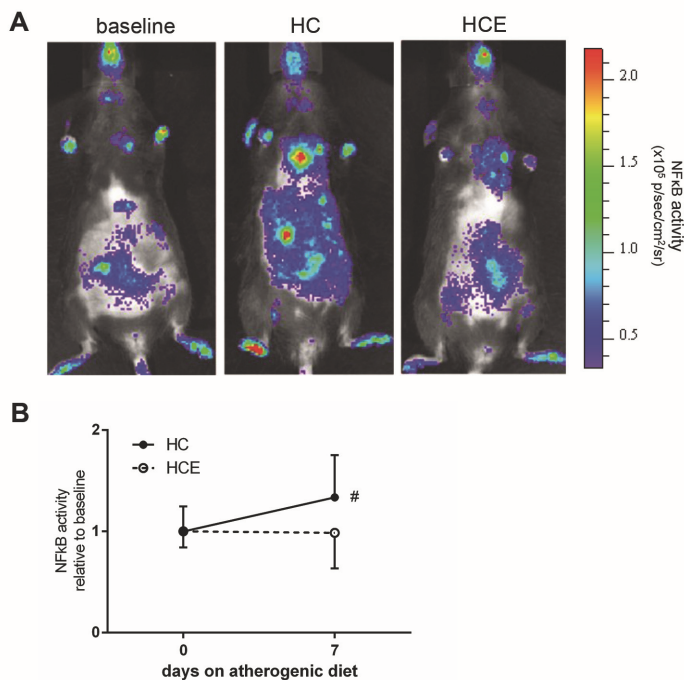
Figure 5. Effects of epicatechin on diet-induced inflammation in NFκB-luciferase reporter mice. (A) representative capture of NFκB activity at baseline, after HC-feeding and HCE-feeding. (B) quantification of whole-body NFκB activity relative to baseline (photon counts/cm^2/second). Data are mean±SD. #p≤0.05 for increase within group.

Discussion

In the present study, we investigated the effects of the flavanol epicatechin on diet-induced early- and late-stage atherosclerosis and the cardiovascular risk factors dyslipidaemia and diet-induced inflammation. Previous studies investigating the effects of flavanol-rich foods have provided indications for potential cardioprotective effects of these foods [18, 19], but the effects of individual flavanols remain unclear. Here, we have shown that epicatechin can attenuate the development of atherosclerosis, independently of effects on plasma lipids. Refined analysis of aortic lesions at early and late stages of the pathogenesis showed that epicatechin specifically reduces the progression from mild to severe lesions. This effect may be mediated by attenuation of several HC induced pro-atherogenic inflammatory factors in the liver (SAA, human-CRP) as well as atherogenic processes in the aorta (e.g. immune cell chemotaxis and cellular movement; matrix remodelling), all of which may at least partly be related to the observed quenching effect of epicatechin on NFκB.

Our atherosclerotic lesion analysis showed that epicatechin can reduce the development of atherosclerosis, resulting in a reduction of total lesion area by 27%. The observed reduction in atherosclerosis was not accompanied by an effect of epicatechin on atherogenic lipids or lipoproteins. A similar lipid-independent anti-atherogenic effect has been reported for another polyphenol quercetin under comparable experimental conditions in E3L mice [26]. The pharmaceutical reference compound atorvastatin did reduce plasma cholesterol and atherosclerotic lesion development, thus confirming that cholesterol modulation is possible under these conditions. These results suggest that the anti-atherogenic effect of epicatechin may be mediated by attenuation of other risk factors such as inflammation.

Here, we demonstrate that epicatechin can mitigate diet-induced inflammation in atherogenesis. In E3L mice, epicatechin attenuated HC-diet-induced SAA expression. This acute phase protein is predominately formed in the liver, indicates increased CVD risk in humans [32], and is considered a potential mediator of atherogenesis [33, 34]. SAA may contribute to atherosclerosis progression by stimulating lipoprotein retention in the vessel wall [35] and by inducing the expression of MMPs [36] involved in degradation of the extracellular matrix. Indeed, SAA directly accelerates atherosclerosis progression independent of plasma lipids [37]. We analysed the effect of epicatechin on liver-derived inflammatory factors in more detail using human-CRP transgenic mice [38]. (N.B. mouse-CRP is not an inflammation marker). Like SAA, human-CRP is a strong predictor of CVD [39] and pharmaceutical reduction of human-CRP levels reduces risk of CVD independently of effects on plasma cholesterol [40]. The observed quenching effect of epicatechin on human-CRP expression is in line with reports of lower plasma CRP levels in humans consuming foods rich in epicatechin [8, 9].

Refined histological analysis of lesion severity in late-stage as well as early-stage atherosclerosis in E3L mice indicates that epicatechin affects the progression of lesions from mild to severe lesion types specifically. This lesion progression is characterised by invasion of the plaque into the media of the vessel wall, a complex process that is driven by local intravascular inflammation and mediated by factors that orchestrate chemotaxis and cellular movement, as well as by remodelling of the extracellular matrix. Microarray analysis of gene expression in the aorta revealed a mitigating effect of epicatechin on HC-induced changes in aortic gene expression, including genes that contribute to the pathways crucial for chemotaxis and cellular movement (e.g. *Ccrl1*, *Ccl7*, *S100A8*) and vascular remodelling (e.g. *Mmp12*, *Mmp13*). To our knowledge, microarray analysis of the effects of epicatechin in aorta has not been performed

previously. Notably, epicatechin did not act on a specific set of 'target' genes or a single inflammatory process, but reduced the overall inflammatory tone within the vasculature, suggesting a damping effect on a more generic inflammatory event upstream of these genes. In reflection of this reduced inflammatory milieu in epicatechin-treated animals, we observed a reduction in the number of lesional myeloperoxidase-positive neutrophilic cells in HCE, a cell type that has been shown to accumulate most prominently in atherosclerotic plaques in regions of high inflammatory activity [41]. Furthermore, neutrophils are a source of large amounts of matrix-degrading proteases that can contribute to matrix degradation and remodelling and are recognised as a cell type that has an important contributory role in atherosclerosis progression (reviewed in [42]).

Many of the HC-induced genes quenched by epicatechin treatment are transcriptionally regulated by the inflammatory transcription factor NFκB. As the liver-derived factors SAA and human-CRP are also controlled by NFκB [43, 44], we sought direct evidence of the potential of epicatechin to inhibit NFκB activation *in vivo*. Imaging of NFκB activation in NFκB-luciferase reporter mice showed that epicatechin can indeed prevent diet-induced activation of this transcription factor, providing a potential lipid-independent mechanism by which epicatechin may exert its anti-atherosclerotic effects. Therapeutic benefits of NFκB inhibition have been demonstrated in earlier studies on the anti-atherogenic effects of systemic [45, 46] and endothelial cell-specific [47] inhibition of NFκB, and pharmaceutical attenuation of vascular NFκB activity resulted in reduced lesion progression from mild towards complex severe lesions [46], consistent with the effects observed here. To our knowledge, no previous studies have investigated the effects of epicatechin on NFκB activation *in vivo*. Results from *in vitro* studies provide conflicting evidence for the potential NFκB-inhibitory effect of epicatechin [48-50] that may be explained by differences in the choice of cell type, stimulus for NFκB activation, concentration of epicatechin used and incubation and exposure times.

Together, the results of the present study provide evidence for beneficial anti-inflammatory effects of the flavanol epicatechin in liver and aorta and a reduction of atherosclerosis, with inhibited progression to severe lesions. Our findings substantiate cardioprotective associations from epidemiological studies on flavanol-rich foods and implicate epicatechin as a possible mediator of these effects.

Acknowledgements

Financial support

Declaration of interests

The authors declare that they have no conflict of interest.

References

1. Weber C, Noels H. Atherosclerosis: current pathogenesis and therapeutic options. Nat Med. 2011;17(11):1410-22. doi:10.1038/nm.2538.
2. Estruch R, Ros E, Salas-Salvado J, Covas MI, Corella D, Aros F, et al. Primary prevention of cardiovascular disease with a Mediterranean diet. N Engl J Med. 2013;368(14):1279-90. doi:10.1056/NEJMoa1200303.
3. Nettleton JA, Polak JF, Tracy R, Burke GL, Jacobs DR, Jr. Dietary patterns and incident cardiovascular disease in the Multi-Ethnic Study of Atherosclerosis. Am J Clin Nutr. 2009;90(3):647-54. doi:10.3945/ajcn.2009.27597.
4. Siri-Tarino PW, Sun Q, Hu FB, Krauss RM. Saturated fatty acids and risk of coronary heart disease: modulation by replacement nutrients. Current Atherosclerosis Reports. 2010;12(6):384-90. doi:10.1007/s11883-010-0131-6.
5. Chait A, Han CY, Oram JF, Heinecke JW. Thematic review series: The immune system and atherogenesis. Lipoprotein-associated inflammatory proteins: markers or mediators of cardiovascular disease? J Lipid Res. 2005;46(3):389-403. doi:10.1194/jlr.R400017-JLR200.
6. Gregor MF, Hotamisligil GS. Inflammatory mechanisms in obesity. Annu Rev Immunol. 2011;29:415-45. doi:10.1146/annurev-immunol-031210-101322.
7. Detopoulou P, Panagiotakos DB, Chrysohoou C, Fragopoulou E, Nomikos T, Antonopoulou S, et al. Dietary antioxidant capacity and concentration of adiponectin in apparently healthy adults: the ATTICA study. Eur J Clin Nutr. 2010;64(2):161-8. doi:10.1038/ejcn.2009.130.
8. Esmaillzadeh A, Kimiagar M, Mehrabi Y, Azadbakht L, Hu FB, Willett WC. Fruit and vegetable intakes, C-reactive protein, and the metabolic syndrome. Am J Clin Nutr. 2006;84(6):1489-97.
9. Holt EM, Steffen LM, Moran A, Basu S, Steinberger J, Ross JA, et al. Fruit and vegetable consumption and its relation to markers of inflammation and oxidative stress in adolescents. J Am Diet Assoc. 2009;109(3):414-21. doi:10.1016/j.jada.2008.11.036.
10. van't Veer P, Jansen MC, Klerk M, Kok FJ. Fruits and vegetables in the prevention of cancer and cardiovascular disease. Public Health Nutr. 2000;3(1):103-7. doi:10.1017/S1368980000000136.
11. Arts IC, Hollman PC, Feskens EJ, Bueno de Mesquita HB, Kromhout D. Catechin intake might explain the inverse relation between tea consumption and ischemic heart disease: the Zutphen Elderly Study. Am J Clin Nutr.

2001;74(2):227-32.

12. Heiss C, Keen CL, Kelm M. Flavanols and cardiovascular disease prevention. Eur Heart J. 2010;31(21):2583-92. doi:10.1093/eurheartj/ehq332.

13. Geleijnse JM, Launer LJ, Van der Kuip DA, Hofman A, Witteman JC. Inverse association of tea and flavonoid intakes with incident myocardial infarction: the Rotterdam Study. Am J Clin Nutr. 2002;75(5):880-6.

14. Buijsse B, Feskens EJ, Kok FJ, Kromhout D. Cocoa intake, blood pressure, and cardiovascular mortality: the Zutphen Elderly Study. Arch Intern Med. 2006;166(4):411-7. doi:10.1001/archinte.166.4.411.

15. Kuriyama S. The relation between green tea consumption and cardiovascular disease as evidenced by epidemiological studies. J Nutr. 2008;138(8):1548S-53S.

16. Larsson SC, Virtamo J, Wolk A. Chocolate consumption and risk of stroke: A prospective cohort of men and meta-analysis. Neurology. 2012;79(12):1223-9. doi:10.1212/WNL.0b013e31826aacfa.

17. Ivey KL, Lewis JR, Prince RL, Hodgson JM. Tea and non-tea flavonol intakes in relation to atherosclerotic vascular disease mortality in older women. Br J Nutr. 2013:1-8. doi:10.1017/S0007114513000780.

18. Arranz S, Valderas-Martinez P, Chiva-Blanch G, Casas R, Urpi-Sarda M, Lamuela-Raventos RM, et al. Cardioprotective effects of cocoa: Clinical evidence from randomized clinical intervention trials in humans. Molecular Nutrition and Food Research. 2013. doi:10.1002/mnfr.201200595.

19. Hooper L, Kroon PA, Rimm EB, Cohn JS, Harvey I, Le Cornu KA, et al. Flavonoids, flavonoid-rich foods, and cardiovascular risk: a meta-analysis of randomized controlled trials. Am J Clin Nutr. 2008;88(1):38-50.

20. Knaze V, Zamora-Ros R, Lujan-Barroso L, Romieu I, Scalbert A, Slimani N, et al. Intake estimation of total and individual flavan-3-ols, proanthocyanidins and theaflavins, their food sources and determinants in the European Prospective Investigation into Cancer and Nutrition (EPIC) study. Br J Nutr. 2012;108(6):1095-108. doi:10.1017/S0007114511006386.

21. Arts IC, Jacobs DR, Jr., Harnack LJ, Gross M, Folsom AR. Dietary catechins in relation to coronary heart disease death among postmenopausal women. Epidemiology. 2001;12(6):668-75. doi:10.1097/00001648-200111000-00015.

22. Noll C, Lameth J, Paul JL, Janel N. Effect of catechin/epicatechin dietary intake on endothelial dysfunction biomarkers and proinflammatory cytokines in aorta of hyperhomocysteinemic mice. Eur J Nutr. 2013;52(3):1243-50. doi:10.1007/s00394-012-0435-0.

23. Loke WM, Proudfoot JM, Hodgson JM, McKinley AJ, Hime N, Magat M, et al. Specific dietary polyphenols attenuate atherosclerosis in apolipoprotein E-knockout mice by alleviating inflammation and endothelial dysfunction. Arterioscler Thromb Vasc Biol. 2010;30(4):749-57. doi:10.1161/ATVBAHA.109.199687.

24. Zadelaar S, Kleemann R, Verschuren L, de Vries-Van der Weij J, van der Hoorn J, Princen HM, et al. Mouse models for atherosclerosis and pharmaceutical modifiers. Arterioscler Thromb Vasc Biol. 2007;27(8):1706-21. doi:10.1161/ATVBAHA.107.142570.

25. Kleemann R, Verschuren L, van Erk MJ, Nikolsky Y, Cnubben NH, Verheij ER, et al. Atherosclerosis and liver inflammation induced by increased dietary cholesterol intake: A combined transcriptomics and metabolomics analysis. Genome Biol. 2007;8(9):R200. doi:10.1186/gb-2007-8-9-r200.

26. Kleemann R, Verschuren L, Morrison M, Zadelaar S, van Erk MJ, Wielinga PY, et al. Anti-inflammatory, anti-proliferative and anti-atherosclerotic effects of quercetin in human in vitro and in vivo models. Atherosclerosis. 2011;218(1):44-52. doi:10.1016/j.atherosclerosis.2011.04.023.

27. Carlsen H, Haugen F, Zadelaar S, Kleemann R, Kooistra T, Drevon CA, et al. Diet-induced obesity increases NF-kappaB signaling in reporter mice. Genes Nutr. 2009;4(3):215-22. doi:10.1007/s12263-009-0133-6.

28. Yakala GK, Wielinga PY, Suarez M, Bunschoten A, van Golde JM, Arola L, et al. Effects of chocolate supplementation on metabolic and cardiovascular parameters in ApoE3L mice fed a high-cholesterol atherogenic diet. Molecular Nutrition and Food Research. 2013. doi:10.1002/mnfr.201200858.

29. Wielinga PY, Yakala GK, Heeringa P, Kleemann R, Kooistra T. Beneficial effects of alternate dietary regimen on liver inflammation, atherosclerosis and renal activation. PLoS One. 2011;6(3):e18432. doi:10.1371/journal.pone.0018432.

30. Verschuren L, Radonjic M, Wielinga PY, Kelder T, Kooistra T, van Ommen B, et al. Systems biology analysis unravels the complementary action of combined rosuvastatin and ezetimibe therapy.

Pharmacogenet Genomics. 2012;22(12):837-45. doi:10.1097/FPC.0b013e328359d274.

31. Manach C, Williamson G, Morand C, Scalbert A, Remesy C. Bioavailability and bioefficacy of polyphenols in humans. I. Review of 97 bioavailability studies. Am J Clin Nutr. 2005;81(1 Suppl):230S-42S.

32. Ridker PM, Hennekens CH, Buring JE, Rifai N. C-reactive protein and other markers of inflammation in the prediction of cardiovascular disease in women. N Engl J Med. 2000;342(12):836-43. doi:10.1056/NEJM200003233421202.

33. King VL, Thompson J, Tannock LR. Serum amyloid A in atherosclerosis. Curr Opin Lipidol. 2011;22(4):302-7. doi:10.1097/MOL.0b013e3283488c39.

34. O'Brien KD, Chait A. Serum amyloid A: the "other" inflammatory protein. Current Atherosclerosis Reports. 2006;8(1):62-8. doi:10.1007/s11883-006-0066-0.

35. O'Brien KD, McDonald TO, Kunjathoor V, Eng K, Knopp EA, Lewis K, et al. Serum amyloid A and lipoprotein retention in murine models of atherosclerosis. Arterioscler Thromb Vasc Biol. 2005;25(4):785-90. doi:10.1161/01.ATV.0000158383.65277.2b.

36. Lee HY, Kim MK, Park KS, Bae YH, Yun J, Park JI, et al. Serum amyloid A stimulates matrix-metalloproteinase-9 upregulation via formyl peptide receptor like-1-mediated signaling in human monocytic cells. Biochem Biophys Res Commun. 2005;330(3):989-98. doi:10.1016/j.bbrc.2005.03.069.

37. Dong Z, Wu T, Qin W, An C, Wang Z, Zhang M, et al. Serum amyloid A directly accelerates the progression of atherosclerosis in apolipoprotein E-deficient mice. Mol Med. 2011;17(11-12):1357-64. doi:10.2119/molmed.2011.00186.

38. Ciliberto G, Arcone R, Wagner EF, Ruther U. Inducible and tissue-specific expression of human C-reactive protein in transgenic mice. EMBO J. 1987;6(13):4017-22.

39. Kaptoge S, Di Angelantonio E, Lowe G, Pepys MB, Thompson SG, Collins R, et al. C-reactive protein concentration and risk of coronary heart disease, stroke, and mortality: an individual participant meta-analysis. Lancet. 2010;375(9709):132-40. doi:10.1016/S0140-6736(09)61717-7.

40. Nissen SE, Tuzcu EM, Schoenhagen P, Crowe T, Sasiela WJ, Tsai J, et al. Statin therapy, LDL cholesterol, C-reactive protein, and coronary artery disease. N Engl J Med. 2005;352(1):29-38.

doi:10.1056/NEJMoa042000.

41. Rotzius P, Thams S, Soehnlein O, Kenne E, Tseng CN, Bjorkstrom NK, et al. Distinct infiltration of neutrophils in lesion shoulders in ApoE-/- mice. Am J Pathol. 2010;177(1):493-500. doi:10.2353/ajpath.2010.090480.

42. Soehnlein O. Multiple roles for neutrophils in atherosclerosis. Circ Res. 2012;110(6):875-88. doi:10.1161/CIRCRESAHA.111.257535.

43. Jensen LE, Whitehead AS. Regulation of serum amyloid A protein expression during the acute-phase response. Biochem J. 1998;334 (Pt 3):489-503.

44. Kleemann R, Gervois PP, Verschuren L, Staels B, Princen HM, Kooistra T. Fibrates down-regulate IL-1-stimulated C-reactive protein gene expression in hepatocytes by reducing nuclear p50-NFkappa B-C/EBP-beta complex formation. Blood. 2003;101(2):545-51. doi:10.1182/blood-2002-06-1762.

45. Chiba T, Kondo Y, Shinozaki S, Kaneko E, Ishigami A, Maruyama N, et al. A selective NFkappaB inhibitor, DHMEQ, reduced atherosclerosis in ApoE-deficient mice. Journal of Atherosclerosis and Thrombosis. 2006;13(6):308-13. doi:10.5551/jat.13.308.

46. de Vries-van der Weij J, Toet K, Zadelaar S, Wielinga PY, Kleemann R, Rensen PC, et al. Anti-inflammatory salicylate beneficially modulates pre-existing atherosclerosis through quenching of NF-kappaB activity and lowering of cholesterol. Atherosclerosis. 2010;213(1):241-6. doi:10.1016/j.atherosclerosis.2010.09.006.

47. Gareus R, Kotsaki E, Xanthoulea S, van der Made I, Gijbels MJ, Kardakaris R, et al. Endothelial cell-specific NF-kappaB inhibition protects mice from atherosclerosis. Cell Metab. 2008;8(5):372-83. doi:10.1016/j.cmet.2008.08.016.

48. Al-Hanbali M, Ali D, Bustami M, Abdel-Malek S, Al-Hanbali R, Alhussainy T, et al. Epicatechin suppresses IL-6, IL-8 and enhances IL-10 production with NF-kappaB nuclear translocation in whole blood stimulated system. Neuro-endocrinology Letters. 2009;30(1):131-8.

49. Granado-Serrano AB, Martin MA, Haegeman G, Goya L, Bravo L, Ramos S. Epicatechin induces NF-kappaB, activator protein-1 (AP-1) and nuclear transcription factor erythroid 2p45-related factor-2 (Nrf2) via phosphatidylinositol-3-kinase/protein kinase B (PI3K/AKT) and extracellular regulated kinase (ERK) signalling in HepG2 cells. Br J Nutr. 2010;103(2):168-79.

doi:10.1017/S0007114509991747.

50. Mackenzie GG, Carrasquedo F, Delfino JM, Keen CL, Fraga CG, Oteiza PI. Epicatechin, catechin, and dimeric procyanidins inhibit PMA-induced NF-kappaB activation at multiple steps in Jurkat T cells. FASEB J. 2004;18(1):167-9. doi:10.1096/fj.03-0402fje.

Supplemental data

Supplement 1. Detailed materials and methods

<u>Atherosclerotic lesion analysis</u>: Hearts were fixed in formaldehyde and embedded in paraffin for analysis of atherosclerosis. Serial cross-sections (5 μm) from the valve area of the aortic root were stained with haematoxylin-phloxine-saffron and atherosclerosis was analysed blindly in 4 cross-sections (at 50 μm intervals) from each specimen. Morphometric analysis of lesion number and area was performed using cell^D software (version 2.7; Olympus Soft Imaging Solutions, Hamburg, Germany). Lesion severity was scored according to the classification of the American Heart Association (AHA). Five lesion types were distinguished using this scoring system: Type I (early fatty streak): up to ten foam cells in the intima, no other changes; Type II (regular fatty streak): ten or more foam cells in the intima, no other changes; Type III (mild plaque): foam cells in the intima with presence of a fibrotic cap; Type IV (moderate plaque): progressive lesion, infiltration into media, elastic fibres intact; Type V (severe plaque): structure of media severely disrupted with fragmented elastic fibres, cholesterol crystals, calcium deposits and necrosis may be present. Monocyte adhesion was determined histologically by counting adherent monocytes in the same four cross-sections that were used for atherosclerosis analysis, using a well-established protocol [1-5]. The average number of monocytes attached luminally to the endothelium per cross-section was used for comparison between groups. Lesional neutrophil content was determined in cross-sections adjacent to those used for atherosclerosis analysis by immunohistochemical staining for myeloperoxidase (Anti-Myeloperoxidase antibody, ab9535, Abcam, Cambridge, UK) and expressed as number of neutrophils /1000 μm^2 lesion area. The null hypothesis for these analyses was that epicatechin may not decrease monocytes/neutrophils.

Analysis of plasma lipids and plasma markers of inflammation

Total plasma cholesterol and triglyceride levels were measured by commercially available enzymatic assays (cholesterol CHOD-PAP 11491458 and triglycerides GPO-PAP 11488872, Roche, Woerden, the Netherlands). Lipoprotein profiles were determined in pooled plasma, fractionated using an ÅKTA fast protein liquid chromatography system (Pharmacia, Roosendaal, the Netherlands) and analysed as reported [6]. Plasma levels of soluble VCAM-1 (CD106), soluble E-selectin (CD62E), human CRP, and serum amyloid A (SAA) were measured by ELISA (R&D Systems, Abingdon, UK, for VCAM-1 and E-selectin and human CRP; Life Technologies, Bleiswijk, the Netherlands for SAA). The activation state of circulating

monocytes was determined at t=16 weeks by flow cytometry (FACSCanto II; BD Biosciences, Breda, the Netherlands). EDTA whole blood samples were taken from the tail vein, red blood cells were lysed and white blood cells were stained with fluorescent-labelled antibodies for CD11a, CD11b, CD162 (BD Biosciences) and CD49d (Biolegend, London, UK). FACSdiva software (BD Biosciences) was used for data acquisition and analysis to determine the number of positive monocytes and mean fluorescence intensity for each marker.

RNA isolation and microarray gene expression analysis

Microarray analysis was performed on individual aortic arches from REF, HC and HCE animals (n=8 per group) from the late-stage atherosclerosis experiment. Total RNA was isolated from aortic tissue with RNAqueous® Kit (Life Technologies) RNA concentration and quality were measured by spectrophotometry using Nanodrop 1000 (Isogen Life Science, De Meern, the Netherlands). All samples had OD 260/280 and OD 260/230 ratios between 1.8 – 2.2 indicating purity of RNA. RNA integrity was verified using 2100 Bioanalyzer (Agilent Technologies, Amstelveen, the Netherlands). All samples showed sharp ribosomal RNA bands, indicating that the RNA was intact. Biotin-labeled cRNA was synthesized from total RNA using the Illumina TotalPrep RNA Amplification Kit (Ambion, Huntington, UK). The biotinylated cRNA was hybridised onto the MouseRef-8 v2 expression BeadChip (Illumina, San Diego CA, USA). Illumina's Genomestudio v1.1.1 software was used for data extraction, using the default settings as advised by Illumina. All the quality control data of this BeadChip were within the specifications of the microarray service provider (Service XS, Leiden, the Netherlands). The probe level background-subtracted expression values were used as input for lumi package [7] of the R/Bioconductor (http://www.bioconductor.org; http://www.r-project.org) to perform quality control and quantile normalisation. Unexpressed probes (p>0.01 in all experiments) were removed from further analysis, and 15725 probes remained in the analysis. Differentially expressed probes were identified using the limma package of R/Bioconductor [8] and the threshold for significance in the aortic arches was set at p values <0.01. Selected differentially expressed probes (DEPs) were used as an input for pathway analysis through Ingenuity Pathway Analysis suite (www.ingenuity.com, accessed 2013) and Ingenuity Pathway Analysis (IPA) software. This analysis determines the activation state of pathways and processes based on the observed differential gene expression in relation to the number of genes present in that particular pathway or process. This results in an overlap p-value and activation z-score for each transcription factor in the IPA knowledgebase. The activation z-score indicates activation (positive z-score) or inhibition (negative z-score) of a particular pathway or biological process.

An activation z-score >2 or <2 indicates significant activation (inhibition) of a pathway or process.

References Supplement 1:

1. Bernhagen J, Krohn R, Lue H, Gregory JL, Zernecke A, Koenen RR, et al. MIF is a noncognate ligand of CXC chemokine receptors in inflammatory and atherogenic cell recruitment. Nat Med. 2007;13(5):587-96. doi:10.1038/nm1567.
2. Kleemann R, Princen HMG, Emeis JJ, Jukema JW, Fontijn RD, Horrevoets AJG, et al. Rosuvastatin Reduces Atherosclerosis Development Beyond and Independent of Its Plasma Cholesterol–Lowering Effect in APOE*3-Leiden Transgenic Mice: Evidence for Antiinflammatory Effects of Rosuvastatin. Circulation. 2003;108(11):1368-74. doi:10.1161/01.cir.0000086460.55494.af.
3. Kleemann R, Verschuren L, Morrison M, Zadelaar S, van Erk MJ, Wielinga PY, et al. Anti-inflammatory, anti-proliferative and anti-atherosclerotic effects of quercetin in human in vitro and in vivo models. Atherosclerosis. 2011;218(1):44-52. doi:10.1016/j.atherosclerosis.2011.04.023.
4. Verschuren L, Kleemann R, Offerman EH, Szalai AJ, Emeis SJ, Princen HM, et al. Effect of low dose atorvastatin versus diet-induced cholesterol lowering on atherosclerotic lesion progression and inflammation in apolipoprotein E*3-Leiden transgenic mice. Arterioscler Thromb Vasc Biol. 2005;25(1):161-7. doi:10.1161/01.ATV.0000148866.29829.19.
5. Verschuren L, Kooistra T, Bernhagen J, Voshol PJ, Ouwens DM, van Erk M, et al. MIF Deficiency Reduces Chronic Inflammation in White Adipose Tissue and Impairs the Development of Insulin Resistance, Glucose Intolerance, and Associated Atherosclerotic Disease. Circ Res. 2009;105(1):99-107. doi:10.1161/circresaha.109.199166.
6. Kooistra T, Verschuren L, de Vries-van der Weij J, Koenig W, Toet K, Princen HM, et al. Fenofibrate reduces atherogenesis in ApoE*3Leiden mice: evidence for multiple antiatherogenic effects besides lowering plasma cholesterol. Arterioscler Thromb Vasc Biol. 2006;26(10):2322-30. doi:10.1161/01.ATV.0000238348.05028.14.
7. Du P, Kibbe WA, Lin SM. lumi: a pipeline for processing Illumina microarray. Bioinformatics (Oxford, England). 2008;24(13):1547-8. doi:10.1093/bioinformatics/btn224.
8. Wettenhall JM, Smyth GK. limmaGUI: a graphical user interface for linear modeling of microarray data. Bioinformatics (Oxford, England). 2004;20(18):3705-6. doi:10.1093/bioinformatics/bth449.

Supplemental table 1. Body weight, food intake and plasma triglycerides quantified in week 16 of the late-stage atherosclerosis experiment in E3L mice.

	REF	HC	HCE	HCA
Body weight (g)	23.5 ± 1.6	25.0 ± 1.3	24.2 ± 1.5	22.9 ± 1.6
Food intake (g/day)	2.2 ± 0.2	2.5 ± 0.2	2.4 ± 0.1	2.4 ± 0.2
Triglycerides (mM)	1.7 ± 0.4	2.5 ± 0.4	2.4 ± 0.6	2.1 ± 0.6

E3L mice were fed an atherogenic diet containing 1% (w/w) cholesterol (HC) supplemented with 0.1% (w/w) epicatechin (HCE) for 16 weeks. A pharmaceutical reference group was fed the HC-diet supplemented with 0.01% (w/w) atorvastatin (HCA), and an ageing control reference group (REF) was fed the diet without added cholesterol. Data are mean ± SD. *$p<0.05$ No significant differences between HC and HCE.

Supplemental table 2. Circulating endothelial cell adhesion molecules and activation state of circulating monocytes quantified in week 16 of the late-stage atherosclerosis experiment in E3L mice.

	HC	HCE
sE-selectin (ng/ml)	105.2 ± 43.7	101.7 ± 25.0
sVCAM-1 (µg/ml)	2.6 ± 0.7	3.3 ± 0.8
Monocyte CD11a		
number of positive cells/100.000 counted	2476 ± 1463	2078 ± 740
expression (MFI)	28700 ± 10917	30039 ± 15685
Monocyte CD11b		
number of positive cells/100.000 counted	916 ± 405	994 ± 648
expression (MFI)	17400 ± 2617	19358 ± 4081
Monocyte CD49d		
number of positive cells/100.000 counted	2523 ± 761	2806 ± 801
expression (MFI)	5155 ± 909	5799 ± 1544
Monocyte CD162		
number of positive cells/100.000 counted	1676 ± 667	1878 ± 816
expression (MFI)	47300 ± 4881	55386 ± 7232

E3L mice were fed an atherogenic diet containing 1% (w/w) cholesterol (HC) supplemented with 0.1% (w/w) epicatechin (HCE) for 16 weeks. Plasma sE-selectin and sVCAM-1 were quantified by ELISA. Monocyte expression of CD11a, CD11b, CD49d, and CD162 was quantified by flow cytometry. MFI: mean fluorescence intensity. Data are mean±SD. *$p<0.05$ No significant differences between HC and HCE.

Chapter 9

Summary & General discussion

Summary

Metabolic inflammation – the inflammatory response to metabolic overload (surplus energy or macronutrients) – is considered to play a crucial role in the development of obesity-associated metabolic diseases such as insulin resistance, non-alcoholic fatty liver disease (NAFLD), and atherosclerosis [1-4]. However, much remains unknown about the origin and mechanisms of metabolic inflammation. Therefore, we aimed to further our understanding of metabolic inflammation, and investigate the effects of interventions targeted to specific aspects of metabolic inflammation on the development of metabolic disease.

In **chapter 2** we explored the sequence of inflammatory events in adipose tissue and liver during high-fat-diet-induced metabolic overload to unravel the contribution of these two organs to the development of obesity-associated insulin resistance and NAFLD. We showed that prolonged high-fat diet feeding induced a progressive obese phenotype with whole-body insulin resistance in C57BL/6J mice. Metabolic inflammation was apparent in the adipose tissue after 24 weeks of high-fat diet feeding, while overt hepatic inflammation did not occur until 40 weeks of high-fat diet feeding. Since systemic insulin resistance was manifest before pronounced hepatic inflammation was observed, results from this study suggest that adipose tissue inflammation is more likely to be associated with systemic insulin resistance than hepatic inflammation, at least in the early stages of disease development. Next, in **chapter 3**, we showed that distinct adipose tissue depots differ in their susceptibility to develop metabolic inflammation during high-fat-diet-induced obesity in C57BL/6J mice. The first depot to develop metabolic inflammation (i.e. macrophage infiltration observed as crown-like structures in the adipose tissue) was the epididymal adipose tissue, which appeared to be related to the maximal expandability of this depot (and its adipocytes). Again, inflammation of this adipose tissue depot preceded the development of hepatic inflammation, and thus the progression from simple steatosis to NASH. We then examined whether inflamed epididymal adipose tissue plays a causal role in the progression of liver steatosis to NASH. We showed that surgical removal of this inflamed adipose tissue depot reduced the development of hepatic inflammation and reduced plasma levels of specific inflammatory factors (such as cytokines and pro-inflammatory fatty acids) that may mediate the effects of inflamed adipose tissue on NASH progression. In **chapter 4** we investigated the effects of an intervention targeted to the NLRP3 inflammasome, i.e. the sensing of metabolic overload, using a caspase-1 inhibitor in high-fat-diet-induced obesity and NAFLD development in LDLr-/-.Leiden mice. Treatment

with this inhibitor did not affect obesity or adipose tissue mass, but did reduce epididymal adipose tissue inflammation, which was paralleled by an improvement in whole-body insulin resistance. In the liver, we observed a mild reduction in hepatic steatosis and, consistent with the observed attenuation of adipose tissue inflammation and the role of inflamed adipose tissue in the aetiology of NASH, a pronounced effect on hepatic inflammation, which was mainly observed as a reduction in the infiltration of neutrophils. In agreement with this reduction in hepatic inflammation we showed that the development of hepatic fibrosis was reduced in mice treated with the caspase-1 inhibitor. Next, we investigated the potential value of nutritional strategies to prevent metabolic inflammation and disease development. In **chapter 5** we showed that (isocaloric) replacement of dietary saturated fat with polyunsaturated fat (PUFA)-rich pumpkin seed oil reduces dyslipidaemia and has beneficial effects in NAFLD (mainly on steatosis) and associated atherosclerosis development in ApoE*3Leiden mice. Furthermore, minor components with putative anti-inflammatory properties (phytochemicals) present only in the virgin (unrefined) pumpkin seed oil had additional beneficial effects on hepatic lipid metabolism and inflammation, leading to profound reductions in metabolic disease endpoints. We then continued with two studies on the potential health effects of phytochemicals with anti-inflammatory effects, focusing either on metabolic inflammation in liver during NASH development or on metabolic inflammation in vasculature during atherosclerosis development. In **chapter 6** we investigated the effects of the anthocyanin-rich bilberry extract Mirtoselect during the development of NASH and fibrosis in ApoE*3Leiden mice. We show that addition of this extract to the diet reduces hepatic steatosis and has pronounced anti-inflammatory effects in the liver. Again, these anti-inflammatory effects were mainly attributable to a reduction in neutrophil infiltration in the liver. The extract also strongly reduced the development of hepatic fibrosis. We found these effects to be strongly related to a reduction in the build-up and crystallisation of free cholesterol in the liver, the levels of which were associated with the observed pathology (histology scores and gene expression data) as well as with NFκB activation, which was also reduced by the extract. Next (**chapter 7**), we studied the potential of the phytochemical (-)-epicatechin to prevent metabolic inflammation in atherosclerosis development in ApoE*3Leiden mice. (-)-Epicatechin reduced the development of atherosclerosis without affecting dyslipidaemia and quenched the formation of liver-derived pro-atherogenic inflammatory factors. Within the vascular wall, (-)-epicatechin reduced inflammatory gene expression, many of which were regulated by NFκB. This quenching effect of (-)-epicatechin on NFκB activation was confirmed in NFκB-luciferase reporter mice in which (-)-epicatechin prevented diet-induced NFκB activation, thus providing a possible

rationale for the anti-atherogenic effects of (-)-epicatechin. In **chapter 8** we studied an intervention targeted at resolution of inflammation during atherosclerosis development. To do so we treated ApoE*3Leiden mice with the endogenous specialised pro-resolving mediator (SPM) Resolvin E1 in a therapeutic study protocol. Treatment with Resolvin E1 did not affect dyslipidaemia but did reduce atherosclerotic lesion area, reducing the progression from mild to severe (vulnerable) lesion types. Resolvin E1 did not affect the liver-derived systemic inflammatory marker serum amyloid A (SAA) but did have anti-inflammatory effects within the aorta, reducing atherogenic gene expression and inactivating pro-inflammatory signalling pathways such as IFN-γ and TNF-α.

Discussion

Experimental models of metabolic inflammation/disease
In this thesis we used several experimental models of metabolic overload, inflammation and disease, which allowed us to study different aspects of metabolic inflammation during disease development. The inbred C57BL/6J mice fed a high-fat diet are a frequently used model of diet-induced obesity and insulin resistance with elevated blood glucose levels and impaired glucose tolerance [5]. Because development of metabolic inflammation and organ dysfunction in this model is relatively slow, it is well-suited for longitudinal studies investigating different stages of disease development [6] (i.e. obesity, insulin resistance, adipose tissue inflammation, NAFLD; **chapter 2 and 3**). Metabolic disease development in this model is quite mild. For instance, NAFLD develops up to the stage of hepatic steatosis with limited development of hepatic inflammation and these mice do not develop atherosclerosis due to the fact that they are normolipidaemic and carry most of their cholesterol in the atheroprotective HDL particles. This means that these mice may not be the optimal model for studies on end-point metabolic disease development. LDLr-/-.Leiden mice, genetically engineered mice that lack the LDL receptor and are highly sensitive to develop obesity and insulin resistance, may be more suited for this purpose. Since the LDL receptor plays a major role in the clearance of chylomicrons and VLDL and LDL particles, these mice have elevated plasma triglyceride and cholesterol levels on a Western-type (cholesterol-containing) diet, confined mainly to the pro-atherogenic lipoproteins [7, 8]. Historically LDLr-/- mice have therefore mainly been used for atherosclerosis research. However, when they are fed a high-fat diet they become obese, insulin resistant and develop metabolic inflammation with gradual and progressive development of NASH with fibrosis as well as atherosclerosis (**chapter 4**), which makes them a comprehensive

model for obesity-associated disease development. A second model that is well-suited for end-point disease studies is the ApoE*3Leiden mouse. ApoE*3Leiden mice are transgenic mice that carry the human ApoE*3Leiden gene, a dominant negative mutant form of the human APOE3 gene, that causes hyperlipidaemia in humans [8]. This ApoE*3Leiden transgene leads to impaired clearance of ApoE-containing lipoproteins which results in elevated levels of VLDL and LDL cholesterol on a Western-type (cholesterol-containing) diet [9]. These mice have a humanised lipid metabolism and lipoprotein profile, and in contrast with other experimental models for atherosclerosis (such as LDLr /- or ApoE /- mice) ApoE*3Leiden mice respond to lipid-modulating therapies in a human-like manner [10]. Cholesterol-fed ApoE*3Leiden mice also develop metabolic inflammation in the liver, which results in the development of NASH with fibrosis (**chapter 5 and 6**). They develop these metabolic diseases in absence of obesity, insulin resistance and white adipose tissue inflammation, which makes them particularly suitable to study the direct effects of cholesterol-induced metabolic inflammation in liver and vasculature (**chapter 7 and 8**).

These different experimental models represent different aetiologies of metabolic overload and inflammation that may contribute to the complexity and heterogeneity of metabolic disease development as it is observed in humans. Although this means that none of these models completely encompasses all aspects of human pathogenesis, it does allow investigation of specific features of metabolic overload and effects of interventions thereupon.

Dietary triggers of metabolic inflammation

The studies described herein employed different dietary triggers of inflammation. In **chapters 2-4**, we used a high-fat diet (24% w/w fat from lard; 38% w/w carbohydrates from sucrose, maltodextrin and corn starch; 23% protein w/w from casein; 0.02% w/w cholesterol) which is frequently used for diet-induced obesity studies. The 25% w/w fat in this diet results in 45 kcal% from fat, which is a fat content that is relatively comparable to Western human diets. The average fat intake in European countries (sampled from the EPIC cohort, a large prospective cohort with 27 centres in 10 countries, mostly recruited from the general population) was found to be ≥34 kcal% in women and ≥36 kcal% in men in the majority of the EPIC centres [11] and similar total fat intakes were observed in a systematic review of fat intake among the general population in 40 countries worldwide, where intakes ranged up to an average of 46 kcal% (in Greece) [12]. It is thought that saturated fats in particular are inducers of metabolic inflammation [13] and this notion is supported by results from observational and intervention studies that show associations between saturated fat intake

and metabolic disease development such as insulin resistance [14] and cardiovascular disease [15], although others have shown that reducing saturated fat intake does not reduce inflammation [16].

While our experimental diet is commonly referred to, and emphasised as a high-fat diet, it is not clear which nutrients in this diet are actually responsible for the observed metabolic overload and inflammation on this diet. Inherently, every diet is a complex mixture of nutrients that may work in synergy to exert net pro- or anti-inflammatory effects. This makes it difficult to separate the specific effects of individual macronutrients. All the more so, since any change in a macronutrient – for instance increasing the fat content of a diet – unavoidably also results in a compensatory change in another macronutrient – e.g. a reduction in carbohydrate content – making it difficult, if not impossible, to dissect the effects of the increase in the one macronutrient from the reduction in the other. In **chapter 4**, that included a low-fat diet control group in which part of the fat in the HFD was replaced by carbohydrates (in the form of sucrose and corn starch), we found that – although this group was initially included as a healthy, non-diseased control group – livers were more steatotic than expected, and not all inflammatory parameters were lower in this group than in the HFD group (for instance, hepatic TNF-α gene expression was comparable). Thus suggesting that the simple carbohydrates in this diet may also contribute to the observed metabolic overload and inflammation. In line with this, observational studies have shown that dietary glycaemic index (the average propensity of carbohydrate in the diet to raise blood glucose) and glycaemic load (the product of glycaemic index and amount of carbohydrates in the diet) are associated with levels of the inflammatory marker C-reactive protein (CRP) [17, 18] and high-sucrose feeding in rodent models of obesity has also been shown to induce metabolic inflammation [19, 20]. Overall, much remains unknown about the role of different macronutrients as triggers of metabolic inflammation, and the question remains whether different macronutrients may trigger distinct forms of metabolic overload and subsequent metabolic inflammation.

In **chapters 5-8** we used a cholesterol-containing Western-type diet (16% w/w fat from cocoa butter, 51% w/w carbohydrates from sucrose and corn starch, 20% w/w protein from casein, 1% w/w cholesterol). As shown in **chapters 6 and 7** (that included a control group that received the same diet without cholesterol), it is the cholesterol in this diet that is the trigger for inflammation and disease development, which is in line with previous observations in the ApoE*3Leiden model [21, 22]. Cholesterol is recognised to play an important role in the pathogenesis of both NASH and atherosclerosis. Epidemiological studies have shown that

dietary cholesterol intake is associated with increased risk and severity of NAFLD [23, 24] and cirrhosis [25] and a short-term intervention study in lean insulin-sensitive subjects showed that cholesterol feeding increases (liver-derived) CRP and SAA levels [26] indicative of cholesterol-induced liver inflammation. The build-up of cholesterol (specifically in its free, unesterified form) within the liver is thought to provide a trigger of inflammation and disease progression in NAFLD [27]. In support of this, studies have shown that hepatic free cholesterol levels are increased in patients with NASH relative to those with simple steatosis (i.e. without the inflammatory component of the disease) [28, 29]. Accumulation of free cholesterol in Kupffer cells [30] and hepatic stellate cells [31, 32] has pro-inflammatory and pro-fibrotic effects and it has been proposed that build-up of cholesterol in lysosomes drives inflammation in both NAFLD and atherosclerosis [33]. The key importance of cholesterol in the development of atherosclerosis is long-established. It was first introduced in 1913, when Nikolai Anitschkow discovered that cholesterol-feeding in rabbits produced atherosclerotic lesions that closely resembled those of human atherosclerosis [34, 35]. Epidemiological evidence has since consistently shown that circulating cholesterol levels (particularly when associated with LDL) are associated with cardiovascular mortality [36]. On a cellular level, it is now known that increased levels of LDL lead to its entry into and retention within the arterial wall, where it may be modified by various processes such as oxidation or aggregation [37]. This modified LDL can either function as a ligand for macrophage PRRs and thereby trigger inflammatory signalling or be engulfed by macrophages, leading to cellular cholesterol accumulation and foam cell formation which in turn amplifies PRR signalling and activation of inflammatory signalling pathways [37-39] driving the process of atherogenesis. Due to the central role of cholesterol in the pathogenesis of atherosclerosis, cholesterol-lowering medication (mainly in the form of statins) has become the cornerstone of cardiovascular disease prevention. However, it is now recognised that despite optimal lowering of circulating cholesterol, there is a substantial residual risk of cardiovascular disease [40], which may be associated with inflammation and could therefore be targeted with anti-inflammatory therapies [41]. We show in **chapters 6-8** that it is possible to attenuate NAFLD and atherosclerosis development independently of circulating cholesterol levels, by exerting local anti-inflammatory effects within the tissue. Notably, the local anti-inflammatory effects observed in these studies were mostly not reflected by an effect on circulating markers of inflammation. This means that evidence from human intervention studies, that often rely largely on analyses of circulating inflammatory markers without taking tissue inflammation into account, could potentially result in dismissal of an efficacious intervention based on the fact that it did not affect

systemic inflammation, even when tissue inflammation is reduced by the intervention.

Regardless of the dietary trigger employed, the diet-induced metabolic overload and inflammation described in this thesis are the result of nutrient excess, not caloric excess. Since the mice used in these experiments do not display hyperphagia (as is known for several non-genetic murine models of obesity [42]) the energy intake in the high-fat diet or Western-type diet groups is not increased relative to their non-diseased controls (chow, low-fat diet, or Western-type diet without cholesterol). Results from our studies therefore provide indication that while metabolic overload and inflammation is commonly thought to be the result of overconsumption of calories, the quality of calories is also of great importance. This is in line with findings from observational studies that report inverse associations between indices of dietary quality (tools that provide an overall numerical rating of an individual's dietary intake, rather than focusing on the intake of individual nutrients) such as the Diet Quality Index [43] and the Healthy Eating Index [44] and systemic inflammation even after adjustment for energy intake. Although as may be expected, observed correlations differ between different indices of dietary quality employed [45]. Furthermore, these indices generally also include additional variables such as fibre intake, alcohol consumption and fruit and vegetable intake (and thus intake of potentially bioactive, anti-inflammatory phytochemicals) which makes it hard to dissect the effects of the macronutrient quality of the diets.

Nutritional interventions in metabolic inflammation
Although logically therapies in obesity would focus on lifestyle modifications (i.e. healthy eating habits and increased physical activity) to reduce metabolic overload and prevent the development and progression of metabolic inflammation and disease, such lifestyle changes are difficult to achieve for many individuals. Lifestyle modifications that do not require caloric restriction, such as alternating dietary regimens [22, 46] or time-restricted feeding [47], may be easier to apply, and have been demonstrated to attenuate metabolic disease development in rodents. A common denominator in these strategies is that they provide windows of time in which the body is not metabolically overloaded, potentially enabling it to return to homeostasis before the next metabolic insult occurs. This may prevent the development of an increasing state of metabolic overload and inflammation that never completely returns to baseline levels, although the mechanisms of such interventions are not yet fully understood. A seemingly contradictory effect is observed in studies on meal frequency, where it is reported that increasing meal frequency (eating small, frequent meals as opposed to fewer, large meals) has metabolic benefits [48, 49] and is associated with a reduction in the inflammatory

marker CRP [50]. A potential explanation for these observations may be found in the fact that these reduced calorie/nutrient meals, although consumed more frequently, are too small to result in metabolic overload and elicit a subsequent metabolic inflammatory response, and may therefore be more favourable than fewer, larger meals.

Another lifestyle modification that may be relatively easy to implement is a change in the quality of fat consumed, as it can be achieved without affecting the amount of fat ingested and therefore does not require caloric restriction or a shift in macronutrient intake. In **chapter 5** we showed that such a dietary modification can have substantial effects on the development of disease, especially when the phytochemical-rich form of the oil is used. This indicates that the addition of potentially anti-inflammatory phytochemicals to the diet may be a valuable strategy to prevent metabolic inflammation and subsequent disease development. Plenty of short-term human intervention studies have investigated the effects of various anti-inflammatory phytochemicals (or phytochemical mixtures/extracts) and frequently report anti-inflammatory effects of such interventions on circulating inflammatory markers (e.g. for quercetin and epicatechin [51], resveratrol [52] and green tea extract [53]). In addition, associations found in observational studies provide indication that consumption of specific phytochemical-rich foods or a high intake of a certain class of phytochemicals may protect against the development CVD (e.g. [54, 55]). However, the concrete effects of individual phytochemicals or phytochemical-rich extracts on end-point disease development often remain unknown. In **chapters 6 and 7** we further explored the effects of specific phytochemicals in this respect, and show that they can be a remarkably powerful tool to attenuate metabolic disease development, even when they are taken as a supplement without any other changes to the diet. However, their potential when administered in a therapeutic setting (starting treatment in established disease) remains to be evaluated. The fact that nutrients are not designed to specifically and potently target a single receptor or signalling pathway may result in them having broad, pleiotropic effects, dampening several pro-inflammatory pathways rather than completely quenching a single target, which could be beneficial in promoting restoration of tissue homeostasis.

Immune cell infiltration

A common component of metabolic diseases is immune cell infiltration into tissues. Macrophages are considered to play an important role in this respect [56, 57], and in line with this we observed infiltration of macrophages in adipose tissue, liver and vasculature in the studies of metabolic inflammation described herein (**chapters 2-8**). However, of all the anti-inflammatory interventions we studied, only the switch in dietary fatty acid composition

described in **chapter 5** had an effect on the infiltration of macrophages. Treatment with the caspase-1 inhibitor (**chapter 4**), the anthocyanin-rich bilberry extract (**chapter 6**) or the flavanol (-)-epicatechin (**chapter 7**) did not affect macrophage content, but specifically attenuated the infiltration of neutrophilic cells during metabolic disease development. In a classical immune response, neutrophils are typically the first to arrive at a site of tissue damage or inflammation, where their presence is short-lived [58]. Uncharacteristically for this cell type, we observed neutrophils in metabolically inflamed tissues at late stages of disease development. This may be due to the persistent presence of the inflammatory trigger(s) (i.e. continuing metabolic overload and resulting tissue damage) which leads to continuous neutrophil recruitment, as supported by data in **chapter 6** in which we show increased hepatic neutrophil chemoattractant expression at this late disease stage. Alternatively (or in addition) to the potential continued recruitment of neutrophils during metabolic inflammation, increased longevity of infiltrated neutrophils could also contribute to observations of increased tissue neutrophil content during metabolic inflammation. Whether these neutrophils play a causal role in the pathogenesis of metabolic disease or are merely innocent bystanders that arrive in response to the tissue damage caused by metabolic overload, remains unclear, although it is thought that their persistence in tissues can be a cause of extensive tissue damage [58, 59]. Recent studies have shown that genetic deletion or inhibition of neutrophil-associated proteins such as myeloperoxidase (MPO) or elastase attenuates adipose tissue inflammation and insulin resistance [60, 61] as well as development of NASH and hepatic fibrosis [62]. This suggests that neutrophil-derived inflammatory mediators may indeed play a role in the development of metabolic inflammation and its pathological consequences. Observational studies in (morbidly) obese subjects have revealed that circulating neutrophils from obese subjects are increased in number and display a more pro-inflammatory/activated phenotype than those from lean controls [63, 64], providing further support for the notion that this immune cell population may be of importance in obesity.

Although the quantity of infiltrating macrophages was not affected in most of our studies, it would be of interest to investigate whether the 'quality' of these macrophages, i.e. their inflammatory phenotype (polarised towards the pro-inflammatory M1 type or the anti-inflammatory, pro-resolving M2 type) was affected by the interventions. Recruitment of macrophages and their polarisation towards a pro-resolving phenotype (while limiting infiltration of neutrophils) is essential during inflammation resolution, to allow clearing up of cellular debris and apoptotic neutrophils and promote restoration of tissue homeostasis [65].

In line with this, treatment with the pro-resolving mediator Resolvin E1 in **chapter 8** did not reduce macrophage plaque content in atherosclerotic lesions, while it did have clear anti-inflammatory and anti-atherosclerotic effects within the vascular wall.

Concluding Remarks and Future Perspectives

Metabolic inflammation triggered by metabolic overload – excess intake of energy or nutrients – is causally involved in the pathogenesis of metabolic diseases such as insulin resistance/type 2 diabetes, non-alcoholic fatty liver disease and atherosclerosis. Interventions that suppress the inflammatory response to metabolic overload may therefore prove valuable in the prevention or retardation of such metabolic disease development. While pharmacological therapies are a logical choice for many, results from this thesis show that nutritional interventions can also be a remarkably powerful tool to dampen metabolic inflammation and prevent development of disease.

Although it is generally accepted that metabolic inflammation differs from classical inflammatory responses, the question whether different macronutrients trigger distinct forms of metabolic overload and inflammation remains largely unexplored. The potential of different macronutrients (e.g. amount and type of carbohydrates and fats) to induce metabolic inflammation, as well as the diverse mechanisms and pathways by which they might do so deserve further investigation. In addition, little is known about differences in individual susceptibility to – these possibly distinct types of – metabolic inflammation. Knowledge on these factors may guide the further development of interventions that alleviate metabolic overload and inflammation and thereby prevent obesity-associated disease development.

References

1. Hotamisligil GS. Inflammation and metabolic disorders. Nature. 2006;444(7121):860-7. doi:10.1038/nature05485.

2. Shoelson SE, Lee J, Goldfine AB. Inflammation and insulin resistance. J Clin Invest. 2006;116(7):1793-801. doi:10.1172/JCI29069.

3. Tilg H, Moschen AR. Evolution of inflammation in nonalcoholic fatty liver disease: The multiple parallel hits hypothesis. Hepatology. 2010;52(5):1836-46. doi:10.1002/hep.24001.

4. Libby P. Inflammation in atherosclerosis. Arterioscler Thromb Vasc Biol. 2012;32(9):2045-51. doi:10.1161/atvbaha.108.179705.

5. Collins S, Martin TL, Surwit RS, Robidoux J. Genetic vulnerability to diet-induced obesity in the C57BL/6J mouse: physiological and molecular characteristics. Physiol Behav. 2004;81(2):243-8. doi:10.1016/j.physbeh.2004.02.006.

6. Williams LM, Campbell FM, Drew JE, Koch C, Hoggard N, Rees WD, et al. The development of diet-induced obesity and glucose intolerance in C57Bl/6 mice on a high-fat diet consists of distinct phases. PLoS One. 2014;9(8):e106159. doi:10.1371/journal.pone.0106159.

7. Knowles JW, Maeda N. Genetic modifiers of atherosclerosis in mice. Arterioscler Thromb Vasc Biol. 2000;20(11):2336-45. doi:10.1161/01.atv.20.11.2336.

8. Zadelaar S, Kleemann R, Verschuren L, de Vries-Van der Weij J, van der Hoorn J, Princen HM, et al. Mouse models for atherosclerosis and pharmaceutical modifiers. Arterioscler Thromb Vasc Biol. 2007;27(8):1706-21. doi:10.1161 /ATVBAHA.107.142570.

9. van Vlijmen BJ, van den Maagdenberg AM, Gijbels MJ, van der Boom H, HogenEsch H, Frants RR, et al. Diet-induced hyperlipoproteinemia and atherosclerosis in apolipoprotein E3-Leiden transgenic mice. J Clin Invest. 1994;93(4):1403-10. doi:10.1172/JCI117117.

10. van de Steeg E, Kleemann R, Jansen HT, van Duyvenvoorde W, Offerman EH, Wortelboer HM, et al. Combined analysis of pharmacokinetic and efficacy data of preclinical studies with statins markedly improves translation of drug efficacy to human trials. The Journal of Pharmacology and Experimental Therapeutics. 2013;347(3):635-44. doi:10.1124/jpet.113.208595.

11. Linseisen J, Welch AA, Ocke M, Amiano P, Agnoli C, Ferrari P, et al. Dietary fat intake in the European Prospective Investigation into Cancer and Nutrition: results from the 24-h dietary recalls. Eur J Clin Nutr. 2009;63(S4):S61-S80. doi:10.1038/ejcn.2009.75.

12. Harika RK, Eilander A, Alssema M, Osendarp SJM, Zock PL. Intake of fatty acids in general populations worldwide does not meet dietary recommendations to prevent coronary heart disease: a systematic review of data from 40 countries. Ann Nutr Metab. 2013;63(3):229-38. doi:10.1159/000355437.

13. Calder PC, Ahluwalia N, Brouns F, Buetler T, Clement K, Cunningham K, et al. Dietary factors and low-grade inflammation in relation to overweight and obesity. Br J Nutr. 2011;106 (Sup.S3):S1-S78. doi:10.1017/S0007114511005460.

14. Hu FB, van Dam RM, Liu S. Diet and risk of Type II diabetes: the role of types of fat and carbohydrate. Diabetologia. 2001;44(7):805-17. doi:10.1007 /s001250100547.

15. Hooper L, Martin N, Abdelhamid A, Davey Smith G. Reduction in saturated fat intake for cardiovascular disease. Cochrane Database of Systematic Reviews. 2015;6. doi:10.1002 /14651858.CD011737.

16. Tierney AC, McMonagle J, Shaw DI, Gulseth HL, Helal O, Saris WHM, et al. Effects of dietary fat modification on insulin sensitivity and on other risk factors of the metabolic syndrome. LIPGENE: a European randomized dietary intervention study. Int J Obes. 2011;35(6):800-9. doi:10.1038

/ijo.2010.209.

17. Gögebakan Ö, Kohl A, Osterhoff MA, van Baak MA, Jebb SA, Papadaki A, et al. Effects of Weight Loss and Long-Term Weight Maintenance With Diets Varying in Protein and Glycemic Index on Cardiovascular Risk Factors: The Diet, Obesity, and Genes (DiOGenes) Study: A Randomized, Controlled Trial. Circulation. 2011;124(25):2829-38. doi:10.1161/circulationaha.111.033274.

18. Levitan EB, Cook NR, Stampfer MJ, Ridker PM, Rexrode KM, Buring JE, et al. Dietary glycemic index, dietary glycemic load, blood lipids, and C-reactive protein. Metabolism. 2008;57(3):437-43. doi:10.1016/j.metabol.2007.11.002.

19. Ishimoto T, Lanaspa MA, Rivard CJ, Roncal-Jimenez CA, Orlicky DJ, Cicerchi C, et al. High-fat and high-sucrose (western) diet induces steatohepatitis that is dependent on fructokinase. Hepatology. 2013;58(5):1632-43. doi:10.1002 /hep.26594.

20. Tallino S, Duffy M, Ralle M, Cortés MP, Latorre M, Burkhead JL. Nutrigenomics analysis reveals that copper deficiency and dietary sucrose up-regulate inflammation, fibrosis and lipogenic pathways in a mature rat model of nonalcoholic fatty liver disease. Journal of Nutritional Biochemistry. 2015;26 (10):996-1006. doi:10.1016/j.jnutbio.2015.04.009.

21. Kleemann R, Verschuren L, van Erk MJ, Nikolsky Y, Cnubben NH, Verheij ER, et al. Atherosclerosis and liver inflammation induced by increased dietary cholesterol intake: A combined transcriptomics and metabolomics analysis. Genome Biol. 2007;8(9):R200. doi:10.1186/gb-2007-8-9-r200.

22. Wielinga PY, Yakala GK, Heeringa P, Kleemann R, Kooistra T. Beneficial effects of alternate dietary regimen on liver inflammation, atherosclerosis and renal activation. PLoS One. 2011;6(3):e18432. doi:10.1371/journal.pone.0018432.

23. Musso G, Gambino R, De Michieli F, Cassader M, Rizzetto M, Durazzo M, et al. Dietary habits and their relations to insulin resistance and postprandial lipemia in nonalcoholic steatohepatitis. Hepatology. 2003;37(4):909-16. doi:10.1053/jhep.2003.50132.

24. Yasutake K, Nakamuta M, Shima Y, Ohyama A, Masuda K, Haruta N, et al. Nutritional investigation of non-obese patients with non-alcoholic fatty liver disease: the significance of dietary cholesterol. Scand J Gastroenterol. 2009;44(4):471-7. doi:10.1080 /00365520802588133.

25. Ioannou GN, Morrow OB, Connole ML, Lee SP. Association between dietary nutrient composition

and the incidence of cirrhosis or liver cancer in the United States population. Hepatology. 2009;50(1):175-84. doi:10.1002/hep.22941.

26. Tannock LR, O'Brien KD, Knopp RH, Retzlaff B, Fish B, Wener MH, et al. Cholesterol feeding increases C-reactive protein and Serum Amyloid A levels in lean insulin-sensitive subjects. Circulation. 2005;111(23):3058-62. doi:10.1161/circulationaha.104.506188.

27. Musso G, Gambino R, Cassader M. Cholesterol metabolism and the pathogenesis of non-alcoholic steatohepatitis. Prog Lipid Res. 2013;52(1):175-91. doi:10.1016/j.plipres.2012.11.002.

28. Puri P, Baillie RA, Wiest MM, Mirshahi F, Choudhury J, Cheung O, et al. A lipidomic analysis of nonalcoholic fatty liver disease. Hepatology. 2007;46(4):1081-90. doi:10.1002/hep.21763.

29. Caballero F, Fernandez A, De Lacy AM, Fernandez-Checa JC, Caballeria J, Garcia-Ruiz C. Enhanced free cholesterol, SREBP-2 and StAR expression in human NASH. J Hepatol. 2009;50(4):789-96. doi:10.1016/j.jhep.2008.12.016.

30. Leroux A, Ferrere G, Godie V, Cailleux F, Renoud ML, Gaudin F, et al. Toxic lipids stored by Kupffer cells correlates with their pro-inflammatory phenotype at an early stage of steatohepatitis. J Hepatol. 2012;57(1):141-9. doi:10.1016/j.jhep.2012.02.028.

31. Teratani T, Tomita K, Suzuki T, Oshikawa T, Yokoyama H, Shimamura K, et al. A high-cholesterol diet exacerbates liver fibrosis in mice via accumulation of free cholesterol in hepatic stellate cells. Gastroenterology. 2012;142(1):152-64.e10. doi:10.1053/j.gastro.2011.09.049.

32. Tomita K, Teratani T, Suzuki T, Shimizu M, Sato H, Narimatsu K, et al. Free cholesterol accumulation in hepatic stellate cells: Mechanism of liver fibrosis aggravation in nonalcoholic steatohepatitis in mice. Hepatology. 2014;59(1):154-69. doi:10.1002/hep.26604.

33. Hendrikx T, Walenbergh SMA, Hofker MH, Shiri-Sverdlov R. Lysosomal cholesterol accumulation: driver on the road to inflammation during atherosclerosis and non-alcoholic steatohepatitis. Obes Rev. 2014;15(5):424-33. doi:10.1111/obr.12159.

34. Anitschkow N, Chalatow S, Müller C, Duguid J. Ueber experimentelle Cholesterinsteatose und ihre Bedeutehung einiger pathologischer Prozesse. Centrbl Allg Pathol Pathol Anat. 1913;24:1-9.

35. Steinberg D. In celebration of the 100th anniversary of the lipid hypothesis of atherosclerosis. J Lipid Res. 2013;54(11):2946-9. doi:10.1194/jlr.R043414.

36. Prospective Studies Collaboration. Blood cholesterol and vascular mortality by age, sex, and blood pressure: a meta-analysis of individual data from 61 prospective studies with 55 000 vascular deaths. Lancet. 2007;370(9602):1829-39. doi:10.1016/S0140-6736(07)61778-4.

37. Tall AR, Yvan-Charvet L. Cholesterol, inflammation and innate immunity. Nature Reviews Immunology. 2015;15(2):104-16. doi:10.1038/nri3793.

38. Moore Kathryn J, Tabas I. Macrophages in the pathogenesis of atherosclerosis. Cell. 2011;145(3):341-55. doi:10.1016/j.cell.2011.04.005.

39. Li Y, Schwabe RF, DeVries-Seimon T, Yao PM, Gerbod-Giannone M-C, Tall AR, et al. Free cholesterol-loaded macrophages are an abundant source of tumor necrosis factor-α and interleukin-6: model of NF-κB- and map kinase-dependent inflammation in advanced atherosclerosis. J Biol Chem. 2005;280(23):21763-72. doi:10.1074/jbc.M501759200.

40. Sampson U, Fazio S, Linton M. Residual cardiovascular risk despite optimal LDL cholesterol reduction with statins: the evidence, etiology, and therapeutic challenges. Current Atherosclerosis Reports. 2012;14(1):1-10. doi:10.1007/s11883-011-0219-7.

41. Golia E, Limongelli G, Natale F, Fimiani F, Maddaloni V, Pariggiano I, et al. Inflammation and cardiovascular disease: from pathogenesis to therapeutic target. Current Atherosclerosis Reports. 2014;16(9):1-7. doi:10.1007/s11883-014-0435-z.

42. West DB, Boozer CN, Moody DL, Atkinson RL. Dietary obesity in nine inbred mouse strains. American Journal of Physiology - Regulatory, Integrative and Comparative Physiology. 1992;262(6):R1025-R32.

43. Dias JA, Wirfält E, Drake I, Gullberg B, Hedblad B, Persson M, et al. A high quality diet is associated with reduced systemic inflammation in middle-aged individuals. Atherosclerosis. 2015;238(1):38-44. doi:10.1016/j.atherosclerosis.2014.11.006.

44. Akbaraly TN, Shipley MJ, Ferrie JE, Virtanen M, Lowe G, Hamer M, et al. Long-term adherence to healthy dietary guidelines and chronic inflammation in the prospective Whitehall II Study. Am J Med. 2015;128(2):152-60.e4. doi:10.1016/j.amjmed.2014.10.002.

45. Fung TT, McCullough ML, Newby P, Manson JE, Meigs JB, Rifai N, et al. Diet-quality scores and

plasma concentrations of markers of inflammation and endothelial dysfunction. Am J Clin Nutr. 2005;82(1):163-73.

46. Yakala GK, van der Heijden R, Molema G, Schipper M, Wielinga PY, Kleemann R, et al. Beneficial effects of an alternating high-fat dietary regimen on systemic insulin resistance, hepatic and renal inflammation and renal function. PLoS One. 2012 ;7(9):e45866. doi:10.1371/journal.pone.0045866.

47. Chaix A, Zarrinpar A, Miu P, Panda S. Time-restricted feeding is a preventative and therapeutic intervention against diverse nutritional challenges. Cell Metab. 2014;20(6):991-1005. doi:10.1016/j.cmet.2014.11.001.

48. Bertelsen J, Christiansen C, Thomsen C, Poulsen PL, Vestergaard S, Steinov A, et al. Effect of Meal Frequency on Blood Glucose, Insulin, and Free Fatty Acids in NIDDM Subjects. Diabetes Care. 1993;16(1):4-7. doi:10.2337/diacare.16.1.4.

49. Jenkins DJ, Ocana A, Jenkins AL, Wolever TM, Vuksan V, Katzman L, et al. Metabolic advantages of spreading the nutrient load: effects of increased meal frequency in non-insulin-dependent diabetes. Am J Clin Nutr. 1992;55(2):461-7.

50. Marinac CR, Sears DD, Natarajan L, Gallo LC, Breen CI, Patterson RE. Frequency and circadian timing of eating may influence biomarkers of inflammation and insulin resistance associated with breast cancer risk. PLoS One. 2015;10(8):e0136240. doi:10.1371/journal.pone.0136240.

51. Dower JI, Geleijnse JM, Gijsbers L, Schalkwijk C, Kromhout D, Hollman PC. Supplementation of the Pure Flavonoids Epicatechin and Quercetin Affects Some Biomarkers of Endothelial Dysfunction and Inflammation in (Pre)Hypertensive Adults: A Randomized Double-Blind, Placebo-Controlled, Crossover Trial. J Nutr. 2015;145(7):1459-63. doi:10.3945/jn.115.211888.

52. Faghihzadeh F, Adibi P, Rafiei R, Hekmatdoost A. Resveratrol supplementation improves inflammatory biomarkers in patients with nonalcoholic fatty liver disease. Nutr Res. 2014 ;34(10):837-43. doi:10.1016/j.nutres.2014.09.005.

53. Bogdanski P, Suliburska J, Szulinska M, Stepien M, Pupek-Musialik D, Jablecka A. Green tea extract reduces blood pressure, inflammatory biomarkers, and oxidative stress and improves parameters associated with insulin resistance in obese, hypertensive patients. Nutr Res. 2012;32(6):421-7. doi:10.1016/j.nutres.2012.05.007.

54. Tresserra-Rimbau A, Rimm EB, Medina-Remón A, Martínez-González MA, de la Torre R, Corella D, et al. Inverse association between habitual polyphenol intake and incidence of cardiovascular events in the PREDIMED study. Nutrition, Metabolism and Cardiovascular Diseases. 2014;24(6):639-47. doi:10.1016/j.numecd.2013.12.014.

55. Arts IC, Hollman PC, Feskens EJ, Bueno de Mesquita HB, Kromhout D. Catechin intake might explain the inverse relation between tea consumption and ischemic heart disease: the Zutphen Elderly Study. Am J Clin Nutr. 2001;74(2):227-32.

56. Chawla A, Nguyen KD, Goh YPS. Macrophage-mediated inflammation in metabolic disease. Nature Reviews Immunology. 2011;11(11):738-49. doi:10.1038/nri3071.

57. McNelis JC, Olefsky JM. Macrophages, immunity, and metabolic disease. Immunity. 2014;41(1):36-48. doi:10.1016/j.immuni.2014.05.010.

58. Kolaczkowska E, Kubes P. Neutrophil recruitment and function in health and inflammation. Nature Reviews Immunology. 2013;13(3):159-75. doi:10.1038/nri3399.

59. Amulic B, Cazalet C, Hayes GL, Metzler KD, Zychlinsky A. Neutrophil function: from mechanisms to disease. Annu Rev Immunol. 2012;30(1):459-89. doi:10.1146/annurev-immunol-020711-074942.

60. Wang Q, Xie Z, Zhang W, Zhou J, Wu Y, Zhang M, et al. Myeloperoxidase deletion prevents high-fat diet–induced obesity and insulin resistance. Diabetes. 2014;63(12):4172-85. doi:10.2337/db14-0026.

61. Talukdar S, Oh DY, Bandyopadhyay G, Li D, Xu J, McNelis J, et al. Neutrophils mediate insulin resistance in mice fed a high-fat diet through secreted elastase. Nat Med. 2012;18(9):1407-12. doi:10.1038/nm.2885.

62. Rensen SS, Bieghs V, Xanthoulea S, Arfianti E, Bakker JA, Shiri-Sverdlov R, et al. Neutrophil-derived myeloperoxidase aggravates non-alcoholic steatohepatitis in low-density lipoprotein receptor-deficient mice. PLoS One. 2012;7(12):e52411. doi:10.1371/journal.pone.0052411.

63. Brotfain E, Hadad N, Shapira Y, Avinoah E, Zlotnik A, Raichel L, et al. Neutrophil functions in morbidly obese subjects. Clin Exp Immunol. 2015;181(1):156-63. doi:10.1111/cei.12631.

64. Xu X, Su S, Wang X, Barnes V, De Miguel C, Ownby D, et al. Obesity is associated with more activated neutrophils in african american male youth. Int J

Obes. 2014. doi:10.1038/ijo.2014.194.

65. Serhan CN. Pro-resolving lipid mediators are leads for resolution physiology. Nature. 2014;510 (7503):92-101. doi:10.1038/nature13479.

Chapter 10

Nederlandstalige samenvatting
(*Summary in Dutch*)

Metabole ontsteking – de ontstekingsreactie die plaatsvindt in respons op metabole overbelasting (een overschot aan energie of macronutriënten) – wordt gedacht een belangrijke rol te spelen bij de ontwikkeling van obesitas-gerelateerde ziekten zoals insulineresistentie, niet-alcoholische leververvetting en atherosclerose. Er is echter nog veel onbekend over de oorsprong en het mechanisme van metabole ontsteking. Het doel van het onderzoek beschreven in dit proefschrift was om het ontstaan van metabole ontsteking beter te begrijpen en mogelijke interventies gericht op specifieke aspecten van metabole ontsteking te onderzoeken.

In **hoofdstuk 2** hebben we de opeenvolging van verschillende ontstekingsprocessen in het vetweefsel en de lever onderzocht gedurende hoog vet geïnduceerde metabole overbelasting. Het doel hiervan was de bijdrage van deze twee organen aan de ontwikkeling van obesitas-gerelateerde insulineresistentie en niet-alcoholische leververvetting te onderzoeken. We hebben laten zien dat het langdurig voeren van een hoog vet dieet aan C57BL/6J muizen een progressief obees fenotype induceert, met ontwikkeling van algehele insulineresistentie. In het vetweefsel was metabole ontsteking waarneembaar na 24 weken hoog vet dieet terwijl leverontsteking pas na 40 weken op het dieet werd waargenomen. Aangezien algehele insulineresistentie zich ontwikkeld had voordat er uitgesproken ontsteking in de lever werd geobserveerd, wijzen de resultaten van deze studie er op dat vetweefselontsteking meer waarschijnlijk geassocieerd is met de ontwikkeling van algehele insulineresistentie dan leverontsteking, in ieder geval in de vroege fases van ziekteontwikkeling. Daarna hebben we in **hoofdstuk 3** laten zien dat verschillende vetweefseldepots verschillen in hun vatbaarheid om metabole ontsteking te ontwikkelen gedurende hoog vet dieet geïnduceerde obesitas in C57BL/6J-muizen. Het eerste vetdepot waarin metabole ontsteking zichtbaar was (d.w.z. macrofaaginfiltratie in het vetweefsel in de vorm van zogenaamde 'crown-like structures') was het epididymale (perigonadale) depot. Deze ontsteking leek gerelateerd te zijn aan de maximale expansie van dit depot en de vetcellen (adipocyten) daarin. Opnieuw ging het ontstaan van ontsteking van dit vetweefseldepot vooraf aan de ontwikkeling van leverontsteking, en daarmee ging het vooraf aan de progressie van leververvetting naar niet-alcoholische steatohepatitis. Vervolgens hebben we onderzocht of dit ontstoken vetweefsel een oorzakelijke rol speelt in deze progressie naar niet-alcoholische steatohepatitis. We hebben laten zien dat wanneer je dit ontstoken epididymale vetdepot operatief verwijdert, de ontwikkeling van leverontsteking vermindert en plasmaniveaus van specifieke ontstekingsfactoren (zoals cytokines en pro-inflammatoire vetzuren) verlaagd worden. Deze circulerende pro-inflammatoire

mediatoren vormen mogelijk de verbinding tussen het ontstoken vetweefseldepot en de progressie van niet-alcoholische steatohepatitis. In **hoofdstuk 4** onderzochten we de effecten van een interventie gericht op het 'NLRP3 inflammasome', één van de sensoren van metabole overbelasting. Dit hebben we bestudeerd in een model van hoog vet geïnduceerde obesitas en niet-alcoholische leververvetting in LDLr-/-.Leiden muizen die we behandelden met een caspase-1 remmer. De behandeling met deze remmer had geen effect op de mate van obesitas of de massa van het vetweefsel, maar verminderde wel de ontsteking in het epididymale vetweefsel en in parallel daaraan nam de algehele insulineresistentie af. In de lever zagen we een milde afname in leververvetting, en consistent met de geobserveerde afname in vetweefselontsteking en de rol van het ontstoken vetweefsel in de ontwikkeling van leverontsteking, observeerden we een uitgesproken effect op leverontsteking. Dit effect was voornamelijk zichtbaar als een afname in de infiltratie van neutrofielen in de lever. In overeenstemming met deze afname in ontsteking van de lever zagen we dat de ontwikkeling van leverfibrose ook afgenomen was in de muizen die behandeld waren met de caspase-1 remmer. Vervolgens onderzochten we de potentiele waarde van verschillende voedingsinterventies als strategie om metabole ontsteking en ziekteontwikkeling te verminderen. In **hoofdstuk 5** hebben we laten zien dat (isocalorische) vervanging van diëtair verzadigd vet met pompoenzaadolie dat rijk is aan poly-onverzadigde vetzuren, de ontwikkeling van dyslipidemie vermindert in ApoE*3Leiden muizen. Ook had de pompoenzaadolie gunstige effecten op niet-alcoholische steatohepatitis (voornamelijk op de vervetting van de lever) en de daarmee geassocieerde atherosclerose. Bovendien vonden we dat bepaalde componenten die alleen in de onverzadigde pompoenzaadolie voorkomen (fytochemicaliën met vermeende anti-inflammatoire effecten), additionele gunstige effecten hadden op het vetmetabolisme en de ontsteking in de lever, wat leidde tot uitgesproken effecten op de ontwikkeling van metabole ziekten. We zijn daarna verdergegaan met twee studies naar de potentiele gezondheidseffecten van fytochemicaliën met anti-inflammatoire eigenschappen, met de nadruk ofwel op de metabole ontsteking in de lever tijdens de ontwikkeling van niet-alcoholische steatohepatitis, ofwel op metabole ontsteking in de vaatwand tijdens de ontwikkeling van atherosclerose. In **hoofdstuk 6** onderzochten we de effecten van een extract van de blauwe bosbes (*Vaccinium myrtillus L.*) dat rijk is aan anthocyanen, gedurende de ontwikkeling van niet-alcoholische steatohepatitis en leverfibrose in ApoE*3Leiden muizen. We hebben laten zien dat toevoeging van dit extract aan het dieet de ontwikkeling van leververvetting vermindert en uitgesproken gunstige effecten heeft op de ontsteking van de lever. Opnieuw waren deze ontstekingsremmende effecten voornamelijk toe te wijzen aan de

afname van neutrofielinfiltratie in de lever. Het extract verminderde ook sterk de ontwikkeling van leverfibrose. We vonden dat deze effecten sterk gerelateerd waren aan een afname van de ophoping en kristallisatie van vrij cholesterol in de lever. De hoeveelheid vrij cholesterol in de lever correleerde met de geobserveerde pathologie (histologische scores en genexpressie data) en met de activatie van NFκB, wat ook gereduceerd werd door het extract. Vervolgens onderzochten we in **hoofdstuk 7** de potentie van de fytochemische stof (-)-epicatechine om metabole ontsteking tijdens de ontwikkeling van atherosclerose in ApoE*3Leiden muizen te voorkomen. (-)-Epicatechine verminderde de ontwikkeling van atherosclerose zonder een effect te hebben op dyslipidemie en onderdrukte de vorming van pro-atherogene ontstekingsfactoren in de lever. In de vaatwand verminderde (-)-epicatechine de expressie van pro-inflammatoire genen, waarvan velen gereguleerd worden door NFκB. Dit onderdrukkende effect op de activatie van NFκB hebben we bevestigd in NFκB-luciferase reportermuizen, waarin (-)-epicatechine de dieetgeïnduceerde NFκB activatie voorkwam. Hiermee vonden we een mogelijk mechanisme van de anti-atherogene effecten van (-)-epicatechine. In **hoofdstuk 8** bestudeerden we een interventie die gericht was op de resolutie van ontsteking tijdens de atheroscleroseontwikkeling. Hiervoor behandelden we ApoE*3Leiden muizen in een therapeutisch behandelprotocol met 'Resolvin E1', een lichaamseigen mediator van ontstekingsresolutie De behandeling met Resolvin E1 had geen effect op dyslipidemie maar resulteerde wel in een afname van de atherosclerose. De totale oppervlakte van atherosclerotische laesies was afgenomen, en er was verminderde progressie van milde naar zware laesietypes (die gekenmerkt worden door hun kwetsbaarheid voor ruptuur). Resolvin E1 had geen effect op de systemische ontstekingsmerker serum amyloid A (SAA) maar had wel ontstekingsremmende effecten in de aorta. Atherogene genexpressie was daar verminderd, en de activatie van ontstekingsbevorderende signaalroutes zoals IFN-γ en TNF-α was gedempt.

Concluderend hebben we laten zien dat metabole ontsteking een belangrijke rol speelt in de ontwikkeling van metabole ziekten zoals insulineresistentie/type 2 diabetes, niet-alcoholische leververvetting en atherosclerose. Interventies die de ontstekingsreactie op metabole overbelasting kunnen onderdrukken kunnen daarom waardevol zijn om de ziekteontwikkeling te voorkomen en vertragen. De resultaten van dit proefschrift laten zien dat naast farmacologische interventies ook voedingsinterventies opmerkelijk krachtige effecten kunnen hebben en daarmee een perspectief bieden om ziekteontwikkeling tegen te gaan.

Appendices

Authors' affiliations

Department of Metabolic Health Research, Netherlands Organization for Applied Scientific Research (TNO), Leiden, the Netherlands

Wim van Duyvenvoorde, Robert Kleemann, Teake Kooistra, Wen Liang, Martine C Morrison, Petra Mulder, Elsbet Pieterman, Kanita Salic, Karin Toet, Lars Verschuren, Peter Y Wielinga

Department of Microbiology and Systems Biology, Netherlands Organization for Applied Scientific Research (TNO), Zeist, the Netherlands

Lars Verschuren

Department of Pathology and Medical Biology, University Medical Center Groningen, University of Groningen, Groningen, the Netherlands

Peter Heeringa, Roel A van der Heijden, Marten H Hofker, Danny Kor, Martine C Morrison

Department of Pediatrics, University Medical Center Groningen, University of Groningen, Groningen, the Netherlands

Alain de Bruin, Nanda Gruben, Pascal PH Hommelberg, Niels J Kloosterhuis, Debby PY Koonen, Fareeba Sheedfar

Top Institute Food and Nutrition, Wageningen, the Netherlands

Roel A van der Heijden, Martine C Morrison

Department of Pathobiology, Dutch Molecular Pathology Center, Faculty of Veterinary Medicine, Utrecht University, Utrecht, the Netherlands

Alain de Bruin, Sameh A Youssef

Department of Physiology, Radboud University Medical Center, Nijmegen, the Netherlands

Fareeba Sheedfar

Department of Cardiovascular Surgery, Leiden University Medical Center, Leiden, the Netherlands

Petra Mulder

Molecular Endocrinology and Molecular Imaging, Department of Endocrinology, Leiden University Medical Center, Leiden, the Netherlands

Eric Kaijzel

Department of Pathology, Academic Medical Center, University of Amsterdam, Amsterdam, the Netherlands
Joanne Verheij

Department of Nutrition, Institute of Basic Medical Sciences, Faculty of Medicine, University of Oslo, Oslo, Norway
Rune Blomhoff

Department of Human and Animal Physiology, Wageningen University, Wageningen, the Netherlands
Robert Kleemann

TNO Triskelion, Zeist, the Netherlands
Aswin Menke

Department of Biochemistry and Biotechnology, Rovira i Virgili University, Tarragona, Spain
Anna Arola-Arnal, Manuel Suárez

Centre Tecnològic de Nutrició i Salut (CTNS), TECNIO, CEICS, Reus, Spain
Anna Arola-Arnal, Manuel Suárez

Bunge Ltd., White Plains, New York, United States of America
P. Mark Stavro

Resolvyx Pharmaceuticals, Inc., Cambridge MA, United States
Per Gjorstrup, Lijun Wu

Curriculum vitae

Martine Morrison was born in Eindhoven, the Netherlands on June 30th 1986. She completed her secondary education at the Lorentz Casimir Lyceum in Eindhoven. In August2009, she obtained her BSc degree in Nutrition and Health from Wageningen University. She then continued with the two-year master program in Nutrition and Health at the same university. She completed her first MSc thesis at the Nutrition, Metabolism and Genomics group of the Division of Human Nutrition, where she worked on a human intervention study on the postprandial effects of different fatty acids on vascular reactivity and leukocyte adhesion in obese subjects. For her second MSc thesis she worked at the chair group Human and Animal Physiology, where she studied the effects of the polyphenol Quercetin on fatty acid metabolism in liver cells *in vitro*. During her internship at the University College Dublin Conway Institute for Biomolecular and Biomedical Research, Martine worked on the role of the protein MIF in the development of obesity and insulin resistance in an experimental disease model. She graduated from Wageningen University in September 2011, obtaining her MSc degree in Nutrition and Health with the specialisations 'Nutritional Physiology' and 'Molecular Nutrition'. From September 2011 onwards she worked as a PhD candidate at the department of Metabolic Health Research at the Netherlands Organization of Applied Scientific Research (TNO) under the guidance of her promotor prof. dr. Peter Heeringa (University Medical Center Groningen) and her co-promotor dr. Robert Kleemann (TNO). Her PhD research was performed within the Top Institute Food and Nutrition project on Cardiovascular Health. The results of this research on the role of metabolic inflammation in hepatic and vascular disease are presented in this thesis.

List of publications

Petra Mulder, <u>Martine C. Morrison</u>, Peter Y. Wielinga, Wim van Duyvenvoorde, Teake Kooistra, Robert Kleemann. **Surgical removal of inflamed epididymal white adipose tissue attenuates the development of non-alcoholic steatohepatitis in obesity.** *International Journal of Obesity* (2015) Oct 26. doi: 10.1038/ijo.2015.226.

<u>Martine C. Morrison</u>, Petra Mulder, P. Mark Stavro, Manuel Suárez, Anna Arola-Arnal, Wim van Duyvenvoorde, Teake Kooistra, Peter Y. Wielinga, Robert Kleemann. **Replacement of dietary saturated fat by PUFA-rich pumpkin seed oil attenuates non-alcoholic fatty liver disease and atherosclerosis development, with additional health effects of virgin over refined oil.** *PLoS One* (2015) 10(9):e0139196. doi: 10.1371/journal.pone.0139196.

Roel A. van der Heijden*, Fareeba Sheedfar*, <u>Martine C. Morrison</u>, Pascal P.H. Hommelberg, Danny Kor, Niels J Kloosterhuis, Nanda Gruben, Sameh A. Youssef, Alain de Bruin, Marten H. Hofker, Robert Kleemann, Debby P.Y. Koonen*, and Peter Heeringa* (*contributed equally). **High-fat diet induced obesity primes inflammation in adipose tissue prior to liver in C57BL/6j mice.** *Aging* (2015)7(4):256-68.

<u>Martine C. Morrison</u>, Robert Kleemann. **Role of macrophage migration inhibitory factor in obesity, insulin resistance, type 2 diabetes, and associated hepatic co-morbidities: a comprehensive review of human and rodent studies.** *Frontiers in Immunology* (2015) 15;6:308. doi: 10.3389/fimmu.2015.00308.

<u>Martine C. Morrison</u>, Wen Liang, Petra Mulder, Lars Verschuren, Elsbet Pieterman, Karin Toet, Peter Heeringa, Peter Y. Wielinga, Teake Kooistra, Robert Kleemann. **Mirtoselect, an anthocyanin-rich bilberry extract, attenuates non-alcoholic steatohepatitis and associated fibrosis in ApoE*3Leiden mice.** *Journal of Hepatology* (2015) 62(5):1180-6. doi: 10.1016 /j.jhep.2014.12.011.

Orla M. Finucane, Clare M. Reynolds, Fiona C. McGillicuddy, Karen A. Harford, <u>Martine Morrison</u>, John Baugh, Helen M. Roche. **Macrophage migration inhibitory factor deficiency ameliorates high-fat diet induced insulin resistance in mice with reduced adipose inflammation and hepatic steatosis.** *PLoS One* (2014) 9(11):e113369. doi: 10.1371 /journal.pone.0113369.

Martine Morrison, Roel van der Heijden, Peter Heeringa, Eric Kaijzel, Lars Verschuren, Rune Blomhoff, Teake Kooistra, Robert Kleemann. **Epicatechin attenuates atherosclerosis and exerts anti-inflammatory effects on diet-induced human-CRP and NFκB** *in vivo.* *Atherosclerosis* (2014) 233(1):149-56. doi: 10.1016/j.atherosclerosis.2013.

Wen Liang, Jan H. Lindeman, Aswin L. Menke, Debby P. Koonen, Martine Morrison, Louis M. Havekes, Anita M van den Hoek*, Robert Kleemann* (*contributed equally). **Metabolically induced liver inflammation leads to NASH and differs from LPS- or IL-1β-induced chronic inflammation.** *Laboratory Investigation* (2014) 94(5):491-502. doi:10.1038/labinvest.2014.11.

Robert Kleemann, Lars Verschuren, Martine Morrison, Susanne Zadelaar, Marjan J. van Erk, Peter Y. Wielinga, Teake Kooistra. **Anti-inflammatory, anti-proliferative and anti-atherosclerotic effects of quercetin in human** *in vitro* **and** *in vivo* **models.** *Atherosclerosis* (2011) 218(1):44-52. doi: 10.1016/j.atherosclerosis.2011.04.023.

Manuscripts in preparation

Martine C. Morrison, Petra Mulder, Kanita Salic, Joanne Verheij, Wen Liang, Wim van Duyvenvoorde, Aswin Menke, Teake Kooistra, Robert Kleemann, Peter Y. Wielinga. **Intervention with a caspase-1 inhibitor reduces obesity-associated hyperinsulinemia, non-alcoholic steatohepatitis (NASH) and hepatic fibrosis in LDLr-/-.Leiden mice.** *In submission.*

Kanita Salic, Martine C. Morrison, Lars Verschuren, Peter Y. Wielinga, Lijun Wu, Robert Kleemann, Per Gjorstrup and Teake Kooistra. **Resolvin E1 attenuates atherosclerosis in absence of cholesterol-lowering effects and on top of atorvastatin.** *In submission.*

Petra Mulder, Martine C. Morrison, Wen Liang, Lars Verschuren, J. Hajo van Bockel, Teake Kooistra, Peter Y. Wielinga, Robert Kleemann. **Reduction of obesity-associated white adipose tissue inflammation attenuates the progression of non-alcoholic fatty liver disease.** *In submission.*

Metabolic inflammation in hepatic and vascular disorders

Strategies to attenuate disease development

1. Although metabolic overload is typically thought to be the result of caloric excess, dietary composition is also an important determinant of the metabolic inflammatory response, even when energy intake is not excessive *(this thesis)*.

2. In order to draw meaningful conclusions from pre-clinical research it is critical that an experimental disease model reflects human pathogenesis and disease aetiology rather than merely reflecting the observed pathology.

3. Inflammation caused by metabolic overload is a promising target for the treatment of metabolic disease, especially when a sustainable reduction in metabolic overload cannot be achieved (*this thesis*).

4. Approaches that categorise dietary components as universally 'good' or 'bad' based on their average beneficial or detrimental health effect in the population may have limited utility for an individual *(Zeevi et al., Cell 2015)*.

5. Statistical significance is an arbitrary convention that is frequently misused as a measure of publication worthiness.

6. Ask someone what constitutes a healthy diet, and 99 out of a 100 people will give you a clear-cut answer. The one person that is not sure is probably a nutrition scientist (adapted from: *Martijn Katan, Wat is nu gezond?).*

Martine Morrison

March 30, 2016